


1995

Photophysics and activity of biological systems containing the optical probes 7-azatryptophan and its analogs

Rebecca Lynne Rich
Iowa State University

Follow this and additional works at: <https://lib.dr.iastate.edu/rtd>

 Part of the [Biophysics Commons](#), and the [Physical Chemistry Commons](#)

Recommended Citation

Rich, Rebecca Lynne, "Photophysics and activity of biological systems containing the optical probes 7-azatryptophan and its analogs " (1995). *Retrospective Theses and Dissertations*. 10974.
<https://lib.dr.iastate.edu/rtd/10974>

This Dissertation is brought to you for free and open access by the Iowa State University Capstones, Theses and Dissertations at Iowa State University Digital Repository. It has been accepted for inclusion in Retrospective Theses and Dissertations by an authorized administrator of Iowa State University Digital Repository. For more information, please contact digirep@iastate.edu.

INFORMATION TO USERS

This manuscript has been reproduced from the microfilm master. UMI films the text directly from the original or copy submitted. Thus, some thesis and dissertation copies are in typewriter face, while others may be from any type of computer printer.

The quality of this reproduction is dependent upon the quality of the copy submitted. Broken or indistinct print, colored or poor quality illustrations and photographs, print bleedthrough, substandard margins, and improper alignment can adversely affect reproduction.

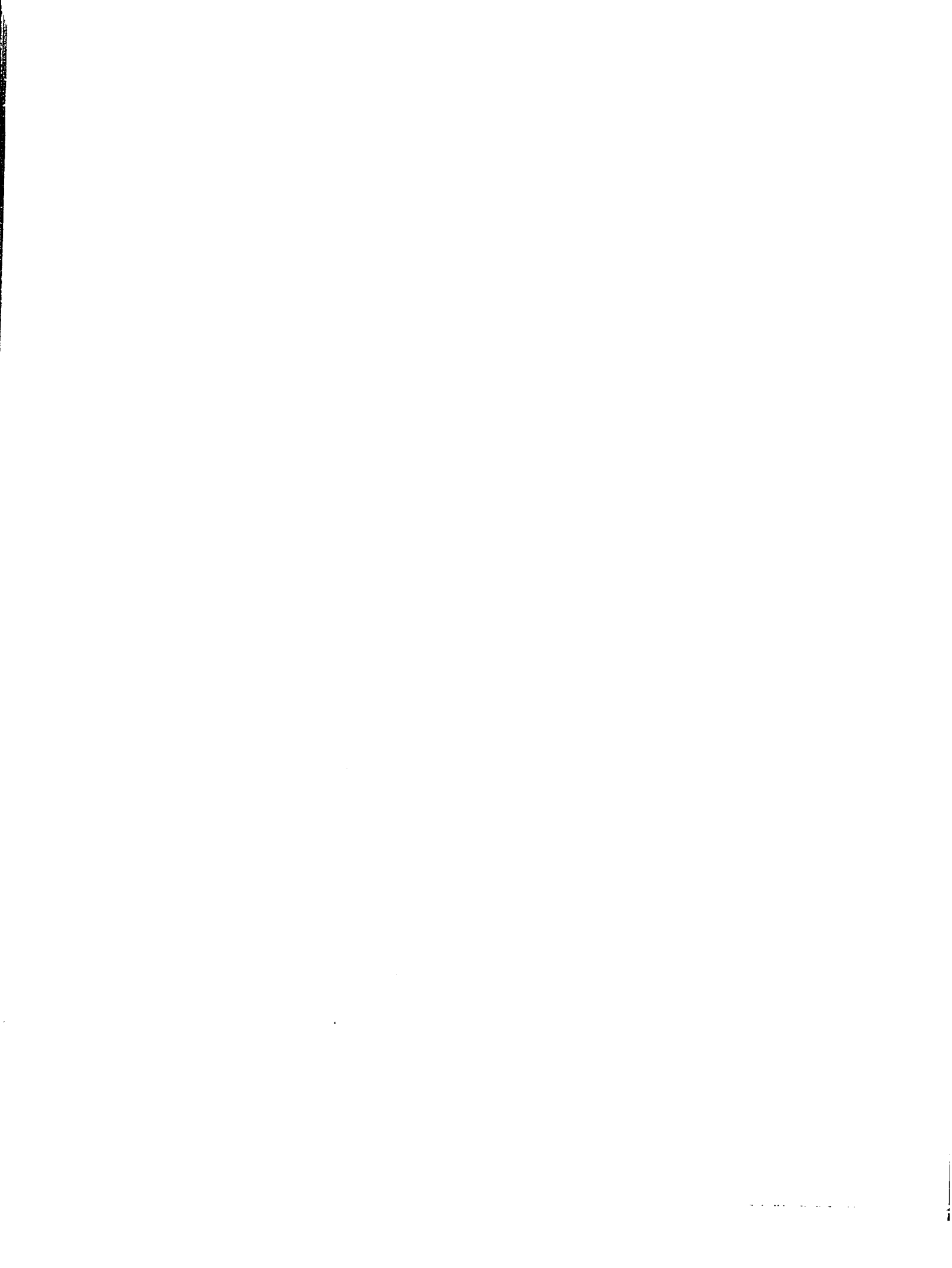
In the unlikely event that the author did not send UMI a complete manuscript and there are missing pages, these will be noted. Also, if unauthorized copyright material had to be removed, a note will indicate the deletion.

Oversize materials (e.g., maps, drawings, charts) are reproduced by sectioning the original, beginning at the upper left-hand corner and continuing from left to right in equal sections with small overlaps. Each original is also photographed in one exposure and is included in reduced form at the back of the book.

Photographs included in the original manuscript have been reproduced xerographically in this copy. Higher quality 6" x 9" black and white photographic prints are available for any photographs or illustrations appearing in this copy for an additional charge. Contact UMI directly to order.

UMI

A Bell & Howell Information Company
300 North Zeeb Road, Ann Arbor, MI 48106-1346 USA
313/761-4700 800/521-0600



Photophysics and activity of biological systems containing the optical probes,

7-azatryptophan and its analogs

by

Rebecca Lynne Rich

A Dissertation Submitted to the
Graduate Faculty in Partial Fulfillment of the
Requirements for the Degree of
DOCTOR OF PHILOSOPHY

Department: Chemistry
Major: Physical Chemistry

Approved:

Signature was redacted for privacy.

In Charge of Major Work

Signature was redacted for privacy.

For the Major Department

Signature was redacted for privacy.

For the Graduate College

Iowa State University
Ames, Iowa

1995

UMI Number: 9540934

UMI Microform 9540934

Copyright 1995, by UMI Company. All rights reserved.

This microform edition is protected against unauthorized
copying under Title 17, United States Code.

UMI

300 North Zeeb Road
Ann Arbor, MI 48103

Tsokonombwe anatha mtunda ndi kulumpha.

— a Chichewa proverb

A rough translation of the proverb is:

Tsokonombwe (a grasshopper that has no wings) can travel an incredibly long distance by hopping or leaping, rather than flying.

Dedicated to my parents with love and gratitude

TABLE OF CONTENTS

ABSTRACT	xiii
GENERAL INTRODUCTION	1
Statement of Purpose and Overview of the Research Project	1
Dissertation Organization	3
PART I. ANALYSIS OF AMINO ACID RESIDUES	5
CHAPTER 1. FLUORESCENT SPECIES OF 7-AZAINDOLE AND 7-AZATRYPTOPHAN IN WATER	6
Abstract	6
Introduction	7
Materials and Methods	11
Results	17
Discussion	32
Conclusions	42
Acknowledgment	44
References and Notes	44
CHAPTER 2. STEADY-STATE AND TIME-RESOLVED FLUORESCENCE ANISOTROPY OF 7-AZAINDOLE AND ITS DERIVATIVES	49
Abstract	49
Introduction	50
Experimental	53
Results	56
Discussion	72
Conclusions	78
Acknowledgment	78
References	79
CHAPTER 3. 7-AZAINDOLE AND 7-AZATRYPTOPHAN DERIVATIVES AS OPTICAL PROBES OF BIOLOGICAL SYSTEMS: METHYLATION OF THE AROMATIC NITROGENS	83
Introduction	83
Syntheses	83
References	86

CHAPTER 4. SYNTHESIS AND PHOTOPHYSICAL ANALYSIS OF THE OPTICAL PROBE, N ₁ -METHYL-7-AZATRYPTOPHAN	87
Abstract	87
Introduction	87
Materials and Methods	88
Results and Discussion	91
Conclusions	98
References	99
PART II. ANALYSIS OF PEPTIDE SEQUENCES	102
CHAPTER 5. INCORPORATION OF 7-AZATRYPTOPHAN INTO PEPTIDE SEQUENCES AND THEIR BINDING INTERACTIONS WITH α -CHYMOTRYPSIN	103
Introduction	103
Incorporation of 7-Azatriptophan into Peptide Sequences	103
Studies of Enzyme Kinetics: Determinations of K_m , k_{cat} , and K_I	105
References	114
CHAPTER 6. THE PHOTOPHYSICAL PROBE, 7-AZATRYPTOPHAN, IN SYNTHETIC PEPTIDES	115
Abstract	115
Introduction	115
Materials and Methods	116
Results and Discussion	118
Conclusions	123
Acknowledgments	123
References	123
CHAPTER 7. SMALL PEPTIDES CONTAINING THE NONNATURAL AMINO ACID, 7-AZATRYPTOPHAN: PROBING STRUCTURE, DYNAMICS, AND BIOLOGICAL ACTIVITY	125
Abstract	125
Introduction	126
Experimental	131
Results	135
Discussion	149
Conclusions	155
Acknowledgment	156
References and Notes	156

CHAPTER 8. INCORPORATION OF N ₁ -METHYL-7-AZATRYPTOPHAN INTO PEPTIDES SEQUENCES AND THEIR BINDING INTERACTIONS WITH THE MAJOR HISTOCOMPATIBILITY COMPLEX MOLECULE, H-2K ^b	161
Introduction	161
Materials and Methods	162
Preliminary Results	163
References	163
PART III. ANALYSIS OF BIOLOGICAL COFACTORS	164
CHAPTER 9. USING 7-AZATRYPTOPHAN TO PROBE SMALL MOLECULE-PROTEIN INTERACTIONS ON THE PICOSECOND TIME SCALE: THE COMPLEX OF AVIDIN AND BIOTINYLATED 7-AZATRYPTOPHAN	165
Abstract	165
Introduction	166
Experimental	168
Results	170
Discussion	179
Conclusions	185
Acknowledgment	186
References	187
CHAPTER 10. SYNTHESIS AND SPECTRAL CHARACTERIZATION OF 5'-PHOSPHOPYRIDOXAL-D,L-7-AZATRYPTOPHAN, A PHOTOPHYSICAL PROBE OF PROTEIN STRUCTURE AND DYNAMICS	190
Abstract	190
Introduction	190
Experimental	192
Results and Discussion	194
Conclusions	195
Acknowledgments	199
References	200
PART IV. ANALYSIS OF PROTEINS	201
CHAPTER 11. PROPOSED INCORPORATION OF 7-AZATRYPTOPHAN INTO BACTERIAL PROTEINS	202
Introduction	202

Materials and Methods	202
References	206
GENERAL SUMMARY AND CONCLUSIONS	207
ACKNOWLEDGMENTS	208
APPENDIX A: FUTURE PROJECTS	209
APPENDIX B: NOTES ON INSTRUMENTATION	212
APPENDIX C: CALCULATIONS TO DETERMINE 90% INHIBITOR BOUND TO ENZYME	217

LIST OF TABLES

Table 1.1 Fluorescence Lifetimes and Quantum Yields of 7-Azaindole and Its Derivatives	18
Table 1.2 Deuterium Isotope Effect on Fluorescence Lifetimes and Quantum Yields	26
Table 1.3 Ground- and Excited-State pK_a Values of 7-Azaindole and Its Analogs	28
Table 2.1 Fluorescence Anisotropy Decay of 7-Azaindole	68
Table 2.2 Steady-State Measurements of 7-Azaindole and Related Compounds	70
Table 4.1 Spectroscopic Data of N_1 -Methyl-7-Azatryptophan and Related Compounds	94
Table 4.2 Fluorescence Lifetimes of Mixtures of N_1 -Methyl-7-Azatryptophan and Tryptophan	95
Table 5.1 Peptides Provided by the Protein Facility	104
Table 5.2 Useful Data of Compounds Used in the Kinetic Studies	107
Table 6.1 Inhibition of α -Chymotrypsin	122
Table 7.1 Summary of Fluorescence and Anisotropy Decay Parameters	129
Table 7.2 Inhibition of α -Chymotrypsin	136
Table 7.3 Temperature Dependence of the Fluorescence Decay of the 7-Azatryptophan D-Octapeptide under Reducing and Oxidizing Conditions	142
Table 7.4 Quenching of 7-Azaindole Fluorescence	145
Table 7.5 Quenching by KI of the Fluorescence from the 7-Azatryptophan D-Octapeptide Under Reducing and Oxidizing Conditions	146
Table 9.1 Fluorescence Lifetime and Anisotropy Decay Parameters	176

LIST OF FIGURES

Figure 1.1	Structures of: (a) 7-azaindole, (b) zwitterionic 7-azatryptophan, (c) N ₁ -methyl-7-azaindole (1M7AT), and (d) 7-methyl-7H-pyrrole[2,3-b]pyridine (7M7AT)	8
Figure 1.2	Comparison of the absorption and fluorescence spectra of: (a) tryptophan and (b) 7-azatryptophan	9
Figure 1.3	Normalized fluorescence spectra of: (a) pure 7-azaindole, (b) isolated impurity 1, and (c) isolated impurity 2	13
Figure 1.4	Normalized fluorescence spectra in water of 7-azaindole	14
Figure 1.5	Normalized fluorescence spectra in water of: (a) impurity 1 and (b) impurity 2 isolated from commercial 7-azaindole	15
Figure 1.6	Fluorescence decay of 7-azaindole in water	20
Figure 1.7	Time-resolved fluorescence spectra of: (a) 7-azaindole and (b) 7-azatryptophan	22
Figure 1.8	Steady-state decomposition of (a) 7-azaindole and (b) 7-azatryptophan	23
Figure 1.9	Arrhenius plots of 7-azaindole in H ₂ O and D ₂ O	25
Figure 1.10	Fluorescence quantum yield of 7-azaindole as a function of pH	29
Figure 1.11	Average fluorescence lifetime of: (a) 1M7AI and (b) 7M7AI as a function of pH	31
Figure 1.12	Steady state emission spectra of: (a) 7-azaindole; (b) 1M7AI; and (c) 7M7AI	34
Figure 1.13	Idealized depictions of 7-azaindole/H ₂ O interactions	36
Figure 2.1	Structures of: (a) indole, (b) 7-azaindole, (c) 7-azatryptophan, (d) N ₁ -methyl-7-azaindole, and (e) 7-methyl-7H-pyrrole[2,3-b]pyridine (7M7AT)	51
Figure 2.2	Structures of 7-azaindole hydrogen-bonded: (a) normal complex and (b) "tautomer" complex	52

Figure 2.3	Fluorescence depolarization data for rose bengal in methanol	58
Figure 2.4	(a) Fluorescence excitation anisotropy and (b) resolved excitation spectrum of indole	61
Figure 2.5	(a) Emission anisotropy, (b) fluorescence excitation anisotropy of 7-azaindole, and (c) resolved excitation spectrum of 7-azaindole	63
Figure 2.6	(a) Emission anisotropy and (b) fluorescence excitation anisotropy of 7-azatryptophan	64
Figure 2.7	(a) Emission anisotropy and (b) fluorescence excitation anisotropy of 1M7AI	65
Figure 2.8	(a) Emission anisotropy and (b) fluorescence excitation anisotropy of 7M7AI	66
Figure 2.9	Fluorescence anisotropy decay of the normal band of 7-azaindole in methanol at 9°C	71
Figure 2.10	Plots of the rotational diffusion time against η/T for the normal band of 7-azaindole in butanol and water	73
Figure 2.11	Energy level diagram for indole, 7-azaindole, and related compounds	75
Figure 3.1	Structures of proposed 7-azatryptophan analogs	85
Figure 4.1	Structures of: (a) tryptophan, (b) 7-azatryptophan, and (c) N ₁ -methyl-7-azatryptophan	89
Figure 4.2	Absorption and emission spectra of tryptophan and N ₁ -methyl-7-azatryptophan	92
Figure 4.3	Fluorescence decay of: (a) N ₁ -methyl-7-azatryptophan; (b) tryptophan; and (c) 7-azatryptophan	93
Figure 4.4	Fluorescence decay of a mixture of N ₁ -methyl-7-azatryptophan and tryptophan at various concentration ratios	96
Figure 5.1	Active-site determination of α -chymotrypsin	109
Figure 5.2	Degradation of α -chymotrypsin over time	110

Figure 6.1	Comparison of: (a) absorption spectra of tryptophan and 7-azatryptophan, and (b) fluorescence spectra of tryptophan and 7-azatryptophan	117
Figure 6.2	Fluorescence decays of mixtures of 7-azatryptophan and <i>N</i> -acetyl-tryptophanamide: (a) at different collection wavelengths and (b) at different concentration ratios	121
Figure 7.1	Structures of tryptophan, 7-azatryptophan, 1-methyl-7-azatryptophan, and sequences of the peptides studied.	127
Figure 7.2	Emission spectra of the reduced and oxidized 7-azatryptophan peptides: (a) D-octapeptide and (b) L-octapeptide	137
Figure 7.3	Fluorescence lifetime decays of the reduced D-7-azatryptophan octapeptide at: (a) $\lambda_{em} = 375$ nm, and (b) $\lambda_{em} \geq 505$ nm	138
Figure 7.4	Fluorescence anisotropy decay of: (a) the D-7-azatryptophan tripeptide and (b) the reduced D-7-azatryptophan octapeptide	140
Figure 7.5	Plots of the rotational diffusion time against η/T for various 7-azatryptophan peptides	141
Figure 7.6	Stern-Volmer plots for the fluorescence quenching of 7-azaindole and indole with acrylamide	144
Figure 7.7	Stern-Volmer plots for the quenching of D-7-azatryptophan octapeptide under both reducing and oxidizing conditions: (a) with KI and (b) with acrylamide	148
Figure 7.8	Stern-Volmer plots for the quenching of the tryptophan octapeptide by KI: (a) for the shorter-lived component and (b) for the longer-lived component	150
Figure 7.9	Stern-Volmer plots for the quenching of the tryptophan octapeptide by acrylamide under both reducing and oxidizing conditions: (a) for the shorter-lived component and (b) for the longer-lived component	151
Figure 7.10	^{13}C spectrum of the 7-azatryptophan tripeptide indicating <i>cis</i> and <i>trans</i> proline conformations	152
Figure 9.1	(a) Fluorescence spectra of avidin, biotinylated 7-azatryptophan and the complex between avidin and biotinylated 7-azatryptophan and	167

(b) excitation spectra of biotinylated 7-azatryptophan and the complex between avidin and biotinylated 7-azatryptophan

Figure 9.2	Fluorescence spectra of the complex of avidin and biotinylated 7-azatryptophan as a function of wavelength	172
Figure 9.3	Fluorescence anisotropy decay of biotinylated 7-azatryptophan	173
Figure 9.4	Fluorescence anisotropy decay of avidin	174
Figure 9.5	Fluorescence anisotropy decay of the complex between avidin and biotinylated 7-azatryptophan	178
Figure 9.6	Percentage of emission observed as a function of time under various experimental conditions for: (a) 7-azatryptophan/4 tryptophans, and (b) 1-methyl-7-azaindole/4 tryptophans	181
Figure 9.7	Relative quantum yields as a function of wavelength for : (a) indole; (b) 5-methoxyindole; (c) 7-azatryptophan; (d) rhodamine B; (e) complex of biotinylated 7-azatryptophan and avidin	181
Figure 9.8	Fluorescence decay of biotinylated 7-azatryptophan bound to avidin at emission wavelengths of 330 ± 8 and ≥ 505 nm	183
Figure 10.1	Structures of: (a) 7-azatryptophan;(b) tryptophan; (c) pyridoxal 5'-phosphate; and (d) 5'-phosphopyridoxal-D,L-7-azatryptophan	191
Figure 10.2	Absorption and emission spectra of pyridoxal 5'-phosphate	196
Figure 10.3	Absorption spectra of: (a) 5'-phosphopyridoxal-L-tryptophan and (b) 5'-phosphopyridoxal-D,L-7-azatryptophan	197
Figure 10.4	Emission spectra of: (a) 5'-phosphopyridoxal-L-tryptophan and (b) 5'-phosphopyridoxal-D,L-7-azatryptophan	198

ABSTRACT

A major use of photophysical apparatus is the study of biological systems, for example, peptides, proteins, and DNA, that contain one or more chromophores. In recent years the incorporation of nonnatural fluorescent compounds into these systems has gained great popularity. A number of optical "tags" have been suggested as detection tools of structure and function; we propose the use of the tryptophan derivative, 7-azatryptophan, as an intrinsic probe in photophysical analyses of proteins. Not only is this chromophore spectroscopically distinct from tryptophan and all other natural amino acids, but we have demonstrated the successful incorporation of 7-azatryptophan into peptide sequences, biological cofactors, and bacterial proteins.

We have performed exhaustive steady-state and time-resolved studies of the chromophoric moiety of 7-azatryptophan, 7-azaindole. Such work is necessary to interpret fully data obtained in different locales within a biological system since the photophysical characteristics of this nonnatural amino acid are unusually sensitive to its surrounding environment. We also have analyzed tri- and octapeptides that mimic substrate active-site sequences. These peptides contain 7-azatryptophan or N₁-methyl-7-azatryptophan at a variety of sites. We have performed binding studies and photophysical analyses of these peptides alone and bound to α -chymotrypsin or H-2K^b (a class I MHC molecule). In addition, we have tagged enzymatic cofactors with 7-azatryptophan or N₁-methyl-7-azatryptophan and studied the behavior of these probes in a protein environment. Lastly, we have begun direct incorporation of this nonnatural amino acid into a variety of bacterial proteins, substituting a tryptophan residue with 7-azatryptophan.

In short, we are currently developing new probes and techniques for the photophysical study of proteins and other biological systems, primarily by direct incorporation of nonnatural amino acids such as 7-azatryptophan and its analogs.

GENERAL INTRODUCTION

Statement of Purpose and Overview of the Research Project

This research entails the study of protein structure and dynamics using time-resolved and steady-state spectroscopic techniques. For such analyses, a chromophore is required; the most commonly employed is the naturally-occurring amino acid, tryptophan. There are a number of disadvantages in the use of tryptophan as an optical probe of biological systems. Two of the most glaring problems are the intrinsically nonexponential fluorescence decay of tryptophan in water, which complicates the interpretation of the data obtained from even a single chromophore, and the occurrence of multiple tryptophan residues in a protein, making the collection of acquired data a compilation of contributions from numerous, heterogeneous sites within the protein.

Alternatives to tryptophan as spectroscopic tools in the study of biological systems are being developed. A variety of fluorescent compounds have gained popularity as intrinsic or extrinsic optical probes of biological systems. Examples of extrinsic probes include dansyl chloride and various fluorescein derivatives; intrinsic probes are often amino acid or nucleic acid derivatives, particularly tryptophan derivatives. Both extrinsic and intrinsic tags have advantages: extrinsic probes do not disrupt the native peptidyl or nucleic acid sequence, but any signal obtained from the chromophore is only an indirect measurement of local motion or structure (it may be argued that, at best, only probe motion is observed); intrinsic probes, on the other hand, may be placed *in situ*, allowing for direct examination of the importance and influence of a particular residue. This technique, however, requires consideration of the possibly deleterious effects caused by such a substitution. Derivatives of tryptophan such as 7-aza, 5-fluoro, 5-methyl-, 5-hydroxy, and 5-methoxytryptophan are currently being used as intrinsic probes in spectroscopic studies of proteins.

Particular characteristics of 7-azatryptophan suggest that this nonnatural amino acid is particularly suited for substitution of tryptophan in a biological system. Although the fluorescence quantum yield of 7-azatryptophan in water is low (0.03), its absorption and emission spectra are dramatically red-shifted from those of tryptophan, 10 and 40 nm, respectively; thereby permitting selective excitation and collection of emission from 7-azatryptophan while ignoring any emission from the tryptophan(s). This is not necessarily true of the other tryptophan derivatives currently being studied: these compounds show

significant spectral (absorption and emission) overlap with tryptophan. In addition, the fluorescence lifetime of 7-azatryptophan in water, when measured over the whole band, is single-exponential (780 ps) and therefore easy to interpret, and its fluorescence spectrum is sensitive to the environment polarity. 7-Azatryptophan can be incorporated into peptides and proteins. By replacing a single tryptophyl residue, we can ensure that all emission collected will be from a specific site.

To use 7-azatryptophan as an alternative to tryptophan, we must first fully characterize the photophysics of this optical probe. The aromatic side chain of 7-azatryptophan, 7-azaindole, determines the photophysics of 7-azatryptophan, so it is necessary to understand the photophysical behavior of 7-azaindole. Tryptophan fluorescence decay is affected by many factors, the most important being charge transfer to the side chain. Such charge transfer does not occur in 7-azatryptophan since the excited state of 7-azaindole is significantly lower in energy than that of tryptophan. Our studies of 7-azaindole include synthesis of 1- and 7-methyl analogs that mimic normal 7-azaindole and its tautomeric species and the subsequent steady-state and time-resolved spectroscopic measurements of these chromophores.

We have begun synthesis and photophysical analysis of 7-azatryptophan analogs that demonstrate even greater viability as optical probes in biological systems. For example, a new amino acid derivative synthesized in our laboratory, N₁-methyl-7-azatryptophan, has a number of distinct advantages. In particular, the fluorescence quantum yield of this derivative in water at room temperature is 0.53, it has a long, single-exponential lifetime (~22 ns), and the optical spectra of this analog are significantly red-shifted from those of tryptophan. These characteristics allow for selective detection of this compound in the presence of ≥ 75 tryptophans and short data collection times. We are currently performing steady-state and time-resolved experiments with N₁-methyl-7-azatryptophan: study of the chromophore's photophysical behavior, incorporation into peptides and cofactors and subsequent protein-binding capabilities, and analysis of these species in a tryptophan-containing protein environment. Other alkylated derivatives currently being synthesized as part of this research project aid in explaining the chromophoric photophysics and some may also be viable as tryptophan substitutes in biological systems.

Incorporation of these compounds into peptides and proteins is of great interest. We have spent much time performing spectroscopic studies of peptides and protein cofactors that contain 7-azatryptophan or N₁-methyl-7-azatryptophan and have begun incorporation of 7-azatryptophan into proteins. It is vital to note, however, that peptides containing 7-

azatryptophan or N₁-methyl-7-azatryptophan must remain functional for these chromophores to be useful probes in the studies of biological systems. We have demonstrated that functionality is retained in our peptide and cofactor studies. Peptides containing 7-azatryptophan inhibit α -chymotrypsin and peptides containing N₁-methyl-7-azatryptophan bind tightly to H-2K^b, a human class I major histocompatibility complex molecule. In addition, the novel avidin cofactor, biotinylated 7-azatryptophan, retains a high binding constant with respect to avidin. We have not performed binding studies of the pyridoxal 5'-phosphate derivative, 5'-phosphopyridoxal-D,L-7-azatryptophan, but previous work with derivatives that incorporate tryptophan show significant binding to tryptophanase. We expect similar results for the 7-azatryptophan derivative.

Tethering 7-azatryptophan or an analog to a coenzyme that binds in the active site ensures that spectrophotometric examinations of the protein would indeed be of the active site; therefore, investigation of these small, tagged molecules in complex with a target protein provides a unique opportunity to study biological systems using a nonnatural probe while disturbing the coenzyme/protein complex insignificantly. Incorporation of 7-azatryptophan or one of its analogs directly into a protein is our ultimate goal. Several mutant proteins have been generously provided to our laboratory that contain only one tryptophan. These are: tryptophanase, luciferase, dihydrofolate reductase, and LDH. It is our hope that by growing auxotrophic bacterial cells that are capable of overexpressing these proteins in 7-azatryptophan-containing media we may isolate proteins containing 7-azatryptophan instead of the natural tryptophan residue. We may then pursue spectroscopic analyses of this nonnatural amino acid within the protein environment.

Dissertation Organization

This dissertation is organized as follows. Four major sections discuss analyses of the nonnatural amino acid, 7-azatryptophan, in different environments: Part I covers our research of the amino acid, its chromophore, and analogs alone in aqueous solution; Part II covers our research of the peptides that contain 7-azatryptophan or N₁-methyl-7-azatryptophan; Part III covers our research of the biological cofactors that contain 7-azatryptophan; and Part IV describes techniques to incorporate 7-azatryptophan into bacterial proteins. The General Summary is an overview of our various projects that implement nonnatural amino acids as intrinsic biological probes. Appendices include ideas concerning future projects, preliminary

results for various experiments, notes on instrumentation in our laboratory, and some miscellaneous calculations required in my research.

In Part I, Chapters 1 and 2 were published in *J. Phys. Chem.* and discuss photophysical characteristics of 7-azatryptophan, while Chapters 3 and 4 outline our syntheses and analyses of new, methylated or otherwise alkylated, 7-azatryptophan derivatives. Chapter 4 has been submitted to *J. Am. Chem. Soc.* for publication.

In Part II, Chapter 5 is a detailed outline of the procedures I used to measure enzyme kinetics. Chapter 6 was published in *Photochem. Photobiol.* and details our initial studies of peptide interactions with α -chymotrypsin; Chapter 7 is a continuation of our peptide/ α -chymotrypsin studies and is undergoing revision before submittal to *J. Phys. Chem.*. Work on the peptide/MHC system discussed in Chapter 8 is currently underway.

In Part III, Chapter 9 was published in *J. Am. Chem. Soc.* and Chapter 10 was published in *Biochem. Biophys. Res. Comm.*. These chapters discuss our work concerning biotinylated 7-azatryptophan and 5'-phosphopyridoxal-D,L-7-azatryptophan, respectively.

In Part IV, Chapter 11 outlines the procedures and techniques I have used in the incorporation of 7-azatryptophan into tryptophanase and isolation of this bacterial protein. This chapter also includes other pertinent information relating to our protein work.

PART I. ANALYSIS OF AMINO ACID RESIDUES

CHAPTER 1. THE FLUORESCENT SPECIES OF 7-AZAINDOLE AND 7-AZATRYPTOPHAN IN WATER

A paper published in the *Journal of Physical Chemistry*¹

Y. Chen², R. L. Rich², F. Gai², and J. W. Petrich^{2,3}

Abstract

A study of the fluorescence lifetimes and quantum yields of 7-azaindole and its methylated derivatives N₁-methyl-7-azaindole (1M7AI) and 7-methyl-7H-pyrrolo[2,3-b]pyridine (7M7AI) in water is performed in order to explain the observation that the fluorescence spectrum of 7-azaindole apparently consists of one band ($\lambda_{\text{max}} = 386$ nm) whereas in alcohols the spectrum is bimodal (e.g., for methanol, $\lambda_{\text{max}} = 374, 505$ nm). Careful measurements of the fluorescence decay as a function of emission wavelength indicate a small amplitude of an ~ 70 -ps decaying component at the bluer wavelengths and a rising component of the same duration at the redder wavelengths. The small amplitude component, which comprises no more than 20% of the fluorescence decay, is attributed to excited-state tautomerization that is mediated by the solvent. Particular attention is paid to the pH dependence of the fluorescence lifetimes and yields. We propose that upon tautomerization the basic 1-nitrogen (N₁) of 7-azaindole is rapidly protonated, giving rise to a species whose emission maximum is at ~ 440 nm. The fluorescence emission maximum and lifetime of 7-azaindole is dominated by the 80% of the solute molecules that are blocked by unfavorable solvation from executing excited-state tautomerization. It is proposed that $> \sim 10$ ns is required for the surrounding water molecules to attain a configuration about 7-azaindole that is propitious for tautomerization.

¹ Reprinted with permission from *Journal of Physical Chemistry* **1993**, *97*, 1770. Copyright © 1993 American Chemical Society.

² Graduate students and Associate Professor, Department of Chemistry, Iowa State University. Syntheses and steady-state measurements performed by R. L. Rich.

³ To whom correspondence should be addressed.

Introduction

7-Azaindole (Figure 1.1) is the chromophoric moiety of the nonnatural amino acid, 7-azatryptophan. Recently, we have proposed 7-azatryptophan as an alternative to tryptophan as an optical probe of protein structure and dynamics [1-4]. 7-Azatryptophan can be incorporated into synthetic peptides and bacterial protein [1]. Its steady-state absorption and fluorescence spectra are sufficiently different from those of tryptophan that selective excitation and detection may be effected. The absorption maximum of 7-azatryptophan is red-shifted by 10 nm with respect to that of tryptophan. There is also a significant red shift of about 50 nm of the fluorescence maximum of 7-azatryptophan with respect to that of tryptophan (Figure 1.2). Most important for its use as an optical probe, however, is that the fluorescence decay for 7-azatryptophan over most of the pH range, when emission is collected over the entire band, is single exponential. For tryptophan, on the other hand, a nonexponential fluorescence decay is observed [5]. The potential utility of 7-azatryptophan as an optical probe suggests a thorough investigation of the photophysics of its chromophore, 7-azaindole, in order to characterize its fluorescence properties and to elucidate its pathways of nonradiative decay.

The photophysics of 7-azaindole were originally studied by Kasha and coworkers [6] in nonpolar hydrocarbon solvents where it was suggested to dimerize by forming two $N_1H \cdots N_7$ hydrogen bonds [6-9]. The major nonradiative decay pathway of these dimers was shown to be a very rapid excited-state tautomerization producing two $N_1 \cdots HN_7$ hydrogen bonds. Recently Hochstrasser and coworkers have shown that in nonpolar solvents at room temperature this tautomerization occurs in 1.4 ps [10].

There is now general agreement that in the linear alcohols an excited-state tautomerization can also occur, which is mediated by an idealized planar cyclic intermediate formed between the 7-azaindole and the -OH of the alcohol. This intermediate is believed to involve two hydrogen bonds: $N_1H \cdots OR$ and $N_7 \cdots HOR$. Once this cyclic intermediate is formed in the excited state, rapid tautomerization (~ 1 ps [2,11-14], as in the dimer case) can occur, producing different hydrogen bonds: $N_1 \cdots HOR$ and $N_7H \cdots OR$. The rate-limiting step for this tautomerization is the formation of the cyclic intermediate.

In alcohols, the fluorescence emission of 7-azaindole is characterized by two bands with distinct and widely separated maxima as well as different fluorescence lifetimes [2,11-14]. The redder of the two bands observed in alcohols is attributed to an excited-state

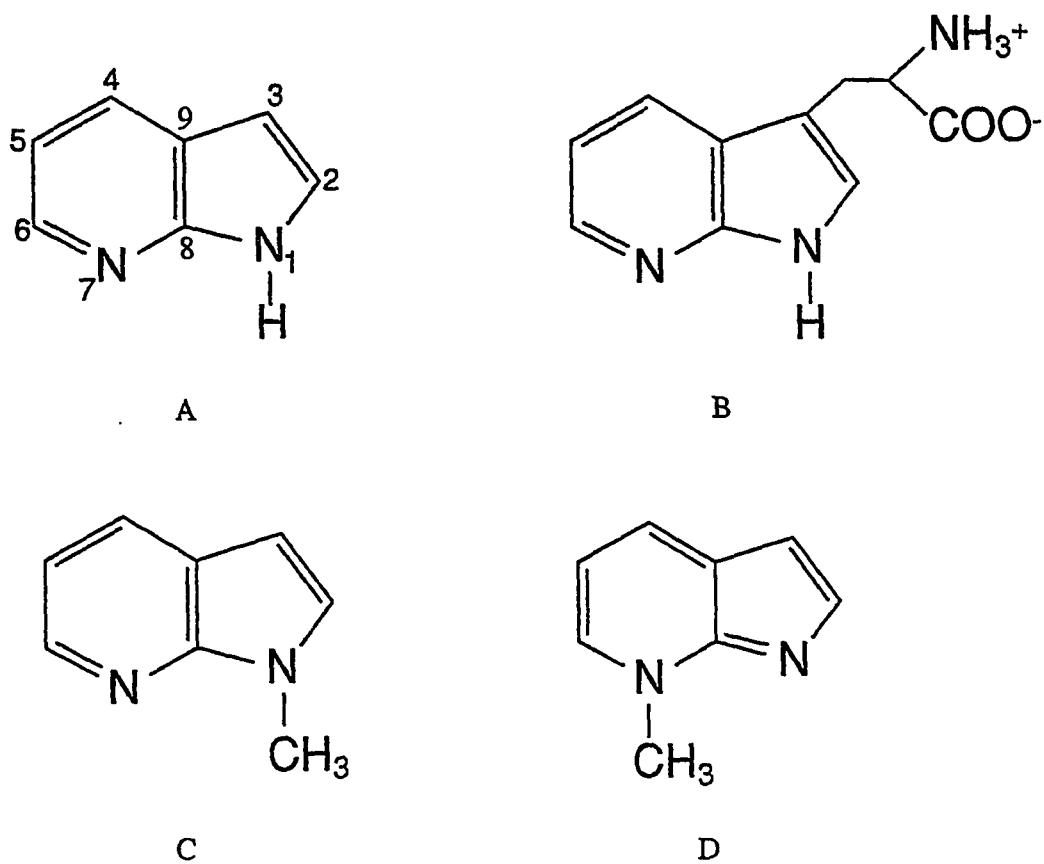


Figure 1.1. Structures of (a) 7-azaindole, (b) zwitterionic 7-azatryptophan, (c) N₁-methyl-7-azaindole (1M7AI), and (d) 7-methyl-7H-pyrrole [2,3-b]pyridine (7M7AI).

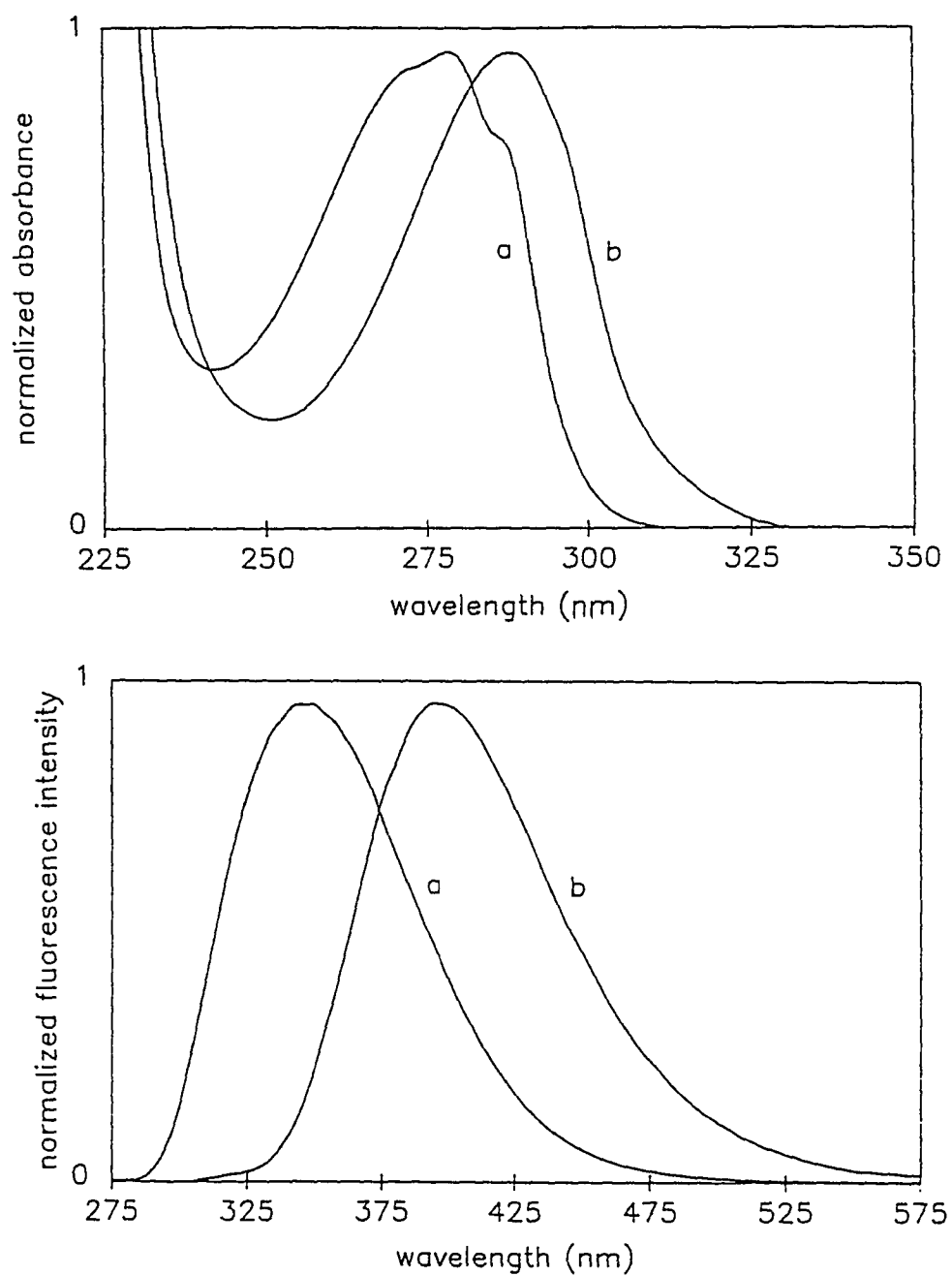


Figure 1.2. Comparison of the absorption and fluorescence spectra of (a) tryptophan and (b) 7-azatryptophan. For tryptophan, $\epsilon_{280 \text{ nm}} \approx 5400 \text{ M}^{-1} \text{ cm}^{-1}$ [45], for 7-azatryptophan, $\epsilon_{288 \text{ nm}} \approx 6200 \text{ M}^{-1} \text{ cm}^{-1}$. Absorbance and fluorescence spectra are normalized to the same peak intensity.

tautomer. Consequently, the bluer of the two bands is attributed to a "normal" species. Because of the interest in using 7-azaindole as a probe of protein structure and dynamics, we began time-resolved studies of 7-azaindole in water [2] to complement the existing steady-state work, carried out predominately in mixed water/alcohol solvents [11,15]. An intriguing characteristic of the emission of 7-azaindole in water is that *only* a smooth band is detected and the fluorescence lifetime is *single exponential* when emission is collected over the entire band over most of the pH range. Previously we suggested that the fluorescent species in water was predominantly "tautomer-like" because the fluorescence quantum yield of this species is similar to that of the tautomer and the deuterium isotope effect of its fluorescence lifetime resembles that of the tautomer in alcohols [2].

Recently we have presented data [3,4] that clarify the nature of the fluorescent state of 7-azaindole in water and broadens the understanding of this chromophore in general. By means of fluorescence-excitation anisotropy measurements [4,16] we have clearly resolved closely-lying excited states (1L_b and 1L_a) in 7-azaindole, just as have been observed in indole [17]. The presence of these states had been suggested by Bulska *et al.* [18]. We observed, at room temperature, photoionization whose origin we attribute to the upper of these two states as well as what we suggest is intersystem crossing. In addition, careful measurements of 7-azaindole fluorescence performed with ~ 16 nm spectral resolution and ~ 100 ps temporal resolution and over many hours to ensure adequate data accumulation unveiled a small amount of excited-state tautomerization.

Here we discuss further experiments to clarify the nature of the fluorescent species in water. Three types of experiments are considered. The fluorescence decay of 7-azaindole is measured as a function of emission wavelength with adequate time resolution to resolve various excited-states. The temperature dependence of the duration of the lifetimes of these excited states and the deuterium isotope effect of these lifetimes are investigated. And a detailed study is made of the protonated and unprotonated forms of 7-azaindole as well as of its methylated derivatives that mimic untautomerized and tautomerized 7-azaindole (Figure 1.1): N₁-methyl-7-azaindole (1M7AI), and 7-methyl-7H-pyrrolo[2,3-b]pyridine (7M7AI).

We propose here that the observations of a smooth emission band of 7-azaindole in water and its corresponding single-exponential fluorescence decay are consequences of the spectral and temporal coarseness with which the measurements are typically made. We conclude that the percentage of 7-azaindole molecules capable of undergoing this reaction is small ($\sim 20\%$) and that the fluorescence lifetime and spectrum is hence dominated by solute molecules that are inappropriately solvated. These molecules are hence "blocked" from

executing an excited-state tautomerization. The coexistence of these two types of solute molecules suggests a time scale for their interconversion. It is argued that $> \sim 10$ ns are required for solvent to rearrange about the "blocked" species, converting it to a form that can undergo tautomerization during the excited-state lifetime.

Materials and Methods

Spectroscopic Measurements

Time-correlated single-photon counting measurements were performed to determine fluorescence lifetimes. A Coherent 701 rhodamine 6G dye laser is pumped with about 1W of 532 nm radiation from an Antares 76-s CW mode-locked Nd:YAG laser. (The remaining 1W of second harmonic pumps a dye laser whose pulses are amplified to 1-2 mJ at 30 Hz by a regenerative amplifier. This branch of the experiment is used to perform pump-probe transient absorption spectroscopy and will be described in detail elsewhere.) The 701 dye laser is cavity-dumped at 3.8 MHz. The pulses have an autocorrelation of about 7 ps full width at half-maximum (fwhm). Excitation of 7-azaindole from 282 to 305 nm is effected by focusing the dye laser pulses with a 5 cm lens into a crystal of LiIO₃ or KDP. Fluorescence is collected at right angles through a polarizer mounted at 54.7° to the excitation polarization and then passed through an ISA H-10 monochromator with a 16 nm band-pass or through cutoff filters. A Hamamatsu 2809u microchannel plate, amplified by a Minicircuits ZHL-1042J, and an FFD 100 EG&G photodiode provide the start and stop signals, respectively. Constant-fraction discrimination of these signals is performed by a Tennelec TC 455, and time-to-amplitude conversion, by an ORTEC 457. Data are stored in a Norland 5500 multichannel analyzer before transfer to and analysis with a personal computer. The instrument function of this system has a fwhm of 50-65 ps and a full width at tenth maximum of 160-170 ps.

Time-resolved fluorescence data were fit to a single exponential or to a sum of exponentials by iteratively convoluting trial decay curves with the instrument response function and employing a least-squares fitting procedure. A good fit was determined largely by the χ^2 criterion [19]: $0.8 \leq \chi^2 \leq 1.2$.

Sample temperature was controlled with a M9000 Fisher refrigerated circulator connected to a brass cell holder and monitored directly at the sample by an HH-99A-T2

Omega thermocouple. Steady-state, corrected fluorescence emission and excitation spectra were obtained with a Spex Fluoromax with emission and excitation bandpasses of 4 nm.

Purification of 7-Azaindole

Commercial preparations of 7-azaindole contain < 1% impurity (Sigma, personal communication). Thin-layer chromatography (TLC) on silica gel plates and ethyl acetate as eluent indicates that commercial 7-azaindole has an $R_f \sim 0.60$ and resolves two fluorescent contaminants having $R_f \sim 0.15$ (impurity 1) and 0.00 (impurity 2). To remove the impurities, flash chromatography [20] was performed using ethyl acetate. Fractions containing 7-azaindole were concentrated and run through the flash column four times to ensure isolation. The 7-azaindole crystals were uniformly white and appeared as a single spot on TLC plates. The two impurities have nonexponential fluorescence lifetimes in water at neutral pH: impurity 1, $F(t) = 0.38 \exp(-t/607 \text{ ps}) + 0.25 \exp(-t/2035 \text{ ps}) + 0.37 \exp(-t/8895 \text{ ps})$; and impurity 2, $F(t) = 0.18 \exp(-t/383 \text{ ps}) + 0.37 \exp(-t/1087 \text{ ps}) + 0.45 \exp(-t/7414 \text{ ps})$. Samples were changed regularly. Subsequent to light exposure they were analyzed by TLC to monitor their integrity.

Several groups have recently commented on the difficulty of obtaining pure 7-azaindole and the problems that impurities may present in the interpretation of high resolution spectra [21], dynamic solvation [14], and the assignment of spectral features in the condensed phase [2]. It is thus important to characterize the spectral characteristics of purified 7-azaindole and of the other products that are contained in commercial 7-azaindole. Figure 1.3 presents the fluorescence emission spectra of purified 7-azaindole and the two isolated impurities in water. The significantly increased purity of our 7-azaindole preparation is supported by the superimposability of the excitation spectra obtained at three different wavelengths (Figure 1.4). These data are to be contrasted with the excitation spectra of the two impurities (Figure 1.5).

At low pH (i.e., < 4), where the fluorescence intensity of 7-azaindole is diminished, a shoulder appears on the blue edge of the spectrum of commercial 7-azaindole [2]. This shoulder is not present in purified preparations of 7-azaindole. We further verified this observation by measuring the sensitivity of the emission spectrum of a mixture of impurities 1 and 2 to pH and buffer. The position of the emission maximum ($\approx 375 \text{ nm}$ at pH 1, unbuffered) corresponds to the blue shoulder observed in commercial 7-azaindole samples. We observe that this impurity emission shifts to the red when sodium acetate/acetic acid buffers are employed. In the presence of this buffer system and at pH $> \sim 3$, the 7-azaindole

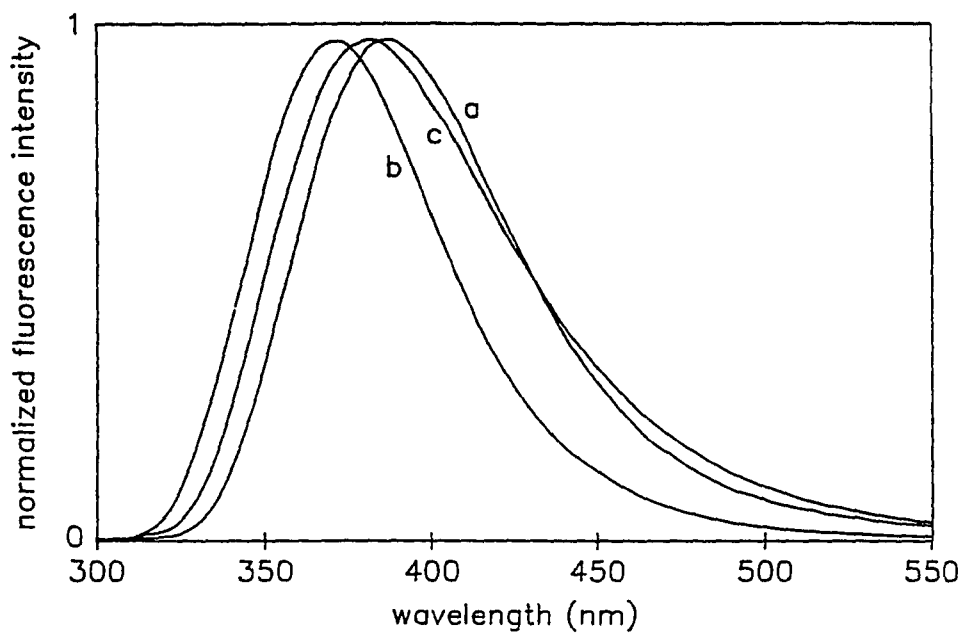


Figure 1.3. Normalized fluorescence spectra in water at 20°C of (A) purified 7-azaindole, (B) isolated impurity 1, and (C) isolated impurity 2.

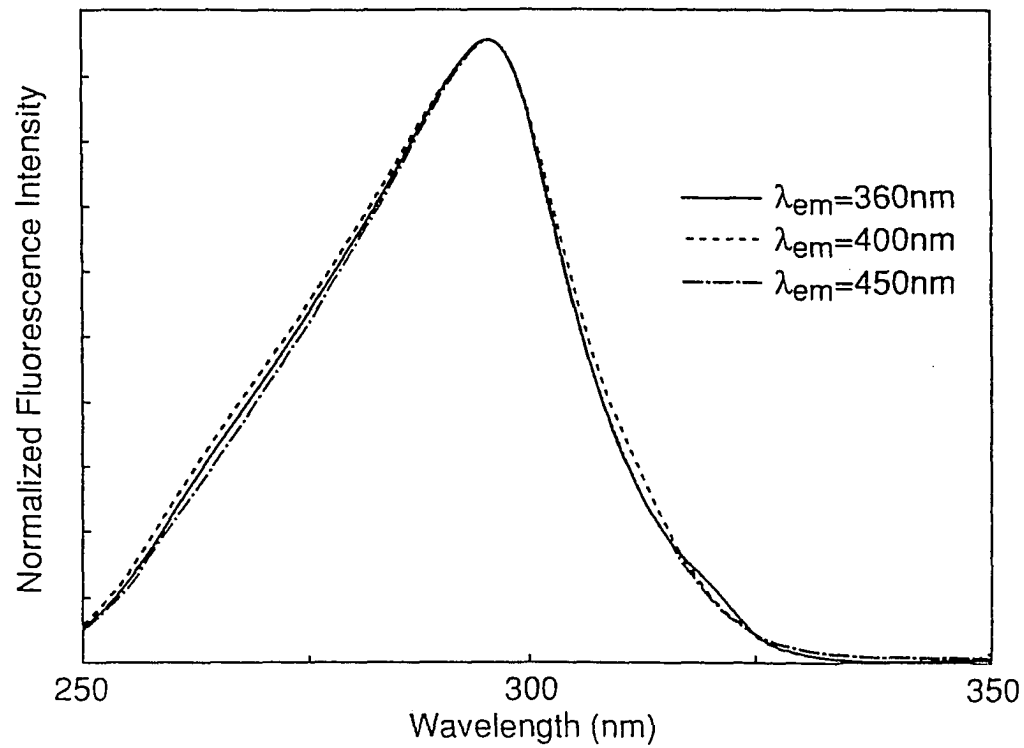


Figure 1.4. Normalized fluorescence excitation spectra in water at 20°C of 7-azaindole. The detection wavelengths are indicated in the Figure.

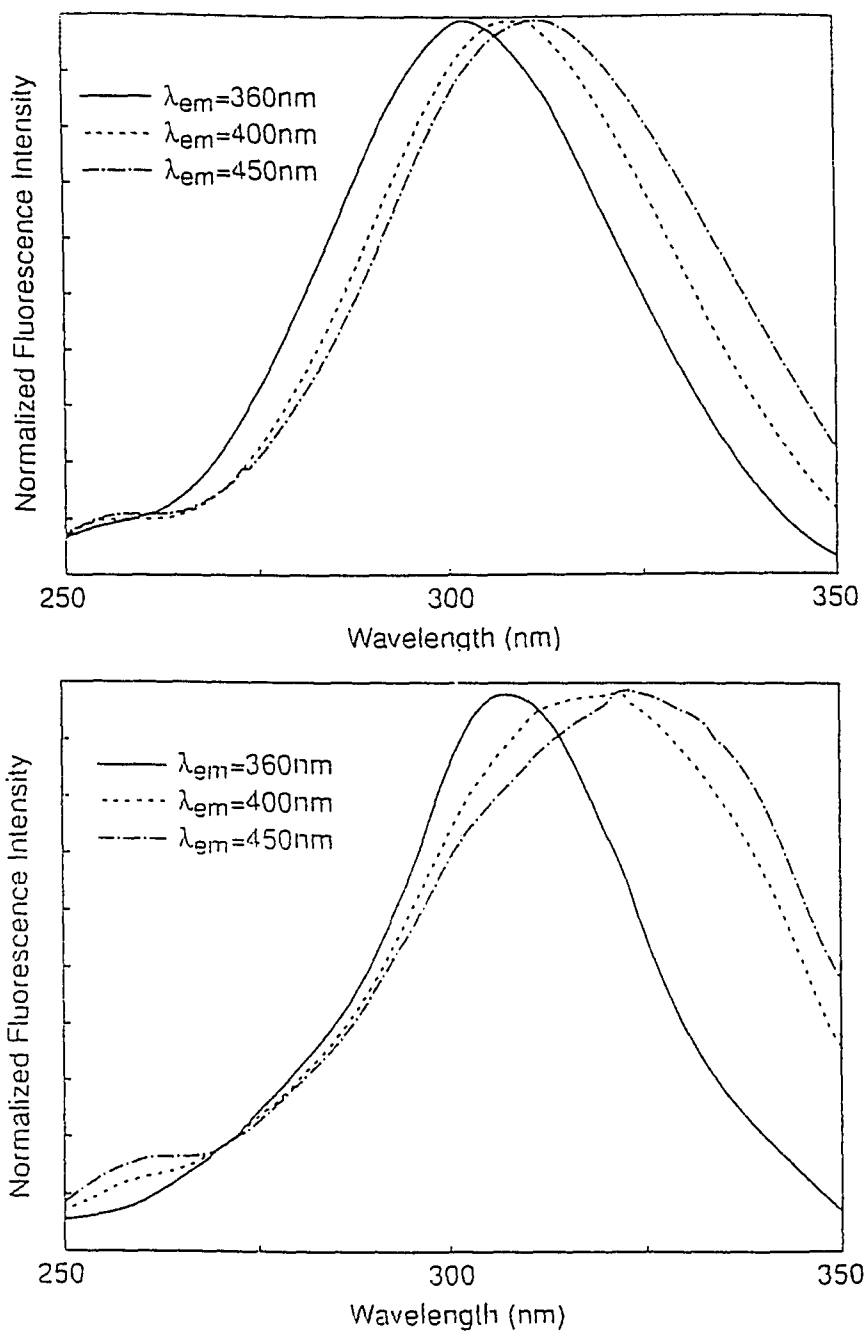


Figure 1.5. Normalized fluorescence excitation spectra in water at 20°C of the two impurities isolated from commercial preparations of 7-azaindole: (a) impurity 1; (b) impurity 2. The detection wavelengths are indicated in the Figure.

emission obscures the impurity emission. The role of the buffer is probably to change the rate at which the acid-base equilibrium of 7-azaindole is attained in the excited state [35]. Purified 7-azaindole preparations, buffered and unbuffered, lack the aforementioned blue shoulder over the entire pH range. We have noted, however, that the fluorescence quantum yield of purified 7-azaindole increases in the presence of 0.01 M acetate: for example, at pH 7 and 4.5 it is greater by a factor of ~ 2.5 . Thus, for measurements discussed here, pH is adjusted only by the addition of HCl or NaOH (or by DCl or NaOD).

Synthesis of N₁-methyl-7-azaindole (1M7AI)

n-Butyl lithium and methyl-*p*-toluenesulfonate were purchased from Aldrich Chemical Co. All other reagents used in the syntheses and purifications were purchased from Sigma Chemical Co. All solvents (Fisher) were reagent grade or higher. Identities of the methylated derivatives and purity of all compounds were determined using NMR, elemental analyses (Oneida Research Services), GC/MS, and TLC.

An alternative to the method of Robison and Robison [22] for the preparation of 1M7AI was employed. 7-Azaindole (5.95 g) was dissolved by stirring in 100 mL dry tetrahydrofuran chilled in ethanol/dry ice bath. Approximately 10 mg *o*-phenanthroline was added as an indicator. *n*-Butyl lithium (approximately 25 mL, 2 M in *n*-hexane) was added until the solution became colored. The mixture was stirred for ten minutes, then methyl iodide (7.20 g) in 50 mL dry tetrahydrofuran was added dropwise to the 7-azaindole/*n*-butyl lithium solution. Upon addition of methyl iodide, the reaction mixture became bright yellow. The mixture was allowed to warm up to room temperature with continued stirring. After twelve hours, the solution was orange and a white crystalline precipitate had formed. The reaction was followed by TLC.

The solution was filtered to remove the precipitate. TLC showed the solution contained 1M7AI, unreacted starting materials, and side products. To isolate 1M7AI, flash chromatography was performed using four successive solvent systems: hexanes, ethyl acetate/hexanes (1:1), ethyl acetate, and methanol. The column set-up, running conditions and fraction collection were as described by Still *et al.* [20]. Fractions containing only 1M7AI were combined and the solvent evaporated. The residue was a colorless oil.

The NMR spectra obtained of our compound agree with those of Cox and Sankar [23] within ± 0.15 ppm and had similar coupling constants. The absorption maximum is 287 nm in water (pH 7) and in methanol. The fluorescence maxima are 395 nm in water (pH 7) and

376 nm in methanol ($\lambda_{\text{ex}} = 285$ nm). Anal. Calcd for $\text{C}_8\text{H}_8\text{N}_2$: C, 72.69; H, 6.11; N, 21.20. Found: C, 71.05; H, 6.34; N, 20.90.

Synthesis of 7-methyl-7H-pyrrolo[2,3-b]pyridine (7M7AI)

7M7AI was prepared as outlined by Robison and Robison [22] using a *p*-toluenesulfonate intermediate. The reaction was followed by TLC and showed that the resulting brownish-yellow oil contained 7M7AI, unreacted starting materials, and side products. 7M7AI was purified using flash chromatography [20]. Initially, ethyl acetate was run through the column to remove the side products and starting materials, then methanol was flushed through the column to collect 7M7AI. Fractions containing only 7M7AI were combined and the solvent evaporated. The residue was a yellow oil.

The NMR spectra obtained for this compound agreed with those of Cox and Sankar [23] within ± 0.14 ppm and had similar coupling constants. The absorption maxima are 294 nm in water (pH 7) and 306 nm in methanol. The fluorescence maxima are 442 nm in water (pH 7) and 509 nm in methanol ($\lambda_{\text{ex}} = 285$ nm). Anal. Calcd for $\text{C}_8\text{H}_8\text{N}_2$: C, 72.69; H, 6.11; N, 21.20. Found: C, 68.40; H, 6.66; N, 19.87.

The *p*-toluenesulfonate intermediate of 7M7AI, 7-methyl-7H-pyrrolo[2,3-b]pyridium *p*-toluenesulfonate, is particularly interesting. This is the penultimate product in the synthesis of 7M7AI. The tosylate group acts as a counterion of 7M7AI that is protonated at N_1 . This tosylate salt is easily synthesized and purified. We obtained white prismatic crystals (m.p. 134-135°C) and observed only one spot on TLC plates. The ground-state pK_a of this compound is 8.52 [24]. The lifetimes of this intermediate over the pH range are similar to those obtained for 7M7AI (Table 1.1): 800 ps for the protonated species; 480 ps for the unprotonated species. Pump-probe experiments using the tosylate intermediate are similar to those of 7M7AI [3]. In short, we propose that the intermediate salt formed in the 7M7AI synthesis may be used as an alternative to 7M7AI in photophysical experiments since it yields similar results and is easy to produce and purify.

Results

Dependence of the Fluorescence Lifetime on Emission Wavelength

7-Azaindole exhibits a single-exponential fluorescence decay of 910 ± 10 ps in water at neutral pH and 20°C if emission from the entire band ($\lambda_{\text{em}} \geq 320$ nm) is collected [2,3].

Table 1.1
Summary of Fluorescence Lifetimes and Quantum Yields of 7-Azaindole (7AI) and Its Derivatives^a

compound	pH	ϕ_F^b	τ_F	k_{rad}^c (10^7 s^{-1})	$\lambda_{\text{em}}^{\text{max}}$ (nm)	$\lambda_{\text{abs}}^{\text{max}}$ (nm)	ϵ^d ($\text{M}^{-1} \text{ cm}^{-1}$)
7AI	7	1.0	$910 \pm 10 \text{ ps}$		386	288	8100 [41]
7AI (N_1H^+) ^e	7		$\sim 1100 \text{ ps}^f$	~ 1.0	~ 440		
1M7AI	11	18.30	$21.0 \pm 0.5 \text{ ns}$	2.6	395	287	8300 ^g
7M7AI	13	0.02	$480 \pm 20 \text{ ps}$	0.14	510	303	8800 [22]
7AI (N_7H^+)	2	0.27	$1.10 \pm 0.03 \text{ ns}$	0.74	444	290	8700 [41]
1M7AI (N_7H^+)	1	0.10	$2.80 \pm 0.20 \text{ ns}$	0.11	456	291	8300 ^g
7M7AI (N_1H^+)	3	0.26	$780 \pm 10 \text{ ps}$	1.0	442	294	8500 [22]

^a Experiments are performed at 20°C.

^b All ϕ_F reported are relative to 7AI at pH 7 and 20°C.

^c Calculations of k_{rad} are based on a value of 0.03 for the quantum yield of 7AI at neutral pH and ambient temperature [11].

^d Decadic molar extinction coefficient at the reported maximum of the absorption band.

^e The protonated tautomer species of 7AI at neutral pH. It is proposed that about 20% of the solute population is converted to this species.

^f This lifetime is recovered from the 980 ps component that is observed when emission is collected at wavelengths longer than 505 nm. It represents a weighted average of the lifetime of the blocked solute (910 ps) and that of the protonated tautomer at *neutral* pH.

^g Estimated using the data of Robison and Robison for compounds dissolved in cyclohexane [22].

The fluorescence decay, however, deviates from single exponential if emission is collected with a limited bandpass. For $\lambda_{em} \leq 450$ nm, a single exponential does not provide a satisfactory fit (Figure 1.6). An acceptable fit is obtained using two exponentially decaying components and indicates that about 20% of the fluorescent emission decays with a time constant between 40 to 100 ps (depending on the full-scale time base chosen for the experiment). Shorter lifetimes are obtained with a full-scale time base of 1.5 ns; longer lifetimes, with a full scale time base of 3.0 ns. The amplitude of this fast component did not depend on the time base chosen. A component with a 70-ps decay time is also detected in the transient absorbance of 7-azaindole in water [3]. There is no such rapid component in the fluorescence decay or the transient absorption of 7M7AI or 1M7AI. We have thus attributed this rapid component to a *small* population of 7-azaindole molecules that undergo excited-state tautomerization. For the duration of the discussion, we shall refer to this transient as the 70-ps component because it is more clearly resolved in the transient absorption measurements [3]. (A 40-100-ps decay is too long to be attributed to solvation dynamics in water, which occur on a time scale of ≤ 1 ps [25].)

The 910 ps component that is resolved for $\lambda_{em} \leq 450$ nm or when emission is collected over the entire band is attributed to the majority of the 7-azaindole molecules that are not capable of excited-state tautomerization. This assignment will be described in more detail below.

When $\lambda_{em} \geq 505$ nm, the fluorescence decay can be fit to the form $F(t) = -0.69 \exp(-t/70 \text{ ps}) + 1.69 \exp(-t/980 \text{ ps})$. The long-lived component is observed to lengthen from 910 to 980 ps. This lengthening of the lifetime at long emission wavelengths was reported earlier [2], but no significance was drawn to it. If the rise time of the fluorescence emission can be attributed to the appearance of tautomer, then for $\lambda_{em} \geq 505$ nm $|0.69/1.69| \sim 0.40$ is the fraction of tautomer present. The rest of the emission arises from 7-azaindole molecules incapable of tautomerization and characterized by a 910 ps lifetime. Thus, 980 ps represents the weighted average of 910 ps and a longer lifetime, namely ~ 1100 ps. This decay time is *identical* to that of protonated (pH < 3) 7 azaindole (Table 1.1).

It is possible to construct time-resolved emission spectra for these species. The fluorescence intensity at a given emission wavelength and time, $F(\lambda, t)$, is given by:

$$F(\lambda, t) = \frac{[A_1(\lambda)\exp(-t/\tau_1) + A_2(\lambda)\exp(-t/\tau_2)]}{A_1(\lambda)\tau_1 + A_2(\lambda)\tau_2} F_{ss}(\lambda) \quad (1)$$

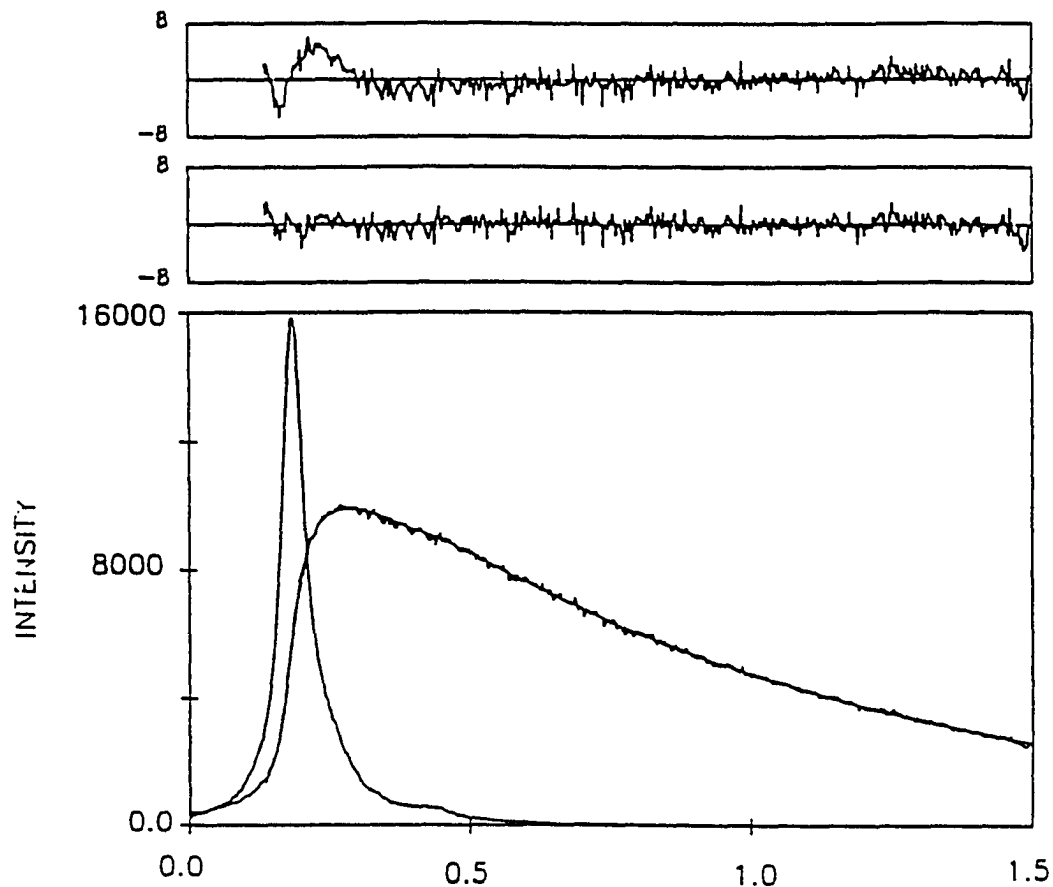


Figure 1.6. Fluorescence decay of 7AI in water, pH 6.1, 20°C, $\lambda_{\text{ex}} = 288 \text{ nm}$, $\lambda_{\text{em}} = 380 \text{ nm}$ (16-nm bandpass). The upper set of residuals corresponds to a single-exponential fit to the data, which yields a decay time of 816 ps with $\chi^2 = 2.6$. The lower set of residuals corresponds to a double-exponential fit yielding $F(t) = 0.20 \exp(-t/41 \text{ ps}) + 0.80 \exp(-t/835 \text{ ps})$, $\chi^2 = 1.2$. 835 ps is obtained for the long-lived component instead of 910 ps because the 1.5-ns time base is too fine to provide enough dynamic range to measure accurately an ~ 1 -ns decay. In preliminary work [2] we could not resolve the short component because experiments were performed on a 6-ns full-scale time base.

where $F_{ss}(\lambda)$ is the steady-state intensity of fluorescent emission. The quantity in square brackets is the fluorescence decay measured at a given emission wavelength. The denominator is the integrated emission at this wavelength. Because solvation in water is extremely rapid [25], this expression differs from those used to evaluate transient Stokes shifts [26] in that τ_1 and τ_2 do not change appreciably over the range of emission wavelengths. Here, τ_1 and τ_2 are considered to have distinct and clear physical meaning, although there are other instances where this may not be the case (see eqs 10 and 11). τ_1 is attributed to the decay of the normal species (or the rise of the tautomer). τ_2 is attributed to another species that does not undergo excited-state tautomerization on the time scale of the fluorescence lifetime. (Owing to the low fluorescence intensity at $\lambda_{em} \geq 505$ nm, not enough data could be collected to resolve the contribution of the ~ 1100 -ps component and hence to distinguish its spectrum from that of the 910-ps component. In the spectral decompositions discussed here, τ_2 refers to either the 910- or the ~ 1100 -ps component.)

Figure 1.7 presents spectra at $t = 0$ and $t = 1$ ns for 7-azaindole and 7-azatryptophan. For 7-azaindole, at 480 nm the $t = 0$ and $t = 1$ ns spectra are scaled to have the same intensity because no short-lived component is resolved at this wavelength. In order to facilitate observation of the spectral evolution between $t = 0$ and $t = 1$ ns, the spectra are subsequently normalized to the same intensity at 380 nm. At 1 ns, the spectra are not as broad because there is no contribution from the short-lived component.

The relative contributions of the short- and long-lived components to the *steady-state* fluorescence spectrum can be estimated as follows. For the short-lived component,

$$F_S(\lambda) = \frac{A_1(\lambda)\tau_1}{A_1(\lambda)\tau_1 + A_2(\lambda)\tau_2} F_{ss}(\lambda) \quad (2)$$

and for the long-lived component,

$$F_L(\lambda) = \frac{A_2(\lambda)\tau_2}{A_1(\lambda)\tau_1 + A_2(\lambda)\tau_2} F_{ss}(\lambda) \quad (3)$$

The decompositions of the steady-state spectra for 7-azaindole and 7-azatryptophan using these relations are depicted in Figure 1.8. The contribution from the short-lived component is multiplied by a factor of 10 in order to facilitate viewing. It is evident that the short-lived

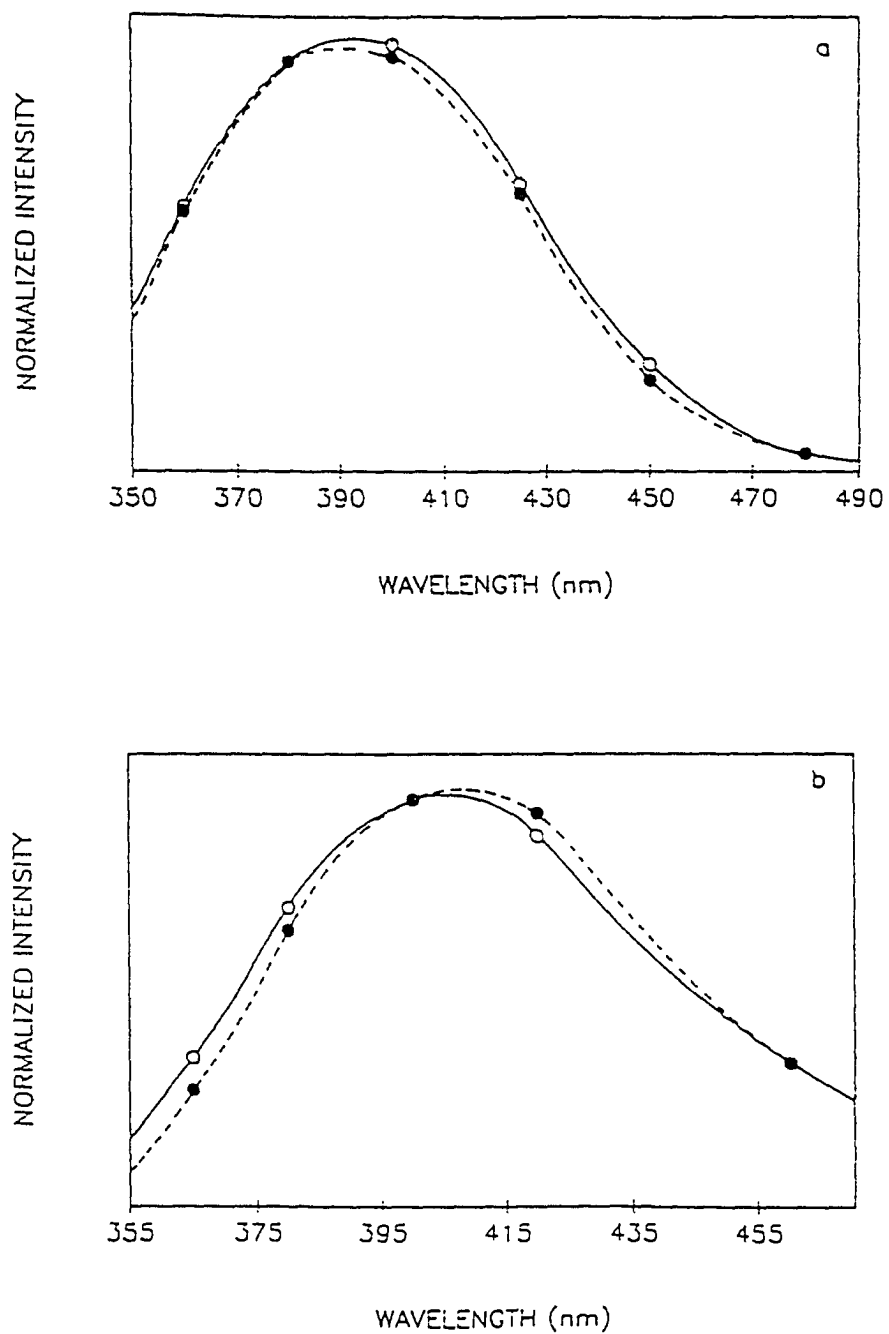


Figure 1.7. Time-resolved fluorescence spectra of (a) 7-azaindole and (b) 7-azatryptophan at pH 6.8 and 20°C. The empty circles represent the spectrum at $t=0$; the solid circles, at $t=1$ ns. The spectra are normalized to have the same intensity at 380 nm.

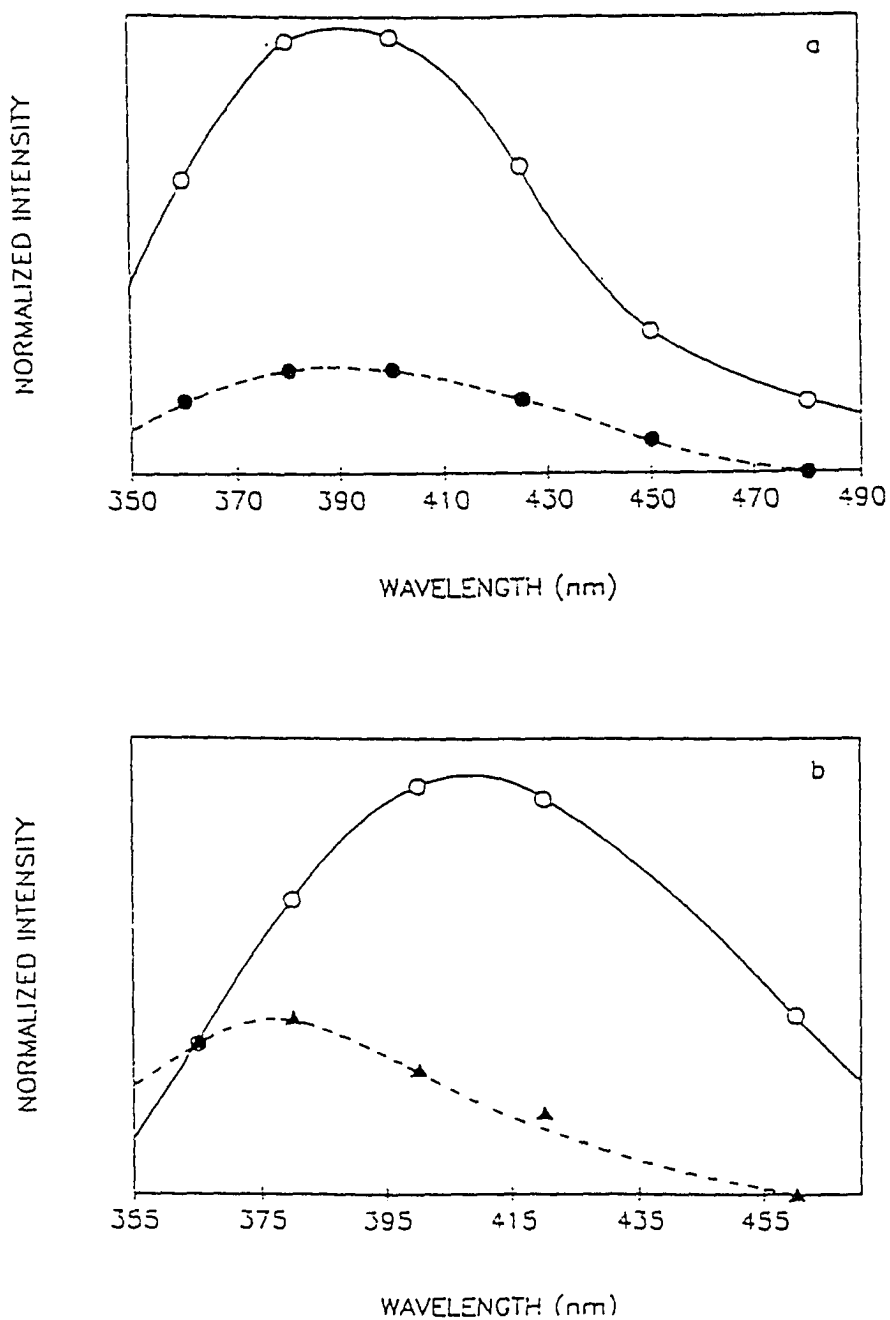


Figure 1.8. Steady-state spectral decomposition of (a) 7-azaindole and (b) 7-azatryptophan at pH 6.8 and 20°C. The empty circles represent the steady-state emission arising from the longer-lived lifetime component; the solid-circles, from the shorter-lived component. The spectrum of the short-lived component is multiplied by a factor of 10.

component contributes negligibly to the total fluorescence spectrum. Note that the spectrum of the short-lived component is different in 7-azaindole than in 7-azatryptophan. In particular, it drops off more quickly to zero in 7-azatryptophan: at 460 nm instead of 480 nm.

Temperature Dependence and Deuterium Isotope Effect

The temperature dependence of the short-lived component in H₂O yields an Arrhenius activation energy of 2.7 ± 1.7 kcal/mol (Figure 1.9). Within the admittedly large experimental error, this result is comparable to the viscosity activation energy of H₂O [27], $E_{\eta}^{\text{H}_2\text{O}} = 3.71$ kcal/mol. In D₂O the short-lived component yields an activation energy of 2.7 ± 1.3 kcal/mol. This result is in accord with the large viscosity activation for D₂O [27], $E_{\eta}^{\text{D}_2\text{O}} = 4.74$ kcal/mol. (More precise measurements of the temperature dependence of the short-lived component are difficult owing to its small amplitude (Figure 1.6). This is especially true in D₂O where the lifetime of the short-lived component is lengthened and hence more difficult to extricate from the double exponential decay.) These data are consistent with those for alcohols [2,12-14] indicating that *large-amplitude solvent motion is required for tautomerization*.

At ambient temperature, the isotope effect on the 7-azaindole short-lived fluorescence lifetime is $\tau_{\text{F}}(\text{D}_2\text{O})/\tau_{\text{F}}(\text{H}_2\text{O}) \sim 3.4$. Table 1.2 summarizes these data for the fluorescence quantum yields and lifetimes of 7-azaindole and indole derivatives. A clear trend is established. For 7-azaindole and its methylated derivatives the presence of a "full" N₁-H bond yields an isotope effect of ≥ 2.6 . The fluorescence quantum yields and lifetimes presented in Table 1.2 were collected over the entire emission band. Hence, since only a small fraction of the 7-azaindole molecules undergo excited-state tautomerization, it is unlikely that the observed isotope effect arises from this process. Under these detection conditions, the decaying and rising contributions will cancel each other out. If we assume that isotopic substitution affects neither the rate of photoionization nor that of intersystem crossing [28], then another nonradiative process must be involved. A likely possibility is S₁-S₀ internal conversion.

The deuterium isotope effect on the lifetimes and quantum yields suggests that the N₁H or N₁H⁺ bond may be a good accepting mode for internal conversion, just as has been demonstrated for the CH bond [30,31]. High frequency vibrations are good acceptors because fewer quanta are required in S₀ than for a lower frequency vibration, thus providing a more favorable Franck-Condon factor for the S₁-S₀ radiationless process. Deuterium substitution lowers the frequency of the acceptor mode and hence decreases the Franck-

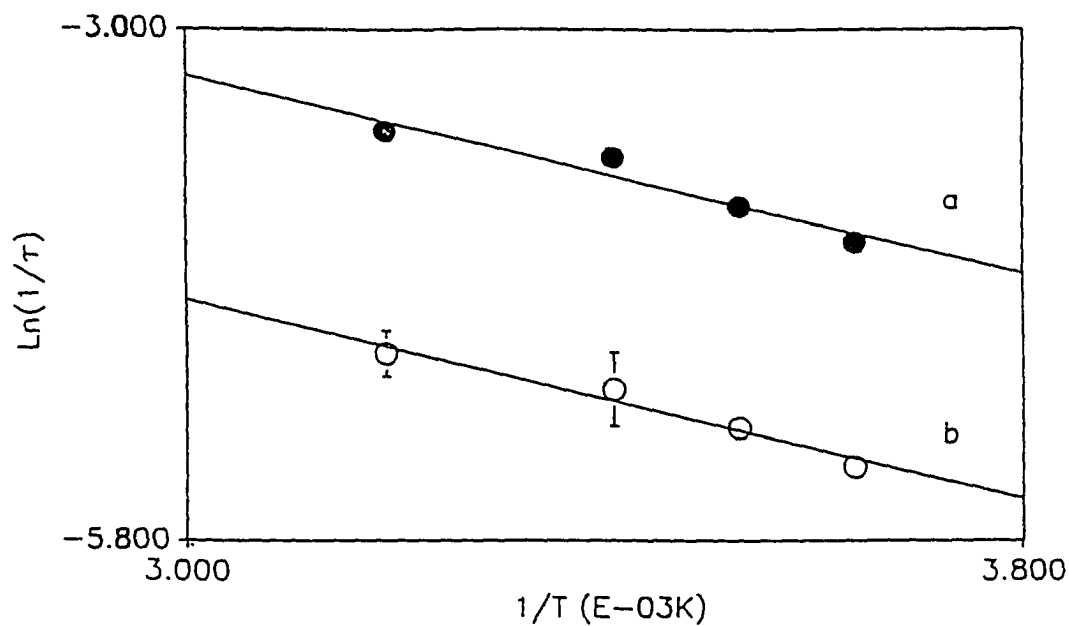


Figure 1.9. Arrhenius plots formed from the inverse of the short-lived lifetime component obtained from 7-azaindole in H_2O (open circles) or D_2O (filled circles). For H_2O , the activation energy is 2.7 ± 1.7 Kcal and the Arrhenius prefactor is $2.3 \pm 0.6 \times 10^{12}$. For D_2O , the activation energy is 2.7 ± 1.3 and the prefactor is $6.7 \pm 1.2 \times 10^{11}$. Experiments were performed at pH 6.8 and pD 7.2.

Table 1.2
Deuterium Isotope Effect on Fluorescence Lifetimes and Quantum Yields^a

compound ^b	$\phi_F(\text{D}_2\text{O})/\phi_F(\text{H}_2\text{O})^c$	$\tau_F(\text{D}_2\text{O})/\tau_F(\text{H}_2\text{O})^c$
7AI (N ₇ , N ₁ H)	3.6	3.5
7AI (N ₇ H ⁺ , N ₁ H)	2.7	2.6
1M7AI (N ₇)	1.19 [11]	1.2
1M7AI (N ₇ H ⁺)	1.8	1.5
7M7AI (N ₁)	1.6	1.4
7M7AI (N ₁ H ⁺)	2.6	3.1
indole (N ₁ H)	1.40 [11]	1.3
1-methylindole	1.19 [11]	1.1

^a Experiments are performed at 20°C.

^b The state of protonation of the relevant nitrogen atom is given by, for example, N₇ or N₇H⁺. The pH regions in which N₇ and N₁ are protonated are presented in Figures 10 and 11.

^c All data obtained in our laboratory were collected over the entire emission band.

Condon factor and the nonradiative rate. The result is an increase in the fluorescence lifetime and quantum yield of S_1 . The enhancement of internal conversion due to hydrogen bonding interactions with the solvent is also a possibility. Inoue *et al.* [47] have demonstrated rapid internal conversion in anthraquinones in which the quinoid oxygen participates in a hydrogen bond. On the other hand, the small isotope effect in indole (Table 1.1) indicates that its lowest excited singlet is not significantly depopulated by internal conversion. The N_1 proton in indole may be less likely to interact strongly with water than that of the corresponding proton in 7-azaindole owing to the higher pK_a of indole (Table 1.3).

7M7AI is a special case in that its fluorescence lifetime and quantum yield are the smallest of all the compounds listed in Table 1.1, yet it does not possess a covalent N_1H bond. Waluk *et al.* [32] have discussed the role of internal conversion in 7M7AI and two of its derivatives in butanol and 3-methylpentane. While a hydrogen-bonding interaction with the solvent may contribute to the short lifetime and low quantum yield of 7M7AI, it is likely that internal conversion is most significantly enhanced by its reduced S_1-S_0 energy gap relative to 7-azaindole: 25,900 as opposed to 19,600 cm^{-1} . For smaller energy gaps, the frequency of the acceptor vibrational mode is less crucial because fewer quanta are required in S_0 [30,31].

pH Dependence of the Fluorescence Lifetimes and Quantum Yields of the Methylated Analogs

In order to understand the nature of the fluorescent species of which the emission band of 7-azaindole at neutral — or any pH — is comprised, it is important to appreciate the pH dependence of the fluorescence lifetimes and quantum yields of the methylated analogs. Earlier we concluded that there was a negligible change in the excited-state pK_a of the N_7 of 7-azaindole owing to the similarity of the potentiometric and the fluorescence titration curves [2]. Figure 1.10 presents the fluorescence quantum yield of 7-azaindole as a function of pH. The form of this titration curve is qualitatively similar to that presented by Ingham and El-Bayoumi [8] except that we observe a more pronounced intensity change with pH. This change is a result of our accounting for the change in shape and position of the 7-azaindole spectrum with pH (Figure 1.10). The data yield an excited-state pK_a of 4.6 and ~ 13 for N_7H^+ and N_1H , respectively (Table 1.3). These values are very near the ground-state values.

We have obtained titration curves based on fluorescence lifetimes for 1M7AI and 7M7AI in order to investigate in detail the excited-state, reversible proton-transfer equilibrium of N_1 and N_7 . If, for example, the proton transfer equilibrium is not rapid on the

Table 1.3
Ground- and Excited-State pK_a Values of 7-Azaindole and Its Analogs

compound	$pK_a(S_0)$	$pK_a(S_1)^a$
pyrrole	16.5 [38], 17.51 (25°C) [39]	
pyridine (H^+)	5.21 (18°C) [40]	
indole (N_1H)	16.97 (25°C) [39]	12.3 [34]
7AI (N_1H)	12.1 (26°C)	~ 13 (23°C) ^b
7AI (N_7H^+)	4.5 (26°C) ^c , 4.59 (20°C) [41]	4.6 (23°C) ^b
7M7AI (N_1H^+)	8.9 ^d [22]	10.3 (20°C)
1M7AI (N_7H^+) ^e		3.1 (20°C)

^a S_1 refers to the fluorescent state, and hence to the lower of the two states, 1L_b and 1L_a [4,16].

^b Obtained from fluorescence quantum yield measurements (Figure 1.10). It is assumed that acid-base equilibrium is established during the excited-state lifetime. No correction to the pK_a value is made for the lifetimes of the protonated and unprotonated species [46].

^c The value reported earlier [2] was the inflection point of the titration curve.

^d Determined by the half neutralization method.

^e Not enough material was available after the optical measurements to perform the ground-state titration.

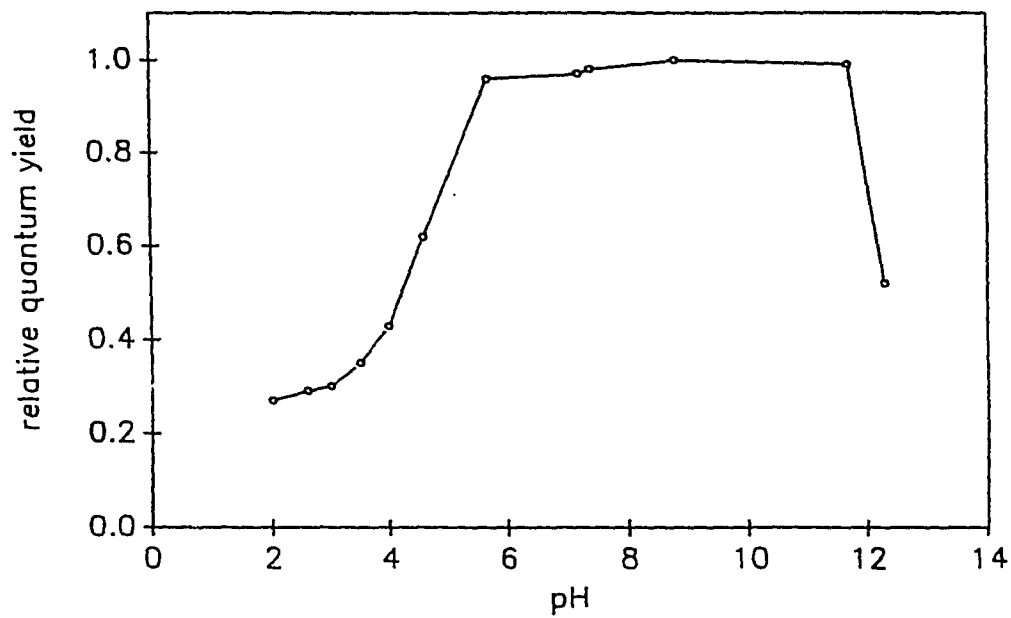
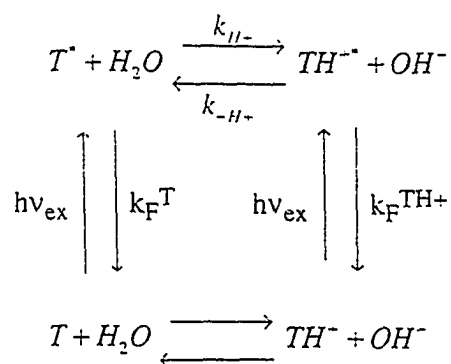


Figure 1.10. Fluorescence quantum yield of 7-azaindole as a function of pH at 20°C. Measurements are relative to those of 7-azaindole at pH 8.8 and 20°C. These results are slightly different from those of Ingham and El-Bayoumi [10] who only measured the 7-azaindole fluorescence intensity at 390 nm and do not take the spectral shift with pH into account. pH measurements are accurate to ± 0.10 units.

time scale of the excited-state lifetimes, then titration curves based on fluorescence of the excited-state lifetimes, then titration curves based on fluorescence measurements, in particular those of quantum yields, will not accurately measure the excited-state pK_a . β -naphthol is a celebrated example of a molecule where the proton transfer equilibrium occurs on the same time scale as the excited-state lifetime [33-36,46]. Fluorescence lifetimes as a function of pH (Figure 1.11) are thus required to clarify the kinetics involved. In particular, we consider the tautomer analog 7M7AI (T) being protonated by water to yield TH^+ at neutral pH.



k_F^T and $k_F^{TH^+}$ are the rates of population decay of the excited-state unprotonated and protonated species, not taking into account k_{H^+} or k_{-H^+} . The solution [31,33,36] to the excited-state rate equations yields two rate constants, λ_1 and λ_2 , where λ_1 represents the rate of decay of T^* ; λ_2 , of TH^{*+} :

$$\lambda_{1,2} = \frac{1}{2} \left[X + Y \mp \left\{ (Y - X)^2 + 4k'_{H^+} k_{-H^+} [OH^-] \right\}^{\frac{1}{2}} \right] \quad (4)$$

The subscript 1 corresponds to the minus sign. Constructing the sum and difference of λ_1 and λ_2 , which can be obtained from any point on the titration curve where two exponentially decaying components are present, permits the determination of k'_1 , k_{-1} , and K_b (or K_a). For 7M7AI at pH 10.4 and 20°C (Figure 1.11), $\lambda_1 = (361 \text{ ps})^{-1}$ and $\lambda_2 = (629 \text{ ps})^{-1}$. $k_F^T = (480 \text{ ps})^{-1}$ and $k_F^{TH^+} = (780 \text{ ps})^{-1}$; these latter values are the rates of population decay of 7M7AI and protonated 7M7AI in regions far away from the inflection point (Table 1.1). Results are tabulated in Table 1.3. There is only a small change in pK_a between the ground and the

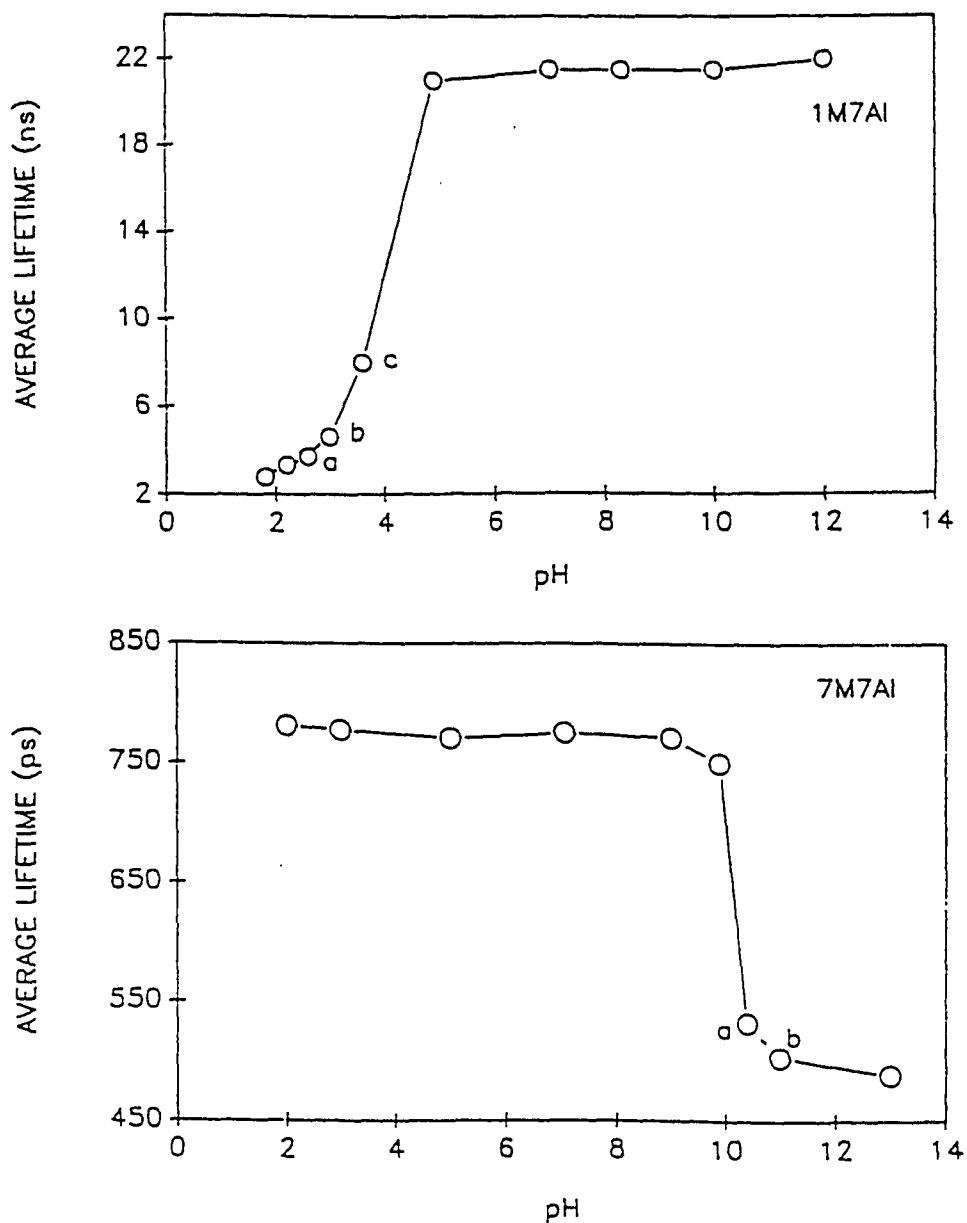


Figure 1.11. Average fluorescence lifetime as a function of pH of 1M7AI and 7M7AI at 20°C. For 1M7AI, the points **a**, **b**, and **c** denote double-exponential lifetimes. **a**: 3.2 ns (81%), 5.6 ns (19%); **b**: 2.3 ns (58%), 7.67 ns (42%); **c**: 1.9 ns (54%), 15.2 ns (46%). For 7M7AI, the points **a** and **b** indicate double-exponential lifetimes. **a**: 629 ps (64%), 361 ps (36%); **b**: 603 ps (50%), 403 ps (50%). Titration curves obtained from fluorescence quantum yields of 1M7AI and 7M7AI demonstrate the same behavior.

excited state for N_7 and N_1 ; and the change that is observed indicates that in the excited state N_7 is slightly more acidic and N_1 is slightly more basic. Large excited-state pK_a changes have been documented in many systems [33-36,46]. The small difference, and its direction, reported here is thus surprising since it has been suggested [37] that the driving force for intramolecular tautomerization in molecules such as methyl salicylate is an excited-state pK_a change. These data indicate that for 7-azaindole another excited-state mechanism is responsible for the tautomerization reaction. One possibility is that the impetus for this reaction is provided by the excited-state dipole moment change, which is responsible for dynamic solvation and the Stokes shift [14] of 7-azaindole. This solvent reorientation would be required to initiate a larger scale solvent reorganization. See discussion below.

Figure 1.12 presents the steady-state fluorescence spectra of 1M7AI and 7M7AI as a function of pH. At pH values below 9, 7M7AI has a maximum at 442 nm; at pH values above 10, the maximum shifts to 510 nm. It is reasonable to assume that the tautomer form of 7-azaindole in water has an N_1 whose pK_a is similar to that of 7M7AI. Therefore, after excited-state, double-proton transfer is effected in 7-azaindole, it is likely that N_1 will very rapidly become protonated and that this cation gives rise to a species with emission maximum at about 440 nm.

Table 1.3 contains pK_a data for pyrrole, pyridine, and indole, which serve as reference compounds. Fusion of a benzene ring to pyrrole to yield indole has a small effect on the pK_a of N_1 . On the other hand, fusion of pyridine to pyrrole to yield 7-azaindole reduces the ground-state pK_a of N_1 by more than 4 units. For indole the excited-state pK_a change is large, whereas in 7-azaindole, both for N_1 and N_7 , it is small as we have mentioned above.

Discussion

The Fluorescent Species in Water

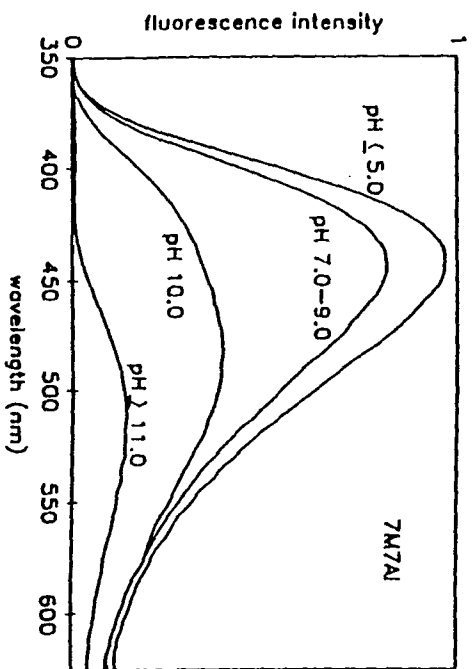
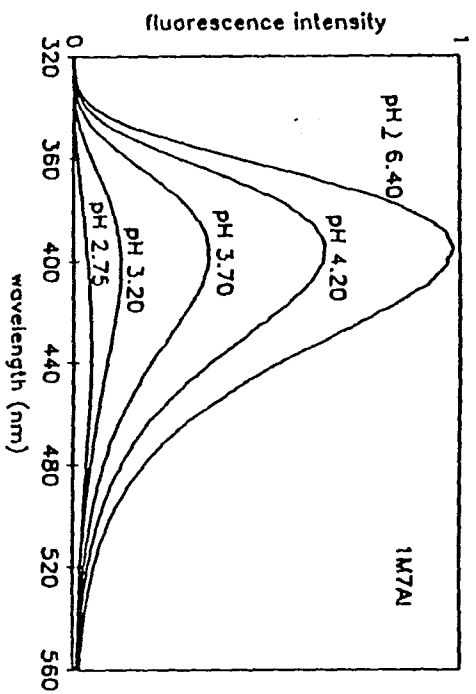
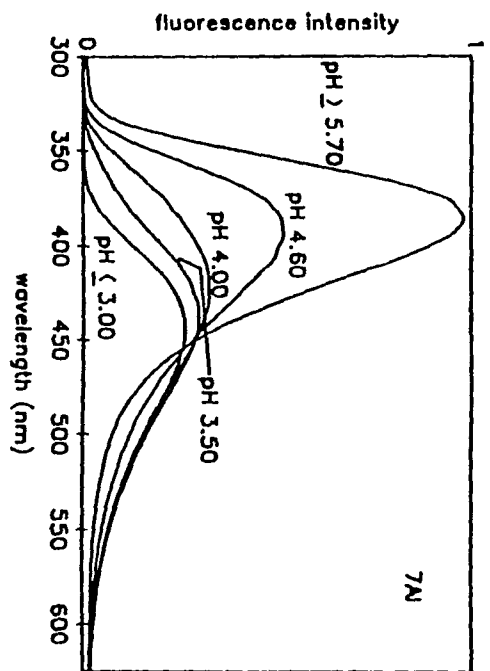
The 70-ps transient that we report elsewhere [3,4] in the transient absorbance of 7-azaindole is consistent with the rapid component that we measure across the emission spectrum for 7-azaindole and 7-azatryptophan in water at neutral pH (Figure 1.6). This rapid decay, which is observed for emission wavelengths towards the blue edge of the spectrum, is matched by a rise time of corresponding duration on the red edge of the spectrum. We note,

Figure 1.12. Steady-state emission spectra of 7AI, 1M7AI, and 7M7AI in water, $\lambda_{\text{ex}} = 285$ nm and 20°C. All spectra are corrected for concentration differences. pH measurements are accurate to ± 0.10 units. The emission maxima as a function of pH are as follows.

For 7AI: pH ≥ 5.70 , $\lambda_{\text{max}} = 387$ nm; pH 4.60, $\lambda_{\text{max}} = 394$ nm; pH 4.00, $\lambda_{\text{max}} = 424$ nm; pH 3.50, $\lambda_{\text{max}} = 437$ nm; pH ≤ 3.00 , $\lambda_{\text{max}} = 444$ nm. These data are more accurate and of higher quality than those presented earlier [2].

For 1M7AI: pH ≥ 4.20 , $\lambda_{\text{max}} = 395$ nm; pH 3.70, $\lambda_{\text{max}} = 398$ nm; pH 3.20, $\lambda_{\text{max}} = 402$ nm; pH 2.75, $\lambda_{\text{max}} = 435$ nm. Not shown are spectra for pH ≤ 2.15 . Below pH 2.15, $\lambda_{\text{max}} = 454$ nm and the peak intensities are significantly less than that at pH 2.75.

For 7M7AI: pH ≤ 9.0 , $\lambda_{\text{max}} = 444$ nm; pH 10.0, $\lambda_{\text{max}} = 482$ nm; pH ≥ 11.0 , $\lambda_{\text{max}} = 510$ nm.



however, that the amplitude of short component *never exceeds 20% of the total fluorescence decay* for 7-azaindole.

This observation leads us to modify slightly our earlier suggestion [2] that the fluorescent species of 7-azaindole in water is tautomer-like. The rapid fluorescence decay and rise times clearly indicate that 20% of the excited-state 7-azaindole molecules are undergoing tautomerization. The Arrhenius plots (Figure 1.9) indicate that this tautomerization is mediated by large-amplitude solvent motion, just as is observed in the alcohols [2,12-14].

At this point, there are two major questions that must be posed:

1. To what does the remaining 80% of the fluorescence decay in water correspond?
2. If excited-state double proton transfer is being effected in water, even for only 20% of the population, why does the fluorescence spectrum apparently consist of only one band whereas in alcohols, which also mediate tautomerization, two emission bands are observed?

The Presence of a "Blocked" Solute Species. To address the first question, we propose that there are three types of species of 7-azaindole in water that give rise to its fluorescence spectrum. These are illustrated in Figure 1.13. Twenty percent of the population is solvated in such a fashion that excited-state tautomerization can be effected in 70 ps. This population then comprises "normal" and "tautomer" species that are formally equivalent to those observed in linear alcohols. The normal species has a lifetime of 70 ps; and the tautomer, which is protonated, has a lifetime of 1100 ps. We suggest that the fluorescence properties of 7-azaindole in water are dominated by the remaining 80% of the solute molecules, which are "blocked" and *unable to tautomerize* during the 910 ps lifetime of this species.

In order to check this assignment, we can estimate the fluorescence quantum yield that would be observed if these three species were present and compare this estimated value to the measured fluorescence quantum yield of 7-azaindole in water, $\phi_F = 0.03$ [11] (Table 1.2). The fluorescence intensity as a function of time, when emission is collected over the entire spectrum, is given by the rate at which photons are emitted from all excited states present:

$$I(t) = \sum_i k_r^i F_i(t) \quad (5)$$

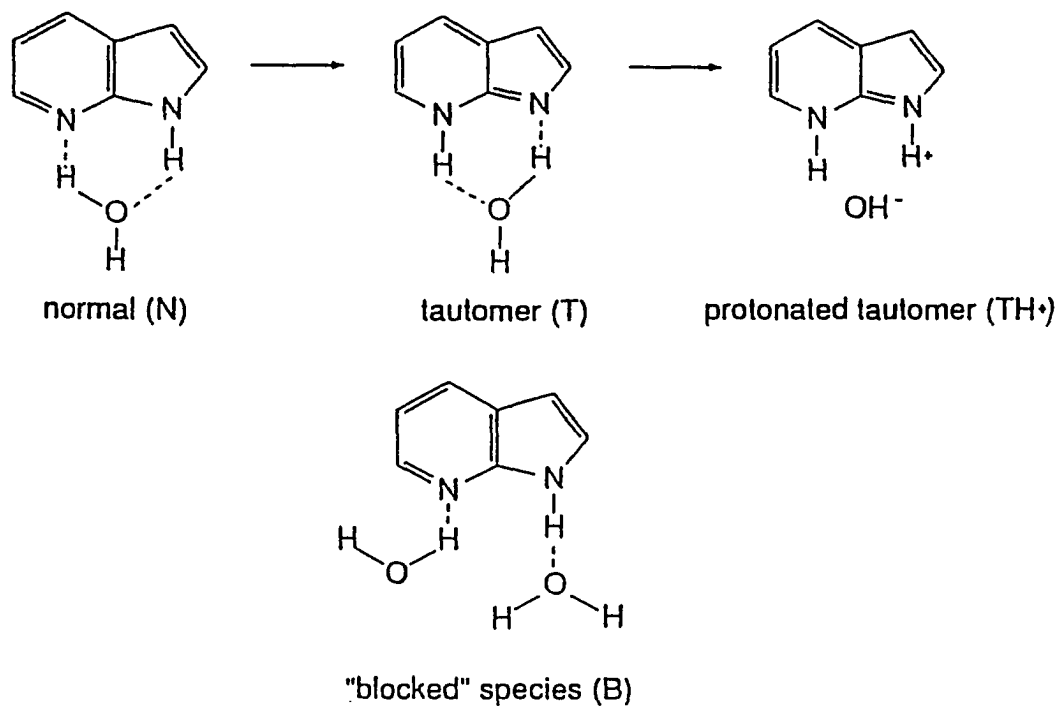


Figure 1.13. Idealized depictions of 7-azaindole/H₂O interactions.

where k_R^i is the radiative rate of species i and $F_i(t)$ is the excited-state population at a given time (the fluorescence decay profile) of species i . In our case, $F_i(t)$ is expressed as an exponential decay or as a sum of exponentially rising and decaying components. The fluorescence quantum yield is obtained by integration of this equation over time:

$$\phi_F = \int_0^{\infty} I(t) dt \quad (6)$$

We thus obtain:

$$\begin{aligned} \phi_{F,calc} = & k_R^{1M7AI} (0.20)(70 ps) + k_R^{7M7AI(N_1H^+)} (-0.20)(70 ps) \\ & + k_R^{7M7AI(N_1H^+)} (0.20)(1100) + k_R^{1M7AI} (0.80)(910 ps) = 0.025 \end{aligned} \quad (7)$$

This estimated result is in good agreement with the measured value of 0.03 when one considers the difficulties in obtaining accurate measurements for quantum yields as well as for the radiative rates and the weight of the short component that represents the 7-azaindole population undergoing tautomerization.

Blocked solvation, referred to above, could be produced if N_1 forms a strong hydrogen bond with water that results in an orientation that is not propitious for proton transfer or if N_7 is also "blocked" by forming another hydrogen bond with a different water molecule (Figure 1.13). Postulating this state of blocked solvation — and most importantly a strong hydrogen bonding interaction of N_1 with the solvent — resolves the following paradoxical observations: the maximum of the fluorescence emission of 7-azaindole in water, 386 nm, is closer to that of unprotonated 1M7AI, 395 nm, than to that of protonated or unprotonated 7M7AI, 442 or 510 nm, respectively. On the other hand, the fluorescence lifetime of 7-azaindole in water is more similar to that of protonated or unprotonated 7M7AI, 780 ps or 480 ps, than to that of unprotonated 1M7AI, 21 ns.

The substitution of the hydrogen by a methyl group at N_1 renders 1M7AI incapable of tautomerizing and hence provides a relatively high fluorescence quantum yield, $\phi_F = 0.55$ - 0.64 [11] (Table 1.1). Presumably, the only significant nonradiative decay channels left to 1M7AI are photoionization and intersystem crossing [3].

The fundamental difference between the blocked species and 1M7AI is the proton at N_1 , which can interact with the solvent. We propose that the presence of this proton bound

to N_1 is responsible for the *position* and *shape* of the fluorescence band of the blocked species of 7-azaindole in water — that is, similar to that of 1M7AI. On the other hand, we suggest that the availability of the high-frequency N_1H bond is responsible for the reduced lifetime and fluorescence quantum yield of this species through S_1-S_0 internal conversion. It is possible that the interaction of the proton with the solvent also enhances the rate of internal conversion to the ground electronic state [37,47].

It is noteworthy that the fluorescence lifetime and quantum yield of this blocked species are more similar to those of *protonated* 7AI, 1M7AI, and 7M7AI than to those of the *unprotonated* tautomer analog, 7M7AI (Table 1.1). This supports the notion that the blocked species is also undergoing an interaction of its N_7 with solvent, as depicted schematically in Figure 1.12.

The Importance of the Relative Acidities of N_1 and N_7 . In order to address the second question raised above, it is important to note that consideration of the steady-state fluorescence spectrum of 7-azaindole in water requires an appreciation of the relative acidities of N_1 and N_7 . A considerable amount of confusion may ensue if one expects to observe, for the fraction of molecules undergoing tautomerization, fluorescence emission in the red ($\lambda_{\max} \sim 510$ nm) as is observed for the tautomer of 7-azaindole in methanol or for 7M7AI in methanol. Instead of bimodal emission at neutral pH, one only detects a long-wavelength tail (Figure 12). This apparent discrepancy is easily resolved when one notes that N_1 in the tautomer (e.g., 7M7AI) is very basic: excited-state $pK_a = 10.3$ (Figure 1.11, Table 1.3). Owing to the basicity of N_1 , upon excited-state tautomerization of the small subset of appropriately solvated molecules, it is likely that N_1 is immediately protonated. Protonated 7M7AI has an emission maximum at 444 nm; and this is consistent with the shape of the 7-azaindole spectrum at low pH (Figure 1.12).

Population Decay, Tautomerization, and Solvent Reorganization ("Dynamics")

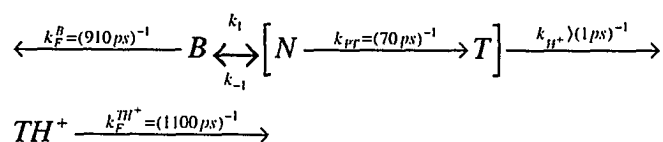
The physical picture that we have so far obtained for the photophysics of the 7-azaindole chromophore in water is the following:

1. At ambient temperature there is a ground-state equilibrium between a set of 7-azaindole molecules that can tautomerize (N) and that is analogous to the normal species referred to in linear alcohols and a set of 7-azaindole molecules that are solvated in such a fashion that tautomerization is blocked (B).

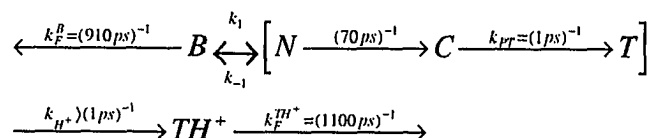
- For 7-azaindole, based on the preexponential factors obtained from wavelength-resolved lifetime measurements, we estimate the equilibrium constant to be at most $K = k_1/k_{-1} = [N]/[B] = 0.25$.
- N and B do not interchange rapidly on the time scale of their fluorescence lifetimes, 70 ps and 910 ps, respectively.
- The tautomer (T) formed by the decay of N is rapidly ($< \sim 1$ ps) protonated (TH^+) owing to the strong basicity of N_1 relative to that of N_7 ($pK_a^*(N_1) = 10.3$ as opposed to $pK_a^*(N_7H^+) = 3.7$).
- The protonated tautomer decays with a time constant of 1100 ps.

There are two reaction schemes that are consistent with these data and conclusions.

Scheme 1



Scheme 2



The difference between these two schemes is contained in the square brackets. While Scheme 1 is the simpler of the two, Scheme 2 introduces another aspect of the tautomerization reaction that makes the physics in water conform more nearly to that of 7-azaindole dimers in nonpolar solvents and 7-azaindole in alcohols. In particular, Hochstrasser and coworkers have observed tautomerization to occur in 1.4 ps in 7-azaindole dimers at ambient temperature. These dimers are considered to be planar complexes in which there are two $N_1H \cdots N_7$ hydrogen bonds [6-8]. Similarly, it has been argued [2,11-

14] that in alcohols, for example methanol, the 140 ps decay time of the normal species represents the time required for a cyclic hydrogen bonding complex to be established between solute and solvent. Upon formation of this complex (Figure 1.13), tautomerization occurs in $< \sim 1$ ps. The proposal of a time constant of $< \sim 1$ ps for the ultimate protonation step is based on the following. First, fast protonation is facilitated by the availability of the proton from the water molecule that participated in the cyclic complex. Thus, this reaction may be considered as essentially intramolecular, insofar as it depends on a solute-solvent complex, rather than as intermolecular. Second, since no long-wavelength emission is observed, the unprotonated tautomer must decay as rapidly as it is formed. Third, a time constant of this duration is consistent with the estimated lifetime of a hydrogen bond, ~ 5 ps [48].

Scheme 2 brings the water problem in line with the dimer and alcohol systems. Here, the 70 ps decay of N is the result of a second solvation step that is much more rapid than k_1 . The large activation energy associated with the 70-ps component is consistent with large-amplitude solvent motion and should be compared with the Arrhenius activation energies obtained from the decay times of the normal species in alcohols: here the activation energy agrees very well with the viscosity activation energy of the solvent. Once the second solvation step occurs to form C, a "cyclic hydrogen-bonded complex," tautomerization occurs as rapidly as in dimers or alcohols.

In the above discussion, we have tacitly assumed that the 910 ps and 70 ps decay components represent the population decay of B and N respectively and are not significantly perturbed by the rate constants for solvent reorganization, k_1 and k_{-1} . These assumptions then require us to place certain limits on k_1 and k_{-1} .

If we consider only the equilibrium between B and N and their population decays, we obtain the following expressions by solving the rate equations using Laplace transform techniques [42]. Here we assume that at $t = 0$, the populations of the excited-state blocked and normal species are nonzero and that $[N]_0/[B]_0 = 0.25$.

$$[B](t) = \frac{[B]_0}{(\lambda_2 - \lambda_1)} [(\lambda_2 - X)\exp(-\lambda_1 t) + (X - \lambda_1)\exp(-\lambda_2 t)] + \frac{k_{-1}[N]_0}{(\lambda_2 - \lambda_1)} (\exp(-\lambda_1 t) - \exp(-\lambda_2 t)) \quad (8)$$

$$[N](t) = \frac{k_1[B]_0}{(\lambda_2 - \lambda_1)} (\exp(-\lambda_1 t) - \exp(-\lambda_2 t)) + \frac{[N]_0}{(\lambda_2 - \lambda_1)} [(\lambda_2 - Y)\exp(-\lambda_1 t) + (Y - \lambda_1)\exp(-\lambda_2 t)] \quad (9)$$

$$\lambda_{1,2} = \frac{1}{2} \left[X + Y \mp \left\{ (Y - X)^2 + 4k_{-1}k_1 \right\}^{\frac{1}{2}} \right] \quad (10)$$

where subscript 1 refers to the negative sign; and subscript 2, to the positive. In general, $\lambda_{1,2}$ depend on the nonradiative and radiative pathways of deactivation of B and N as well as on k_1 and k_{-1} . Thus,

$$X = k_1 + k_F^B; \quad Y = k_{-1} + k_F^N \quad (11)$$

where k_F^B and k_F^N are the inverse of the fluorescence lifetimes of B and N, *neglecting the contribution from k_1 and k_{-1}* .

From eqs 10 and 11 it can be seen that if $k_F^B \gg k_1$ and if $k_F^N \gg k_{-1}$, then $\lambda_1 = k_F^B$ and $\lambda_2 = k_F^N$. It is interesting to consider the physical implications of how small k_1 and k_{-1} must be relative to k_F^B and k_F^N in order for $\lambda_1 \sim k_F^B$ and $\lambda_2 \sim k_F^N$. If we arbitrarily choose $k_1 = 0.1 \times 10^9 \text{ s}^{-1}$, the equilibrium between B and N requires $k_{-1} = 0.4 \times 10^9 \text{ s}^{-1}$. Then from eqs 10 and 11 we obtain $1/\lambda_1 = 837 \text{ ps} \sim \tau_F^B$ and $1/\lambda_2 = 68 \text{ ps} \sim \tau_F^N$. In other words, if we require that the solvation step converting B to N occurs on a time scale of *10 ns or longer*, we recover decay components that are qualitatively similar to the measured 910 ps and 70 ps that we have attributed to the population decay times of B and N, respectively.

Two additional self-consistency checks arise from these assumptions. First, the *total* fluorescence intensity, which is proportional to the sum of the transient populations of B and N, assuming that their radiative rates are identical, yields from eq 5 $I(t) = k_R[B](t) + k_R[N](t) \propto 0.80 \exp(-\lambda_1 t) + 0.20 \exp(-\lambda_2 t)$. Thus, we retrieve 20% of a species decaying rapidly, which is in agreement with the experimental observation of the proportion of the 7-azaindole population that is capable of tautomerization. Second, using the above values, we find that $(X - \lambda_1) \sim 0$ and that $[B]_0(\lambda_2 - X)/k_{-1}[N]_0 \gg 1$. Thus, B decays essentially as a single exponential, as is observed.

One may ask whether the reorganization of water molecules about the solute can occur on such a slow time scale. It is important to distinguish the time scales involving reorientational dynamics of solvent molecules, which can be extremely rapid [10,43], and "diffusive redistribution" of solvent. In particular, one must distinguish between the kind of solvent reorientation that is induced by dipole moment changes in the excited state of a probe molecule and reorganization of the solvent that involves the breaking and making of

hydrogen bonds. It has been noted that in polyalcohols such as ethylene glycol and glycerol there is a severe deviation, characterized by unusually slow tautomerization, from the good correlation of tautomerization rate with $E_T(30)$ that is observed with monoalcohols [14]. It has been suggested that this deviation is a signature of solvents capable of donating more than one hydrogen bond per molecule and that such solvents reduce the probability of forming solute molecules with the "correct" solvation for tautomerization [14,43]. The detailed mechanism of the rate reduction peculiar to these solvents is still unknown.

Conclusions

Recently two related studies of 7-azaindole have been performed. Chou *et al.* [44] investigated 7-azaindole in mixtures of water and aprotic solvents. Small additions of water to polar aprotic solvents produced tautomer-like emission. They proposed that excited-state tautomerization is possible only when there are significant concentrations of 1:1 complexes of 7-azaindole and water. They further proposed that in pure water the formation of higher-order aggregates inhibits tautomerization during the excited-state lifetime.

Chapman and Maroncelli have studied 7-azaindole fluorescence in water and in mixtures of water and diethyl ether [43]. They too observe long-wavelength, tautomer-like emission at low water concentrations. In pure water they also observe a rapid rise time at long wavelengths. They, however, take a different point of view, namely that excited-state tautomerization occurs for the entire 7-azaindole population in pure water and that the 7-azaindole fluorescence lifetime is dominated by this reaction. Using a two-state kinetic model in conjunction with steady-state spectral data they conclude that the rapid rise time is associated with the nonradiative decay rate of the tautomer. They propose that the longer, ~ 900 ps, decay time of the entire emission band is a measure of the tautomerization rate. Their scheme requires that the nonradiative decay rate of the tautomer is greater than the rate of tautomerization. They estimate that the rate of tautomerization is $1.2 \times 10^9 \text{ s}^{-1}$.

Our observations and conclusions more nearly approach those of Chou *et al.*, although there is a small population of 7-azaindole molecules that do tautomerize in addition to the majority of the population in which this reaction is frustrated. That the fluorescence lifetime of 7-azaindole is *not* dominated by excited-state tautomerization is demonstrated by the observation of three distinct fluorescence lifetimes: ~ 70 ps, the normal decay time; ~ 980 ps (i.e., 1100 ps (Table 1.3)), the tautomer decay time; and 910 ps, the decay time of the

blocked solute. Further evidence is provided by the spectral inhomogeneity of the emission band (Figures 1.7 and 1.8).

The major conclusions of this article can be summarized as follows:

1. Only a small fraction (<~ 20%) of 7-azaindole molecules in pure water are capable of excited-state tautomerization on a 1-ns time scale.
2. The majority of the 7-azaindole molecules are solvated in such a fashion that tautomerization is blocked. More than 10 ns are required to achieve a state of solvation that facilitates tautomerization, that is, to convert the "blocked" species into a "normal" species.
3. The 70-ps time constant that is observed in fluorescence and absorption measurements reflects a subsequent reorientation of the solvent that establishes a "cyclic complex" between solvent and solute. Formation of this complex permits an ~ 1 ps tautomerization step, as has been discussed for 7-azaindole in alcohols and 7-azaindole dimers in nonpolar solvents.
4. No significant emission intensity is observed for 7-azaindole in water at 510 nm because so little tautomer is produced and because the tautomer that is produced is rapidly protonated and has an emission maximum at ~ 440 nm.
5. Optical titration of the methylated 7-azaindole analogs confirms that there is a negligible pK_a change of N_7 and N_1 of 7-azaindole in the excited state. Thus, an excited-state pK_a change cannot be the "driving force" for the tautomerization reaction, as has been suggested for other systems.
6. For 7-azaindole in water, excited-state tautomerization and intersystem crossing seem to be relatively minor pathways of nonradiative decay. Photoionization from a higher-lying excited singlet has been suggested to be quite facile [3,4]. In addition S_1 - S_0 internal conversion may play an important role when N_1 is bound to a hydrogen or interacts strongly through hydrogen bonding with the solvent. This latter process is most likely responsible for the previously mentioned [2] "tautomer-like" behavior of the species in water (i.e., relatively short fluorescence lifetime, low quantum yield, deuterium isotope effect).
7. Most importantly these results clarify the photophysics of 7-azaindole for use as the intrinsic chromophore of the probe molecule, 7-azatryptophan. In particular, the minor amount of tautomerization will contribute to the decay kinetics only if emission is collected at wavelengths red of 505 nm or with a relatively narrow spectral bandpass (with adequate temporal resolution). This is not a serious restriction since

experiments are not likely to be performed with such spectral resolution owing to the low fluorescence intensity. When emission is collected over a large spectral region and on a full-scale time base coarser than 3 ns, the tautomerization reaction is imperceptible. On the other hand, the appearance of long-wavelength emission of a protein containing 7-azatryptophan in water would definitely signal a change of environment that facilitates tautomerization.

Acknowledgment

We thank Mark Maroncelli for sharing his preliminary results with us and for providing a preprint. Alan Schwabacher provided many helpful suggestions for synthetic and purification procedures. This work was partially supported by the ISU Biotechnology Council, University Research Grants, and IPRT. J.W.P. is an Office of Naval Research Young Investigator.

References and Notes

1. Négrerie, M.; Bellefeuille, S. M.; Whitham, S.; Petrich, J. W.; Thornburg, R. W. *J. Am. Chem. Soc.* **1990**, *112*, 7419.
2. Négrerie, M.; Gai, F.; Bellefeuille, S. M.; Petrich, J. W. *J. Phys. Chem.* **1991**, *95*, 8663.
3. Gai, F.; Chen, Y.; Petrich, J. W. *J. Am. Chem. Soc.* **1992**, *114*, 8343.
4. Négrerie, M.; Gai, F.; Lambry, J.-C.; Martin, J.-L.; Petrich, J. W. In *Ultrafast Phenomena VIII*, Eds. Martin, J.-L.; Migus, A.; Springer: New York, 1993; p. 621.
5. Petrich, J. W.; Chang, M. C.; McDonald, D. B.; Fleming, G. R. *J. Am. Chem. Soc.* **1983**, *105*, 3824; Szabo, A. G.; Rayner, D. M. *J. Am. Chem. Soc.* **1980**, *102*, 554.

6. Taylor, C. A.; El-Bayoumi, M. A.; Kasha, M. *Proc. Natl. Acad. Sci. USA* **1969**, *63*, 253.
7. Ingham, K. C.; Abu-Elgheit, M.; El-Bayoumi, M. A. *J. Am. Chem. Soc.* **1971**, *93*, 5023.
8. Ingham, K. C.; El-Bayoumi, M. A. *J. Am. Chem. Soc.* **1974**, *96*, 1674.
9. Hetherington, W. M., III; Micheels, R. M.; Eisenthal, K. B. *Chem. Phys. Lett.* **1979**, *66*, 230.
10. Share, P. E.; Sarisky, M. J.; Pereira, M. A.; Repinec, S. T.; Hochstrasser, R. M. *J. Lumin.* **1991**, *48/49*, 204.
11. Avouris, P.; Yang, L. L.; El-Bayoumi, M. A. *Photochem. Photobiol.* **1976**, *24*, 211.
12. McMorrow, D.; Aartsma, T. J. *Chem. Phys. Lett.* **1986**, *125*, 581.
13. Konijnenberg, J.; Huizer, A. H.; and Varma, C. A. G. O. *J. Chem. Soc. Faraday Trans. 2.* **1988**, *84*, 1163.
14. Moog, R. S.; Maroncelli, M. *J. Phys. Chem.* **1991**, *95*, 10359.
15. Collins, S. T. *J. Phys. Chem.* **1983**, *87*, 3202.
16. Rich, R. L.; Chen, Y.; Neven, D.; Négrerie, M.; Gai, F.; Petrich, J. W. *J. Phys. Chem.* **1993**, *97*, 1781.
17. Valeur, B.; Weber, G. *Photochem. Photobiol.* **1977**, *25*, 441.
18. Bulska, H.; Grabowska, A.; Pakula, B.; Sepiol, J.; Waluk, J.; Wild, U. P. *J. Lumin.* **1984**, *29*, 65.

19. Chang, M. C.; Courtney, S. J.; Cross, A. J.; Gulotty, R. J.; Petrich, J. W.; Fleming, G. R. *Anal. Instrum.* **1985**, *14*, 33; Cross, A. J.; Fleming, G. R. *Biophys. J.* **1984**, *46*, 45.
20. Still, W. C.; Kahn, M.; Mitra, A. *J. Org. Chem.* **1978**, *43*, 2923.
21. Kim, S. K.; Bernstein, E. R. *J. Phys. Chem.* **1990**, *94*, 3531.
22. Robison, M. M.; Robison, B. L. *J. Am. Chem. Soc.* **1955**, *77*, 6555.
23. Cox, R. H.; Sankar, S. *Org. Mag. Reson.* **1980**, *14*, 150.
24. Timpe, H.-J.; Müller, U.; Worschech, R. *J. Prakt. Chem.* **1980**, *322*, 517.
25. Jarzeba, W.; Walker, G. C.; Johnson, A. E.; Kahlow, M. A.; Barbara, P. F. *J. Phys. Chem.* **1988**, *92*, 7039; Barbara, P. F.; Jarzeba, W. *Adv. Photochem.* **1990**, *15*, 1.
26. Maroncelli, M.; Fleming, G. R. *J. Chem. Phys.* **1987**, *86*, 6221.
27. Viswanath, D. S.; Natarajan, G. *Data Book on the Viscosity of Liquids*; Hemisphere Publishing: New York, 1989.
28. This assumption is based on the analogy with the effect of isotopic substitution on the fluorescence quantum yield of derivatives of tryptophan and indole, where photoionization and intersystem crossing are significant nonradiative decay pathways [29]: $1 \sim \phi_F(D_2O)/\phi_F(H_2O) \sim 2$. Robbins, R. J.; Fleming, G. R.; Beddard, G. S.; Robinson, G. W.; Thistlethwaite, P. J.; Woolfe, G. J. *J. Am. Chem. Soc.* **1980**, *102*, 6271; Kirby, E. P.; Steiner, R. F. *J. Phys. Chem.* **1970**, *74*, 4880. See also the data for indole in Table I.
29. Bent, D. V.; Hayon, E. *J. Am. Chem. Soc.* **1975**, *97*, 2612.
30. Siebrand, W. *J. Chem. Phys.* **1967**, *46*, 440; *47*, 2411; Siebrand, W.; Williams, D. F. *J. Chem. Phys.* **1968**, *49*, 1860; Avouris, P.; Gelbart, W. M.; El-Sayed, M. A. *Chem. Rev.* **1977**, *77*, 793.

31. Birks, J. B. *Photophysics of Aromatic Molecules*; Wiley-Interscience: London, 1970, Chapter 7.
32. Waluk, J.; Pakula, B.; Komorowski, S. J. *J. Photochem.* **1987**, *39*, 49.
33. Weller, A. *Progr. Reaction Kinetics* **1961**, *1*, 187.
34. Vander Donckt, E. *Progr. Reaction Kinetics* **1970**, *5*, 273.
35. Parker, C. A. *Photoluminescence of Solutions*; Elsevier: Amsterdam, 1968.
36. Laws, W. R.; Brand, L. *J. Phys. Chem.* **1979**, *83*, 795.
37. Flom, S. R.; Barbara, P. F. *J. Phys. Chem.* **1985**, *89*, 4489.
38. McEwen, W. K. *J. Am. Chem. Soc.* **1936**, *58*, 1124.
39. Yagil, G. *Tetrahedron* **1967**, *23*, 2855.
40. Britton, H. T. S.; Williams, W. G. *J. Chem. Soc.* **1935**, 796.
41. Adler, T. K.; Albert, A. *J. Chem. Soc.* **1960**, 1794.
42. Arfken, G. *Mathematical Methods for Physicists*; Academic Press, Inc.: San Diego, 1985.
43. Chapman, C. F.; Maroncelli, M. *J. Phys. Chem.* **1992**, *96*, 8430.
44. Chou, P.-T.; Martinez, M. L.; Cooper, W. C.; Collins, S. T.; McMorrow, D. P.; Kasha, M. *J. Phys. Chem.* 1992, **96**, 5203.
45. Wetlaufer, D. B.; *Advan. Protein Chem.* **1962**, *17*, 303.
46. Ireland, J. F.; Wyatt, P. A. H. *Adv. Phys. Org. Chem.* **1976**, *12*, 643.

47. Inoue, H.; Hida, M.; Nakashima, N.; Yoshihara, K. *J. Phys. Chem.* **1982**, *86*, 3184.
48. Crooks, J. E. In *Comprehensive Chemical Kinetics*, Vol. 8. Eds. Bamford, C. H.; Tipper, C. F. H. (Elsevier, Amsterdam, 1977).

CHAPTER 2. STEADY-STATE AND TIME-RESOLVED FLUORESCENCE ANISOTROPY OF 7-AZAINDOLE AND ITS DERIVATIVES

A paper published in the *Journal of Physical Chemistry*¹

R. L. Rich², Y. Chen², D. Neven², M. Négrerie³, F. Gai², and J. W. Petrich^{2,4}

Abstract

The fluorescence excitation and excitation anisotropy spectra at -60°C in a propylene glycol glass are reported for 7-azaindole and three related derivatives: 7-azatryptophan, N₁-methyl-7-azaindole (1M7AI), and 7-methyl-7H-pyrrolo[2,3-*b*]pyridine (7M7AI). At the reddest excitation wavelengths, steady-state anisotropy values are observed in the range 0.17 to 0.23, which is significantly less than the theoretical limiting anisotropy of 0.4. The anisotropy spectra indicate the presence of closely-spaced ¹L_a and ¹L_b bands as in indole. The low temperature anisotropies are compared with results from time-dependent measurements. An alternative method of collecting fluorescence depolarization data in time-correlated single-photon counting experiments is also presented. It is reliable, provides long-term stability, which is essential for weakly fluorescent samples, and obviates the need for "tail matching" scaling procedures. This method is tested with the well-characterized fluorescein derivative, rose bengal, and is employed to compare the rotational diffusion times of the normal and the tautomer species of 7-azaindole in methanol and butanol with that of the fluorescent, "blocked," species of 7-azaindole in water.

¹ Reprinted with permission from *Journal of Physical Chemistry* **1993**, *97*, 1781. Copyright © 1993 American Chemical Society.

² R. L. Rich, Y. Chen, and F. Gai (graduate students), D. Neven (undergraduate researcher), and J. W. Petrich (Associate Professor) in the Department of Chemistry, Iowa State University.

³ Postdoctoral Fellow under J. W. Petrich. Currently employed by Laboratoire d'Optique Appliquée, Ecole Polytechnique, ENSTA, INSERM U275, 91128 Palaiseau Cedex, FRANCE.

⁴ To whom correspondence should be addressed.

Introduction

7-Azaindole (Figure 2.1) is the chromophoric moiety of the nonnatural amino acid, 7-azatryptophan. We have proposed 7-azatryptophan as an alternate to tryptophan for use as an optical probe of protein structure and dynamics [1-5]. The suitability of 7-azatryptophan is based on its single-exponential (780 ps) fluorescence decay (when emission is collected over the entire band), its spectroscopic distinguishability from tryptophan in both absorption and emission, and its amenability to peptide synthesis and bacterial incorporation.

To use 7-azatryptophan as a probe of protein structure and dynamics it is crucial to understand the photophysics of the 7-azaindole chromophore in water. We have obtained evidence for four nonradiative processes: photoionization, intersystem crossing, internal conversion, and excited-state tautomerization [3-5]. Unlike its dimer [6-10] or when it is in alcohols [11-14], 7-azaindole in water exhibits only a minor amount, $< \sim 20\%$, of excited-state tautomerization [3-5] (Figure 2.2). In fact, when emission is collected over the entire band, tautomerization is imperceptible because the fluorescence decay time of the population which can tautomerize, the "normal" species, is compensated for by the fluorescence rise time of the tautomer [3-5]. Chou *et al.* [15] have also discussed the inability of 7-azaindole in water to execute double-proton transfer [16]. Because tautomerization of 7-azaindole in water is not facile, the fluorescence spectrum is smooth with a single maximum at 386 nm instead of bimodal as it is in alcohols (e.g., for methanol $\lambda_{\text{max}} = 374, 505$ nm). The small fraction of molecules that do tautomerize are most likely rapidly protonated and have an emission maximum at ~ 440 nm [5].

While much has been learned about the photophysics of 7-azaindole, there are outstanding questions that must be resolved in order to appreciate fully its use as a biological probe: how does the electronic structure of 7-azaindole differ from that of indole and how do these differences result in the "well-behaved" photophysics of 7-azatryptophan, which are exemplified by its single-exponential fluorescence lifetime as opposed to the nonexponential fluorescence lifetime of tryptophan [1,17]?

In order to provide answers to these questions, we have performed fluorescence excitation anisotropy measurements of 7-azaindole in order to compare its excited-state level structure with that of indole. Valeur and Weber [18] resolved the fluorescence excitation spectrum of indole into overlapping 1L_a and 1L_b bands at -58°C in propylene glycol and reported the 1L_b transition to be quite structured with maxima at 282.5 and 289.5 nm. They reported the 1L_a transition to be broader and to absorb farther to the red than the 1L_b

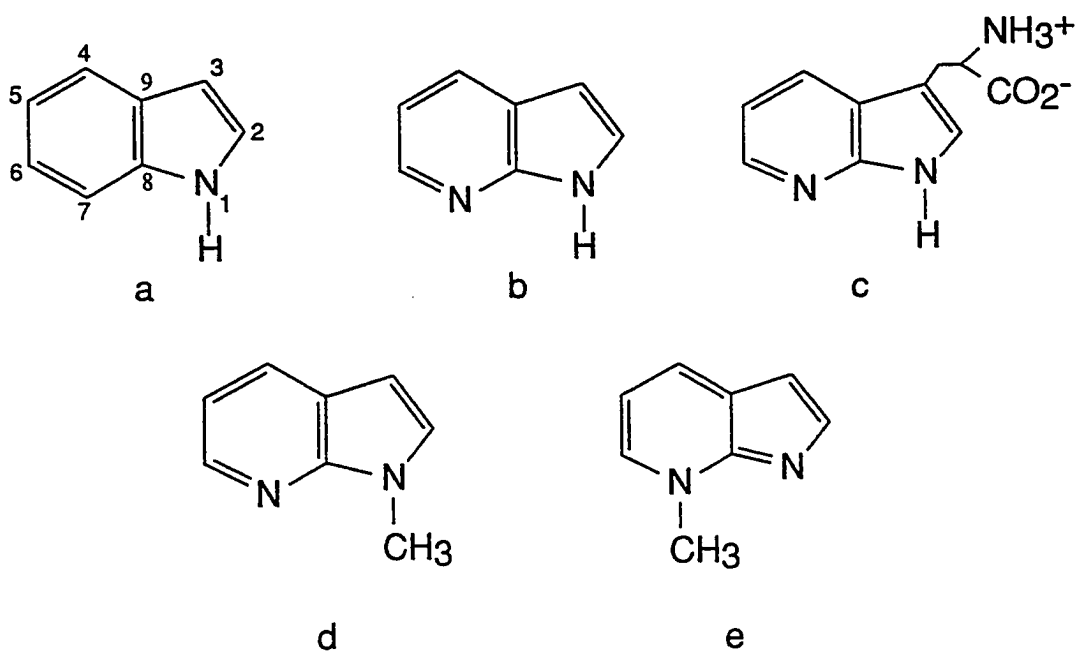


Figure 2.1. Structures of (a) indole; (b) 7-azaindole; (c) 7-azatryptophan; (d) N_1 -methyl-7-azaindole; and (e) 7-methyl-7H-pyrrolo [2,3-b]pyridine (7M7AI).

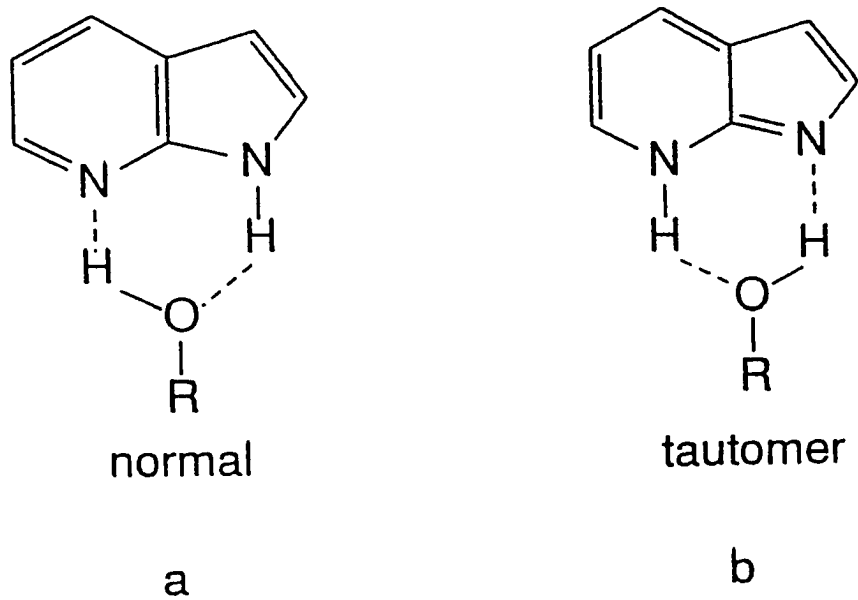


Figure 2.2. Structures of (a) hydrogen-bonded cyclic complex of 7-azaindole with a linear alcohol or water molecule and (b) the tautomeric form of this complex.

transition. An important question is whether 7-azaindole and related compounds share these features in common with indole or whether the nitrogen at the 7 position is sufficient to perturb significantly the overlap of these two bands. The purpose of this article is thus to investigate, through fluorescence excitation spectra and fluorescence excitation anisotropy spectra, the lowest lying electronic transitions of 7-azaindole and its analogs. In addition to 7-azaindole and 7-azatryptophan, we investigate derivatives that mimic untautomerized and tautomerized 7-azaindole: N₁-methyl-7-azaindole (1M7AI) and 7-methyl-7*H*-pyrrolo[2,3-*b*]pyridine (7M7AI) (Figure 2.1). We reproduce the results of Valeur and Weber for indole. The fluorescence excitation spectra for indole and the 7-azaindoles are decomposed into ¹L_a and ¹L_b components using the conventional analysis [18,21]. We shall discuss in detail when such an analysis may be inappropriate. For 7-azaindole, we compare the steady-state low temperature anisotropy, *r*₀, with the limiting anisotropy, *r*(0), obtained in time-dependent measurements in the liquid phase.

Experimental

Materials

Indole and D,L-7-azatryptophan (Sigma Chemical Co.) were used without further purification. 7-Azaindole (Sigma) was purified via flash chromatography [3,5,19] using ethyl acetate as a solvent. Detailed methods of synthesis and purification for 1M7AI and 7M7AI have been described elsewhere [5,20]. For the steady-state measurements, compounds were dissolved in propylene glycol to make 10-50 μM solutions. Solutions of low concentration are required to prevent aggregation of the solute during cooling.

Steady-State Measurements

Steady-state measurements were performed using a Spex Fluoromax (error of ± 0.5 nm) adapted to hold a quartz-windowed Dewar flask containing a 5 mm-diameter quartz sample tube. A methanol/dry ice slurry maintained a sample temperature of less than -60°C. All spectra were corrected. A 1-nm band-pass was used for excitation and emission.

We follow the procedure outlined by Valeur and Weber [18] and utilized by Eftink *et al.* [21] for the resolution of the excitation anisotropy spectra into two bands arising from ¹L_a and ¹L_b electronic transitions.

The steady-state anisotropy, r_0 , of a system is given by

$$r_0 = \frac{I_{\parallel} - I_{\perp}}{I_{\parallel} + 2I_{\perp}} \quad (1)$$

where I_{\parallel} is the emission polarized parallel to the excitation source and $I_{\perp} = gI_{\perp}^*$. g is a correction factor for the polarization dependence of the emission monochromator; and I_{\perp}^* is the uncorrected intensity of emission polarized perpendicular to the excitation source. g is obtained for a sample at room temperature, where the *steady-state* emission is expected to be completely depolarized. For our experiments, we define

$$g = \frac{I_{\parallel}}{I_{\perp}^*}$$

where the excitation source is polarized vertically in the laboratory frame for both emission measurements.

Time-Resolved Measurements

The time-correlated single-photon counting apparatus [5] and the data analysis for fluorescence anisotropy measurements are described elsewhere [22,23]. The time-dependent anisotropy, $r(t)$, is constructed in a manner similar to that of its steady-state counterpart. It is related to the correlation function of the transition dipole moment for absorption to state i at time zero, $\mu_{\text{abs}}^i(0)$, with the transition dipole moment for emission from state i at subsequent times, t , $\mu_{\text{em}}^i(t)$. For a sphere undergoing rotational diffusion by Brownian motion [24]:

$$r(t) = \frac{I_{\parallel}(t) - I_{\perp}(t)}{I_{\parallel}(t) + 2I_{\perp}(t)} = \frac{2}{5} \langle P_2[\mu_{\text{abs}}^i(0) \cdot \mu_{\text{em}}^i(t)] \rangle = \frac{2}{5} P_2(\cos\theta) \exp(-t/\tau_r) \quad (2)$$

$I_{\parallel}(t)$ and $I_{\perp}(t)$ are the time dependent fluorescence intensities parallel and perpendicular to the excitation polarization. P_2 is the second Legendre polynomial, θ is the angle formed by $\mu_{\text{abs}}(0)$ and $\mu_{\text{em}}(0)$, and τ_r is the diffusion relaxation time for a sphere (i.e., $\tau_r = 1/6 D$, D being

the diffusion coefficient). Accurate construction of the fluorescence anisotropy decay function demands that the sample be exposed to equivalent excitation intensity during the collection of the parallel and perpendicular emission profiles. Numerous methods have been proposed for the normalized collection of $I_{\parallel}(t)$ and $I_{\perp}(t)$. They have been summarized by Cross and Fleming [23]. In general, these methods fall into two categories: genuine simultaneous collection or alternate sampling procedures. If these methods are not adequate, the two curves must be scaled, "tail-matched," to have equal intensity at times where the fluorescence emission is *expected* to be depolarized. In the following, we present a method for acquiring fluorescence depolarization data without recourse to scaling procedures. This technique is based upon alternate detection of $I_{\parallel}(t)$ and $I_{\perp}(t)$, obviates the need for scaling procedures, and permits very precise measurements of fast reorientation times.

Automation of both polarizer movement and multichannel analyzer (MCA) operation provides our apparatus with the capability of sampling fluorescence at multiple orientations of the analyzer polarizer. A polarizer (Polaroid, HNP,B) is mounted on a modified motorized rotation stage (RSA-1TM, Newport Corp.) and is synchronously controlled in conjunction with the MCA (Norland 5500), making possible alternate readings of $I_{\parallel}(t)$ and $I_{\perp}(t)$. Polarization bias in our system is negligible. By alternately acquiring $I_{\parallel}(t)$ and $I_{\perp}(t)$, one may compensate for drift in the laser system over long periods of time, at least up to seven hours, thereby allowing for the collection of fluorescence depolarization data without recourse to scaling procedures. (Long-term drift in electronic components may still present a problem that is more difficult to compensate for.) Such compensation is crucial if the sample is weakly fluorescent and many hours of data accumulation are required. An IBM 386 clone controls both the rotation stage and the MCA under the direction of Asyst software, an advanced fourth-generation data acquisition and analysis language. Data transfer and MCA control are achieved over an RS-232 serial link connecting the computer to the MCA. The motorized rotation stage is interfaced to the computer via a parallel port connection to a manual-stage controller (Newport 860 SC-C). The operator specifies the data names in which to store the $I_{\parallel}(t)$ and $I_{\perp}(t)$ data, the maximum count of any channel that will terminate the experiment, the length of the $I_{\parallel}(t)$ and $I_{\perp}(t)$ acquisition times (usually 1-5 minutes), and the present orientation of the analyzer polarizer. Approaches similar to ours have been presented [25-32]. For example, Fayer and coworkers use a Pockels cell to rotate the polarization of their excitation beam by 90° every 20 seconds [33,34]. Millar *et al.* [35] describe an apparatus for sampling parallel and perpendicular emission intensities; but they

do not discuss the long-term reliability of their system, nor are the results calibrated against a standard.

One of the most thoroughly investigated dye molecules is the fluorescein derivative, rose bengal [33,34]. Figure 2.3 presents the data obtained for rose bengal in methanol at 20° C using an acquisition time of one minute for the $I_{\parallel}(t)$ and $I_{\perp}(t)$ curves. These data yield results that are in excellent agreement with literature values: ten measurements of $I_{\parallel}(t)$ and ten measurements of $I_{\perp}(t)$ yield a limiting anisotropy, $r(0) = 0.360 \pm 0.003$, and a rotational diffusion time, $\tau_r = 173 \pm 5$ ps. Above Figure 3 are displayed three sets of residuals corresponding, from top to bottom, to sampling times of 15, 2, and 1 min. As the sampling time is decreased, the fit of the data to a monoexponential anisotropy decay progressively improves, as measured by the χ^2 criterion, from $\chi^2 = 1.60, 1.26$, and 1.05. More importantly, attendant to this improvement in the fit is an increasingly more accurate value of the rotational diffusion time: 166 ps for a 15-min. sampling time and 179 ps for a 1-min. sampling time. The deviation in the residuals for the 15-minute sampling clearly indicates drift in the laser intensity on this time scale. In these experiments we have made no special effort to ensure long-term stability of our excitation source since our main concern is to demonstrate that *in its absence* it may be compensated for — especially when long accumulation times are required.

Results

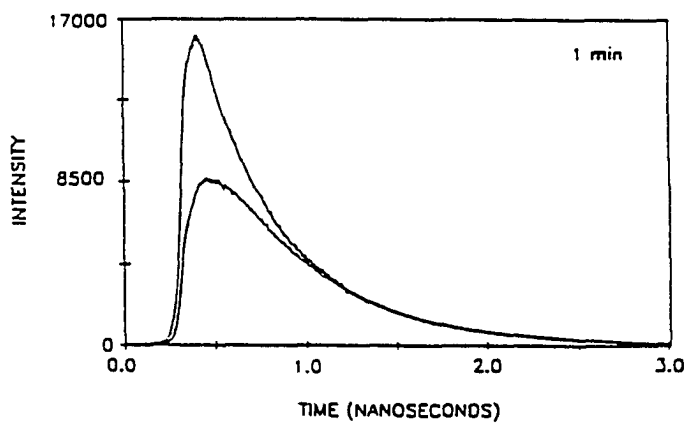
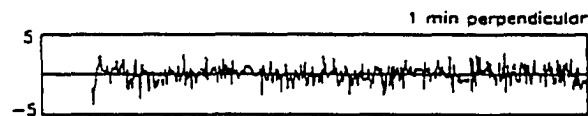
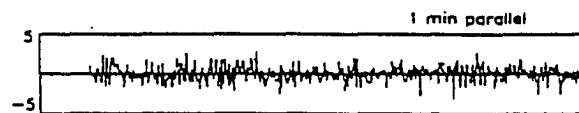
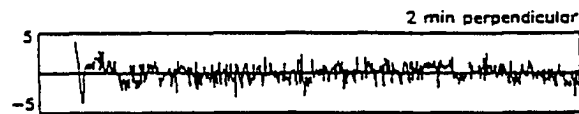
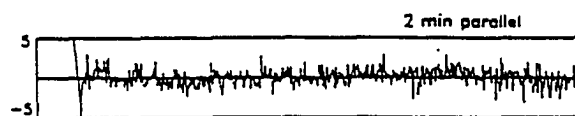
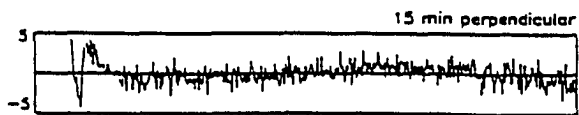
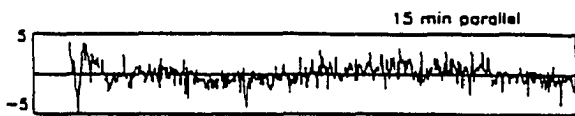
Resolution of the Steady-State Fluorescence Excitation Spectrum into 1L_a and 1L_b Bands

Valeur and Weber [18] and Eftink *et al.* [19] have used the results of steady-state fluorescence excitation anisotropy spectra to resolve the fluorescence excitation spectra of indole and its analogs into 1L_a and 1L_b spectra. The procedure is as follows. The measured steady-state anisotropy, $r_o(\lambda)$, is considered to be the sum of the contributions of the transitions connecting 1L_a and 1L_b with the ground state

$$r_o(\lambda) = f^a(\lambda)r_{oa} + f^b(\lambda)r_{ob} \quad (3)$$

where r_{oa} and r_{ob} are the anisotropies of each transition and $f^a(\lambda) + f^b(\lambda) = 1$. r_{ob} is obtained from r_{oa} by the relation

Figure 2.3. Fluorescence depolarization data for rose bengal in methanol at $20 \pm 0.5^\circ\text{C}$ using 1-minute accumulations: the upper trace corresponds to raw data for $I_{\parallel}(t)$; the lower, to $I_{\perp}(t)$. $\lambda_{\text{ex}} = 570 \text{ nm}$, $\lambda_{\text{em}} \geq 650 \text{ nm}$. Residuals obtained by fitting rose bengal anisotropy decays to one exponential are displayed above. The different sets of residuals correspond to different accumulation times for the rose bengal experiment. In descending order, we have: 15-minute accumulations (2.5-hour total acquisition time), $r(t) = 0.361 \exp(-t/166 \text{ ps})$, $\chi^2 = 1.60$; 2-minute accumulations (3.0-hour total acquisition time), $r(t) = 0.360 \exp(-t/172 \text{ ps})$, $\chi^2 = 1.26$; 1-minute accumulations (3.5-hour total acquisition time), $r(t) = 0.360 \exp(-t/179 \text{ ps})$, $\chi^2 = 1.05$. In all cases, the data were collected to 16,000 counts in the maximum channel. The excited-state decay was well-described by a single exponential with a 532-ps time constant. The rose bengal experiments were performed with an excitation wavelength at 570 nm and a power of 60 mW. For the 7-azaindole experiments, approximately 60 mW of 570-610 nm radiation was frequency doubled in a KDP crystal and used as the excitation pulse. The dye laser, pumped with $\sim 1 \text{ W}$ of the second harmonic of a cw mode-locked Nd:YAG was cavity dumped at 3.8 MHz. The instrument response function had a full-width at half maximum of 50-70 ps.



$$r_{ob} = r_{oa} P_2(\mu_{em}^{1L_a} \bullet \mu_{em}^{1L_b})$$

assuming $r_{oa} = r_o$ at the reddest excitation wavelengths. For indole, the angle formed by the emission dipole moments of 1L_a and 1L_b is believed to be very close to 90° [35]. It is also assumed that $(\mu_{abs}^{1L_a} \bullet \mu_{em}^{1L_a}) = 1$ and $(\mu_{abs}^{1L_b} \bullet \mu_{em}^{1L_b}) = 1$. The 1L_a and 1L_b fluorescence excitation spectra, $I_a(\lambda)$ and $I_b(\lambda)$, are thus resolved using the following relations. r_{oa} and r_{ob} are defined as the limiting steady-state anisotropies of a single emissive transition

$$f^a(\lambda) = \frac{r_o(\lambda) - r_{ob}}{r_{oa} - r_{ob}} \quad (4)$$

$$f^b(\lambda) = \frac{r_{oa} - r_o(\lambda)}{r_{oa} - r_{ob}}$$

$$I_a(\lambda) = f^a(\lambda)I(\lambda) \quad (5)$$

$$I_b(\lambda) = f^b(\lambda)I(\lambda)$$

involving either 1L_a or 1L_b , respectively. (Eftink *et al.* [19] describe some empirical criteria for determining whether a single state is responsible for the observed steady-state anisotropy spectrum.)

The assumptions underlying the spectral decomposition indicated by eqs 4 and 5 are quite severe and must be stated explicitly and commented upon.

1. In their original analysis of the steady-state anisotropy spectrum of indole, Valeur and Weber [18] assumed that at the very reddest excitation wavelengths the steady-state anisotropy arose *entirely* from 1L_a , which was known to lie below 1L_b in polar solvents [36,37]. Their assignment, however, of $r_{oa} = 0.3$ still required rationalization since this value is less than 0.4, the theoretical limiting value of the anisotropy (eq 2). The diminished anisotropy has been attributed to either an angle between $\mu_{abs}^{1L_a}$ and $\mu_{em}^{1L_a}$ that was greater

than 0° or, which is less likely, to exceedingly rapid depolarizing motion that could occur even in a glass [18,19,38].

2. The assumption that at the reddest excitation wavelengths the steady-state anisotropy arises entirely from 1L_a implies that at these wavelengths only 1L_a absorbs and emits radiation and that it is kinetically isolated from the 1L_b state. This assignment seems increasingly less valid as the measured values become lower. Eftink *et al.* [19] have arbitrarily picked 0.3 as the value below which the assumption is no longer valid.

3. The $I_a(\lambda)$ and $I_b(\lambda)$ excitation spectra resulting from the spectral decomposition must be carefully interpreted. It has been tacitly assumed that $I_a(\lambda)$ and $I_b(\lambda)$ represent the absorption spectra connecting 1L_a and 1L_b to the ground electronic state. But the fluorescence intensity is proportional to $I_0 \epsilon \phi_F$, where I_0 is the excitation intensity, ϵ is the extinction coefficient of the absorbing species, and ϕ_F is the fluorescence quantum yield. If ϕ_F varies with excitation wavelength, the fluorescence excitation spectra cannot be identified with absorption spectra. Such an excitation wavelength dependence of the quantum yield has been cited for indole [39]. We have also observed this dependence for both indole and 7-azaindole [40]. This will be discussed in greater detail elsewhere.

With these caveats in mind, we tested our experimental procedure by resolving the fluorescence excitation anisotropy spectrum of indole in propylene glycol at -60°C into contributions from the 1L_a and 1L_b electronic transitions (Figure 2.4). For purposes of comparison, we have resolved the excitation anisotropy spectrum by means of eqs 3-5 and have assumed that for 7-azaindole $\epsilon_{cm}^{1L_a} \cdot \mu_{cm}^{1L_b} \neq 0$. Our result is in excellent agreement with those of Valeur and Weber [18], except that our spectrum is blue-shifted by 2 nm with respect to theirs. We find anisotropy minima at 280.5 and 287.5 nm and a local maximum at 284.0 nm.

Figures 2.5-2.8 present the fluorescence excitation and emission spectra, and the fluorescence excitation anisotropy spectra for 7-azaindole and its derivatives. Resolved 1L_a and 1L_b spectra are presented for 7-azaindole (Figure 2.5). Substitution of a nitrogen for a carbon at the 7 position of indole produces a significant change in the anisotropy and the resolved 1L_a and 1L_b excitation spectra with respect to those observed for indole. The presence of the 1L_a and 1L_b bands in 7-azaindole had been suggested by the measurements of

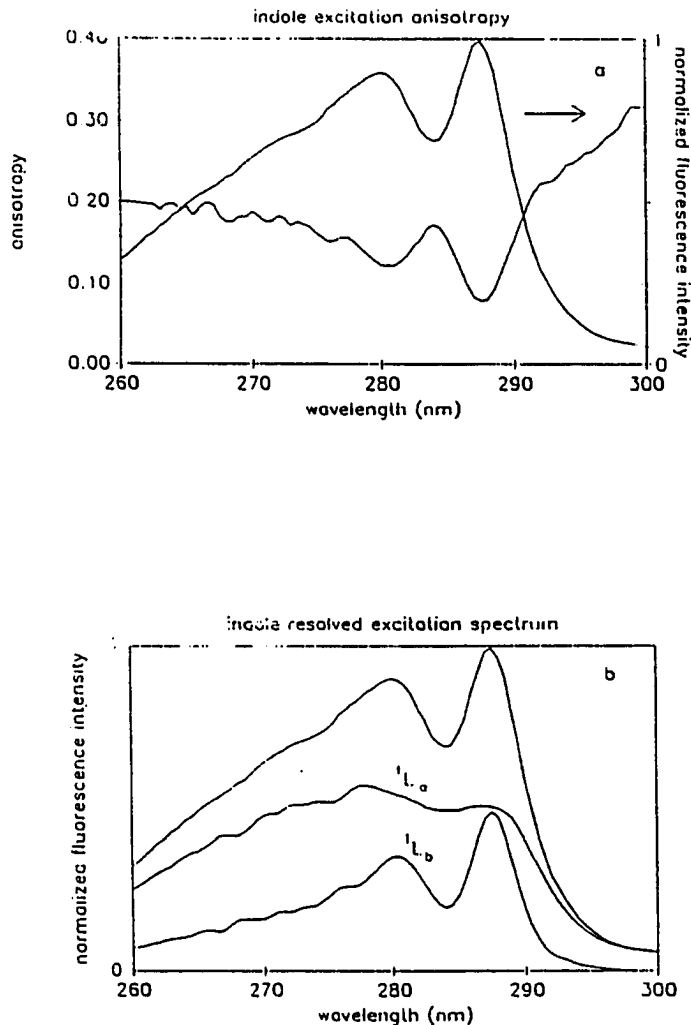
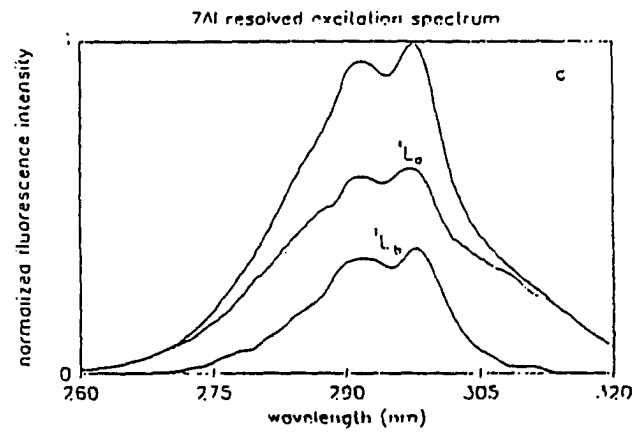
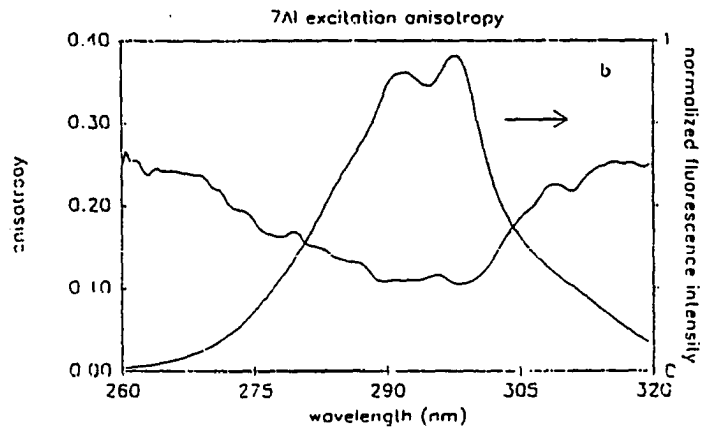
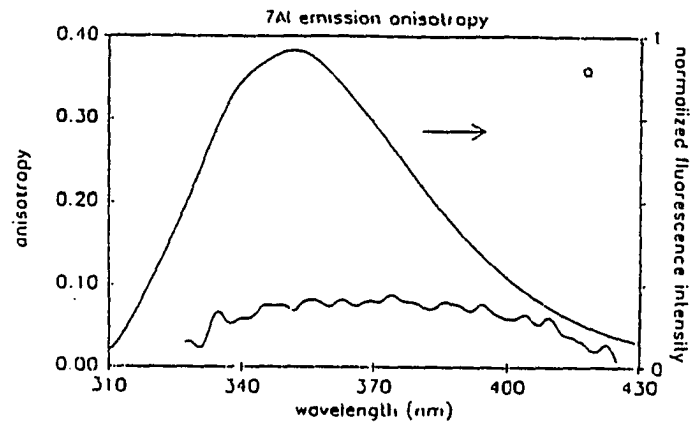


Figure 2.4. (a) The fluorescence excitation anisotropy of indole ($\lambda_{em} = 350$ nm). The emission anisotropy ($\lambda_{ex} = 286$ nm) was flat across the wavelength region studied and agreed with previous reports [18,19]. (b) The excitation spectrum of indole resolved into contributions from the 1L_a and 1L_b bands. $r_{0a} = 0.31$ and $r_{0b} = -0.16$. The values for r_{0a} and r_{0b} reported here and in Figures 5-8 were determined using the methods of Valeur and Weber [18] and Eftink *et al.* [19]. This technique requires the assumption that at the reddest wavelengths only 1L_a absorbs and emits radiation. Refer to the text for further discussion of these calculations.

Figure 2.5. (a) The emission anisotropy of 7-azaindole ($\lambda_{\text{ex}} = 295.5$ nm). At wavelengths less than 330 nm and greater than 425 nm, the emission anisotropy became too noisy to resolve. (b) The fluorescence excitation anisotropy of 7-azaindole ($\lambda_{\text{em}} = 372$ nm). $r_0 = 0.19$ at $\lambda_{\text{ex}} = 305$ nm; $r_0 = 0.14$ at $\lambda_{\text{ex}} = 285$ nm. (c) The excitation spectrum of 7-azaindole resolved into contributions from the 1L_a and 1L_b bands. $r_{0a} = 0.25$ and $r_{0b} = -0.13$.



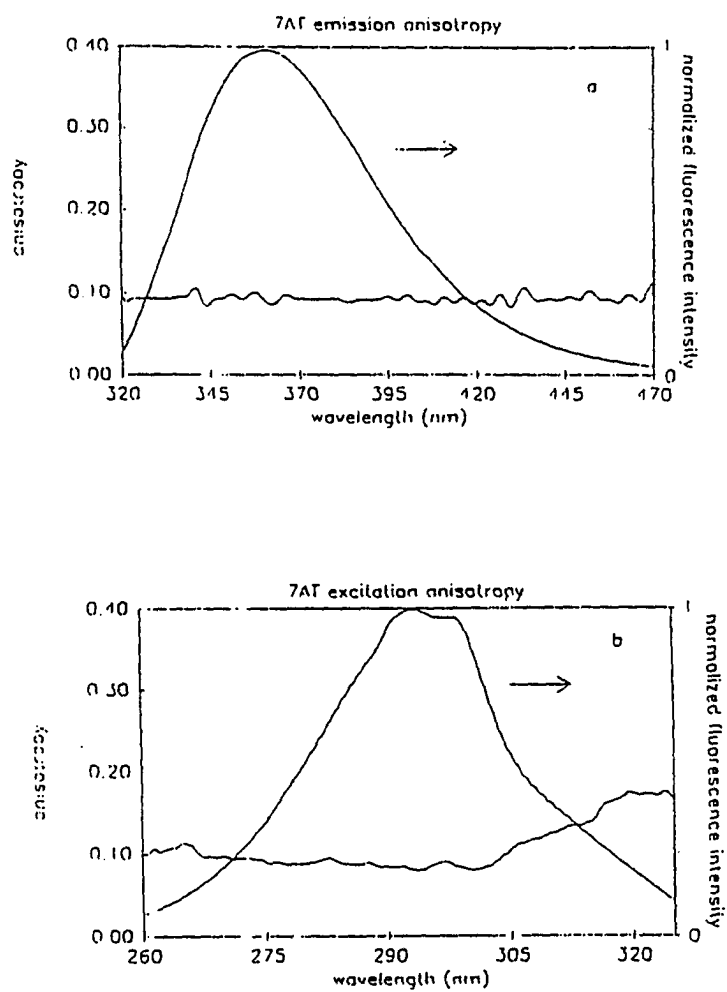


Figure 2.6. (a) The emission anisotropy of 7-azatryptophan ($\lambda_{\text{ex}} = 295$ nm). (b) The fluorescence excitation anisotropy of 7-azatryptophan ($\lambda_{\text{em}} = 362$ nm).

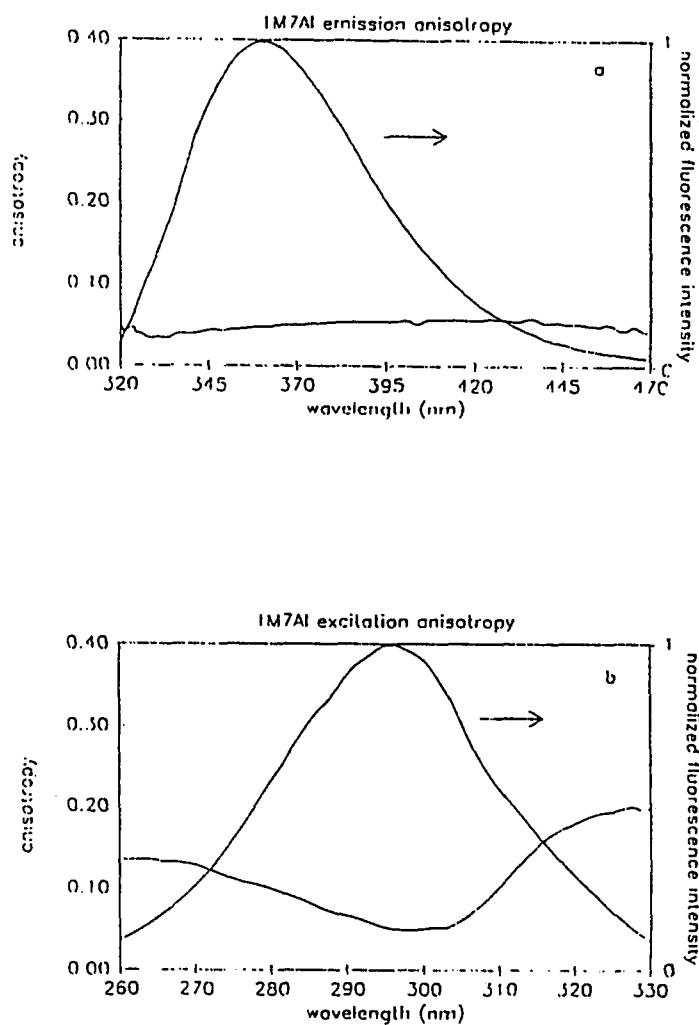


Figure 2.7. (a) The emission anisotropy of 1M7AI ($\lambda_{\text{ex}} = 295$ nm). (b) The fluorescence excitation anisotropy of 1M7AI ($\lambda_{\text{em}} = 361$ nm).

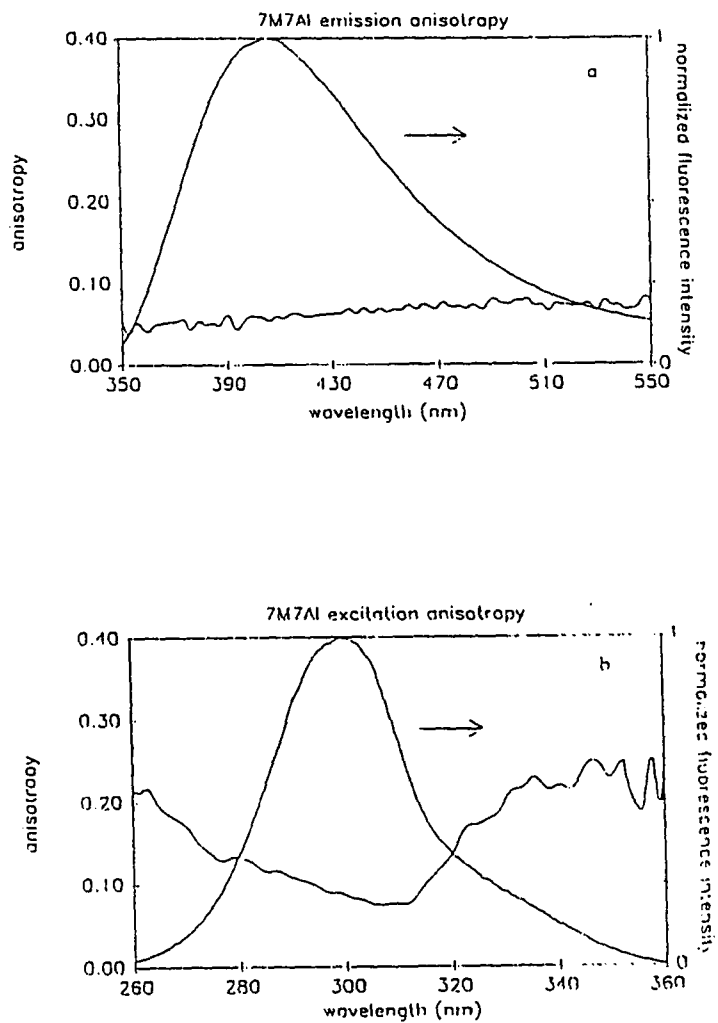


Figure 2.8. (a) The emission anisotropy of 7M7AI ($\lambda_{\text{ex}} = 300$ nm). (b) The fluorescence excitation anisotropy of 7M7AI ($\lambda_{\text{em}} = 420$ nm).

Bulska *et al.* [41]. For indole, a strong 1L_b 0-0 transition is apparent at 287.5 nm, yet the analogous transitions at 298.0 nm for 7-azaindole and 300.5 nm for 7-azatryptophan are much less pronounced. Resolved excitation spectra of the methylated derivatives (not shown) lack the structure observed in those of 7-azaindole and 7-azatryptophan, showing only a slowly varying change in the proportions of the 1L_a and 1L_b transitions. Similar to that of indole, the 1L_a contribution of these compounds is broad, absorbing over a much larger wavelength region than that of 1L_b , and is less structured than the 1L_b contribution. For reasons that are listed above and elaborated in detail in the Discussion, the resolution of the fluorescence excitation spectrum of indole, 7-azaindole, and their derivatives can only be considered to be qualitative.

Fluorescence Anisotropy Decay

For 7-azaindole in water, the limiting anisotropy, $r(0)$, was examined at 285 and 305 nm. At each wavelength, the time-resolved measurement agrees closely with that determined via steady-state techniques (Table 2.1 and Figure 2.5a). Table 2.2 demonstrates that the fluorescence excitation spectra at 20° and -60°C are essentially the same for all the compounds considered here. The fluorescence anisotropy decay of the normal and the tautomer bands of 7-azaindole were measured in butanol and in methanol (Table 2.1 and Figure 2.9). A notable result is that in methanol at $\eta = 0.93$ cP (-9.0°C), the parallel and perpendicular emission curves of the tautomer are superposable and hence the tautomer *appears* to be completely depolarized. On the other hand, the parallel and perpendicular emission of the normal band are distinct and may be fit to yield $r(0) = 0.11$ when $\lambda_{ex} = 285$ and $r(0) = 0.21$ when $\lambda_{ex} = 305$ nm. A rotational diffusion time, τ_r , of 34 ps is obtained in both cases (Table 2.1).

For 7-azaindole in the alcohols the limiting anisotropy, $r(0)$, for the tautomer appears to be significantly less than that for the normal species: in fact, for viscosities such that $\eta < \sim 3$ cP, $r(0)$ for the tautomer is ~ 0 (Table 2.1). At higher viscosities, for example $\eta = 6.96$ cP, one begins to discern a measurable $r(0)$, (i.e., $r(0) = 0.004$), for the tautomer and hence becomes able to resolve a rotational diffusion time that is comparable to that obtained from the normal band, 174 ps. This is reasonable, since *a priori* there is no reason why the rotational diffusion time of the tautomer should be different from that of the normal species.

The power of the time-correlated single-photon counting technique, coupled with our method of data collection, is demonstrated by our ability to obtain consistent limiting

Table 2.1
Fluorescence Anisotropy Decay of 7-Azaindole

solvent, T(°C) ^a	η (cP) ^b	species, λ_{em} (nm)	τ_F (ps) ^c	$r(0)^d$	$r(0)^e$	τ_r (ps) ^{e,f}
				$\lambda_{ex} = 305$ nm	$\lambda_{ex} = 285$ nm	
butanol, -9.0	6.96	normal, 320-460	358 ± 6	--	0.10 ± 0.01	191 ± 9
		tautomer, > 505	$254 \pm 19; 1552 \pm 36$	--	0.004^g	174
butanol, 20.0	2.92	normal, 320-460	241 ± 6	--	0.10 ± 0.01	82 ± 13
		tautomer, > 505	$210 \pm 7; 989 \pm 19$	--	unresolved	unresolved
methanol, -9.0	0.93	normal, 320-460	211 ± 6	0.21 ± 0.01	0.11 ± 0.02	34 ± 8
		tautomer, > 505	$192 \pm 6; 837 \pm 16$	--	unresolved	unresolved
water, 2.0	1.67	entire band ^h , > 320	1263 ± 14	0.21 ± 0.01	0.11 ± 0.01	41 ± 6
water, 23.5	0.92	entire band ^h , > 320	886 ± 15	0.20 ± 0.05	0.12 ± 0.06	20 ± 2

- ^a Temperatures are certain to within $\pm 0.5^\circ\text{C}$.
- ^b From reference 54. $1 \text{ cP} = 1.0 \times 10^{-3} \text{ N m}^{-2} \text{ s}$.
- ^c The normal form in alcohols and the species in water are characterized by a single-exponential fluorescence decay. The time-resolved emission of the tautomer band in alcohols is fit to the function $K(t) = A_1 \exp(-t/\tau_1) + A_2 \exp(-t/\tau_2)$, where $A_1 < 0$ for the rising component of the fluorescence, whose contribution to the emission is normalized to unity and is given in parentheses by $|A_1|/(|A_1| + |A_2|)$. For the tautomer, the first number is the risetime; the second, the decay time.
- ^d The absence of a value indicates that the measurement was not performed.
- ^e "Unresolved" indicates that the emitting species was not sufficiently polarized at time zero to obtain a meaningful result, in other words $r(0) \sim 0$.
- ^f Where applicable, we present averages of experiments performed at both $\lambda_{\text{ex}} = 285 \text{ nm}$ and $\lambda_{\text{ex}} = 305 \text{ nm}$.
- ^g This low value reflects the similar time scales of tautomerization and rotational diffusion. If the transition dipole moment for emission from the excited-state tautomer were different from the transition dipole moment for the absorbing species by approximately 50° , the $r(0)$ for 7-azaindole in methanol would be reduced by a factor of 10, thus rendering its measurements very difficult. As appealing as it may be to invoke this explanation to explain the low values of $r(0)$ for the tautomer, the data may be rationalized without it. It is sufficient to note that at all viscosities except that for butanol at -9°C , 6.96 cP, the rise time of the tautomer emission is at least 2.5 times longer than the rotational diffusion time (as obtained from the normal species). Clearly, one cannot detect polarized fluorescence if the time scale for the formation of the polarized species is longer than that for its depolarization.
- ^h The majority of the 7-azaindole population in water is not capable of tautomerization [3-5], hence it is inappropriate to refer to it as "normal." And even though its fluorescence lifetime, quantum yield, and behavior with respect to deuterium substitution are tautomer-like, it is not a "tautomer." Because of these distinctions, we have referred to this species as "blocked" [5].

Table 2.2
Steady-State Measurements of 7-Azaindole and Related Compounds

compound ^a	$\lambda_{\text{ex}}^{\text{max}}$, nm (20°C)	$\lambda_{\text{ex}}^{\text{max}}$, nm (-60°C)	$\lambda_{\text{em}}^{\text{max}}$, nm (20°C)	$\lambda_{\text{em}}^{\text{max}}$, nm (-60°C)
indole	272, 287	287	330	~290 ^b
7-azaindole	290.5, 297	290.5, 297	371	353
7-azatryptophan	297.5 ^c	287.5, 290.5 ^{c,d}	380	361
1M7AI	285	285	381	361
7M7AI	291	291	440	405

^a All compounds were dissolved in propylene glycol and diluted to a final concentration of 10-50 μM .

^b Valeur and Weber [18] report an emission maximum of ~ 330 nm for indole at -58°C. This is the maximum we observe at room temperature. We observe a distinct blue-shift of the emission maximum as the sample is cooled. At -60°C, the emission maximum is slightly less than 300 nm. We are unable to obtain fluorescence spectra below 300 nm that have been corrected for instrument response.

^c A shoulder is apparent at 298 nm in the excitation spectrum of 7-azatryptophan.

^d The excitation spectra of each compound at 20°C and -60°C have similar shapes and maxima. When 7-azatryptophan is cooled, however, structure becomes apparent and two relative maxima are observed.

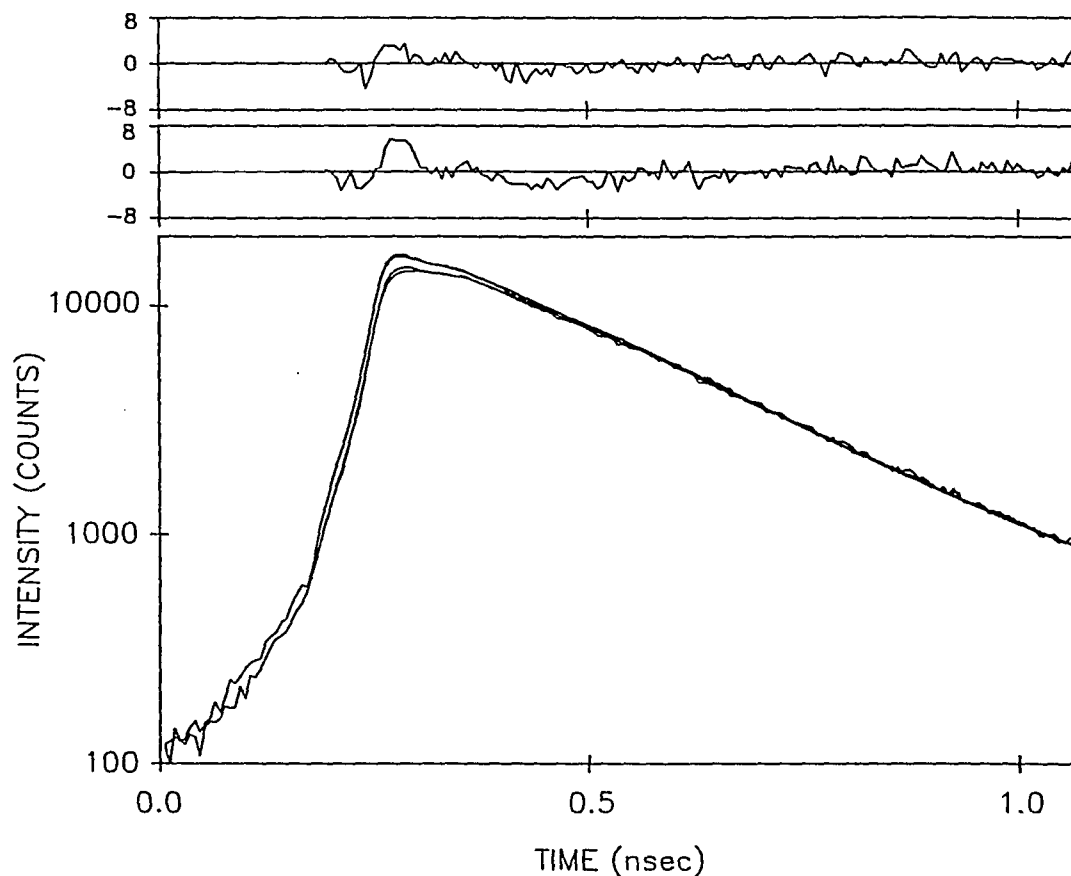


Figure 2.9. Fluorescence anisotropy decay of the normal band of 7-azaindole in methanol at -9°C (0.93 cP). For the normal band, $r(t) = 0.10 \exp(-t/36 \text{ ps})$, $\chi^2 = 1.43$. The upper set of residuals refers to $I_{||}$; the lower, to I_{\perp} . For the tautomer band, no difference was observed between the parallel and perpendicular fluorescence intensities, and hence, a limiting anisotropy and a rotational diffusion time could not be resolved. The excitation wavelength was 285 nm. See the text and Table I for further details. Two-minute acquisition times are typically employed for $I_{||}(t)$ and $I_{\perp}(t)$. Modeling the anisotropy as a double exponential does not significantly improve the fit and, in fact, produces unphysical results such as negative amplitudes or exceedingly long rotation times.

anisotropy and rotational diffusion times (Table 2.1) with parallel and perpendicular emission curves that differ only slightly on the rising edges and the maxima (Figures 2.9 and 2.10).

Discussion

Comparison of Steady-State and Time-Dependent Measurements

From a comparison of Table 2.1 and Figure 2.5b, it can be seen that, for the excitation wavelengths investigated, the low limiting anisotropy, $r(0)$, obtained in time-dependent measurements is the same, within experimental error, as that obtained in steady-state measurements, r_0 . Because the same results are obtained in liquid butanol, methanol, and water on the one hand and in propylene glycol glass on the other hand, the low limiting anisotropy may be attributed to nonmotional factors rather than to a rapid component of rotational diffusion that lies beyond the time resolution of our apparatus and that is expected to be viscosity dependent.

Similarly, the limiting anisotropy extrapolated for tryptophan using data obtained on time scales > 5 ps is less than 0.4, is wavelength dependent, and agrees with the steady-state results for indole [42]. First Cross *et al.* [43] and then Szabo [44] demonstrated how the presence of two excited electronic states whose energy gap is close to kT can influence the short time anisotropy decay and hence give rise to apparently anomalously low $r(0)$ values if the anisotropy measurement is not performed with sufficient time resolution. Subsequently, Fleming and coworkers [45] experimentally observed these effects in tryptophan and in the single-tryptophan-containing hormone and protein, melittin and *Pseudomonas aeruginosa* azurin, respectively. Subpicosecond resolution reveals $r(0) = 0.4$ and rapid components of anisotropy decay in the range of 1-4 ps.

In the specific case where there are two closely lying excited states, 1L_a and 1L_b , the measured anisotropy decay function is a function of both wavelength and time [43].

$$r(\lambda, t) = \frac{k_R^a g^a(\lambda) r^a(t) K^a(t) + k_R^b g^b(\lambda) r^b(t) K^b(t)}{k_R^a g^a(\lambda) K^a(t) + k_R^b g^b(\lambda) K^b(t)} \quad (6)$$

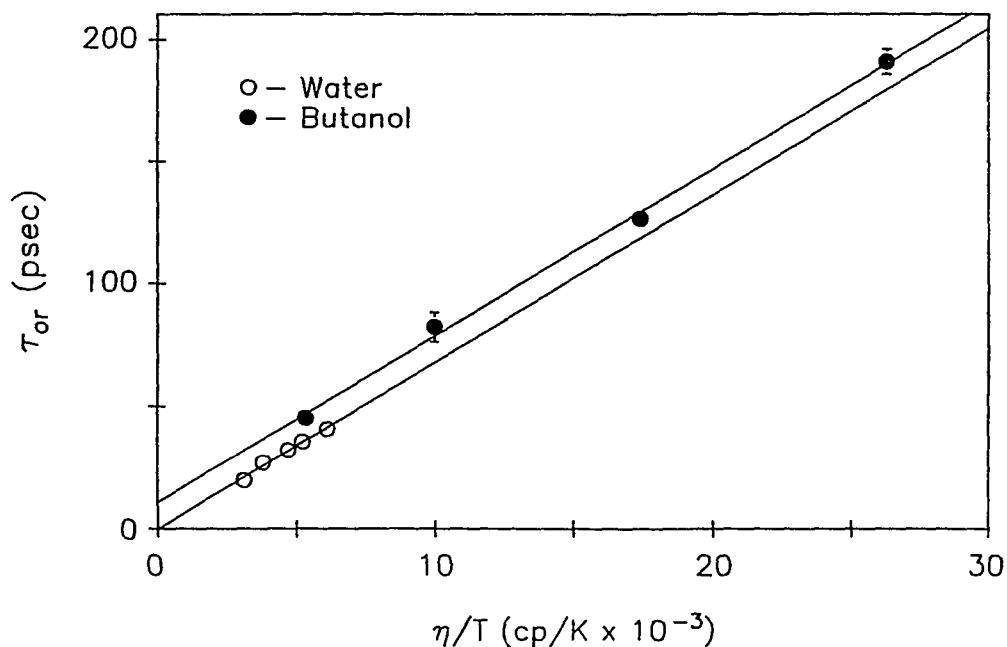


Figure 2.10. Plots of the rotational diffusion (reorientation) time, τ_r , against η/T for the normal band of 7-azaindole in butanol (●) and for 7-azaindole in water (○). Emission wavelengths are noted in Table I. The τ_r data presented are averages from at least four measurements at a given viscosity using either an excitation wavelength of 285 or 305 nm. The data are fit to the relation, $\tau_r = c\eta + \tau_0$, where $c = V/kT$ if the diffusing species is a sphere. Both the butanol and the water data yield slopes such that $V = 94.1 \pm 3.2 \text{ \AA}^3$. This volume is corrected in the text for an oblate ellipsoid. The intercepts are the "free rotor" times and are 10.6 ± 3.8 and -0.2 ± 2.4 ps for butanol and water, respectively. These are in good agreement with the estimated free rotor time of about 1 ps.

where $k_R^{a,b}$ are the radiative rate constants, $K^{a,b}(t)$ are the population (fluorescence) decay laws, and $g^{a,b}(\lambda)$ are the emission line shapes, whose integrals are normalized to unity, of the 1L_a and 1L_b states. Thus, when two nearby states can be reached from the ground state in an optical transition (or if the upper state can be thermally populated), the observed anisotropy decay is a superposition of the individual anisotropy decays. The form of the observed anisotropy decay will depend strongly on the extinction coefficient connecting the ground electronic state to 1L_a or 1L_b , which will determine $K^{a,b}(t=0)$, as well as on the relative contribution of emission from the two states that is detected at a given wavelength.

Using the level scheme depicted in Figure 2.11, the following rate constants [46] are defined.

$$k^a = k^b = k_R^a + k_{NR}^a \quad (7)$$

Here we assume that $k_R^a = k_R^b$. We also assume that the sum of the rate constants of the nonradiative processes depleting 1L_a and 1L_b , neglecting internal conversion, is the same for both levels: $k_{NR}^a = k_{NR}^b$. Further aspects of the kinetic analysis are described in detail elsewhere [42-44].

The steady-state anisotropy obtained in a glass, r_0 , and the limiting anisotropy obtained at room temperature, $r(0)$, are expected to be very similar if the 1L_b - 1L_a energy gap and if the internal conversion rate do not change significantly with temperature. r_0 can be determined from the approximation

$$r_0 \equiv \int_0^{\infty} r(t) dt \quad (8)$$

that is valid as long as the nonmotional contributions to the anisotropy are very rapid compared to those from rotational diffusion. In a glass, where $\tau_r \sim 0$, this condition is easily satisfied. $r(0)$ is determined by extrapolating the long-time behavior of eq 6 back to $t=0$.

We assume that $g^a(\lambda) = g^b(\lambda)$ and that only 1L_a is optically excited. For tryptophan, $k^a = k^b = 3.3 \times 10^8 \text{ s}^{-1}$ [42]. 10^{12} s^{-1} and 500 cm^{-1} are taken for the values of k_{ba} and the 1L_b - 1L_a energy gap [42,43]. For -60°C and 20°C , r_0 and $r(0)$ are calculated to be 0.38 and 0.36, respectively.

This calculation indicates that thermal population of the 1L_b level will reduce the limiting anisotropy. But the limiting anisotropy is still much larger than those obtained for 7-azaindole and its derivatives. In fact, in order to obtain $r(0) = 0.20$, it is necessary that for the

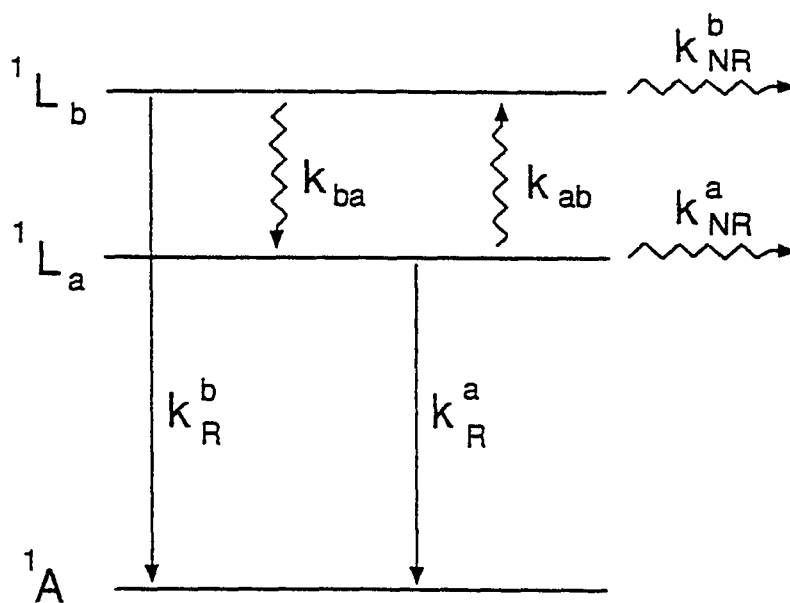


Figure 2.11. Energy level diagram for the ground electronic state and the two closely-lying excited electronic states, 1L_a and 1L_b , in 7-azaindole and indole. In the text, we assume that $k_R^a = k_R^b$. We also assume that the sum of the nonradiative rates depopulating 1L_a and 1L_b in the absence of internal conversion and thermal equilibration are the same, $k_{NR}^a = k_{NR}^b$. k_{ab} is calculated from given values of the internal conversion rate, k_{ba} , and the 1L_b - 1L_a energy gap.

same emission profiles, internal conversion rate, and energy gap, there is significant optical population of 1L_b . In other words, this requires the initial populations of the 1L_a and 1L_b states, $K^a(0)$ and $K^b(0)$ are such that $K^a(0):K^b(0) = 2.4:1$ at -60°C and $K^a(0):K^b(0) = 2.1:1$ at 20°C . For simplicity, in these analyses we have not taken into consideration the depletion of the 1L_b state by the production of solvated electrons [4,40].

These calculations lead us to conclude that the low $r(0)$ values observed for the normal form of 7-azaindole in alcohols and for the fluorescent species of 7-azaindole in water are a result of both level kinetics *and* of absorption by 1L_b *even at the reddest excitation wavelengths*. We noted earlier that a standard assumption used in decomposing fluorescence excitation anisotropy spectra is that at the reddest excitation wavelengths only the lower of the two states is optically populated. This assumption may not be a good one for indole, where it has been asserted that $r_0 = r_{0a} = 0.3$ [18]; and it is most likely not appropriate for 7-azaindole and its derivatives. We have, nevertheless, employed this method of analysis because it indicates clearly, albeit only qualitatively, the presence of the 1L_a and 1L_b states.

In discussing the low values of $r(0)$, we have assumed that $(\mu_{abs}^{1L_a} \bullet \mu_{em}^{1L_a}) = 1$ and that $(\mu_{abs}^{1L_b} \bullet \mu_{em}^{1L_b}) = 1$. An angle between the absorption and emission moments for these respective transitions would, however, contribute to a lowering of $r(0)$ (eq 2). Fleming and coworkers [42] have proposed a mechanism that provides such an angle. If there is vibronic mixing between the 1L_a and 1L_b states and if the rate of vibrational relaxation is much larger than the rates of interconversion between these two states, k_{ba} and k_{ab} , then an angle is introduced between the initially excited Franck-Condon vibronic state and the vibronic state that is detected in emission.

Solvent Interactions with Normal, Tautomer, and "Blocked" 7-Azaindole Species

In alcohols, the fluorescence emission of 7-azaindole is characterized by two bands with distinct and widely separated maxima as well as different fluorescence lifetimes [2-5, 11-14]. The redder of the two bands observed in alcohols is attributed to an excited-state tautomer. Consequently, the bluer of the two bands is attributed to a "normal" species. An intriguing characteristic of the emission of 7 azaindole in water is that *only* a smooth band is detected and the fluorescence lifetime is *single exponential* when emission is collected over the entire band over most of the pH range. Previously we suggested that the fluorescent species in water was predominantly "tautomer-like" because it bears some similarities with respect to fluorescence quantum yield and the deuterium isotope effect of its fluorescence

lifetime with the tautomer in alcohols [2]. As mentioned in the Introduction and discussed in detail elsewhere [5], although a small fraction of the population in water is capable of tautomerization, the majority of the 7-azaindole molecules do not tautomerize [16]. We have referred to this solute population as "blocked" in order to distinguish it from the "normal" and the "tautomer" species. We have suggested that tautomerization is not possible for the "blocked" species because of its inability to form the appropriate geometry with the solvent, the idealized cyclic intermediate (Figure 2.2), during the lifetime of the excited state. Chou *et al.* [15] have commented on this phenomenon and have made the distinction between a 7-azaindole monohydrate and a 7-azaindole polyhydrate, the latter being incapable of tautomerization.

The blocked species possesses a short fluorescence lifetime and low quantum yield relative to the normal analog (1M7AI); 910 ps and 0.03 as compared with 21 ns and 0.55, respectively [5]. These traits, along with the deuterium isotope effect [5], render the photophysics of the blocked species more like that of the tautomer species. On the other hand, in water the emission maximum is at 386 nm instead of 510 nm, as it is for the tautomer analog (7M7AI) [5].

In the light of our recent results, we no longer consider it useful to discuss the "blocked" species as being "tautomer-like." We thus feel that referring to the blocked species as either normal or tautomer is not appropriate when all the data are taken into account since it shares features of both.

The reorientation times obtained for 7-azaindole (Table 2.1 and Figure 2.10) allow us to compare the bulk solute-solvent interactions in different solvents. Figure 2.0 indicates that the normal form of 7-azaindole in butanol and the blocked species of 7-azaindole in water have, within experimental error, the same linear dependence of rotational diffusion time with respect to η/T . This indicates that the bulk interactions of 7-azaindole with butanol and water are the same. Bauer *et al.* [47] have suggested the empirical relationship, $\tau_r = c\eta + \tau_0$. From the slopes of the data presented in Figure 2.10, the apparent volume of the rotationally diffusing species may be determined. If the species is a sphere, $c = V/kT$; and the data presented in Figure 2.10 yield $V = 94 \text{ \AA}^3$ for both butanol and water, (for other molecular shapes, however, a correction must be applied) [47,48]. This experimental volume is in very good agreement with the "theoretical volume" of 104 \AA^3 that may be determined from a consideration of van der Waals increments [51]. This agreement is somewhat surprising since the experimental value is determined by assuming a spherical shape for the solute and

by completely ignoring specific solute-solvent interactions, such as those depicted in Figure 2.2, for example.

Conclusions

Despite the single-exponential fluorescence decay of the nonnatural amino acid, 7-azatryptophan, compared with the nonexponential decay of tryptophan and the significant spectroscopic differences between 7-azaindole and indole [2-5], these two chromophores are much more similar to one another than might have been expected. Not only do they share the same pathways of nonradiative decay in water, photoionization and intersystem crossing [3,4,40,49], but they also possess similar excited-state structure as is manifested by closely-lying 1L_a and 1L_b states. The proximity of these two states is responsible for the wavelength dependence and the low value of the limiting anisotropy in steady-state and time-dependent measurements. Because of these effects, 7-azaindole can only be used as a probe of protein dynamics (in fluorescence depolarization measurements) on time scales of greater duration than the nonmotional depolarizing event (i.e., ~ 5 ps). Absorption anisotropy must be performed if motion is to be detected unambiguously on a finer time scale.

Acknowledgment

We thank Professor G. R. Fleming for making available to us the simultaneous fitting programs developed by A. J. Cross. J.W.P. is an Office of Naval Research Young Investigator. D.E.N. was supported by a NASA summer internship. Additional support was provided by the Iowa State University Biotechnology Council and IPRT. Travel support was provided to M.N. by NATO.

References

1. Négrerie, M.; Bellefeuille, S. M.; Whitham, S.; Petrich, J. W.; Thornburg, R. W. *J. Am. Chem. Soc.* **1990**, *112*, 7419.
2. Négrerie, M.; Gai, F.; Bellefeuille, S. M.; Petrich, J. W. *J. Phys. Chem.* **1991**, *95*, 8663.
3. Gai, F.; Chen, Y.; Petrich, J. W. *J. Am. Chem. Soc.* **1992**, *114*, 8343.
4. Négrerie, M.; Gai, F.; Lambry, J.-C.; Martin, J.-L.; Petrich, J. W. In *Ultrafast Phenomena VIII*, Eds. Martin J.-L.; Migus, A.; Springer: New York, 1993; p. 621.
5. Chen, Y.; Rich, R. L.; Gai, F.; Petrich, J. W. *J. Am. Chem. Soc.* **1993**, *97*, 1770.
6. Taylor, C. A.; El-Bayoumi, M. A.; Kasha, M. *Proc. Natl. Acad. Sci. USA* **1969**, *63*, 253.
7. Ingham, K. C.; Abu-Elgheit, M.; El-Bayoumi, M. A. *J. Am. Chem. Soc.* **1971**, *93*, 5023.
8. Ingham, K. C.; El-Bayoumi, M. A. *J. Am. Chem. Soc.* **1974**, *96*, 1674.
9. Hetherington, W. M., III; Micheels, R. M.; Eisenthal, K. B. *Chem. Phys. Lett.* **1979**, *66*, 230.
10. Share, P. E.; Sarisky, M. J.; Pereira, M. A.; Repinec, S. T.; Hochstrasser, R. M. *J. Lumin.* **1991**, *48/49*, 204.
11. Avouris, P.; Yang, L. L.; El-Bayoumi, M. A. *Photochem. Photobiol.* **1976**, *24*, 211.
12. McMorrow, D.; Aartsma, T. J. *Chem. Phys. Lett.* **1986**, *125*, 581.

13. Konijnenbeg, J.; Huizer, A. H.; Varma, C. A. G. O. *J. Chem. Soc. Faraday Trans. 2* **1988**, *84*, 1163.
14. Moog, R. S.; Maroncelli, M. *J. Phys. Chem.* **1991**, *95*, 10359.
15. Chou, P.-T.; Martinez, M. L.; Cooper, W. C.; Collins, S. T.; McMorrow, D. P.; Kasha, M. *J. Phys. Chem.* **1992**, *96*, 5203.
16. While the conclusions of Chou *et al.* [15] are qualitatively consistent with our results [5], another report of the photophysics of 7-azaindole in water has been submitted by C. F. Chapman and M. Maroncelli (*J. Phys. Chem.* **1992**, *96*, 8430). In their study, Chapman and Maroncelli propose that all of the 7-azaindole population tautomerizes in water with a rate constant of $1.2 \times 10^9 \text{ s}^{-1}$. We have discussed this proposal in detail [5].
17. Petrich, J. W.; Chang, M. C.; McDonald, D. B.; Fleming G. R. *J. Am. Chem. Soc.* **1983**, *105*, 3824; Szabo, A. G.; Rayner, D. M. *J. Am. Chem. Soc.* **1980**, *102*, 554.
18. Valeur, B.; Weber, G. *Photochem. Photobiol.* **1977**, *25*, 441.
19. Eftink, M. R.; Selvidge, L. A.; Callis, P. R.; Rehms, A. A. *J. Phys. Chem.* **1990**, *94*, 3469.
20. Still, W. C.; Kahn, M.; Mitra, A. *J. Org. Chem.* **1978**, *43*, 2923.
21. Robison, M. M.; Robison, B. L. *J. Am. Chem. Soc.* **1955**, *77*, 6555.
22. Chang, M. C.; Courtney, S. J.; Cross, A. J.; Gulotty, R. J.; Petrich, J. W.; Fleming, G. R. *Anal. Instrum.* **1985**, *14*, 33.
23. Cross, A. J.; Fleming, G. R. *Biophys. J.* **1984**, *46*, 45.
24. Tao, T. *Biopolymers*, **1969**, *8*, 609.

25. Hanson, D. C.; Ygeurabide, J.; Schumaker, V. N. *Biochemistry* **1981**, *20*, 6842.
26. Ricke, J.; Amsler, K.; Binkert, Th. *Biopolymers* **1983**, *22*, 1301.
27. Martin, C. E.; Foyt, D. C. *Biochemistry* **1978**, *17*, 3587.
28. Easter, J. H.; DeToma, R. P.; Brand, L. *Biophys. J.* **1976**, *16*, 571.
29. Munro, I.; Pecht, I.; Stryer, L. *Proc. Natl. Acad. Sci. USA* **1979**, *76*, 55.
30. Stein, A. D.; Peterson, K. A.; Fayer, M. D. *J. Chem. Phys.* **1990**, *92*, 5622.
31. Stein, A. D.; Hoffman, D. A.; Frank, C. W.; Fayer, M. D. *J. Chem. Phys.* **1992**, *96*, 3269.
32. Millar, D. P.; Robbins, R. J.; Zewail, A. H. *J. Chem. Phys.* **1982**, *76*, 2080.
33. Fleming, G. R.; Morris, J. M.; Robinson, G. W. *Chem. Phys.* **1976**, *17*, 91.
34. Cramer, L. E.; Spears, K. G. *J. Am. Chem. Soc.* **1978**, *100*, 221.
35. Yamamoto, Y.; Tanaka, J. *Bull. Chem. Soc. Jpn.* **1972**, *45*, 1362.
36. Strickland, E. H.; Horwitz, J.; Billups, C. *Biochemistry* **1970**, *9*, 4914.
37. Mataga, N.; Torihashi, Y.; Ezumi, K. *Theor. Chim. Acta* **1964**, *2*, 158.
38. Jablonski, A. *Acta Phys. Pol. B* **1965**, *28*, 717.
39. Steen, H. B. *J. Chem. Phys.* **1974**, *61*, 3997.
40. Gai, F.; Rich, R. L.; Petrich, J. W. *J. Am. Chem. Soc.* **1994**, *116*, 735.
41. Bulska, H.; Grabowska, A.; Pakula, B.; Sepiol, J.; Waluk, J.; Wild, U. P. *J. Lumin.* **1984**, *29*, 65.

42. Ruggiero, A. J.; Todd, D. C.; Fleming, G. R. *J. Am. Chem. Soc.* **1990**, *112*, 1003.
43. Cross, A. J.; Waldeck, D. H.; Fleming, G. R. *J. Chem. Phys.* **1983**, *78*, 6455; *79*, 3173.
44. Szabo, A. *J. Chem. Phys.* **1984**, *81*, 150.
45. Hansen, J. E.; Rosenthal, S. J.; Fleming, G. R. *J. Phys. Chem.* **1992**, *96*, 3034.
46. The expressions in references 46 and 47 for l_1 and l_2 need to be interchanged.
47. Bauer, D. R.; Brauman, J. I.; Pecora, R. *J. Am. Chem. Soc.* **1974**, *96*, 3034.
48. Shimizu, H. *J. Chem. Phys.* **1962**, *37*, 765.
49. Bent, D. V.; Hayon, E. *J. Am. Chem. Soc.* **1975**, *97*, 2612.
50. Viswanath, D. S.; Natarajan, G. *Data Book on the Viscosity of Liquids*. 1989, Hemisphere Publishing Company, New York.
51. Edward, J. T. *J. Chem. Educ.* **1970**, *47*, 261.

CHAPTER 3. 7-AZAINDOLE AND 7-AZATRYPTOPHAN DERIVATIVES AS OPTICAL PROBES OF BIOLOGICAL SYSTEMS: METHYLATION OF THE AROMATIC NITROGENS

Introduction

In previous chapters the role of the chromophoric N_1 in the photophysical behavior of 7-azatryptophan has been discussed. The proton on N_1 is responsible for many of the fluorescence characteristics of 7-azatryptophan. This proton may interact with the solvent and undergo internal conversion to the ground state or states of solvation that favor excited-state tautomerization [1,2]. Methylation of N_1 inhibits such interactions. Methylation of N_1 and N_7 of 7-azaindole and the justifications for performing these syntheses are discussed in Chapters 1 and 2; the synthesis and discussion of N_1 -methyl-7-azatryptophan is found in Chapter 4. We propose here that other 7-azatryptophan derivatives may have significant advantages as optical probes of biological systems. Current work on these syntheses are outlined below.

Syntheses

In published syntheses, methylation at the N_1 position in tryptophan has required "preparing the disodium salt of tryptophan in liquid ammonia and then allowing it to react with alkyl halides" [3]. We propose an alternative method of methylation that requires little precaution. We have employed this procedure in the synthesis of N_1 -methyl-7-azatryptophan and assume that it may become generally applicable in the alkylation of aromatic nitrogens. Suitable methylating agents and various reaction conditions have been outlined by Epling and Kumar [4].

Proposed Methylation of 7-Azatryptophan at the N_7 Position to Yield D,L-7-Methyl-7-Azatryptophan

In the event we should want to further study the tautomeric form of 7-azatryptophan, a methylated- N_7 derivative should be simple to synthesize. This is expected to require four steps: (1) blocking the alkyl nitrogen with a protecting group such as *N-t*-Boc; (2)

methylating N₇ by preparing N-*t*-Boc-7-methyl-7-azatryptophan-*p*-toluenesulfonate; (3) isolating N-*t*-Boc-7-methyl-7-azatryptophan; and (4) deprotecting the alkyl nitrogen. The protection and deprotection steps should be the same as those used in the synthesis of N₁-methyl-7-azatryptophan (see Chapter 4). The preparation of 7-methyl-7-azaindole via a *p*-toluenesulfonate intermediate is simple [2] and produces product in high yield, so the method of Robison and Robison is recommended for the methylation steps [5].

Synthesis of N₁-Alkyl-7-Azatryptophan Analogs

Our previous syntheses have focused on preserving the original tryptophan-like configuration in the methylations of 7-azaindole and 7-azatryptophan. We now suggest that alkylation of the 7-azaindole N₁ with an amino acid side chain would yield a chromophore suitable for tryptophan substitution. Two significant advantages of this new molecule are: (1) its overall size matches that of tryptophan, thereby eliminating any concerns about a protruding methyl group, as in N₁-methyl-7-azatryptophan, and (2) the end product amino acids obtained are stereochemically pure. The compounds we are currently synthesizing are depicted in Figure 3.1. The synthesis of the N₁-substituted-7-azaindole is a two-step procedure: (1) formation of the β -lactone precursor, and (2) reaction between the β -lactone and 7-azaindole to form the N₁-alkylated-7-azaindole. The procedure of Arnold *et al.* [6] is followed in this synthesis and the steps are outlined below. Synthesis of the other compounds is performed using this method, but replacing 7-azaindole with the appropriate indole derivative.

Synthesis of N-t-Boc-L-Serine- β -Lactone. 0.500 g Ph₃P is dissolved in five mL dry THF under argon at -78°C. 390 μ L diethylazodicarboxylate is added dropwise and the solution is allowed to stir for ten minutes at -78°C. N-*t*-Boc-serine dissolved in five mL dry THF is added dropwise to the mixture. After 20 minutes, the chilling bath is removed and the yellow slurry is stirred at room temperature for three hours.

Formation of N₁-Alkyl-7-Azaindole. 57 mg 7-azaindole in four mL CH₃CN is added to 100 mg N-*t*-Boc-L-serine- β -lactone dissolved in six mL CH₃CN. This mixture is heated at 50°C for 12 hours. The solvent is removed *in vacuo*.

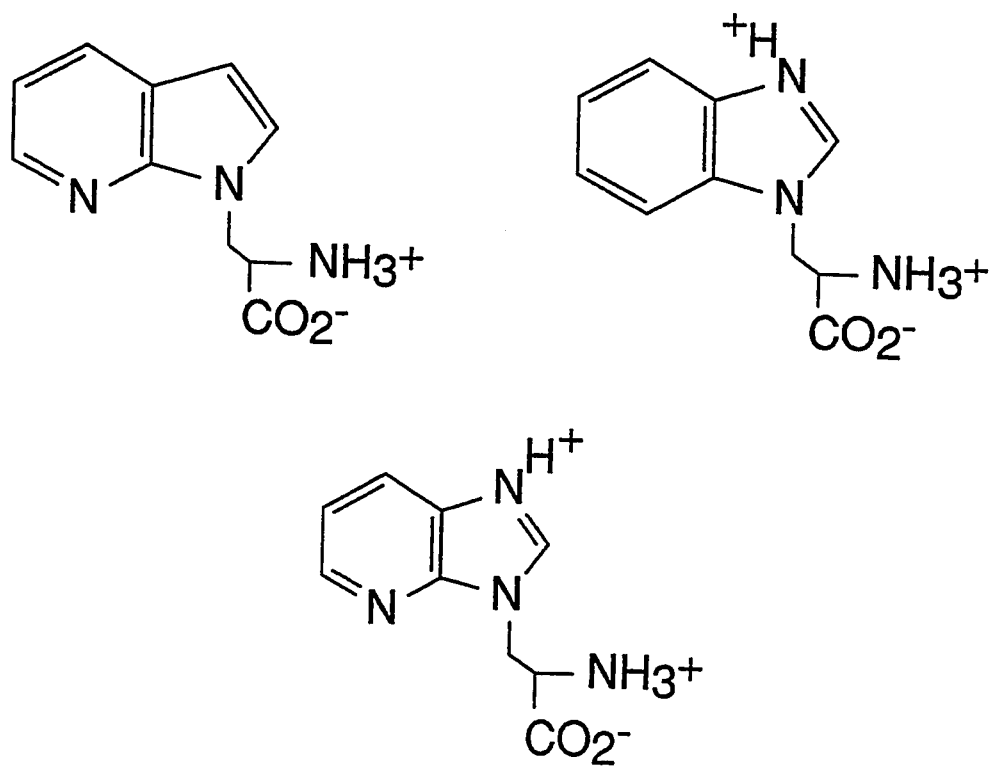


Figure 3.1. Structures of proposed 7-azatryptophan analogs.

References

1. Gai, F.; Chen, Y.; Petrich, J. W. *J. Am. Chem. Soc.* **1992**, *114*, 8343; Chen, Y.; Gai, F.; Petrich, J. W. *J. Am. Chem. Soc.* **1993**, *115*, 10158; Chen, Y.; Gai, F.; Petrich, J. W. *Chem. Phys. Lett.*, **1994**, *222*, 329.
2. Chen, Y.; Rich, R. L.; Gai, F.; Petrich, J. W. *J. Phys. Chem.* **1993**, *97*, 1770.
3. Yamada, S., Shiori, T., Taisuke, I., Hara, T., Matsueda, R. *Chem. Pharm. Bull.* **1965**, *12*, 88.
4. Epling, G. A.; Kumar, A. *Synlett.* **1991**, 347.
5. Robison, M. M. and Robison, B. L. *J. Am. Chem. Soc.* **1955**, *77*, 6554.
6. Arnold, L. D.; Kalantar, T. H.; Vederas, J. C. *J. Am. Chem. Soc.*, **1985**, *107*, 7105.

CHAPTER 4. SYNTHESIS AND PHOTOPHYSICAL ANALYSIS OF THE OPTICAL PROBE, N₁-METHYL-7-AZATRYPTOPHAN

A paper submitted to *J. Am. Chem. Soc.*

R. L. Rich¹, A. V. Smirnov¹, A. W. Schwabacher¹, and J. W. Petrich^{1,2}

Abstract

The development of a new intrinsic optical probe of protein structure and dynamics, N₁-methyl-7-azatryptophan, is reported. The utility of this nonnatural amino acid derivative lies in its single-exponential, long-lived fluorescence decay (21.7 ± 0.4 ns) and in its high fluorescence quantum yield (0.53 ± 0.07). Its absorption and emission maxima are red-shifted 10 and 65 nm, respectively, from those of tryptophan. These characteristics permit its unambiguous detection with unprecedented discrimination against emission from multiply occurring native tryptophan residues. In a mixture of these two amino acids, no tryptophan signal is detected until the tryptophan:N₁-methyl-7-azatryptophan ratio exceeds 75:1. Consequently, N₁-methyl-7-azatryptophan is ideal for studying the interactions of small peptides containing it with large proteins.

Introduction

The difficulties in using tryptophan as an optical probe of protein structure and dynamics are well known. Tryptophan has an intrinsic nonexponential fluorescence decay and it occurs multiply in most proteins of interest [1-7]. Consequently, we have devoted considerable effort to the development and characterization of the nonnatural amino acid, 7-azatryptophan, as an alternative optical probe [8-19], and other groups have subsequently begun to exploit its properties [20,21]. 7-Azatryptophan has a single exponential

¹ Graduate students, Assistant Professor, and Associate Professor, respectively; Department of Chemistry, Iowa State University.

² To whom correspondence should be addressed.

fluorescence decay (780 ps in water, pH 7 and 20°C) and the location of its absorption and emission maxima permit it to be detected unambiguously in the presence of up to ten tryptophan residues [8,11,16]. Furthermore, it is amenable to peptide synthesis and can be incorporated into bacterial protein [8,11]. These qualities are extremely useful, especially when short-time dynamics are of interest and when there are a limited number of tryptophans present. We have, however, demonstrated in a recent study of biotinylated 7-azatryptophan in complex with avidin that the relatively low fluorescence quantum yield of 7-azatryptophan (0.03 in water, pH 7) can diminish its utility when long-time dynamics are of interest [19].

In order to address problems where long-time dynamics are of interest and many tryptophan residues are present, it is necessary that the optical probe have both a long-lived excited state and a high fluorescence quantum yield. We had already suggested that N₁-methyl-7-azatryptophan (Figure 4.1) conformed to these requirements [19] based on our understanding of the photophysics of the 7-azaindole chromophore [9-19]. The most significant nonradiative properties of 7-azaindole (in particular, those that distinguish it from indole) are determined by the N₁ proton and its interactions with the solvent. In alcohols [9,15,17,22,23] (and to a small degree in water [13,24-26]) this proton participates in an excited-state double-proton transfer. Internal conversion promoted by the interaction of this proton with the solvent has also been suggested [27]. The importance of the N₁ proton in the nonradiative process of 7-azaindole is demonstrated most vividly by the methylation of N₁: in water, the fluorescence lifetime and quantum yield increase from 910 ps and 0.03 to 21.0 ns and 0.55 [13]. We anticipated that the methylated analog of 7-azatryptophan would possess the same characteristics [13,19]. This article demonstrates that it does and comments on the utility of this result.

Materials and Methods

Synthesis

The preparation of N₁-methyl-7-azatryptophan was performed in three steps: blocking the alkyl nitrogen of D,L-7-azatryptophan with a protecting group to form N-*t*-Boc-D,L-7-azatryptophan, deprotonation using lithium diisopropylamide and subsequent methylation of the pyrrolic nitrogen with methyl mesylate to form N-*t*-Boc-N₁-methyl-D,L-7-azatryptophan, and deprotection of the alkyl nitrogen to yield the final product, N₁-methyl-D,L-7-azatryptophan.

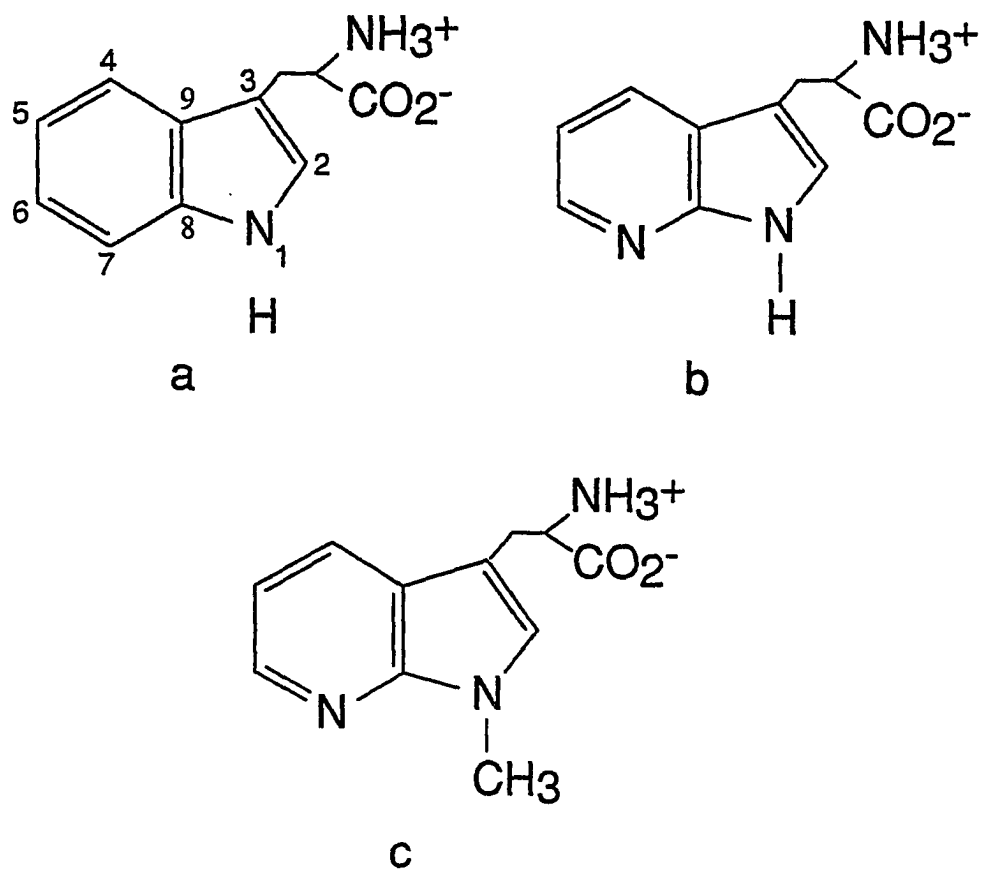


Figure 4.1. Structures of (a) tryptophan, (b) 7-azatryptophan, and (c) N_1 -methyl-7-azatryptophan.

Synthesis of N-t-Boc-D,L-7-azatryptophan. The method used was slightly modified from that of Bodansky and Bodansky [28] and has been briefly outlined in our previous work [11]. Triethylamine (515 μ L, 3.67 mmol, Kodak) was added to D,L-7-azatryptophan (500 mg, 2.44 mmol, Sigma) stirring in 1.5 mL water/1.5 mL dioxane. As 2-butoxycarbonyloxyimino-2-phenylacetonitrile (665 mg, 2.70 mmol, BOC-ON, Aldrich) was added, the mixture became yellow. After stirring for one hour, all material had dissolved. The solution was stirred for three more hours. Four mL water and five mL ethyl acetate were added to the solution, and the aqueous fraction was extracted twice with five mL portions of ethyl acetate. The aqueous layer was acidified to pH 4 with crystalline citric acid and was filtered. The precipitate was washed with dilute citric acid and ethyl acetate, and dried *in vacuo* to yield N-t-Boc-D,L-7-azatryptophan (0.70 g, 94%). m.p. = 232-236 $^{\circ}$ C. 1 H NMR (300 MHz, $(\text{CD}_3)_2\text{SO}$): δ 12.60 (s, 1H), 11.41 (s, 1H), 8.21 (d, 1H, 3.9 Hz), 7.98 (d, 1H, 7.8 Hz), 7.30 (s, 1H), 7.08 (dd, 1H, $J_1=7.5\text{Hz}$, $J_2=3.3\text{Hz}$), 4.18 (br, 1H), 3.19-2.94 (m, 3H), 1.34 (s, 9H). Calcd for $\text{C}_{15}\text{H}_{19}\text{N}_3\text{O}_4$: C, 59.01, H, 6.27, N, 13.76. Found: C, 58.77, H, 6.29, N, 13.52. MS (EISP): 305.1 [M] $^+$.

Methylation of N-t-Boc-D,L-7-azatryptophan. Diisopropylamine (595 μ L, 4.23 mmol, Sigma) was added to seven mL anhydrous THF and stirred under argon at -78°C for 15 minutes. *n*-Butyl lithium (2.35 mL, 2.1 M, 4.94 mmol, Johnson Matthey Catalog Co.) in hexanes was added dropwise to the amine solution. This mixture was stirred at -78°C for one hour, then warmed to room temperature. At this time, the solution was added dropwise to a slurry of N-t-Boc-D,L-7-azatryptophan (500 mg, 1.64 mmol) stirring in seven mL anhydrous THF/1.5 mL anhydrous DMSO chilled to -78°C under an argon atmosphere. The slurry became yellow upon addition of the amide. This mixture was kept at -78°C for one hour, then allowed to warm to room temperature. The solution was again chilled to -78°C and methyl methanesulfonate (220 μ L, 2.60 mmol, Aldrich) [29] was added. The acetone/dry ice bath is removed after three hours and the solution continued to stir for 15 hours. The reaction was quenched with 15 mL water and extracted three times with ethyl acetate. Isolation of this product was as for N-t-Boc-D,L-7-azatryptophan to yield N-t-Boc-D,L-N₁-methyl-7-azatryptophan. m.p. = 217-218 $^{\circ}$ C. 1 H NMR:(300 MHz, $(\text{CD}_3)_2\text{SO}$) δ 12.67 (s, 1H), 8.27 (d, 1H, 4.2 Hz), 8.01 (d, 1H, 7.2 Hz), 7.34 (s, 1H), 7.10 (dd, 1H, $J_1=6.9\text{Hz}$, $J_2=4.2\text{Hz}$), 4.17 (br, 1H), 3.80 (s, 3H), 3.18-3.04 (m, 3H), 1.35 (s, 9H). Calcd for $\text{C}_{16}\text{H}_{21}\text{N}_3\text{O}_4\cdot\text{H}_2\text{O}$: C, 56.97; H, 6.82; N, 12.46. Found: C, 57.91; H, 6.82; N, 12.65. MS (EISP): 319.2 [M] $^+$.

Deprotection of N-t-Boc-D,L-N₁-methyl-7-azatryptophan. N-t-Boc-N₁-methyl-7-azatryptophan (100 mg, 0.32 mmol) was dissolved in one mL concentrated hydrochloric acid

and allowed to stir for one hour. The solution was then concentrated to near dryness by rotary evaporation. One mL water was added and the solution was again evaporated to near dryness. This last step was repeated, then one mL water was added to the solution and solid lithium hydroxide was added to neutralize the solution. The solution was then evaporated to dryness. After addition of two mL isopropanol to dissolve the lithium chloride, the solution was filtered and the remaining solids were washed repeatedly with isopropanol to yield N₁-methyl-7-azatryptophan. The NMR spectrum confirmed the absence of the N-*t*-Boc protecting group, but otherwise agreed with that obtained for N-*t*-Boc-D,L-N₁-methyl-7-azatryptophan. m.p.: decomposition began at ~235 °C, with sharp melting at 292 °C.

Spectroscopic Measurements

Fluorescence lifetimes were obtained by means of time-correlated single-photon counting [13,14]. Owing to the long fluorescence lifetime (Table 4.1) of N₁-methyl-7-azatryptophan, a 50-ns full-scale time window was required to characterize it properly. The fluorescence decays of mixtures of one N₁-methyl-7-azatryptophan to varying amounts of tryptophan were measured in order to determine what level of tryptophan produces an appreciable background signal. These measurements were performed on a 3-ns time scale in order to be more sensitive to onset of the tryptophyl fluorescence lifetime, especially its subnanosecond component (Table 4.2). The fluorescence decays of the mixtures were adequately fit to one or a sum of two exponentially decaying components: $F(t) = A_1 \exp(-t/\tau_1) + A_2 \exp(-t/\tau_2)$, where $A_1 + A_2 = 1.00$. Two exponentials only became necessary at probe:tryptophan ratios of less than 1:75. Consequently, we made no attempt to attach physical significance to the lifetimes or their weights, but concentrated on the visual deviation of the fluorescence decays of the mixtures with respect to the probe alone and on the average fluorescence lifetime computed from the decay parameters: $\langle \tau \rangle = A_1 \tau_1 + A_2 \tau_2$ (Figure 4.4 and Table 4.2). The N₁-methyl-7-azatryptophan concentration was 2-20 μM for these experiments and the tryptophan concentration was adjusted accordingly.

Results and Discussion

The absorption and emission spectra of N₁-methyl-7-azatryptophan and tryptophan are shown in Figure 4.2. Table 4.1 summarizes the steady-state and the time-resolved data. Because of the shift in the absorption and emission spectra of N₁-methyl-7-azatryptophan

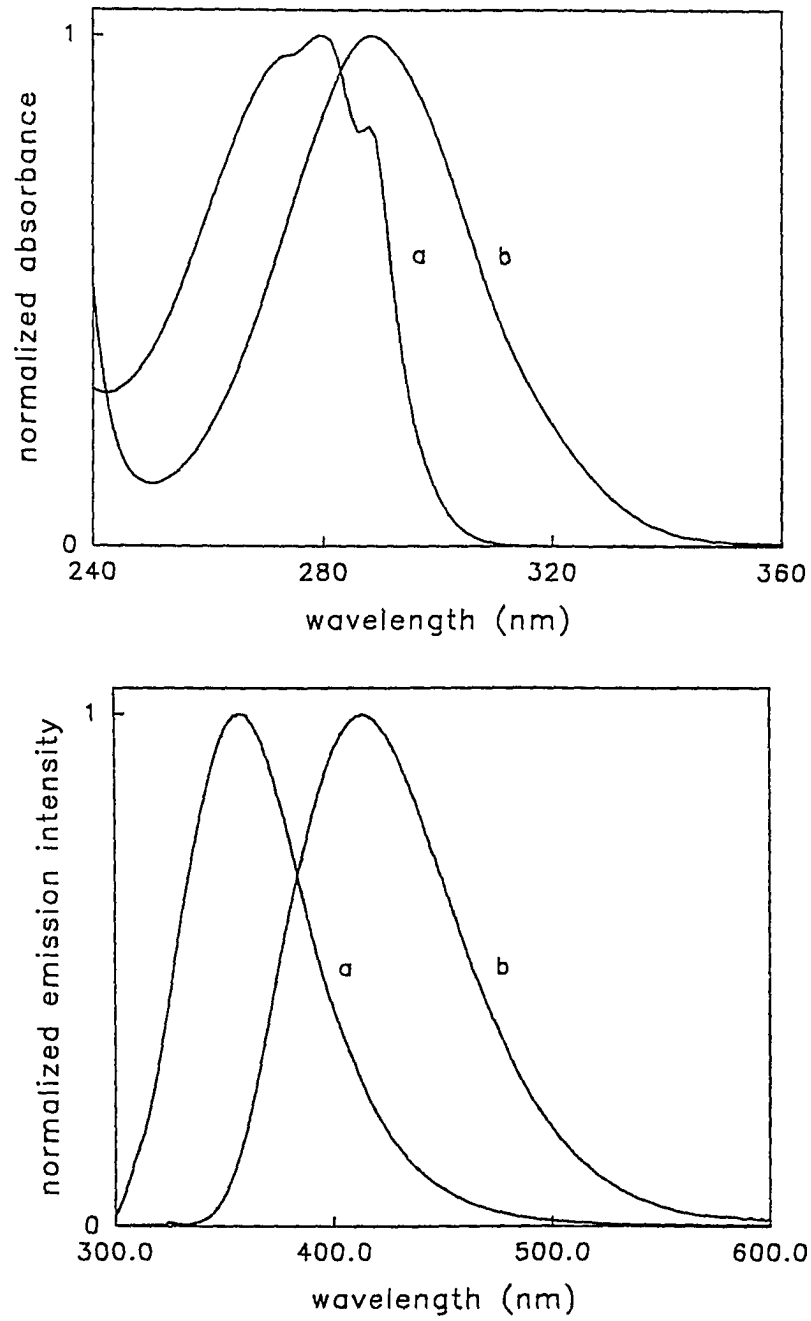


Figure 4.2. Comparison of the normalized absorption (top) and emission (bottom) of (a) tryptophan and (b) N₁-methyl-7-azatryptophan.

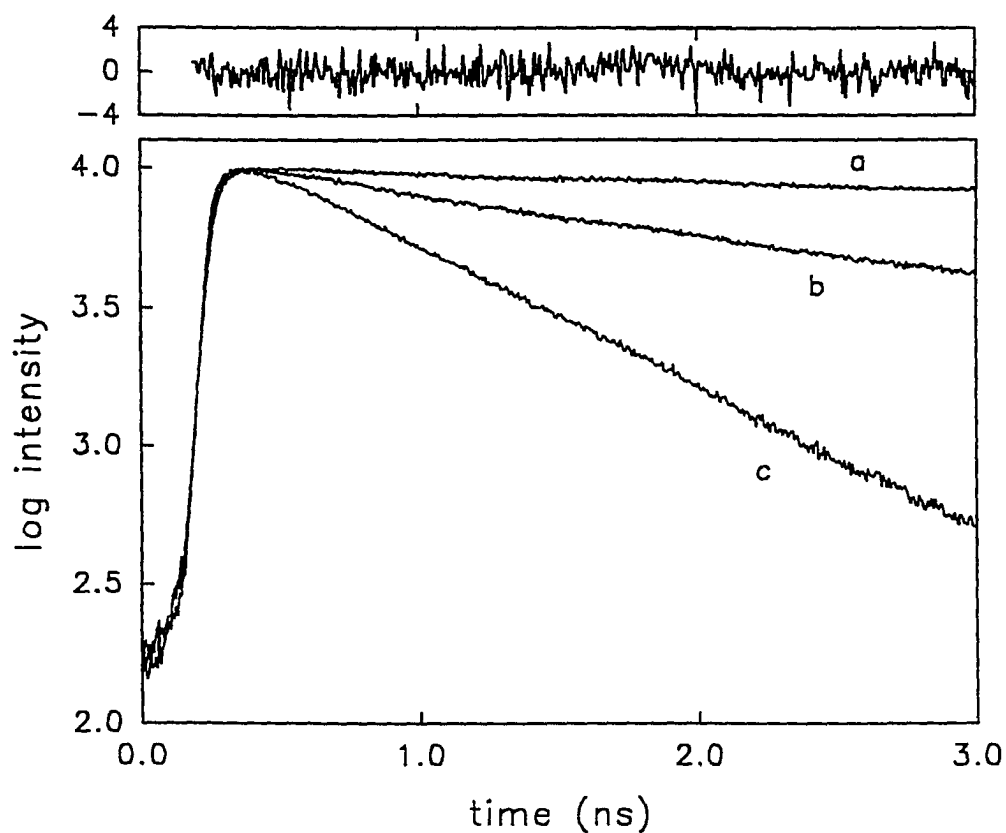


Figure 4.3. Fluorescence decay of (a) N_1 -methyl-7-azatryptophan in water: pH 7.0, 20°C; $\lambda_{\text{ex}} = 310\text{nm}$; $\lambda_{\text{em}} \geq 455\text{ nm}$, $F(t) = 1.00 \exp(-t/22.8\text{ns})$, $\chi^2 = 1.07$; (b) tryptophan: pH 7.0, 20°C; $\lambda_{\text{ex}} = 310\text{nm}$; $\lambda_{\text{em}} \geq 320\text{ nm}$, $F(t) = 0.16 \exp(-t/332\text{ps}) + 0.84 \exp(-t/3.08\text{ns})$, $\chi^2 = 1.13$; and (c) 7-azatryptophan in water: pH 7.0, 20°C; $\lambda_{\text{ex}} = 310\text{nm}$; $\lambda_{\text{em}} \geq 375\text{ nm}$, $F(t) = 1.00 \exp(-t/812\text{ps})$, $\chi^2 = 1.16$. Fluorescence decay parameters of each species are listed in Table 1. These experiments were performed on a 3-ns time scale to emphasize the monoexponential fluorescence decay lifetime of N_1 -methyl-7-azatryptophan.

Table 4.1. Summary of Photophysical Data.

compound ^a	$\lambda_{\text{abs}}^{\text{max}}$ (nm)	$\lambda_{\text{em}}^{\text{max}}$ (nm)	ϵ (M ⁻¹ cm ⁻¹) ^b	ϕ_f	A_1^c	τ_1 (ns)	τ_2 (ns) ^d
tryptophan	280 [35]	351 [16]	5400 [35]	0.18 [22]	0.22 ± 0.01	0.62 ± 0.050	3.2 ± 0.1 [1]
7-azatryptophan	288 [11]	397 [16]	6200 [11]	0.03 [22]	1.00	0.78 ± 0.10 ^e [16]	---
NAc-P(7AT)N-NH ₂	289	397	6200 ^g		1.00	0.83 ± 0.010	---
NAc-KACP(7AT)- NCD-NH ₂ ^f	289	396	6200 ^g		0.84 ± 0.04	0.85 ± 0.010	0.19 ± 0.03
N- <i>t</i> -Boc-N ₁ -methyl-7- azatryptophan	289	414	8300 ^h	0.47 ± 0.02	1.00	16.1 ± 1.1	---
N ₁ -methyl-7-aza tryptophan	289	409	8300 ^h	0.53 ± 0.07	1.00	21.7 ± 0.4	---
SIIN(1M7AT)EKL ⁱ	289	406	8300 ^h	0.52 ± 0.06	1.00	16.4 ± 0.3	---

^a Zwitterionic forms of all amino acids, measured at 20°C.

^b The extinction coefficients are measured at the absorption maxima.

^c Fluorescence lifetimes are fit to a double exponential of the form $F(t) = A_1 \exp(-t/\tau_1) + A_2 \exp(-t/\tau_2)$, where $A_1 + A_2 = 1.00$

^d The absence of an entry indicates that the fluorescence decay was best fit to a single exponential.

^e Nonexponential fluorescence decay can be detected in 7-azatryptophan in water if emission is collected with a sufficiently narrow bandwidth on the blue or red edge of the spectrum [13].

^f Experiments were performed under aqueous conditions in which the cysteine residues were assumed to be reduced thiols.

^g The extinction coefficient was assumed to be equal to that of 7-azatryptophan [11].

^h The extinction coefficient was assumed to be equal to that of N₁-methyl-7-azaindole [13].

ⁱ Peptide dissolved in phosphate-buffered saline containing 0.5% gelatin and 0.02% NaN₃.

Table 4.2. Average Fluorescence Lifetime of Mixtures of N₁-Methyl-7-azatryptophan and Tryptophan

1M7AT:Trp	$\langle\tau\rangle$ (ns) ^a
1:0	21.7 ± 0.4
1:50	23.8 ± 0.3
1:75	22.3 ± 0.4
1:100	9.4 ± 1.5
1:150	9.1 ± 2.3
1:175	6.6 ± 1.5
1:200	5.2 ± 0.9

^a Data are collected at pH 7 and 20°C. $\langle\tau\rangle = A_1\tau_1 + A_2\tau_2$; see Materials and Methods.

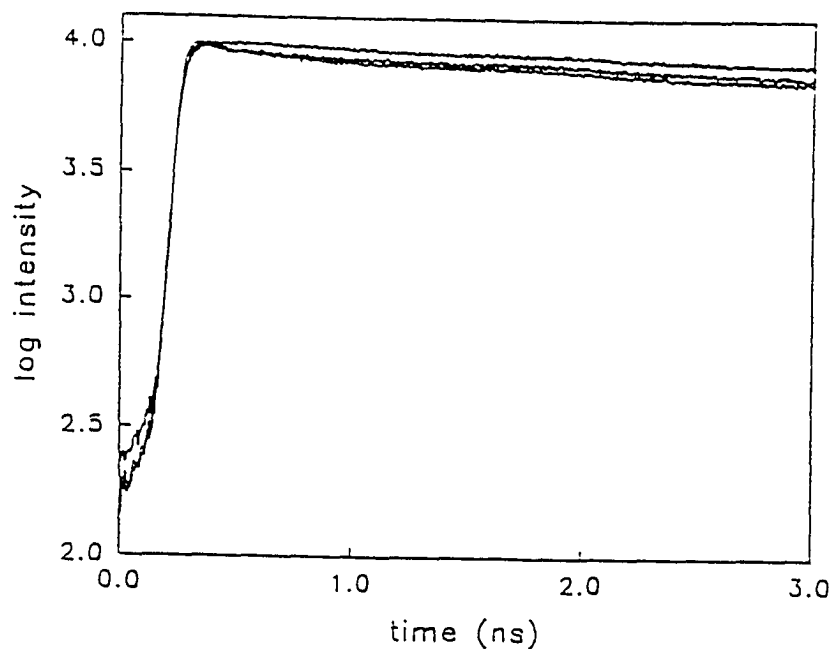


Figure 4.4. Fluorescence decay of (top trace) N_1 -methyl-7-azatryptophan, $F(t) = 1.00 \exp(-t/22.8\text{ns})$, $\chi^2 = 1.07$; and mixtures of N_1 -methyl-7-azatryptophan and tryptophan: (middle trace) 1:100, $F(t) = 0.35 \exp(-t/83\text{ps}) + 0.65 \exp(-t/12.3\text{ns})$, $\chi^2 = 1.28$; and (bottom trace) 1:200, $F(t) = 0.41 \exp(-t/96\text{ps}) + 0.59 \exp(-t/10.4\text{ns})$, $\chi^2 = 1.21$; pH 7.0, 20°C; $\lambda_{\text{ex}} = 310\text{nm}$, $\lambda_{\text{em}} \geq 455\text{ nm}$. No contribution from tryptophan to the fluorescence decay lifetime is apparent up to a 75-fold excess of tryptophan. In our work with 7-azatryptophan, we performed similar measurements [11] with mixtures of N-acetyl-tryptophanamide (NATA) because it is known to have an anomalous single exponential lifetime of 3-ns duration. This lifetime component consequently provides a telling contrast to the 780-ps lifetime of 7-azatryptophan. In the measurements displayed in this Figure and reported in Table 2, tryptophan itself affords the more rigorous test because of the presence of its subnanosecond component, which is expected to stand out in starkest contrast against the 21-ns lifetime of the probe. The nonnatural amino acid, 5-hydroxytryptophan, has also been proposed as an optical probe [34]. Its fluorescence lifetime is not, however, sufficiently different from that of tryptophan to provide a significant contrast in mixtures [16].

with respect to tryptophan, and because of the very large fluorescence quantum yield of N_1 -methyl-7-azatryptophan (0.53 ± 0.07), it is expected that its fluorescence decay can be uniquely detected in the presence of many background tryptophan residues. A comparison of the fluorescence decays of N_1 -methyl-7-azatryptophan, tryptophan, and 7-azatryptophan is given in Figure 4.3. To illustrate the usefulness of N_1 -methyl-7-azatryptophan as an optical probe in an environment containing multiple tryptophans, we measured the fluorescence decay lifetime of a mixture of these two amino acids. The fluorescence decay profile of the mixture exactly overlaid that of N_1 -methyl-7-azatryptophan up to a 75-fold excess of tryptophan, where the average fluorescence lifetime begins to become perceptibly shorter. The tryptophyl contribution to the fluorescence decay becomes much more apparent as the probe:tryptophan ratio approaches 1:200 (Table 4.2, Figure 4.4). Few, if any, naturally occurring biological systems contain this many tryptophans; clearly, emission from our optical probe would be unambiguously observed when incorporated into proteins. Finally, the single exponential fluorescence decay of N_1 -methyl-7-azatryptophan permits a simplified interpretation of time-resolved data. Any change in its fluorescence decay can be directly attributed to its environment.

Hogue and Szabo [20] have presented a study of the aminoacyladenylate of 7-azatryptophan in *B. subtilis* tryptophyl tRNA synthetase. While they seem to recognize the importance of the N_1 proton for the photophysics of 7-azatryptophan, this recognition is not completely brought to bear upon their interpretation of data [9,30] using this chromophore. Unlike the photophysics of tryptophan where blue shifts or red shifts of the fluorescence spectrum can only crudely be interpreted in terms of, respectively, nonpolar or polar *continuous* environments and where nonexponential decay can only be rationalized by a sweeping invocation of conformational heterogeneity, the delicate nature of the photophysics of 7-azaindole provides the possibility of gleaning much more detailed and specific information on the environment of the chromophore. *This is because the photophysics of 7-azaindole can only be satisfactorily explained by understanding in microscopic detail its interactions with its solvation environment: a continuum picture of the environment is not sufficient.*

Hogue and Szabo observe a 10-ns lifetime of 7-azatryptophan in its aminoacyladenylate complex with tRNA synthetase. This is most likely a result of the inability of the N_1 proton to form a significant hydrogen bonding interaction with a water molecule or any amino acid residues. Contrary to their claim [20], however, it is not necessarily true that just because the 7-azaindole chromophore is located in a hydrophobic

pocket it will exhibit a long fluorescence lifetime. It must be noted that 7-azaindole forms dimers under suitable conditions and that this system was first studied by Kasha and coworkers in 3-methylpentane [31] because it provided a model for hydrogen bonding in DNA base pairs. In the course of this work, it was realized that these dimers undergo excited-state double-proton transfer. Subsequent work has revealed that in alcohols [9,15,17,22,23] (and to a lesser extent in water [13,24-26]) excited-state tautomerization can occur if an appropriate hydrogen bonding interaction is established between the solvent molecule, the N_1 proton, and N_7 . Consequently, the ability of 7-azaindole to tautomerize does not necessarily depend on the presence of either a hydrophobic or a hydrophilic environment but rather on the specific nature of the available molecular species that can provide suitable hydrogen bonding partners.

Table 4.1 is also very instructive in this regard. While 7-azatryptophan and the tripeptide, NAc-Pro-7-azatrp-Asn-NH₂, exhibit single-exponential fluorescence decay, the octapeptide, NAc-Lys-Ala-Cys-Pro-7-azatrp-Asn-Cys-Asp-NH₂, provides a nonexponential fluorescence decay. Clearly, the nonexponential fluorescence decay in the octapeptide must be induced directly by the amino acid side chain residues or indirectly by their ability to reorganize water about the chromophore [25]. On the other hand, both N_1 -methyl-7-azatryptophan and the octapeptide Ser-Ile-Ile-Asn-(1M7AT)-Glu-Lys-Leu display single exponential fluorescence decay because of the absence of the N_1 proton.

Conclusions

Previously we have shown that 7-azatryptophan can be uniquely detected in an environment of up to a 10-fold tryptophan excess. We have improved the optical selectivity of the probe by methylating N_1 . N_1 -Methyl-7-azatryptophan has numerous advantages over other intrinsic fluorescent probes currently in use: It has red-shifted absorption and emission spectra with respect to those of tryptophan and a very high fluorescence quantum yield. This latter feature allows for shorter data collection time and analysis of smaller or more dilute sample volumes. This probe is characterized by a long-lived monoexponential fluorescence decay that is also clearly distinguishable from that of tryptophan. In addition, this tryptophan derivative is amenable to incorporation into peptide sequences. These combined factors allow for unambiguous detection of the probe signal in biological systems where site-specific analyses are expected to be difficult, if not impossible, owing to an overwhelming tryptophan

content. The immediate and most powerful use of N₁-methyl-7-azatryptophan will be to incorporate it into small peptides of known biological interest and to study the interactions of these tagged peptides with larger proteins.

References

1. Petrich, J. W.; Chang, M. C.; McDonald, D. B.; Fleming, G. R. *J. Am. Chem. Soc.* **1983**, *105*, 3824.
2. Petrich, J. W.; Longworth, J. W.; Fleming, G. R. *Biochemistry*, **1987**, *26*, 2711.
3. Donzel, B.; Gauduchon, P.; Wahl, Ph. *J. Am. Chem. Soc.* **1974**, *96*, 801.
4. Szabo, A. G. and Rayner, D. M. *J. Am. Chem. Soc.* **1980**, *102*, 554.
5. Gudgin, E.; Lopez-Delgado, R.; Ware, W. R. *J. Phys. Chem.* **1983**, *87*, 1559.
6. Creed, D. *Photochem. Photobiol.* **1984**, *39*, 537.
7. Beechem, J. M. and Brand, L. *Annu. Rev. Biochem.* **1985**, *54*, 43.
8. Négrerie, M.; Bellefeuille, S. M.; Whitham, S.; Petrich, J. W.; Thornburg, R. W. *J. Am. Chem. Soc.* **1990**, *112*, 7419.
9. Négrerie, M.; Gai, F.; Bellefeuille, S. M.; Petrich, J. W. *J. Phys. Chem.* **1991**, *95*, 8663.
10. Gai, F.; Chen, Y.; Petrich, J. W. *J. Am. Chem. Soc.* **1992**, *114*, 8343.
11. Rich, R. L.; Négrerie, M.; Li, J.; Elliott, S.; Thornburg, R. W.; Petrich, J. W. *Photochem. Photobiol.* **1993**, *58*, 28.
12. Négrerie, M.; Gai, F.; Lambry, J.-C.; Martin, J.-L.; Petrich, J. W. *J. Phys. Chem.* **1993**, *97*, 5046.

13. Chen Y.; Rich, R. L.; Gai, F.; Petrich, J. W. *J. Phys. Chem.* **1993**, *97*, 1770.
14. Rich, R. L.; Chen, Y.; Neven, D.; Négrerie, M.; Gai, F.; Petrich, J. W. *J. Phys. Chem.* **1993**, *97*, 1781.
15. Chen, Y.; Gai, F.; Petrich, J. W. *J. Am. Chem. Soc.* **1993**, *115*, 10158.
16. Chen, Y.; Gai, F.; Petrich, J. W. *J. Phys. Chem.* **1994**, *98*, 2203.
17. Chen, Y.; Gai, F.; Petrich, J. W. *Chem. Phys. Lett.* **1994**, *222*, 329.
18. Smirnov, A. V.; Rich, R. L.; Petrich, J. W. *Biochem. Biophys. Res. Comm.* **1994**, *198*, 1007.
19. Rich, R. L.; Gai, F.; Lane, J. W.; Petrich, J. W.; Schwabacher, A. W. *J. Am. Chem. Soc.* **1995**, *117*, 733.
20. Hogue, C. W. V.; Szabo, A. G. *Biophys. Chem.* **1993**, *48*, 159.
21. Hasselbacher, C. A.; Rusinova, E.; Waxman, E.; Lam, W.; Guha, A.; Rusinova, R.; Nemerson, Y.; Ross, J. B. A. *Proc. SPIE* **1994**, *2137*, 312.
22. Avouris, P.; Yang, L. L.; El-Bayoumi, M. A.; *Photochem. Photobiol.* **1976**, *24*, 211.
23. Moog, R. S. and Maroncelli, M. *J. Phys. Chem.* **1991**, *95*, 10359.
24. Chou, P.-T.; Matinez, M. L.; Cooper, W. C.; Collins, S. T.; McMorrow, D. P.; Kasha, M. *J. Phys. Chem.* **1992**, *96*, 5203.
25. Charge transfer to the side chain is generally attributed as the major nonradiative process in tryptophan [1, 16, 32] and different charge transfer rates owing to a distribution of ground-state conformers is attributed to the origin of the the nonexponential fluorescence decay in tryptophan. Although 7-azaindole is capable of photoionization [12, 33], we have argued that charge transfer to the side chain is not operative in 7-

azatryptophan because it is not thermodynamically favorable [16]. This argument is confirmed by the absence of nonexponential decay in the 7-azatryptophan tripeptide and its universal appearance in all tryptophan-containing tripeptides [1, 16].

26. Chapman, C. F.; Maroncelli, M. *J. Phys. Chem.* **1992**, *96*, 8430.
27. Waluk, J.; Pakula, B.; Komorowski, S. *J. Photochem.* **1987**, *39*, 49.
28. Bodansky, M.; Bodansky, A. *The Practice of Peptide Synthesis*; Springer-Verlag: Berlin, 1984.
29. Epling, G. A.; Kumar, A. *Synlett.* **1991**, 347.
30. Schlesinger, S. *J. Biol. Chem.* **1968**, *243*, 3877.
31. Taylor, C. A.; El-Bayoumi, M. A.; Kasha, M. *Proc. Natl. Acad. Sci. U.S. A.* **1969**, *63*, 253.
32. Arnold, S.; Tong, L.; Sulkes, M. *J. Phys. Chem.* **1994**, *98*, 2325.
33. Collins, S. T. *J. Phys. Chem.* **1983**, *87*, 3202.
34. Hogue, C. W. V.; Rasquinha, I.; Szabo, A. G.; McManus, J. P. *FEBS Lett.* **1992**, *310*, 269. Senear, D. F.; Laue, T. M.; Ross, J. B.; Waxman, E.; Easton, S.; Rusinova, E. *Biochemistry* **1993**, *32*, 6179. Ross, J. B. A.; Senear, D. F.; Waseman, E.; Kombo, B. B.; Rusinova, E.; Huang, Y. T.; Laws, W. R. Hasselbacher, C. A. *Proc. Nat. Acad. Sci. U.S.A.* **1992**, *89*, 12023. Kishi, T.; Tanaka, M.; Tanaka, J. *Bull. Chem. Soc. Jpn.* **1977**, *50*, 1267.
35. Wetlaufer, D. B. *Adv. Protein. Chem.* **1962**, *17*, 303.

PART II. ANALYSIS OF PEPTIDE SEQUENCES

CHAPTER 5. INCORPORATION OF 7-AZATRYPTOPHAN INTO PEPTIDE SEQUENCES AND THEIR BINDING INTERACTIONS WITH α -CHYMOTRYPSIN

Introduction

The incorporation of 7-azatryptophan and its derivatives into peptides and proteins is the next step in validating these compounds as optical probes of biological systems. The continued function of the peptide or protein upon replacement of a residue with 7-azatryptophan proves the biological viability of this nonnatural amino acid. In particular, a small peptide or protein containing 7-azatryptophan may be studied alone and in complex with a larger protein that may contain many tryptophans.

With such an intent in mind, we have begun to analyze peptides containing 7-azatryptophan. We have examined three- and eight-residue sequences that mimic the active site of potato proteinase inhibitor II, with 7-azatryptophan replacing Leu at the P₁ position, and determined the spectroscopic and α -chymotrypsin-inhibiting properties of these peptides. A more detailed description of each of the peptide/ α -chymotrypsin project and justification for the specific peptide sequences chosen in this study is described later in this chapter. The following is some information concerning the synthesis and upkeep of the peptides we use.

Incorporation of 7-Azatryptophan into Peptide Sequences

Except for a tryptophan-containing octapeptide synthesized for us by Genosys Biotechnologies, Inc., all peptides used in our laboratory have been prepared by the Protein Facility, Department of Biochemistry and Biophysics, Iowa State University. The person to contact at the Protein Facility regarding peptide synthesis, incorporation of nonnatural amino acids, and subsequent enantiomeric separation by HPLC is Siquan Luo at 294-3267, email: sluo@iastate.edu. The peptide sequences we have had made at the Protein Facility and their sample numbers are listed in Table 5.1.

The peptides are fluffly, white powders. Decomposition or contamination would be evident if any discoloration, waxiness, or compacting of the peptides was observed. To preserve the peptides, they should be kept dessicated at -60°C until use. When removing the

Table 5.1. Peptides Provided by the Protein Facility

sequence ^a	sample number	date
PLN	104	4/20/92
L-P(7AT)N ^b	85	8/13/91
D-P(7AT)N	85	8/13/91
KACPLNCD	117	9/11/92
L-KACP(7AT)NCD		
D-KACP(7AT)NCD		

^a All peptides are of the form NAc-X-Y-NH₂.

^b D- and L-notation refers to the 7-azatryptophan enantiomers only. The other residues are all L-conformers.

samples from the freezer, allow the dessicator to warm to room temperature before opening vials containing peptides to prevent moisture from entering the vials. Concentrations of peptide solutions should be determined using the optical density, rather than the weight of the peptide dissolved in solution. This is particularly important for samples of disulfide-containing peptides that contain DTT as reducing agents. Using the weight of powder to determine solution concentration will yield an erroneously high molarity.

Up to now, assignment of the D- and L-enantiomers has been made by elution time by HPLC. It was assumed that the L-peptides in general elute prior to the D-enantiomer under the conditions used for purification of our peptides. This, in fact, may not hold true for all peptides. An alternative method of assignment may be made using selective enzymatic enantiomer cleavage; e.g., some enzymes selectively cleave peptides containing a L-amino acid in the P₁ position.

Studies of Enzyme Kinetics: Determinations of K_m , k_{cat} , and K_I

An ideal protein-protein complex of which to study interactions and dynamics is that of an enzyme and inhibitor. The enzyme/inhibitor system we have chosen for our studies is that of potato proteinase inhibitor II bound to a serine proteinase, α -chymotrypsin. Serine proteinases (those proteinases requiring a serine residue for function) such as trypsin, α -chymotrypsin, and elastase perform protein digestion and are endopeptidases; that is, they cleave a peptide chain between non-terminal residues, thereby yielding two smaller fragments. α -Chymotrypsin is a globular protein consisting of three polypeptide chains, contains a hydrophobic pocket, and requires a bulky, nonpolar, hydrophobic residue at the P₁ position, but has little, if any, selectivity for the P₁' position. Small molecules that mimic a substrate, but are unreactive, (e.g., indole) can inhibit α -chymotrypsin since these compounds also bind in the active site pocket. These characteristics, the abundance of data for this enzyme, and its availability and inexpensive make α -chymotrypsin a prime candidate for our studies.

The Protein Facility has synthesized peptides that contain 7-azatryptophan at the P₁ position, but otherwise duplicate the potato proteinase inhibitor II sequence [1], about the active site. Potato proteinase inhibitor II was chosen as the inhibitor of interest for several reasons, the most significant being the existence of a published crystal structure of this

inhibitor bound to an proteinase. This modified inhibitor has been complexed with α -chymotrypsin and active-site dynamic studies have been performed.

Active-site Determination of α -Chymotrypsin

The α -chymotrypsin commercially available is not 100% active. In fact, the typical percentage of active chymotrypsin in the lots we purchase was 55-80%. Almost exclusively, we used α -chymotrypsin purchased from Sigma (e.g., lot 128F8035) Type 1-S from bovine pancreas for these studies. Prior to each experiment, the active-site concentration of the α -chymotrypsin stock solution to be used was determined. The techniques and calculations discussed below are from Schonbaum's work [2].

solutions. Stock solutions of α -chymotrypsin are prepared by dissolution in 0.1 M sodium acetate buffer pH 5.05 (acidified to pH 5.05 with acetic acid), to a final concentration of approximately 0.4 mM. Stock solutions of *N*-transcinnamoylimidazole (NTCI) are prepared by dissolution in acetonitrile to a concentration of approximately 0.2 M. Concentrations are determined spectrophotometrically using extinction coefficients. Table 5.2 is a compilation of useful parameters of several compounds used in the binding studies. For use in experiments, dilute the NTCI solution to approximately four mM. The titrations are run using three mL buffer in cuvettes, 100 μ L α -chymotrypsin solution, and 100 μ L NTCI solution. The volumes must be exact: weigh 3.00 ± 0.01 g buffer into a cuvette and carefully inject 100 μ L each of enzyme and substrate. Enzyme solutions should be kept on ice throughout the experiment. If all solutions, except the buffer solution, are not used up during a set of experiments, quickly freeze the remaining solutions by immersion of the solution vial in liquid nitrogen and store in a -60°C freezer. The buffer solution should be kept refrigerated when not in use and new buffer solution should be made periodically.

analytical conditions. Experiments were run on a Beckman DU 7400 or HP 8452A diode array UV/vis spectrophotometer thermostatted to maintain a temperature of $24 \pm 2^{\circ}\text{C}$. The instrument was set to scan in kinetics mode at an absorption wavelength of 410 nm. Scan time for each active site run should be 6-8 minutes, with data collection every 2 seconds. Stirring was maintained throughout the runs by including a cuvette stir bar in each cuvette. The cuvettes used for the active site determination were disposable methacrylate 4.5 mL cuvettes from Fisher Scientific.

experimental procedure. After specifying the data-collection parameters of the spectrophotometer, place a cuvette containing 3.00 mL buffer and a cuvette stir bar in the spectrophotometer. Begin a run and collect data for the absorbance of the buffer alone for

Table 5.2. Useful data of compounds used in the kinetic studies

compound	molecular weight (g/mol)	ϵ ($M^{-1} \text{ cm}^{-1}$)	$\lambda_{\text{abs}}^{\text{max}}$ (nm)
indole		5850 at 269 nm	
pNA		8800	
P7ATA		6200 at 288 nm	288
NTCI		9370 335 nm	
α -chymotrypsin [2]	24800	50,000 at 280 nm	280
PLA		approx. 450 at 240 nm	
SAAPFpNA [7]	624.5	12,700 at 316 nm	
7-azaindole		8500	

20-30 seconds. Add 100 μL α -chymotrypsin solution between spectrophotometer readings (which are every 2 seconds) and collect data for approximately 45-60 seconds. Add 100 μL NTCI solution between readings and collect data for 90-120 seconds. Remove this cuvette and replace it with another containing buffer only. Collect data for this buffer for 20-30 seconds, then inject 100 μL NTCI solution between readings. Collect data for 60-120 seconds, then terminate the run. A typical scan is shown in Figure 5.1. Usually, three or four runs of this type are required to determine an average and standard deviation for the concentration of active sites in the α -chymotrypsin stock solution. The exchange of cuvettes and multiple injections between absorbance readings throughout the run requires much practice to obtain consistency. The calculations for the active site concentration are:

$$\begin{aligned}A_1 &= A_1^* - B_2 \\A_4 &= A_4^* - B_1 \\A_2 &= A_4 + 0.969A_1 \\M &= (A_2 - A_3)/279.7\end{aligned}$$

where A_{1-4} are described in the figure caption and M is the concentration of active sites. Note that these formulae are for three mL buffer and 100 μL injection volumes. These equations must be rederived if different volumes of solutions are to be used.

Another concern with the use of α -chymotrypsin is the possible degradation of this enzyme over the time required for a set of experiments (12-24 hours). To discover if this concern was valid, we chose to run a number of active site titrations over 24 hours. Type II-S α -chymotrypsin was used since this experiment requires such a large quantity of enzyme and Type II-S is significantly less expensive than Type I-S. The solution used was approximately three mM and was kept at room temperature (to encourage degradation) throughout the experiment. The method described above for determination of active sites was used and the results obtained are shown in Figure 5.2. We assume that using Type II-S α -chymotrypsin and keeping the solution at room temperature is the worst-case scenario; during the actual kinetic runs I have observed that the α -chymotrypsin active-site percentage remained unchanged for three or four days in a buffered solution kept at 4°C.

Verification of the Experimental Procedure by Determination of K_m and k_{cat} for a Known Enzyme/Substrate System: α -Chymotrypsin and SAAPFpNA

Before each set of experiments to determine an inhibition constant, a verification of the concentrations of the enzyme and substrate solutions and a familiarization with the required techniques was necessary. These checks were performed by measuring the K_m and

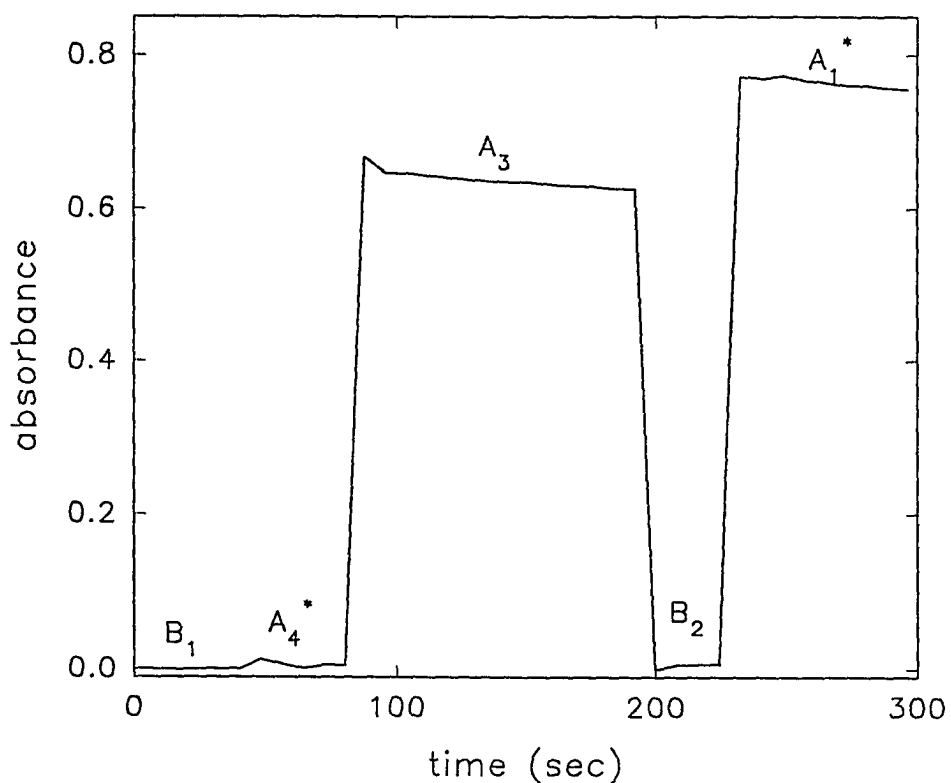


Figure 5.1. Plot of a typical titration to determine the active-site concentration of α -chymotrypsin. Linear regressions are necessary to find the value for A_4^* , A_3 , and A_1^* . Averages are necessary for B_1 and B_2 .

B_1 : blank of the first cuvette

A_4^* : addition of the enzyme to the first cuvette

A_3 : addition of NTCI to the first cuvette

B_2 : blank of the second cuvette

A_1^* : addition of NTCI to the second cuvette

Calculations to determine $A_{1,2,4}$ are given in the text.

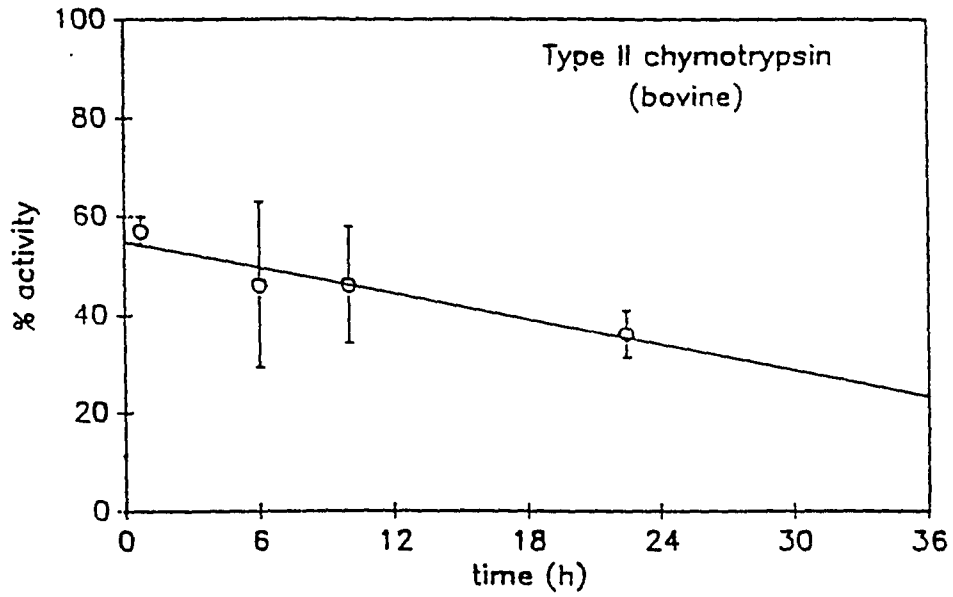


Figure 5.2. Plot of the degradation of Type II-S α -chymotrypsin over time.

k_{cat} of α -chymotrypsin and Succinyl-Ala-Ala-Pro-Phe-*p*-nitroanilide, SAAPFpNA. Previous work [3] has shown that $K_m = 43 \mu\text{M}$ and $k_{\text{cat}} = 45 \text{ s}^{-1}$ for this system. I could consistently duplicate these results. The conditions for this experiment are outlined below.

Solutions. α -Chymotrypsin (Sigma) was dissolved in 0.1 M sodium acetate, pH 5.05 buffer solution (adjusted to correct pH with dilute acetic acid) and the active-site concentration was determined. The α -chymotrypsin stock solution was kept on ice throughout the binding studies. SAAPFpNA was dissolved in DMSO. The concentration of this solution did not change over the course of the measurements. Contamination of the substrate solution by α -chymotrypsin would be obvious if the solution became yellow. This did not happen during these experiments; absorption spectra were taken periodically to ensure that the substrate solution did not decompose. A series of dilutions were made to ensure a range of substrate concentrations for the analyses. Concentrations were determined by weighing a known amount of substrate and dissolving appropriately. A rough estimate of the extinction coefficient of SAAPFpNA is $14,000 \text{ cm}^{-1} \text{ M}^{-1}$. Using this value, the concentration determined spectrophotometrically agreed, within expected error, with the value calculated from weighing and diluting the substrate. The buffer solution for these experiments was 0.1 M tris-HCl, 0.02 M CaCl_2 , 0.005% Triton X-100 (w/v) adjusted to pH 7.8 with 1 M HCl. $1.00 \pm 0.01 \text{ mL}$ of this buffer solution was added to a cuvette; $\sim 1\text{-}5 \mu\text{M}$ α -chymotrypsin solution and $\sim 1\text{-}10 \text{ mM}$ SAAPFpNA solution were typical concentration used in the reaction.

Analytical Conditions. Experiments were run on a Beckman DU 7400 or HP 8452A diode array UV/vis spectrophotometer thermostatted to maintain a temperature of $24 \pm 2^\circ\text{C}$. The instrument was set to scan in kinetics mode at an absorption wavelength of 380 nm. Data were collected every 0.5 seconds and the total run time for each measurement was eight minutes. Richard Wynn, a graduate student in M. Laskowski, Jr.'s group at Purdue who does similar work [4], suggested collecting absorption from 380 to 410 nm and subtracting the background (650-700 nm). Under the conditions I was using, the instrument lacked the memory to store all these parameters. As a consequence, the background was not subtracted during the runs. However, the absorbance of the blank (enzyme + inhibitor) solution was subtracted at the beginning of each run. This appeared to be sufficient. Data points were collected over the time in which the absorption curve was linear. The cuvettes used for these experiments were disposable methacrylate 1.5 mL semi-micro cuvettes purchased from Fisher Scientific. Since a cuvette stir bar does not fit in these small cuvettes, stirring was performed briefly, but vigorously, with the injection syringe upon addition of the substrate.

Calculations. The program used to fit the data was ENZFITTER version 1.05, a non-linear regression data analysis program produced by Robin J. Leatherbarrow, Department of Chemistry, Imperial College of Science and Technology, London, and published and distributed by Biosoft in Cambridge, U.K.. The original software package is kept in our laboratory and has been loaded onto the c: and/or e: drive of some of our computers. To use this program, enter the enzfit directory (c:\enzfit), then type "ef" to begin the program. The initial parameters I use are:

Robust weighting:	on
Weighting:	simple
Equation:	Michaelis Menton kinetics
Directory:	c:\enzfit
Printer:	off
Auto guess:	on

Under "File and data" menu, enter the substrate concentrations and rates as x and y coordinates. Note that the rates reported by the spectrophotometer (dA/dt) must undergo conversion to be the actual reaction rates (dc/dt). The conversion is:

$$dc(M)/dt(sec) = dA/dt(min) \times 1 \text{ min}/60 \text{ sec} \times 1/\epsilon l$$

where $\epsilon_{pNA} = 8800 \text{ cm}^{-1} \text{ M}^{-1}$ and the length (l) is a pathlength of 1 cm. Also, there is an error in the ENZFITTER program. The results obtained upon fitting the entered data are reported to be K_m and k_{cat} . This is incorrect. The actual results reported are K_m and v_{max} . To determine the k_{cat} , divide the reported v_{max} by the concentration of α -chymotrypsin in the reaction.

Determination of Inhibition Constants

Solutions. The inhibitors were dissolved in 0.1 M tris-HCl, 0.02 M CaCl_2 , 0.005% Triton X-100 (w/v) pH 7.8 buffer (adjusted to the correct pH with 1 M HCl) and the concentrations of the solutions were determined spectrophotometrically. Chilling the concentrated solutions of indole and other amino acid derivatives caused precipitation of the solute, so reactions were run with these inhibitors kept at room temperature. New solutions of these compounds were made every two days since discoloration occurred after some time.

A minimal volume of the peptide solution was prepared at one time, so that no peptide inhibitor was in solution for more than a few hours, thereby reducing the possibility of degradation. Since the stability of the peptides at this pH was unknown, all analyses using these solutions were completed within six hours. It was assumed that the solutions remained unchanged over this period. All reactions were run in 0.7-1.0 mL inhibitor solutions. Small (μL) volumes of enzyme and substrate were added to the inhibitor solution. Dilutions due to addition of reactants was accounted for in the calculations. Wynn [4] suggests an incubation time of "ten half-lives of the enzyme-inhibitor second-order association reaction ($t_{1/2} = 1/(E_0 \times k_{on})$ ". k_{on} for this enzyme-inhibitor complex is $1 \times 10^6 \text{ M}^{-1} \text{ s}^{-1}$ [4] For the peptide studies, this required an incubation time of less than 20 seconds; all reaction mixtures were incubated far longer than the required minimum (0.5 - 5 min). For inhibition to occur, the concentration of inhibitor must approximate the inhibition constant. Peptide solutions of millimolar concentration required a great amount of compound, so only a few runs of various inhibitor concentrations were possible for the peptides since each run required about 25 mg peptide. The enzyme and substrate concentrations in these experiments approximated those used for the α -chymotrypsin/SAAPFpNA experiments discussed above.

Analytical Conditions. Experiments were run on a Beckman DU 7400 or HP 8452A Diode array UV/vis spectrophotometer thermostatted to maintain a temperature of 24 ± 2 °C. Data were collected at 380 nm and were collected every 0.2 seconds. Since the inhibition constant of the inhibitors is about 1 mM, the concentration of total enzyme must also be unusually great. For these reactions, it was necessary for the enzyme concentration in the reaction mixture to be about 0.1 μM . With such a high enzyme concentration, the reaction proceeds very quickly. Since only the linear portion of the absorption change curve may be used, the total run time became very short (less than one minute). This produced a greater spread in the rate results; even with precise injections and consistent technique, data points varied significantly. This resulted in a large number of data points being eliminated when calculating the inhibition constants.

Calculations. ENZFITTER was used as described previously to determine K_m' . To determine K_I , I used the following formula:

$$K_m' = K_m (1 + [I] / K_I)$$

A check of my techniques and calculations was performed by measuring the inhibition constant of native potato chymotrypsin inhibitor II in complex with α -chymotrypsin. The K_I reported in the literature is 2×10^{-8} M [1]; I obtained $2.3 \pm 0.4 \times 10^{-8}$ M.

References

1. Bryant, J.; Green, T. R.; Gurusaddaiah, T.; Ryan, C. A. *Biochemistry*, **1976**, *15*, 3418.
2. Schonbaum, G. R., Zerner, B., Bender, M. L. *J. Biol. Chem.* **1961**, *236*, 2930.
3. Park, S. 1985, Ph.D. dissertation, Purdue University.
4. Wynn, R., 1990, Ph.D. dissertation, Purdue University.

CHAPTER 6. THE PHOTOPHYSICAL PROBE, 7-AZATRYPTOPHAN, IN SYNTHETIC PEPTIDES

A paper published in *Photochemistry and Photobiology*¹

R. L. Rich², M. Négrerie³, J. Li⁴, S. Elliott⁴, R. W. Thornburg⁵, and J. W. Petrich^{2,6}

Abstract

7-azatryptophan is proposed as an alternative to tryptophan as a photophysical probe in the study of protein structure and dynamics. Not only are the spectral characteristics of 7-azatryptophan easily distinguishable from those of tryptophan, but this nonnatural amino acid is shown to be amenable to incorporation into peptides. We present the first synthesis and purification of a synthetic peptide containing 7-azatryptophan, NAc-Pro-7-azatryptophan-Asn-NH₂, which is shown to be a competitive inhibitor of α -chymotrypsin.

Introduction

The standard optical probe of protein structure and dynamics has been tryptophan. The use of tryptophan, however, presents a number of problems. Among these are the difficulties in the interpretation of the data posed by its intrinsic nonexponential fluorescence decay, demonstrated by Szabo and Rayner [1] and Petrich *et al.* [2], and the occurrence of

¹ Reprinted with permission from *Photochemistry and Photobiology* **1993**, 58, 28. Copyright © 1993, American Society for Photobiology.

² Graduate student and Associate Professor, respectively, in the Department of Chemistry, Iowa State University.

³ Postdoctoral fellow under J. W. Petrich, Department of Chemistry, Iowa State University, 1989-1991. Currently employed by Laboratoire d'Optique Appliquée, Ecole Polytechnique -- ENSTA, INSERM U275, 91128, Palaiseau Cedex, FRANCE.

⁴ Employees of the Protein Facility, Department of Biochemistry and Biophysics, Iowa State University.

⁵ Associate Professor, Department of Biochemistry and Biophysics, Iowa State University.

⁶ To whom correspondence should be addressed.

multiple-tryptophan-containing proteins. We have suggested that the nonnatural analog of tryptophan, 7-azatryptophan, is a promising alternative to tryptophan as a photophysical probe. In addition to having a single-exponential lifetime decay in water over most of the pH range, 7-azatryptophan has optical spectra that differ significantly from those of tryptophan (Figures 6.1a and 6.1b). The absorption and emission spectra of 7-azatryptophan are red-shifted 10 nm and 70 nm, respectively, from those of tryptophan. Négrerie *et al.* [3,4] have shown that 7-azatryptophan thus has great potential as a probe of protein structure and dynamics, especially for investigations of protein-protein interactions in which one of the proteins involved may contain several tryptophans. In order, however, for 7-azatryptophan to be useful as a biological probe and not merely a photophysical curiosity, it must be demonstrated that 7-azatryptophan can be incorporated into proteins and peptides and that these modified systems remain functional. Here we show that 7-azatryptophan is suitable for use in peptide synthesis by producing an analog of the active site of the potato proteinase inhibitor II, which is a strong inhibitor of α -chymotrypsin: $K_1 = 2.3 \times 10^{-8}$ M. This analog is NAc-Pro-7-azatryptophan-Asn-NH₂ where 7-azatryptophan is substituted for Leu in the P₁ site. α -Chymotrypsin was subsequently challenged by the L and D forms of this tripeptide. In addition, we determined the inhibition constants for the native active-site sequence of potato chymotrypsin inhibitor II, NAc-Pro-Leu-Asn-NH₂, and a series of related compounds. Kowalski *et al.* [5] demonstrated that soybean trypsin inhibitor (Kunitz) becomes a strong inhibitor against α -chymotrypsin when the P₁ Arg is substituted with Trp.

Materials and Methods

Synthesis and Purification of NAc-Pro-7-azatryptophan-Asn-NH₂ Peptides

Unless otherwise specified, reagents for peptide synthesis and amino acid analysis were purchased from Applied Biosystems, Inc. Other materials were reagent grade. The *t*-Boc-D,L-7-azatryptophan was prepared by reacting 2-butoxycarbonyloxyimino-2-phenylacetonitrile (Aldrich) with D,L-7-azatryptophan (Sigma). Owing to the solubility characteristics of 7-azatryptophan, the procedure was altered from the protocol by Itoh *et al.* [6] for tryptophan. The water layer was acidified with 5% citric acid causing a precipitate to form. The precipitate was determined to be *t*-Boc-7-azatryptophan by chemical ionization mass spectrometry, using ammonia as a reagent gas. The acetylated peptide, NAc-Pro-7-azatryptophan-Asn-NH₂ was synthesized using tetrabutylloxycarbonyl solid-phase peptide

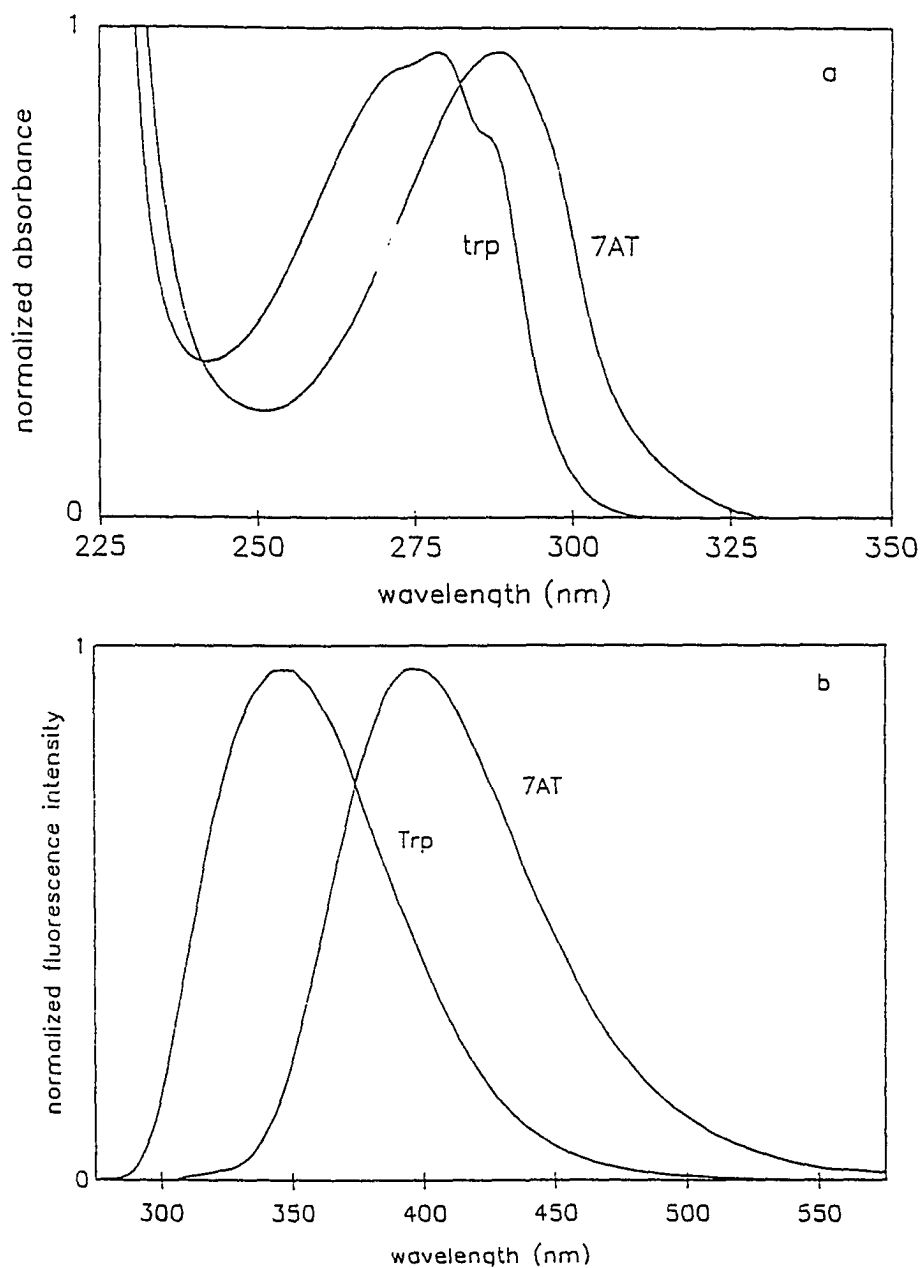


Figure 6.1. (a) Comparison of the absorption spectra of tryptophan (Trp, $\lambda_{\text{max}}^{\text{abs}} = 280\text{nm}$, $\epsilon_{278\text{ nm}} \approx 5550\text{ M}^{-1}\text{ cm}^{-1}$ [8]) and 7-azatryptophan (7AT, ($\lambda_{\text{max}}^{\text{abs}} = 288\text{ nm}$, $\epsilon_{288\text{ nm}} \approx 6200\text{ M}^{-1}\text{ cm}^{-1}$); (b) Comparison of the fluorescence spectra of tryptophan (Trp, $\lambda_{\text{max}}^{\text{em}} = 348\text{ nm}$) and 7-azatryptophan (7AT, $\lambda_{\text{max}}^{\text{em}} = 395\text{ nm}$). Absorption and emission spectra are normalized to the same peak intensity.

synthesis. Most of the synthesis was carried out on an Applied Biosystems 430A Peptide Synthesizer starting with benzhydrylamine resin. *t*-Boc-D,L-7-azatryptophan is insoluble in methylene chloride and only slightly soluble in *N*-methylpyrrolidone. Thus, the formation of the active ester and the addition of this residue were carried out manually. The diastereoisomeric peptides were separated on a Beckman high-performance liquid chromatography (HPLC) system with a Vydac reverse-phase C18 semipreparative column (10 x 250 mm) using HPLC grade reagents (Fisher Scientific). Buffers were 0.1% trifluoroacetic acid (TFA) in water and 0.08% TFA in acetonitrile. The L-peptide eluted from the column with a retention time of 10.96 minutes in a 20 minute gradient from 0% to 20% acetonitrile buffer. The retention time for the D-peptide was 11.75 minutes. D and L forms were distinguished by analogy with the elution profiles of racemic mixtures of other amino acids. Amino acid analysis using constant boiling hydrochloric acid (Pierce Chemical Company) revealed that the D and L forms contained the same amino acids in identical ratios. 7-azatryptophan is not destroyed by acid hydrolysis as is tryptophan. Fast atom bombardment (FAB) mass spectrometry revealed the same peak for both fractions at 456.3. The peptide NAc-Pro-Leu-Asn-NH₂ was synthesized by standard techniques.

Reagents and Conditions for Kinetic and Binding Studies

Bovine α -chymotrypsin was dissolved in 0.1 M sodium acetate buffer solution adjusted to pH 5.05 with dilute acetic acid, and the active-site concentration was determined as described by Schonbaum *et al.* [7]. The substrate, succinyl-Ala-Ala-Pro-Phe-*p*-nitroanilide (CalBiochem), was dissolved in dimethylsulfoxide. The weak inhibitors were dissolved in 0.1 M tris-HCl, 0.02 M CaCl₂, 0.005% Triton X-100 (w/v) buffer solution adjusted to pH 7.8 with dilute hydrochloric acid. Potato proteinase inhibitor II (CalBiochem) was dissolved in deionized water. For kinetic measurements, absorbance was monitored at 410 nm and experiments were run at $24 \pm 2^\circ\text{C}$. For all analyses the enzyme concentration in the reaction cell was nanomolar and the substrate concentration was in the range $0.1 K_M \leq [S]_{\text{rxn}} \leq 10 K_M$.

Results and Discussion

We have measured the fluorescence decays of mixtures of tryptophan and 7-azatryptophan. Only when the ratio of tryptophan to 7-azatryptophan is as great as 10:1 does

the tryptophyl emission become detectable (Figure 6.2). The fluorescence maximum of the model tripeptide containing either D- or L-7-azatryptophan is 414 nm at 20°C and pH 7. Its fluorescence lifetime is single-exponential (870 ps). Thus, not only is the fluorescence decay of 7-azatryptophan in water single-exponential, but so is that of the tripeptide containing 7-azatryptophan. In contrast, Szabo and Rayner [1] and Petrich *et al.* [2] determined that most derivatives of tryptophan except for the anomalous *N*-acetyl-tryptophanamide (NATA) exhibit fluorescence decays that can be fit only to a sum of exponentials. (NATA is a poor model system for the fluorescence decay of tryptophan in peptides and proteins, as even simple tripeptides are generally well characterized by nonexponential fluorescence decay — usually commensurate amplitudes of 1 and 3 ns components [2].)

Classical kinetic studies (Table 6.1) indicate the following.

1. Indole and 7-azaindole inhibit equally well indicating that the substitution of a nitrogen for a carbon in the 7 position does not affect the binding interactions.
2. Both indole and 7-azaindole bind more than 10 times stronger than the zwitterionic amino acids, Leu and Trp. But within experimental error, Leu and Trp have identical binding constants with respect to α -chymotrypsin.
3. The above results suggest that the improved inhibition afforded by substituting the P₁ Leu with 7-azatryptophan is a result of conformational change in the peptide rather than a specific interaction afforded by the 7-nitrogen of the azaindole moiety.
4. It is unlikely that the 7-azatryptophan tripeptides are being hydrolyzed on the time scale of the experiment as both Pro-Leu and Pro-Trp exhibit much higher K_I values. If Pro-Trp or the 7-azatryptophan peptides were being cleaved, similar K_I values would be expected for the di- and tripeptides.
5. The strong inhibition provided by potato proteinase inhibitor II must be afforded by additional contacts from amino acids in both the N- and C-terminal directions. We are investigating which of these amino acids are essential for providing strong inhibition.
6. The similar K_I values of the D- and L-7-azatryptophan tripeptides suggest a certain degree of flexibility of the active site of α -chymotrypsin for accommodating a tryptophyl-like residue.

Figure 6.2. Fluorescence decays of mixtures of 7-azatryptophan and *N*-acetyltryptophanamide at 20°C and pH 6.0. (a) [7AT]/[NATA] = 1/1 and $\lambda_{\text{ex}} = 310$ nm. The upper curve is the emission monitored at $\lambda_{\text{em}} \geq 320$ nm. The fluorescence decay, $F(t)$, is well described by two exponentials, the second of which is the contribution from the tryptophyl moiety: $F(t) = 0.95\exp(-t/826 \text{ ps}) + 0.05\exp(-t/2482 \text{ ps})$; $\chi^2 = 1.05$. The lower curve is the emission monitored at $\lambda_{\text{em}} \geq 400$ nm. It is well described by a single exponential: $F(t) = \exp(-t/851 \text{ ps})$; $\chi^2 = 1.10$. (b) For both curves, $\lambda_{\text{ex}} = 310$ nm and $\lambda_{\text{em}} \geq 450$ nm. The lower curve corresponds to [7AT]/[NATA] = 1/3. The fluorescence decay is single exponential, $F(t) = \exp(-t/856 \text{ ps})$; $\chi^2 = 1.04$. The upper curve corresponds to [7AT]/[NATA] = 1/10. $F(t) = 0.91\exp(-t/848 \text{ ps}) + 0.09\exp(-t/2475 \text{ ps})$; $\chi^2 = 1.10$. The high tryptophan concentration begins to become apparent and gives rise to the second component. Fitting the upper curves in both (a) and (b) to a single exponential yields lifetimes of 983 ps ($\chi^2 = 2.40$) and 898 ps ($\chi^2 = 1.81$), respectively. At 310 nm, the extinction coefficients of tryptophan and 7-azatryptophan are approximately 100 and 100 M⁻¹ cm⁻¹, respectively. For an excitation wavelength of 310 nm, the ratio of the integrated fluorescence intensity of 7-azatryptophan to tryptophan for $\lambda_{\text{em}} \geq 450$ nm is ~ 15. Based on these values and these excitation and detection parameters, a solution whose zwitterionic tryptophan to 7-azatryptophan ratio is 10-to-1 is expected to yield only ~ 6% emission from tryptophan. This is in very good agreement with the results obtained from the time-resolved measurements of the upper curve presented in panel (b). (NATA, instead of tryptophan, was specifically used for the time-resolved measurements because of its anomalous single-exponential fluorescence decay. This facilitates the quantitative resolution of the fluorescence decays into components from indole and 7-azaindole chromophores, as the decay from zwitterionic tryptophan is intrinsically nonexponential).

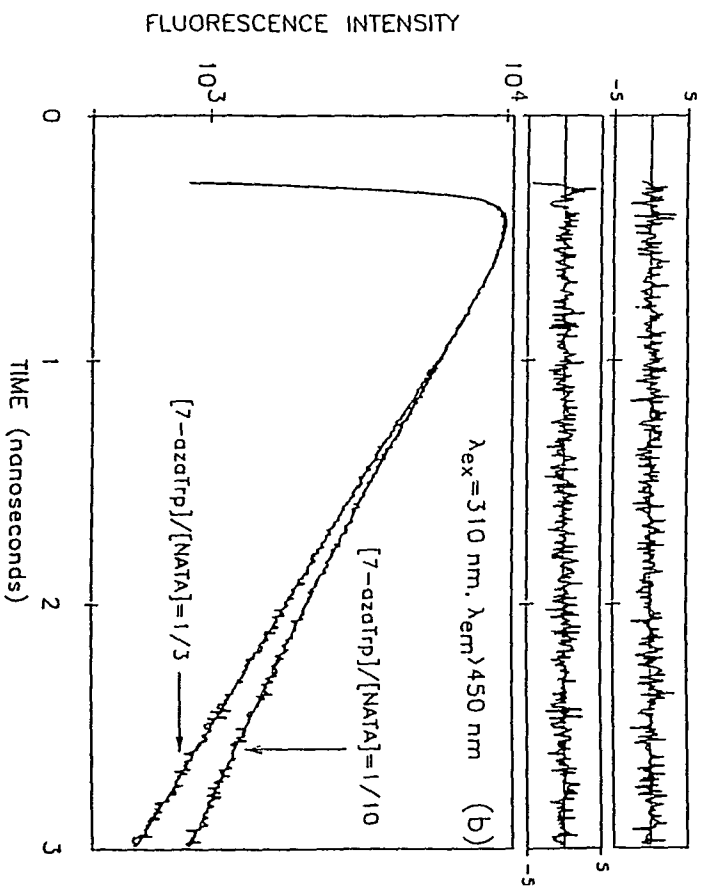
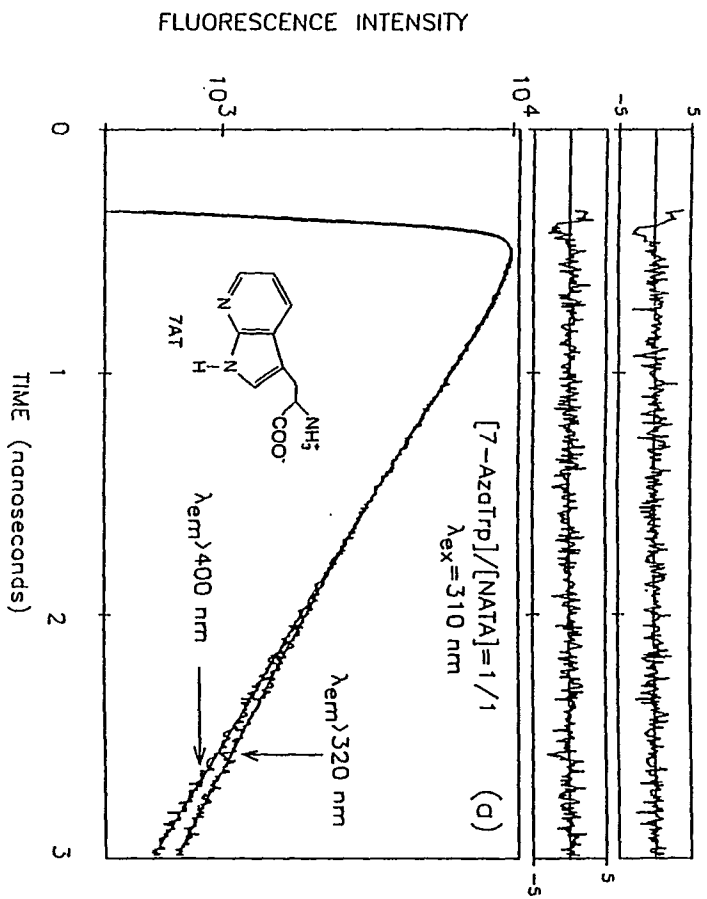


Table 6.1 Inhibition of α -Chymotrypsin

species	K_I (mM)
indole	$0.4 \pm 0.2, 0.8 \pm 0.2$ [9]
7-azaindole	$0.4 \pm 0.1, 1.3 \pm 0.2$ [10]
leucine	10 ± 4
L-tryptophan ^a	$16 \pm 6, 6 \pm 2$ [11]
7-azatryptophan	42 ± 10
Pro-Leu	45 ± 4
Pro-Trp	22 ± 7
Nac-Pro-Leu-Asn-NH ₂	7 ± 3
NAc-Pro-L-7AT-Asn-NH ₂	0.3 ± 0.2
NAc-Pro-D-7AT-Asn-NH ₂	0.5 ± 0.1
Potato Proteinase Inhibitor II	$2.3 \pm 0.4 \times 10^{-8}, 2 \times 10^{-8}$ [1 2]

^a Our experiments used the L form of tryptophan, Foster and Niemann [39] used the D form.

Conclusions

A great value of 7-azatryptophan will be to probe the interactions of a smaller peptide or protein containing it with another protein that may contain several tryptophans. These intrinsically tagged molecules can then be studied individually or in complex with their target. This approach will be useful in studying complexes between a small protein or polypeptide containing 7-azatryptophan and a large globular protein that may contain many tryptophans.

Acknowledgments

Support was provided by the Iowa State Biotechnology Council, IPRT, and University Research Grants. J.W.P. is an Office of Naval Research Young Investigator. The tripeptides were prepared in the ISU Protein Synthesis Laboratory. Travel support was provided to M. N. by NATO. R. L. R. is the recipient of a GAANN fellowship.

References

1. Szabo, A. G.; Rayner, D. M. *J. Am. Chem. Soc.* **1980**, *102*, 554.
2. Petrich, J. W.; Chang, M. C.; McDonald, D. B.; Fleming, G. R. *J. Am. Chem. Soc.* **1983**, *105*, 3824.
3. Négrerie, M.; Bellefeuille, S. M.; Whitham, S.; Petrich, J. W.; Thornburg, R. W. *J. Am. Chem. Soc.* **1990**, *112*, 7419.
4. Négrerie, M.; Gai, F.; Bellefeuille, S. M.; Petrich, J. W. *J. Phys. Chem.* **1991**, 8663.
5. Kowalski, D.; Leary, T. R.; McKee, R. E.; Sealock, R. W.; Wang, D.; Laskowski, Jr., M. Bayer Symposium V "Proteinase Inhibitors" 1974, (Edited by H. Fritz, H. Tschesche, and L. J. Greene), pp. 311-324. Springer-Verlag, Berlin.

6. Itoh, M.; Hagiwara, D.; Karniya, T. *Tetrahedron Letters* **1975**, *49*, 4393.
7. Schonbaum, G. R.; Zerner, B.; Bender, M. L. *J. Biol. Chem.* **1961**, *236*, 2930.
8. Greenstein, J. P.; Winitz, M. *Chemistry of the Amino Acids*, p. 1689. John Wiley and Sons, Inc., New York and London.
9. Foster, R. J.; Niemann, C. *J. Am. Chem. Soc.* **1955**, *77*, 3370.
10. Wallace, R. A.; Kurtz, A. N.; Niemann, C. *Biochemistry* **963**, *2*, 824.
11. Foster, R. J.; Niemann, C. *J. Am. Chem. Soc.* **1955**, *77*, 3365.
12. Bryant, J.; Green, T. R.; Gurusaddaiah, T.; Ryan, C. A. *Biochemistry* **1976**, *15*, 3418.

CHAPTER 7. SMALL PEPTIDES CONTAINING THE NONNATURAL AMINO ACID, 7-AZATRYPTOPHAN: PROBING STRUCTURE, DYNAMICS, AND BIOLOGICAL ACTIVITY

A paper in preparation for submittal to *J. Phys. Chem.*

R. L. Rich¹, D. S. English¹, R. W. Thornburg², and J. W. Petrich^{1,3}

Abstract

7-Azatriptophan is an alternative to tryptophan as an optical probe of protein structure and dynamics. 7-Azatriptophan is synthetically incorporated into a tripeptide and an octapeptide that mimic the active site of potato chymotrypsin inhibitor II, which is known to be a strong inhibitor of α -chymotrypsin. Both tripeptides and octapeptides containing 7-azatriptophan inhibit α -chymotrypsin. The model octapeptide has the sequence: NAc-Lys-Ala-Cys-Pro-7-Azatriptophan-Asn-Cys-Asp-NH₂. This is the first compound containing the 7-azaindole chromophore to display a nonexponential fluorescence decay in water when fluorescence is collected over the entire emission band. 7-Azatriptophan is clearly more sensitive than tryptophan to the onset of whatever secondary structure or partial secondary structure the peptide may have assumed. This result is discussed in terms of three effects: (1) the solvation of the 7-azaindole chromophore itself, which promotes or impedes excited-state tautomerization, and which we have discussed for solvation in water (*J. Phys. Chem.* **1993**, *97*, 1770) and in alcohols (*Chem. Phys. Lett.* **1994**, *222*, 329); (2) the secondary structure imposed by reduction or oxidation of the thiol groups of the two cysteine residues of the octapeptide; (3) inhomogeneities in the secondary structure imposed by the *cis* to *trans* isomerization about the proline residue. It is the thesis of this article that the nonexponential fluorescence decay of the 7-azatriptophan octapeptide is a consequence of excited-state tautomerization of the 7-azaindole chromophore. This tautomerization is suggested to be

¹ Graduate students and Associate Professor, Department of Chemistry, Iowa State University.

² Associate Professor, Department of Biochemistry and Biophysics, Iowa State University.

³ To whom correspondence should be addressed.

promoted by solvent reorganization induced by the peptide backbone or by direct interactions of the 7-azaindole with neighboring amino acid side chains.

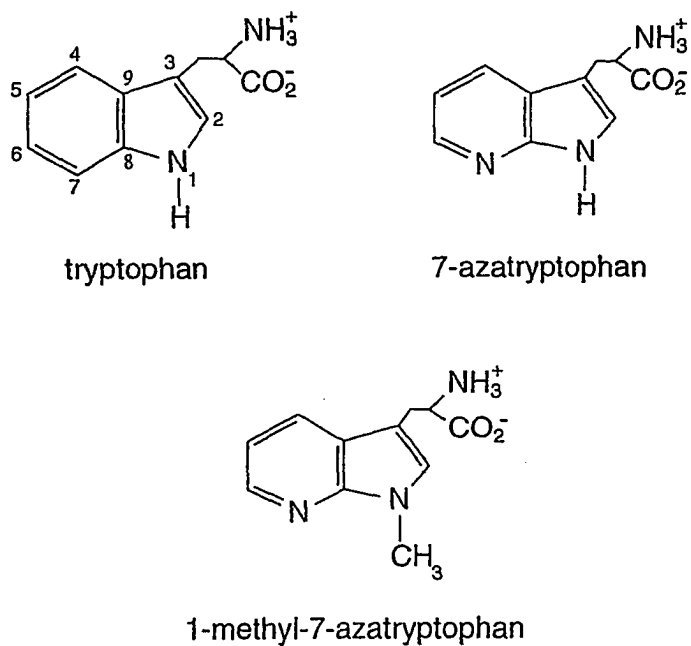
Introduction

The standard optical probe of protein structure and dynamics has been tryptophan (Figure 7.1). The use of tryptophan, however, presents a number of problems. Most significant are the difficulties in the interpretation of the data posed by the intrinsic nonexponential fluorescence decay of tryptophan [1-10] and the occurrence of proteins containing more than one tryptophan residue (which consequently renders the origin of the signal derived from the multiple probes ambiguous).

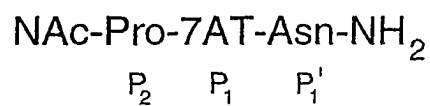
In a series of papers, we have presented the nonnatural analog of tryptophan, 7-azatryptophan, as a promising alternative to tryptophan as a photophysical probe. In addition to having a single-exponential lifetime decay in water over most of the pH range, (e.g. 780 ps at pH 7 and 20°C), 7-azatryptophan has optical spectra that differ significantly from those of tryptophan [11-18]. The absorption and emission spectra of 7-azatryptophan are red shifted 10 nm and 46 nm, respectively, from those of tryptophan.

7-Azatryptophan thus has great potential as a probe of protein structure and dynamics, especially for investigations of protein-protein interactions in which one of the proteins involved may contain several tryptophans. A dramatic illustration of the optical selectivity afforded by the lifetime and the spectroscopic distinguishability of 7-azatryptophan is that in a mixture of tryptophan and 7-azatryptophan, only when the ratio of tryptophan to 7-azatryptophan is as great as 10:1 does the tryptophyl emission become detectable [11,18]; and even when the ratio is 40:1 the 7-azatryptophan is easily detected in the mixture. 5-Hydroxytryptophan, which has been proposed as a useful biological probe [19], has a fluorescence lifetime comparable to that of tryptophan (3.8 ns) and consequently cannot provide the same degree of optical selectivity [18].

Kasha and coworkers were the first to realize that dimers of 7-azaindole can undergo excited-state tautomerization [20]. It was subsequently observed [21-23] that alcohols can provide a state of solvation that predominates at room temperature [15] in which such a double proton transfer is possible with the monomer. In water, on the other hand, we [13] and Kasha and coworkers [24] have provided evidence that such a state of solvation is largely prohibited. Nevertheless, in water at room temperature, the fluorescence lifetimes of



tripeptide:



octapeptide:

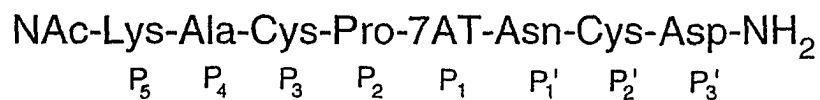


Figure 7.1. Structures of tryptophan, 7-azatryptophan, 1-methyl-7-azatryptophan, and sequences of the peptides studied. The sequences are labelled according to the notation of Berger and Schechter [41] for substrates of proteinases.

7-azaindole and 7-azatryptophan are relatively short-lived (~ 900 and 780 ps, respectively), owing most likely to internal conversion [13,24,25] facilitated by the N₁-H stretch or to dissociation of the bond itself. The 7-azaindole chromophore is thus remarkably sensitive to its state of solvation. The N₁-H interacts strongly with the solvent and the chromophore is poised to undergo an excited-state double proton transfer. The nonradiative pathways permitted by the N₁-H group are very effectively shut down by methylation of the 1-nitrogen [13,20]. 1-Methyl-7-azaindole has a fluorescence lifetime of 21 ns and a fluorescence quantum yield of 0.55 in water at 20°C [13,20]. This suggests that 1-methyl-7-azatryptophan (Figure 7.1) will have a similarly long-lived fluorescence decay and hence be an excellent probe of events transpiring on a more extended time scale [17] (see Conclusions).

We have proposed that the "well-behaved" fluorescence properties of 7-azatryptophan are a result of the interactions of the 1-nitrogen with the solvent [13] and the relatively low energy of its fluorescent state with respect to that of tryptophan [18].

In order for 7-azatryptophan to be useful as a biological probe and not merely a photophysical curiosity, it is required that 7-azatryptophan be amenable to incorporation into proteins and peptides and that these modified systems remain functional [11]. We have begun studies of a number of protein systems. For example, we have synthesized 5'-phosphopyridoxyl-7-azatryptophan [16] for use as a probe of tryptophanase, tryptophan synthase, and other enzymes requiring a vitamin B₆ derivative as a coenzyme. We have demonstrated that biotinylated 7-azatryptophan retains a high binding constant with respect to avidin and can usefully probe local motion (rapid restricted motion) with respect to overall tumbling of avidin — even in the presence of excess tryptophan residues [17]. Finally, the suitability of 7-azatryptophan for use in peptide synthesis was demonstrated by producing a tripeptide analog of the active site of the potato chymotrypsin inhibitor II (a degradation product of potato proteinase inhibitor II), which is a strong inhibitor of α -chymotrypsin: $K_I \sim 2 \times 10^{-8}$ M [14]. The sequence of this tripeptide is NAc-Pro-7-Azatryptophan-Asn-NH₂, where 7-azatryptophan is substituted for Leu, which occurs in the native protein.

In this article we report the synthesis of a 7-azatryptophan-containing octapeptide that mimics the active site of the potato chymotrypsin inhibitor II: NAc-Lys-Ala-Cys-Pro-7-Azatryptophan-Asn-Cys-Asp-NH₂. Both tripeptides and octapeptides containing 7-azatryptophan inhibit α -chymotrypsin. *Unlike the tripeptide, the octapeptide displays a nonexponential fluorescence decay (Table 7.1). In fact, the octapeptide is the first compound containing the 7-azaindole chromophore reported to display a nonexponential fluorescence decay in water when fluorescence is collected over the entire emission band.* This result is

Table 7.1 Summary of Fluorescence and Anisotropy Decay Parameters

species ($\lambda_{\max}^{\text{em}}$)	τ_1 (ps)	τ_2 (ps)	A_1	τ_r (ps) ^b	$\lambda_{\text{ex}}, \lambda_{\text{em}}$ (nm)
7-azaindole (386 nm) [13]	886 ± 15	---	1.00	$20 \pm 2^{\text{f}}$	$305, \geq 320$
7-azaindole/MeOH, (364, 505 nm) [36]	730	147^{c}	0.10	$34 \pm 8^{\text{g}}$ [12]	$285, \geq 320$
7-azatryptophan (397 nm)[13,18]	780 ± 10	---	1.00	50 ± 3	$305, \geq 320$
7-azatryptophan (MeOH, 382 nm) [18]	350	$150 \pm 8^{\text{d}}$	0.10	57 ± 8	$305, 320-460$
tripeptide (397 nm)	833 ± 2	---	1.00	103 ± 13	$310, \geq 345$
reduced octapeptide (396 nm)	845 ± 9	189 ± 31	0.84 ± 0.04	312 ± 17	$290, \geq 335$
reduced octapeptide (TCEP, 460 nm)	846 ± 35	278 ± 82	0.80 ± 0.04	426 ± 103	$305, \geq 320$
alkylated octapeptide (398 nm)	931	232	0.72	465	$285, \geq 335$
oxidized octapeptide (389 nm)	874 ± 11	216 ± 30	0.82 ± 0.02	297 ± 48	$290, \geq 335$
tryptophan [1]	3210 ± 120	620 ± 50	0.78 ± 0.01	33.2 ± 5.5 [40]	$295, \geq 320$
Arg-Trp-Gly ^c [6]	1910 ± 20	730 ± 70	0.78 ± 0.01	140 ± 20	$295, \geq 335$
reduced tryptophan octapeptide (350 nm)	1928 ± 198	281 ± 33	0.53 ± 0.04	407 ± 26	$290, \geq 335$
oxidized tryptophan octapeptide (350 nm)	1636 ± 94	274 ± 56	0.56 ± 0.04	275	$290, \geq 335$

Table 7.1 (continued)

- ^a Unless otherwise specified, the measurement is carried out in water at 20°C. Fluorescence lifetimes are best described by two exponentially decaying components and are fit to the form: $K(t) = A_1 \exp(-t/\tau_1) + A_2 \exp(-t/\tau_2)$.
- ^b In all cases the fluorescence anisotropy decay is adequately described by a single exponentially decaying component: $r(t) = r(0) \exp(-t/\tau_r)$. For the oxidized 7-azatryptophan octapeptide, a double-exponential model does not significantly improve the fit. See Results and Discussion.
- ^c The rise time for the formation of the tautomer band of 7-azaindole in methanol is 150 ps at room temperature [12,13].
- ^d When emission is collected at wavelengths greater than 505 nm, a rise time commensurate to this decaying component is observed, i.e., 127 ps.
- ^e ACTH(8-10).
- ^f 23.5°C [12].
- ^g -9°C [12].

discussed in terms of three effects, whose importance, in order of decreasing significance is believed to be:

1. The solvation of the 7-azaindole chromophore itself, which to different extents may promote or impede excited-state tautomerization, alluded to above, and which we have discussed for solvation in water [13] and in alcohols [15].
2. The secondary structure imposed by reduction or oxidation of the thiol groups of the two cysteine residues of the octapeptide. The existence of this secondary structure is demonstrated both by classical chemical spot tests as well as by fluorescence quenching experiments and rotational diffusion times obtained from fluorescence anisotropy decays.
3. Inhomogeneities in the secondary structure imposed by the *cis* to *trans* isomerization about the proline residue [26,27].

It is the thesis of this article that the nonexponential fluorescence decay of the 7-azatryptophan octapeptide is a consequence of excited-state tautomerization of the 7-azaindole chromophore. This tautomerization is promoted by solvent reorganization induced by the peptide backbone or by direct interactions of the 7-azaindole with neighboring amino acid side chains.

Experimental

Peptide Synthesis

Synthesis of peptides containing 7-azatryptophan was performed as described elsewhere [14] using an Applied Biosystems 430A Peptide Synthesizer starting with benzhydrylamine resin. The purity of the tripeptides and octapeptides was verified by HPLC. An important distinction between the octapeptide and the tripeptide, however, is that the octapeptide contains two cysteine residues, which provide the potential for disulfide formation. This eventuality is discussed and considered in the following experimental procedures and in the Results and Discussion sections.

Since the octapeptide yielded a double-exponential fluorescence lifetime (see below) the octapeptide preparations (i.e, reduced, oxidized, and alkylated forms) were frequently checked for impurities or degradation by TLC using Sigma T-6770 precoated plates and several solvent systems: EtOH/H₂O, EtOAc/H₂O, and BuOH/H₂O/HOAc in various proportions. All results gave a single spot when viewed under UV light or after development in an I₂ chamber.

An octapeptide containing tryptophan in the P₁ position (Figure 7.1) was purchased from Genosys Biotechnologies, Inc. The purity of the sample was >95%. Results of time-resolved experiments using the tryptophan octapeptide were compared with those obtained from the 7-azatryptophan octapeptide.

Derivatization of the 7-Azatryptophan Octapeptide

Several routes were employed to ensure complete reduction or oxidation of the cysteine thiols. Identical results were obtained for both the D- and the L-octapeptides.

Reduction of Cysteine Residues. Two methods for reducing the disulfide linkages within the octapeptide were employed. Dithiothreitol (DTT) was added to solutions of the octapeptide to a final concentration of 0.05 M DTT and allowed to react for four hours under inert atmosphere before analysis to ensure significant reduction of the cysteine thiols.

Alternatively, a solution of tris(2-carboxyethyl)phosphine hydrochloride (TCEP•HCl) [28] was prepared by dissolving 11.5 μmol in 100 μL water. This TCEP•HCl solution was added to a solution of octapeptide (0.1 μmol) in 100 μL water. The reduction of disulfide bonds appears to be immediate since there is no change in the fluorescence lifetime data when the reaction mixture is monitored over several hours.

Alkylation of Cysteine Residues. Another strategy employed to remove disulfide linkages was to alkylate all the cysteine residues. Disulfide linkages in the octapeptide were reduced using TCEP•HCl as described above. 2-Methylaziridine (Aldrich) was added undiluted in a quantity representing a greater than 40-fold excess of methylaziridine to sulfhydryl groups [29]. The solution was evaporated to dryness using an argon stream to remove all excess 2-methylaziridine. The alkylated octapeptide was reconstituted in water.

Analyses of the thiol-containing (reduced) and alkylated octapeptides were performed under an inert atmosphere, while the studies of the disulfide-containing (oxidized) octapeptides were not. The solutions of the reduced and alkylated octapeptides were deoxygenated with argon. The concentration of dissolved oxygen was less than 6.25×10^{-6} M as measured by a Hach OX-2P kit. A positive pressure of argon was maintained throughout the measurements.

Oxidation of Cysteine Residues. Aqueous samples of D-octapeptide were bubbled under pure oxygen using needle and septa at room temperature. The sample volume was maintained so that the peptide concentration was $\sim 10^{-5}$ M.

The oxidation state of the thiols in the octapeptides was verified by a spot test [30]. The spot test depends on the ability of the thiol groups to catalyze the reaction, $2\text{NaN}_3 + \text{I}_2$

→ 2NaI + 3N₂ (g). The presence of thiol groups is indicated by bubbling due to the evolution of N₂ and the loss of yellow color due to the consumption of I₂. This test is somewhat subjective and may not be sensitive enough for concentrations below 10⁻⁵ M. The results, however, indicate clearly the presence of -SH groups for the octapeptide under reducing conditions and are negative for the octapeptide under oxidizing conditions.

Measurements of Peptide Conformation

Peptidyl-prolyl-*cis/trans*-isomerase (PPIase) was obtained from Sigma. Solutions of 2×10^{-4} M D-7-azatryptophan octapeptide were prepared in tris buffer at pH 8.0 and maintained at 10°C. Enough PPIase was added to the solution to obtain a 40:1 ratio of proline residues to enzyme. These experimental conditions are similar to those described by Lang *et al.* [26]. Time-correlated single photon counting measurements were taken before and after the addition of PPIase.

In addition, samples of the D-7-azatryptophan tripeptide were dissolved in D₂O and submitted for natural abundance ¹³C NMR measurements. Concentrations were ~ 20 mg/mL. In this range the spectra have been reported to be independent of concentration [43]. Measurements were performed in a 5-mm tube on a Unity 500 spectrometer. 9,700 acquisitions were collected at 125 MHz with a 45° pulse. A 2.6-second recycle time was used between acquisitions to allow full relaxation of nuclei. NOE was suppressed by gated decoupling to make results suitable for quantitative analysis. The probe temperature was maintained at 20°C. The FID was processed using NMR1 software on a Digital DEC station 5000/200. *Cis/trans* ratios were determined by fitting the peaks to a lorentzian and integrating. Chemical shifts were calibrated to an internal standard of CS₂, which was assigned a value of 192.5 ppm.

Other NMR experiments were carried out in order to confirm that PPIase did not change the *cis/trans* ratio of the peptide. These were performed on a VXR 300 under similar conditions except that the sample was maintained at 10°C at pH 8.0. Here, the sample was monitored before and after addition of PPIase (1:70 ratio of enzyme to peptide). 12,000-13,000 acquisitions were collected in order to give suitable signal-to-noise ratios for accurate peak integrations.

Classical Kinetic Studies

Kinetic and binding studies of the peptide inhibitors was performed by monitoring the hydrolysis of a substrate catalyzed by α-chymotrypsin. Bovine α-chymotrypsin was

dissolved in 0.1 M sodium acetate buffer solution adjusted to pH 5.05 with dilute acetic acid, and the active-site concentration was determined [31]. The substrate, succinyl-Ala-Ala-Pro-Phe-*p*-nitroanilide (CalBiochem), was dissolved in dimethylsulfoxide. The weak inhibitors were dissolved in 0.1 M tris-HCl, 0.02 M CaCl₂, 0.005% Triton X-100 (w/v) buffer solution adjusted to pH 7.8 with dilute HCl. Potato chymotrypsin inhibitor II (CalBiochem) was dissolved in deionized water. Concentrations of the 7-azatryptophan peptide solutions were determined spectrophotometrically using $\epsilon_{288\text{nm}} = 6200 \text{ cm}^{-1} \text{ M}^{-1}$. Absorbance changes due to substrate hydrolysis were most effectively monitored at 410 nm. Experiments were run at $24 \pm 2^\circ\text{C}$. For all analyses the enzyme concentration in the reaction cell was nanomolar and the substrate concentration approximated $0.1 K_M \leq [S]_{\text{rxn}} \leq 10 K_M$. Fresh inhibitor solutions were used for each kinetic run. As a check of the experimental conditions and procedure, the K_I of potato chymotrypsin inhibitor II was determined and the result agreed with published results [32].

We measured the K_I of the octapeptide reduced with 0.05 M DTT. This concentration of DTT did not damage the α -chymotrypsin disulfide linkages within the time required for each measurement. Measurements of the K_I of the alkylated and TCEP•HCl-reduced octapeptides were not performed, since these procedures yielded the same fluorescence lifetimes as the DTT-reduced species. The K_I for the 7-azatryptophan octapeptide under oxidizing conditions agreed within experimental error with that for the reduced species.

Time-Resolved Experiments

Fluorescence lifetimes and fluorescence anisotropy decays were obtained by means of time-correlated single-photon counting using the apparatus described elsewhere [13]. In most cases the emission wavelength was selected by cutoff filters. Standard sample concentrations were $\sim 10^{-5}$ M. When more spectral resolution was required the samples were concentrated to $\sim 10^{-4}$ M (OD ~ 0.7 at 290 nm for the 7-azatryptophan octapeptide) and emission was collected with an ISA H-10 monochromator with 2-mm slits. This provided a 16-nm bandpass.

Fluorescence quenching experiments were carried out by adding aliquots of 1.5-M solutions of the respective quencher (KI or acrylamide) to a 1-mL sample ($\sim 10^{-5}$ M) of the fluorescing molecule. The reduced and oxidized samples were kept in cuvettes sealed with septa under argon and oxygen, respectively. The quencher was injected with a glass syringe, and the sample was thoroughly agitated.

Data were fit to one or two decaying exponentials by an iterative convolution procedure using a nonlinear least squares algorithm. The quality of the fit was determined by visual inspection of the residuals and the χ^2 criterion [12,13]. Results reported with error estimates are obtained from at least three and as many as seven experiments.

Results

Steady-State Kinetics: Determination of Inhibition Constants

Classical kinetic studies (Table 7.2) indicate that the D- and L-peptides (Figure 7.1) are competitive inhibitors of α -chymotrypsin. Thus, not only do the model peptides bind to the target enzyme, but each binds at the active site and inhibits proteolytic activity. The presence of the nitrogen at the 7 position in 7-azatryptophan is shown not to introduce additional binding interactions by the identical K_I values for indole and 7-azaindole. Kinetic studies using the octapeptide containing 7-azatryptophan as an inhibitor indicate that the additional five amino acid residues do not improve the K_I with respect to the tripeptide (Table 7.2). Both the D- and L-enantiomers yield the same result within experimental error.

Steady-State Spectra and Fluorescence Decay

The fluorescence maximum of the model tripeptide containing D- or L-7-azatryptophan is 397 nm at 20°C and pH 7 [33]. The fluorescence spectra of the reduced and the oxidized 7-azatryptophan and tryptophan octapeptides are compared in Figure 7.2.

The fluorescence lifetime of the 7-azatryptophan tripeptide is single-exponential of 830-ps duration. Thus, not only is the fluorescence decay of 7-azatryptophan in water single-exponential, but so is that of the tripeptide containing 7-azatryptophan. In contrast, most derivatives of tryptophan except for the anomalous N-acetyl-tryptophanamide exhibit fluorescence decays that can be fit only to a sum of exponentials. [1,2].

The fluorescence lifetime of the 7-azatryptophan octapeptide is nonexponential under all conditions (Table 7.1 and Figure 7.3), i.e. whether the octapeptide contains D- or L-7-azatryptophan or whether the octapeptide is reduced, oxidized, or alkylated.

It is unlikely that an impurity is the cause of the nonexponentiality of the fluorescence decay of the octapeptide. One would expect a species contributing 20% to the fluorescence lifetime decay to be apparent in the steady-state emission spectrum. This is not the case,

Table 7.2 Inhibition of α -Chymotrypsin

species	K_i (mM)
indole	$0.4 \pm 0.2, 0.8 \pm 0.2$ [38]
7-azaindole	$0.4 \pm 0.1, 1.3 \pm 0.2$ [43]
leucine	10 ± 4
tryptophan ^a	$16 \pm 6, 6 \pm 2$ [39]
7-azatryptophan	42 ± 10
Pro-Leu	45 ± 4
Pro-Trp	22 ± 7
Nac-Pro-Leu-Asn-NH ₂	7 ± 3
NAc-Pro-L-7AT-Asn-NH ₂	0.3 ± 0.2
NAc-Pro-D-7AT-Asn-NH ₂	0.5 ± 0.1
NAc-Lys-Ala-Cys-Pro-L-7AT-Asn-Cys-Asp-NH ₂	0.5 ± 0.2
NAc-Lys-Ala-Cys-Pro-D-7AT-Asn-Cys-Asp-NH ₂	0.5 ± 0.1
Potato Chymotrypsin Inhibitor II	$2.3 \pm 0.4 \times 10^{-8}, 2 \times 10^{-8}$ [32]

^a Our experiments used the L form of tryptophan, Foster and Niemann [39] used the D form.

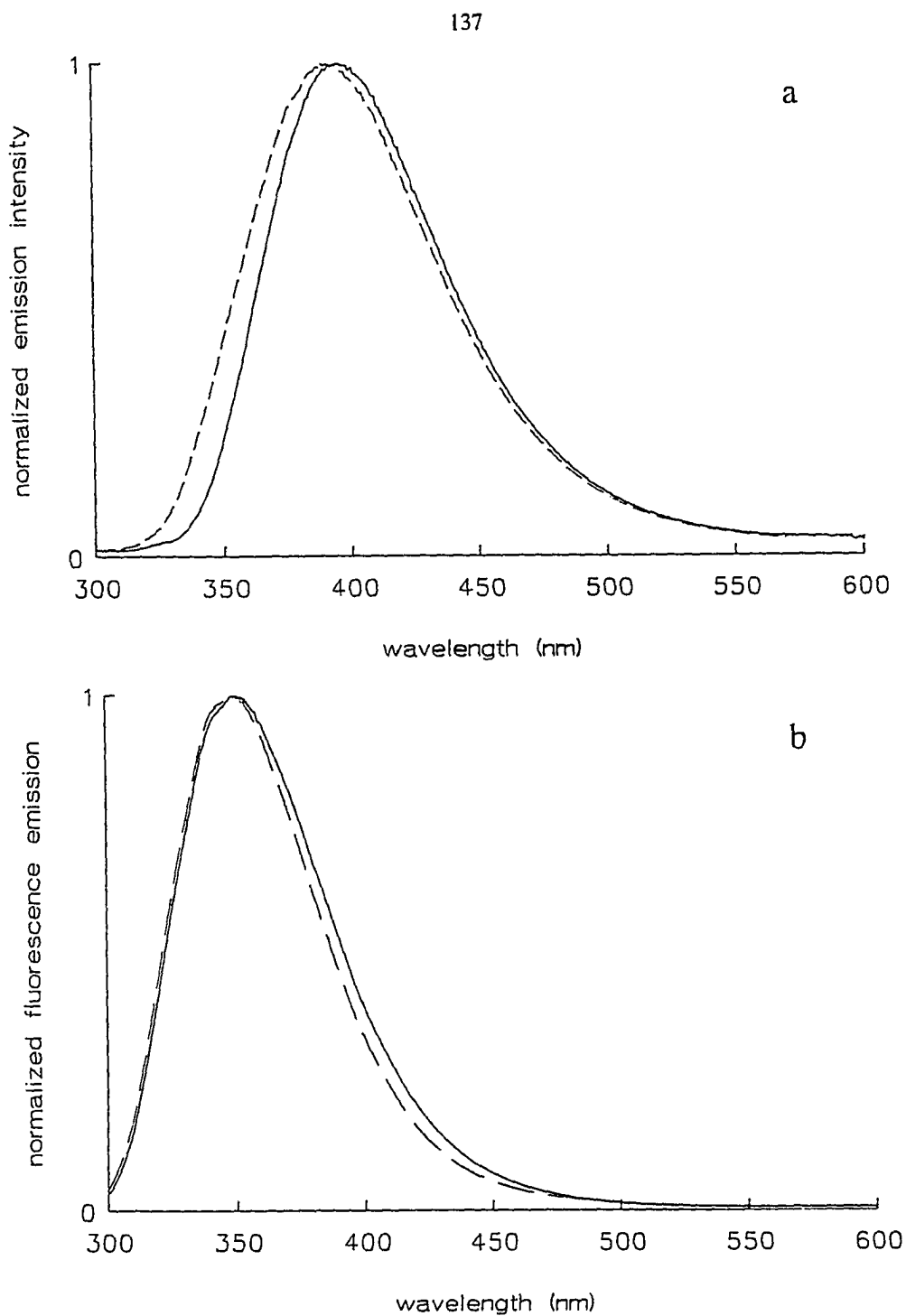


Figure 7.2. Emission spectra (a) the reduced and oxidized D-7-azatryptophan octapeptides and (b) the reduced and oxidized L-tryptophan octapeptides. All spectra were measured in water at neutral pH. In both panels the dashed curve represents the oxidized species.

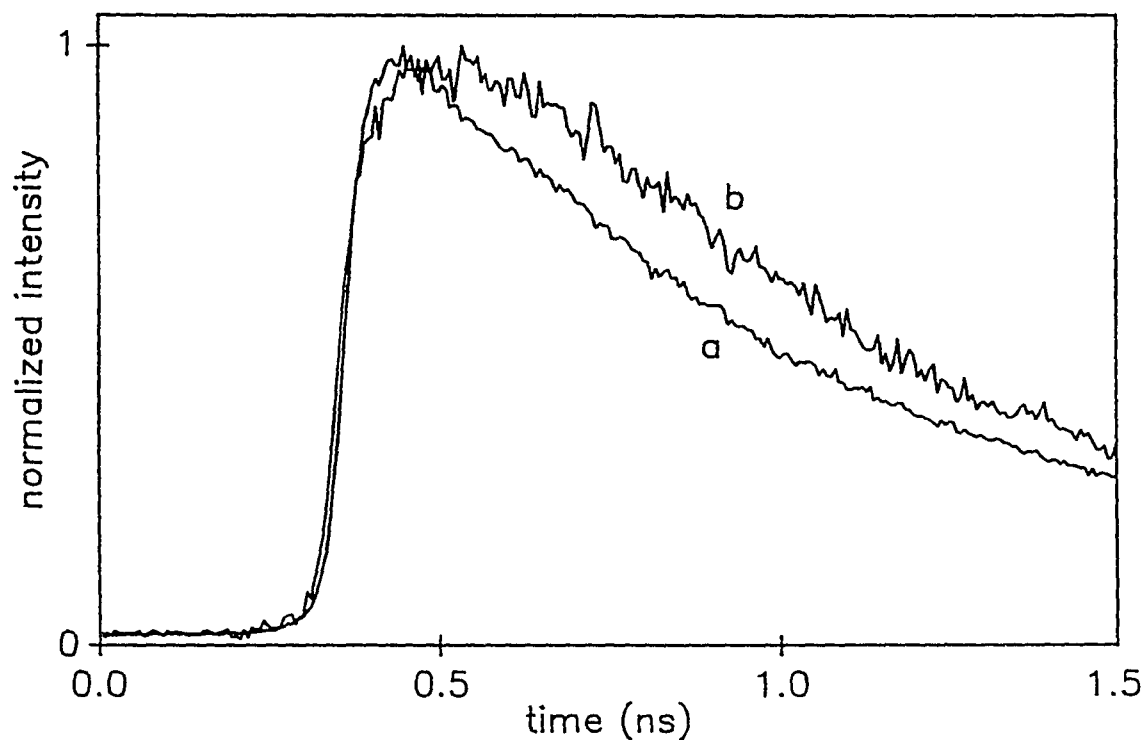


Figure 7.3. Fluorescence lifetime decays of the reduced D-7-azatryptophan octapeptide at 20 °C. (a) $\lambda_{em} = 375$ nm, $K(t) = 0.19\exp(-t/100 \text{ ps}) + 0.68\exp(-t/706 \text{ ps}) + 0.13\exp(-t/1658 \text{ ps})$; $\chi^2 = 1.55$. (b) $\lambda_{em} \geq 505$ nm, $K(t) = -0.24\exp(-t/151 \text{ ps}) + 0.92\exp(-t/656 \text{ ps}) + 0.32\exp(-t/1504 \text{ ps})$; $\chi^2 = 1.12$. The latter measurement was collected to a maximum of 2000 counts instead of 10,000 owing to the low fluorescence intensity in this region.

since the reduced and alkylated octapeptide emission spectra (measured at pH 7.8) are nearly identical to that of 7-azatryptophan in water.

Fluorescence Anisotropy Decay

The fluorescence anisotropy decay of the 7-azatryptophan tripeptide and the 7-azatryptophan octapeptide in the reduced and oxidized states were measured as a function of temperature. Identical results were obtained for both the D and the L forms.

The fluorescence anisotropy decays of the 7-azatryptophan tripeptide and reduced octapeptide are both very well described by a single-exponential ($\chi^2 \sim 1.1-1.3$) (Figure 7.4). On the other hand, the fit of the anisotropy decay of the 7-azatryptophan oxidized octapeptide to a single exponential is typically not very good ($\chi^2 \sim 2$); but a double-exponential fit does not yield a significantly better result.

Assuming the peptide solvent complex is spherical, plots of the anisotropy decay against temperature can be used to estimate a hypothetical volume [12] (see Figure 7.5 and caption). The volume obtained for the tripeptide is $470 \pm 10 \text{ \AA}^3$. The volume obtained for both the reduced and oxidized octapeptides is $1700 \pm 200 \text{ \AA}^3$. Given that the reduced and oxidized forms are likely to have extended and hairpin geometries, respectively, we conclude that the 7-azatryptophan is in both cases probing similar forms of local depolarizing motion that is independent of the gross conformation of the octapeptide. (Similar results have been observed for a series of ACTH fragments of varying lengths [6].)

Temperature Dependence of the Fluorescence Lifetimes of the 7-Azatryptophan Octapeptide

An Arrhenius plot constructed from the single exponential fluorescence lifetimes of the D-7-azatryptophan tripeptide yields a straight line and an activation energy of 2.9 ± 0.1 kcal/mol, which is identical, within experimental error, to that of 7-azaindole in water [13]. The temperature dependence of the fluorescence lifetimes of the 7-azatryptophan octapeptide is, however, much more complicated. Table 7.3 summarizes the dependence of the fluorescence decay of the 7-azatryptophan octapeptide under reducing and oxidizing conditions as a function of temperature. Contrary to what is observed for tryptophan peptides, for example, the two fluorescence lifetime components do not show a marked tendency to decrease with increasing temperature. In fact, *both* increases and decreases in the lifetimes are observed with increasing temperature. We suggest that this complicated behavior is indicative of the presence of several thermally activated processes: local

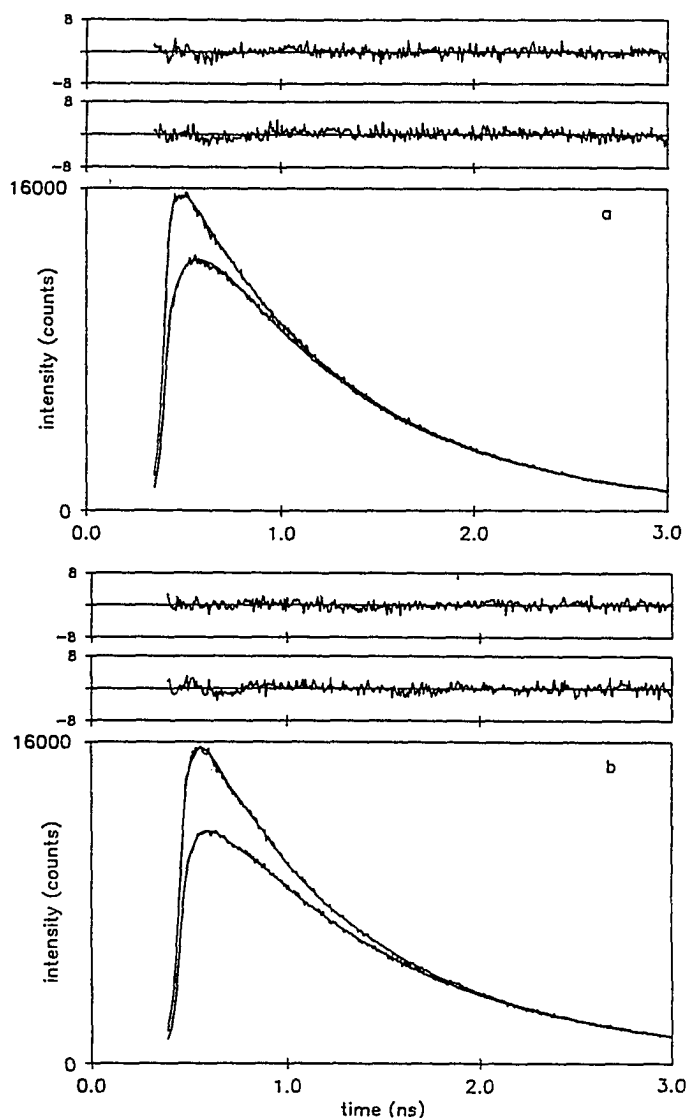


Figure 7.4. Fluorescence anisotropy decay of 7-azatryptophan containing peptides at $20 \pm 1^\circ$ C:

(a) the D-7-azatryptophan-tripeptide ($\lambda_{\text{ex}} = 310$ nm, $\lambda_{\text{em}} \geq 345$ nm); $K(t) = \exp(-t/833$ ps), $\chi^2 = 1.31$; $r(t) = 0.19\exp(-t/103$ ps), $\chi^2 = 1.26$;

(b) the reduced D-7-azatryptophan-octapeptide ($\lambda_{\text{ex}} = 310$ nm, $\lambda_{\text{em}} \geq 345$ nm); $K(t) = 0.22\exp(-t/184$ ps) + $0.78\exp(-t/833$ ps), $\chi^2 = 1.35$; $r(t) = 0.13\exp(-t/312$ ps), $\chi^2 = 1.10$. In both cases, the upper set of residuals corresponds to fluorescence polarized parallel to the excitation beam (I_{\parallel}); the lower set, to fluorescence polarized perpendicular to the excitation beam (I_{\perp}).

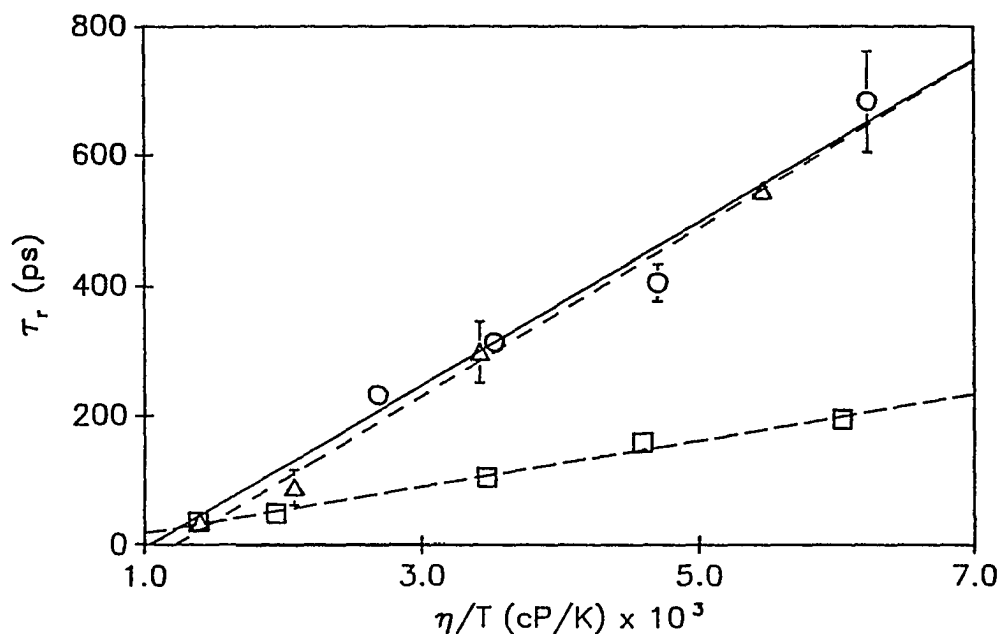


Figure 7.5. Plots of the rotational diffusion (reorientation) time, τ_r , against η/T for the D-7-azatryptophan tripeptide (\square) and the reduced (O) and the oxidized (—) D-7-azatryptophan-octa-peptides. Identical results were obtained for the L forms.

The τ_r data presented are averages from at least three measurements at a given viscosity. $\lambda_{ex} = 310$ nm and $\lambda_{em} \geq 345$ nm. The samples were dissolved in tris buffer (see Materials and Methods), but the viscosity values used were those of water [42].

The data are fit to the relation, $\tau_r = c\eta + \tau_0$, where $c = V/kT$ if the diffusing species is a sphere. The tripeptide data yield a volume of $470 \pm 10 \text{ \AA}^3$. The reduced and oxidized octapeptide data both yield a volume of $1700 \pm 200 \text{ \AA}^3$.

Table 7.3 Temperature Dependence of the Fluorescence Decay of the 7-Azatriptophan D-Octapeptide Under Reducing and Oxidizing Conditions

Reduced (RSH HSR) 7-Azatriptophan Octapeptide			
T (°C)	τ_1 (ps)	τ_2 (ps)	A_1
1.5	210 ± 47	1278 ± 22	0.07 ± 0.01
20	191 ± 9	830 ± 11	0.18 ± 0.04
30	196 ± 17	710 ± 11	0.18 ± 0.01
50	240 ± 24	555 ± 7	0.22 ± 0.03
70	379 ± 3	1219 ± 197	0.93 ± 0.02
Oxidized (RS-SR) 7-Azatriptophan Octapeptide			
T (°C)	τ_1 (ps)	τ_2 (ps)	A_1
1.5	264 ± 43	1362 ± 17	0.17 ± 0.02
20	417 ± 22	1084 ± 32	0.38 ± 0.03
30	430 ± 11	1354 ± 232	0.62 ± 0.06
45	455 ± 78	1354 ± 42	0.84 ± 0.01
50	448 ± 23	2112 ± 225	0.87 ± 0.03
70	364 ± 2	2251 ± 146	0.89 ± 0.01

solvation of 7-azaindole by both water and the peptide, peptide conformational changes (including most notably *cis/trans* isomerization — see below), and the nonradiative processes intrinsic to the 7-azaindole chromophore in water.

Fluorescence Quenching as a Probe of Conformational Inhomogeneity

In order to verify that the thiol groups of the octapeptide were either reduced and free or oxidized and existing as disulfide bonds, fluorescence lifetimes were measured as a function of concentration of a quencher. One would expect that the oxidation state of the thiols would subject the 7-azaindole chromophore to different local environments and that these different environments would render the chromophore more or less accessible to an external fluorescence quencher.

Control experiments were performed with free 7-azaindole and indole. The Stern-Volmer plots obtained using KI and acrylamide as quenchers are displayed in Figure 7.6. For 7-azaindole, the Stern-Volmer plots are constructed for both quenchers with the *average* lifetime. This was necessary because 7-azaindole in the presence of KI or acrylamide, *unlike indole*, yields a fluorescence decay that is well described by a sum of two exponentials (Table 7.4). We shall address this point later.

The control experiments (Figure 7.6) indicate that indole is quenched much more efficiently than 7-azaindole by either KI or acrylamide. Assuming that acrylamide quenches by an electron transfer process, these results are consistent with our earlier analysis for the absence of nonexponential fluorescence decay for 7-azatryptophan in water. Namely, nonexponential fluorescence decay is not observed for 7-azatryptophan, whereas it is for tryptophan, because excited-state 7-azatryptophan is not a good electron donor. This is a result of the energy of the 7-azatryptophan singlet being lower than that of tryptophan [18].

7-Azatryptophan Octapeptide and KI. The concentration dependence of the fluorescence quenching of the 7-azatryptophan octapeptide by KI is given in Table 7.5. The presence of KI does not significantly perturb the weight of the shorter-lived component with respect to that of the longer-lived component on going from reducing to oxidizing conditions. The data in the Table also indicate that the lifetime itself is not affected so much as the relative weights of the two decaying components. This suggests that a nonfluorescent (or weakly fluorescent) complex is formed between the 7-azaindole chromophore and KI in the ground state.

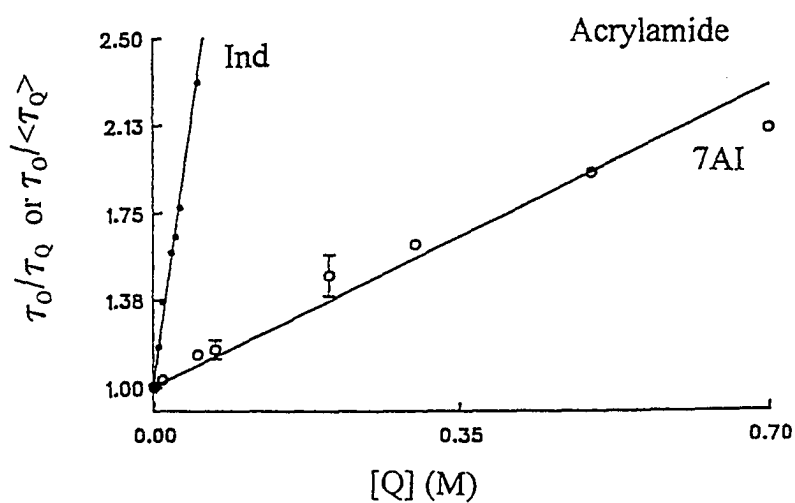
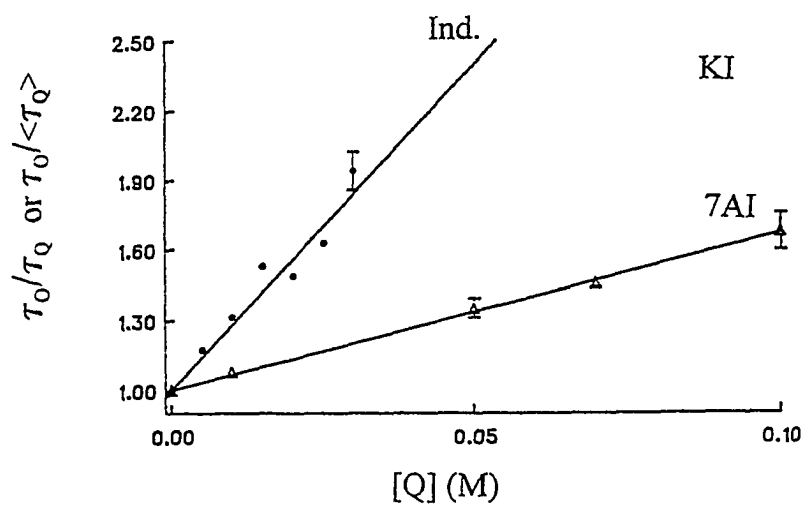


Figure 7.6. Stern-Volmer plots for the fluorescence quenching of 7-azaindole and indole with KI and acrylamide. Since the fluorescence lifetime for 7-azaindole in the presence of quencher is nonexponential, the quantity plotted is actually the single exponential lifetime in the absence of the quencher divided by the *average fluorescence lifetime in the presence of the quencher*. There is a marked difference between 7-azaindole and indole. The slopes for 7-azaindole and indole are 6.7 M^{-1} and 28.0 M^{-1} , respectively, when KI is the quencher. The slopes for 7-azaindole and indole are 1.8 M^{-1} and 26.0 M^{-1} , respectively, when acrylamide is the quencher.

Table 7.4 Quenching of 7-Azaindole Fluorescence^a

KI				
[Q] (M)	τ_1 (ps)	τ_2 (ps)	A_1	$\langle\tau\rangle$ (ps)
0	886 ± 15	---	1.00	891
0.01	857	338	0.93	821
0.05	805	431	0.57	644
0.07	831	440	0.43	608
0.10	1039	415	0.16	515
0.20	1043	286	0.08	344

acrylamide				
[Q] (M)	τ_1 (ps)	τ_2 (ps)	A_1	$\langle\tau\rangle$ (ps)
0	886 ± 15	---	1.00	896
0.01	878	---	1.00	878
0.05	813	601	0.87	785
0.07	1032	665	0.23	794
0.20	1218	503	0.11	582
0.50	2107	312	0.07	438
0.90	2634	207	0.07	377

^a Experiments are performed at 20°C. Data are fit to the function $K(t) = A_1 \exp(-t/\tau_1) + A_2 \exp(-t/\tau_2)$. When 7-azaindole was quenched with acrylamide in the range of 0.05-0.07 M, the results of the fits were not always reproducible; but the average lifetime was always conserved. The data presented here represent one run.

Table 7.5 Quenching by KI of the Fluorescence from the 7-Azatriptophan D-Octapeptide Under Reducing and Oxidizing Conditions

Reducing (RSH HSR) Conditions				
[KI] (M)	τ_1 (ps)	τ_2 (ps)	A_1	$\langle\tau\rangle$ (ps)
0	845 ± 9	189 ± 31	0.84 ± 0.04	732
0.01	883	285	0.69	698
0.03	960	331	0.51	652
0.05	893	318	0.50	606
0.07	808	346	0.53	591
0.10	1033	383	0.35	611
0.15	892	353	0.35	542
0.20	959	294	0.32	509

Oxidizing (RS-SR) Conditions				
[KI] (M)	τ_1 (ps)	τ_2 (ps)	A_1	$\langle\tau\rangle$ (ps)
0	874 ± 11	216 ± 30	0.82 ± 0.02	756
0.01	949	323	0.73	780
0.03	975	396	0.64	767
0.05	1222	447	0.43	780
0.07	1270	441	0.39	764
0.10	1224	396	0.40	727
0.15	1249	401	0.32	672
0.20	1128	388	0.28	556

Most importantly, the concentration dependence is qualitatively very similar to that for 7-azaindole itself. To the extent that the nonexponential decay of the octapeptide is due to all of the chromophores in an identically solvated environment that is suitable for excited-state tautomerization (see Introduction and Conclusions) and not to conformational heterogeneity (which is most likely an oversimplification), it was considered most convenient to construct Stern-Volmer plots using the average fluorescence lifetime. Figure 7.7 compares the dependence of the average lifetime of 7-azaindole with that of the 7-azatryptophan octapeptide under reducing and oxidizing conditions, respectively. It is seen that the oxidized octapeptide to a small extent impedes the quenching of the 7-azaindole chromophore more efficiently than the reduced octapeptide. The slopes of the Stern-Volmer plots for the oxidized and the reduced species are 1.4 and 2.2 M^{-1} , respectively.

7-Azatryptophan Octapeptide and Acrylamide. In contrast to KI, however, acrylamide affects both the relative weights of the shorter- and longer-lived components as well as the duration of the longer-lived decay component (Figure 7.7). For example, in going from 0 to 0.5 M acrylamide, the weight and the lifetime of the longer-lived component decrease from 0.82 and 878 ps to 0.55 and 661 ps. This is suggestive of a combination of different quenching mechanisms and modes of interaction between the peptide and KI and acrylamide.

For reasons identical to those enumerated above, Stern-Volmer plots were constructed using average lifetimes. There is very little difference in the sensitivity of the average fluorescence lifetime of the oxidized and the reduced peptides to acrylamide, whose Stern-Volmer plots yield slopes of 1.1 and 1.3 M^{-1} , respectively.

Tryptophan Octapeptide. For purposes of comparison, quenching studies of the tryptophan octapeptide were performed. The origin of the nonexponential fluorescence decay in tryptophan and tryptophan-containing compounds is generally attributed to the presence of several conformations, in which the tryptophan has different nonradiative rates, that do not equilibrate rapidly during the excited-state lifetime [1,2,8,34,45-47]. Insofar as one is justified in assigning the nonexponential fluorescence decay in tryptophan-containing compounds to different conformations of the chromophore with respect to a quencher (e.g., a charge-transfer acceptor [1,18,35]) it is reasonable to construct Stern-Volmer plots based on the quenching characteristics of the two lifetime components instead of the average lifetime as we have done above with the 7-azatryptophan peptide.

Figures 7.8 and 7.9 present the behavior the shorter- and longer-lived lifetime components for the reduced and oxidized tryptophan octapeptide in the presence of KI and

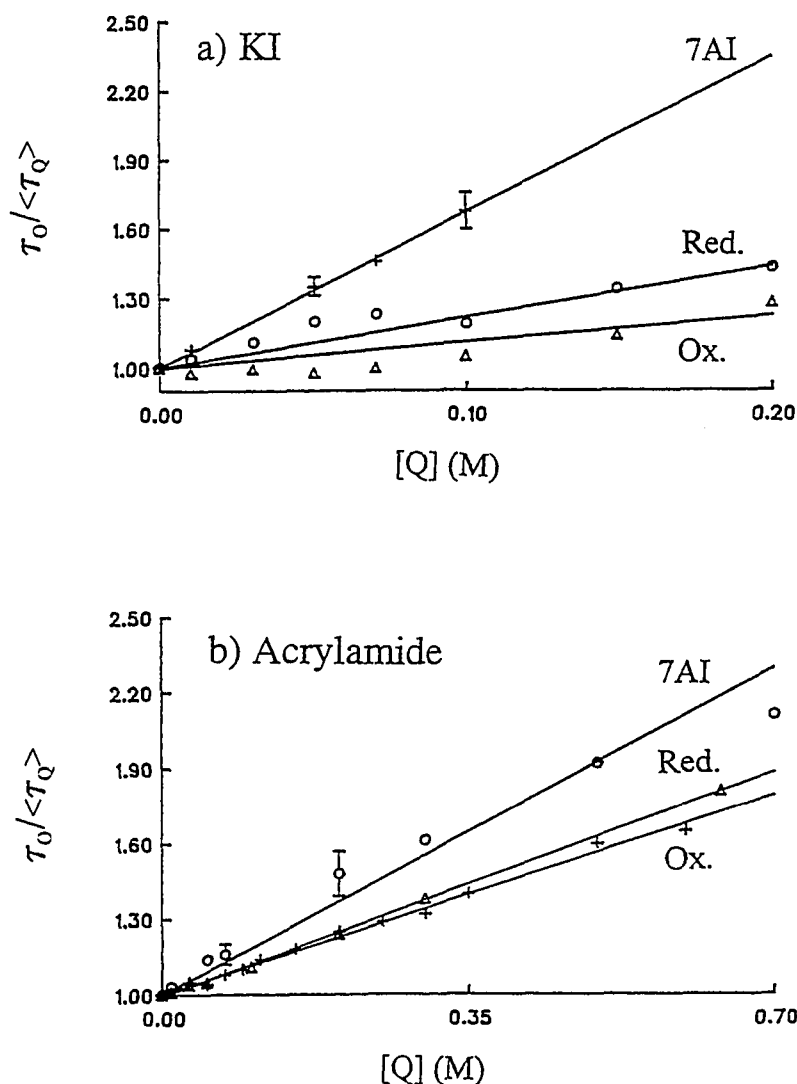


Figure 7.7. (a) Stern-Volmer plots for the quenching of 7-azatryptophan D-octapeptide fluorescence with KI under both reducing and oxidizing conditions. The slopes of the Stern-Volmer plots for the oxidized and the reduced forms are 1.4 M^{-1} and 2.2 M^{-1} , respectively.

(b) Stern-Volmer plots for the quenching of 7-azatryptophan D-octapeptide fluorescence with acrylamide under both reducing and oxidizing conditions. The slopes of the Stern-Volmer plots for the oxidized and the reduced forms are 1.1 M^{-1} and 1.3 M^{-1} , respectively.

In both panels, the quenching behavior of 7-azaindole itself (Figure 6) is reproduced as a reference. The data presented in parts (a) and (b) represent the *average fluorescence lifetime* for reasons that are described in the text.

acrylamide. As with the 7-azatryptophan peptide, the difference between the oxidized and the reduced forms is most pronounced with KI. In contrast to the 7-azatryptophan octapeptide, the Stern-Volmer plots exhibit a marked levelling off at acrylamide concentrations of ~ 0.1 M. Such behavior may be present for the 7-azatryptophan peptide, but it is not apparent until acrylamide concentrations as high as 0.7 M (Figure 7.7b).

Possible Role of Proline Isomerization

A factor that may contribute to the nonexponential fluorescence decay of the 7-azatryptophan octapeptide (and possibly to the tryptophan octapeptide) is the isomerization of the proline residue. Proline is the only amino acid that occurs significantly in the *cis* conformation in peptides and proteins [27] (Figure 7.10). 5.7% of the Pro residues occurring in proteins have *cis* peptide bonds [27]. On the other hand, all the other residues combined occur in the *cis* conformation only 0.5% of the time.

In the octapeptide, it is possible that a *cis* conformation of the Cys-Pro peptide bond contributes to a different state of solvation of the 7-azatryptophan residue, which in turn gives rise to a population of chromophores capable of undergoing excited-state tautomerization.

Attempts to perturb the *cis/trans* population of the reduced octapeptide by addition of the enzyme peptidyl-prolyl-*cis/trans*-isomerase (PPIase) produced no measureable changes in the weights or the lifetimes of the fluorescence decay. This was also verified by NMR. A sample of tripeptide with a 70:1 ratio of peptide to enzyme was monitored over a 24-hour period. There was no observable change in the *cis* population over this time. These results can be rationalized by noting that time constants of 10-100 sec are typical for *cis/trans* isomerization of X-Pro bonds in denatured proteins [27]. The PPIase will not perturb the relative populations if equilibrium between them is reached rapidly with respect to the time required to perform the optical or the NMR experiment.

Discussion

The 7-Azaindole Chromophore and the Solvent Environment

In a series of articles we have discussed the role of water and alcohols in solvating 7-azaindole in such a fashion as either to promote or to impede excited-state tautomerization [13,15,36,37] (see Introduction). Solvation of 7-azaindole by hydrogen-bonding molecules

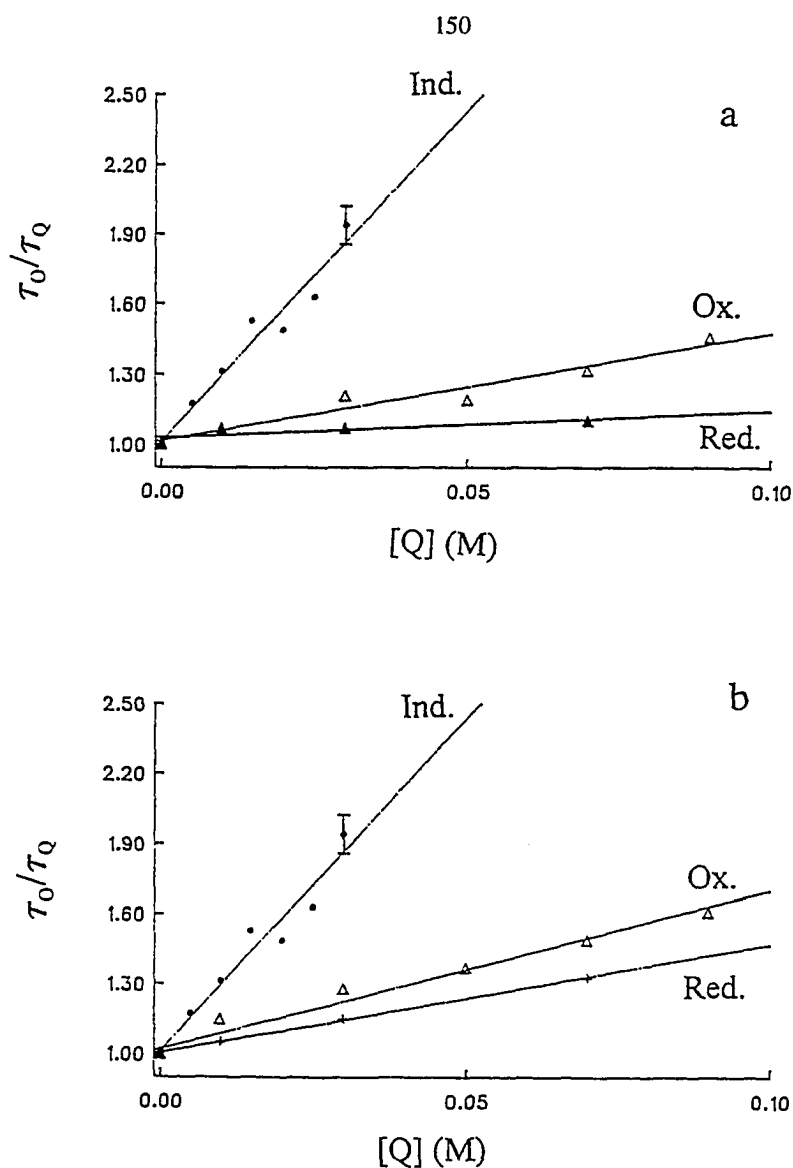


Figure 7.8. Stern-Volmer plots for the quenching of the tryptophan octapeptide by KI.

(a) Quenching behavior of the shorter lived component under reducing and oxidizing conditions. The slopes of the Stern-Volmer plots for the reduced and the oxidized forms are 1.2 M^{-1} and 4.6 M^{-1} , respectively.

(b) Quenching behavior of the longer lived component under reducing and oxidizing conditions. The slopes of the Stern-Volmer plots for the reduced and the oxidized forms are 4.7 M^{-1} and 6.8 M^{-1} , respectively.

In both panels, the quenching behavior of indole itself (Figure 6) is reproduced as a reference.

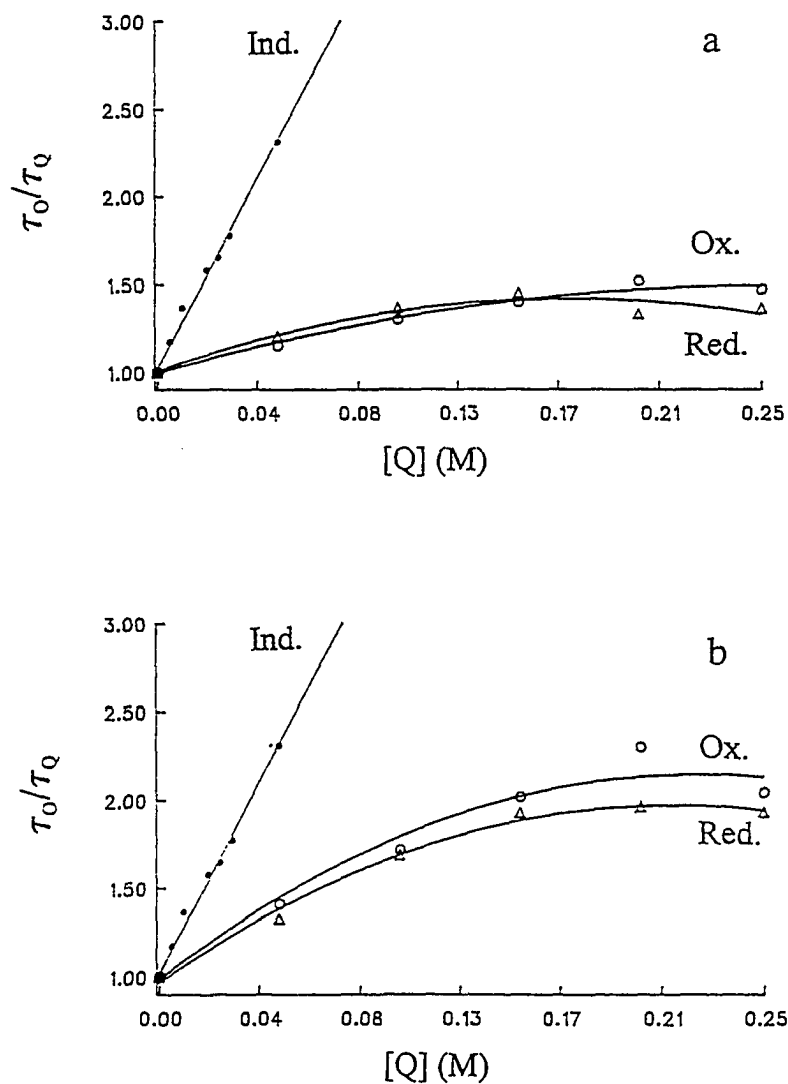


Figure 7.9. Stern-Volmer plots for the quenching of the tryptophan octapeptide by acrylamide.

(a) Quenching behavior of the shorter lived component under reducing and oxidizing conditions.

(b) Quenching behavior of the longer lived component under reducing and oxidizing conditions.

In both panels, the quenching behavior of indole itself (Figure 6) is reproduced as a reference.

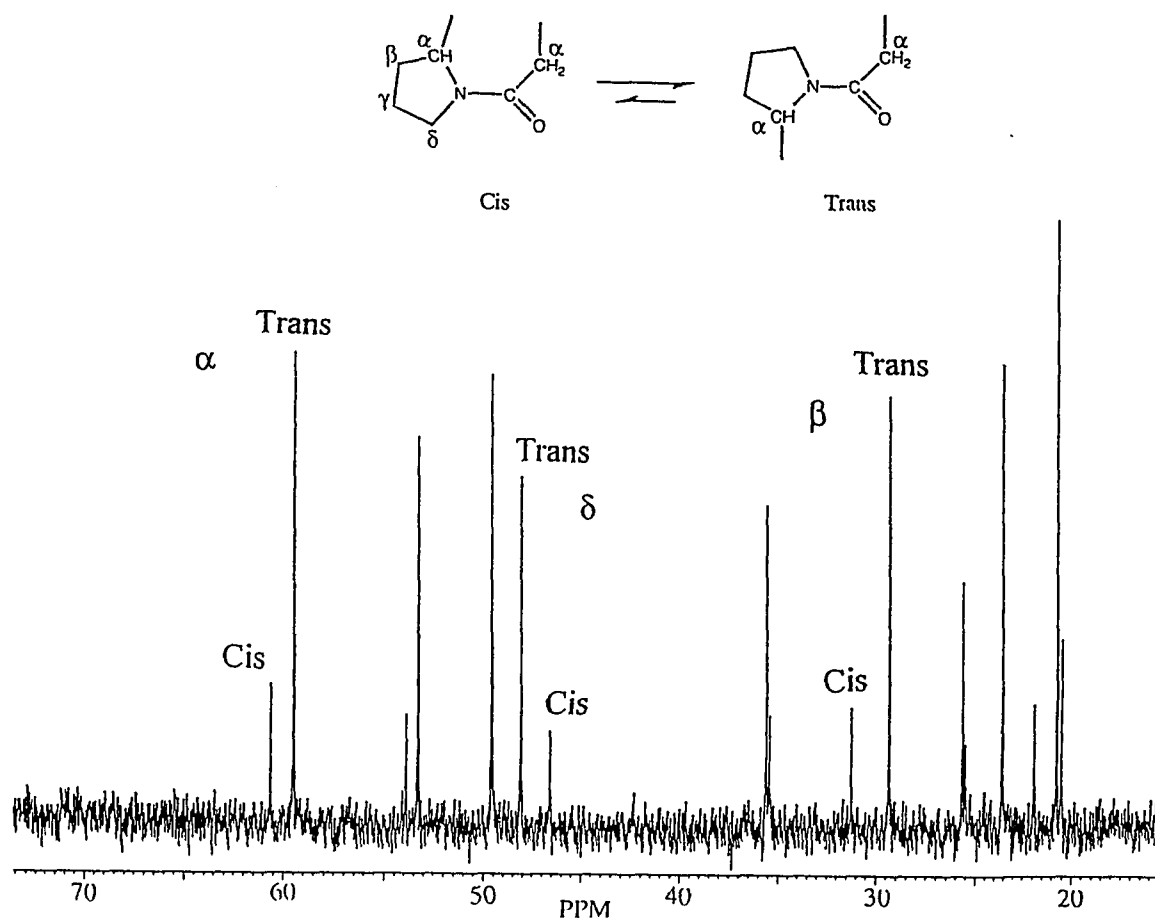


Figure 7.10. ¹³C spectrum indicating *cis* and *trans* proline conformations for the tripeptide, NAc-Pro-7-Azatriptophan-Asn-NH₂. The *cis* and *trans* peaks for the α , β , and δ carbons of proline are labelled. Analysis of this spectrum in terms of that of Stimson *et al.* [44] gives a *cis* population of 19.0 ± 0.4 % for the proline residue. The octapeptide is expected to have a similar *cis* population. Use of the tripeptide, however, simplifies the spectrum and, consequently, its analysis.

(e.g., HOR) can be divided into two crude, idealized categories. The first is a "cyclic" complex that is believed to involve two hydrogen bonds *with the same solvent molecule*: $N_1H\cdots OR$ and $N_7\cdots HOR$ (the normal species). N_1 and N_7 denote the two nitrogens of 7-azaindole (Figure 7.1). Subsequent to optical excitation, the cyclic complex facilitates the double proton transfer producing two different hydrogen bonds: $N_1\cdots HOR$ and $N_7H\cdots OR$ (the tautomer species). The second is a state of "blocked" solvation in which 7-azaindole forms two hydrogen bonds, but *with different solvent molecules*. This blocked configuration is believed to impede excited-state tautomerization.

In the context of the categories of solvent and peptide heterogeneity discussed here, it is important to bear in mind that given the above description of solvation of 7-azaindole, a homogeneous "cyclic" state of solvation can yield a nonexponential fluorescence decay. For example, the fluorescence decay of 7-azaindole (and 7-azatryptophan) in methanol at room temperature that is obtained by collecting all emission wavelengths is nonexponential owing to the presence of tautomer that is formed by the normal species (Table 7.1). On the other hand, in water at room temperature [13] or in alcohols below 0°C [15], the blocked configuration is more apparent in the fluorescence decay of 7-azaindole.

In interpreting the results described above, our organizing assumption is that the double-exponential decay observed for the 7-azatryptophan octapeptide is a consequence of excited-state tautomerization that is induced by the peptide itself. The outstanding question is then to what extent this production of chromophores susceptible to excited-state tautomerization is a result of direct interaction with the peptide, the ability of the peptide to reorganize solvent about the chromophore, or a distribution of solvation environments.

That the octapeptide does undergo excited-state tautomerization is evident from the fluorescence decay profiles obtained as a function of emission wavelength (Figure 7.3). Emission collected on the red edge of the spectrum yields a rise time commensurate to the shorter-lived component observed when emission is collected either over the entire spectrum or at individual bluer wavelengths: 150 ps. This result demonstrates that excited-state tautomerization occurs in the octapeptide. *What distinguishes the octapeptide from 7-azatryptophan, 7-azaindole, and the tripeptide in water is the prominence of the shorter-lived decay component and the observation of nonexponential fluorescence decay even when emission is collected over the entire band.* This implies that for the octapeptide in water the tautomer band and the normal band are essentially centered upon one another.

Photophysics of the 7-Azatryptophan Octapeptide

There are several results in whose context the remainder of the data must be considered.

1. The 7-azatryptophan octapeptide is the only compound containing 7-azaindole considered up to now whose fluorescence lifetime is nonexponential in pure water when emission is collected over the entire band.
2. The fluorescence decays of the reduced and the oxidized octapeptide are not significantly different from each other (Table 7.1), but they are qualitatively similar to that of 7-azaindole in the presence of quenchers. It is noteworthy that 7-azaindole in the presence of quenchers such as KI or acrylamide exhibits nonexponential fluorescence decay. This phenomenon is not observed with indole over the same range of concentrations. We tentatively attribute the nonexponential fluorescence decay of 7-azaindole induced by these quenching agents to a perturbation of the equilibrium solvation by water. By comparison with the 7-azaindole quenching experiments, we suggest that the secondary structure of the octapeptide either perturbs the solvent environment of the 7-azaindole chromophore and consequently modifies the population that is poised for excited-state tautomerization or that the octapeptide interacts directly with the chromophore and assumes the role of the solvent.
3. That reducing and oxidizing conditions significantly influence the secondary structure of the octapeptide is demonstrated by the spot tests, by the different rotation times, and by the different (although relatively small) responses of the reduced and oxidized octapeptides to the fluorescence quenchers, KI and acrylamide. We cannot rule out additional heterogeneity resulting from *cis/trans* isomerization of the proline bond. The importance of these latter contributions is suggested by the complicated temperature dependence of the fluorescence decay of the 7-azatryptophan octapeptide.

Biochemical Activity

The similar K_I values for the D- and L-7-azatryptophan tripeptides suggest a certain degree of flexibility of the active site in α -chymotrypsin for accommodating a tryptophyl-like residue.

Classical kinetic studies (Table 7.2) indicate the following:

1. Indole and 7-azaindole inhibit equally well, suggesting that the substitution of a carbon for a nitrogen in the 7 position does not affect the binding interactions.

2. Both indole and 7-azaindole bind more than 10 times stronger than the zwitterionic amino acids, Leu and Trp. But within experimental error, Leu and Trp have identical inhibition constants with respect to α -chymotrypsin.
3. The above results suggest that the improved inhibition afforded by substituting the P₁ Leu with 7-azatryptophan is a result of a conformational change in the tripeptide rather than a specific interaction afforded by the 7-nitrogen of the azaindole moiety.
4. It is unlikely that the 7-azatryptophan tripeptides or octapeptides are being hydrolyzed on the time scale of the measurements as both Pro-Leu and Pro-Trp exhibit much higher K_I values. If Pro-Leu-Asn or the 7-azatryptophan peptides were being cleaved, K_I values similar to those of the dipeptides would be expected.
5. The similar K_I values of the D- and L-7-azatryptophan tripeptides and octapeptides suggest a certain degree of flexibility of the active site of α -chymotrypsin for accomodating a tryptophyl-like residue.
6. The strong inhibition provided by potato chymotrypsin inhibitor II must be provided by additional contacts from amino acids in both the N- and C-terminal directions with respect to the P₁ Leu or 7-azatryptophan residues.

Conclusions

The octapeptide containing the 7-azaindole chromophore discussed here is the first 7-azaindole derivative reported to display a nonexponential fluorescence decay in water when its emission is collected over the entire band. Clearly there is a structural change in going from the tripeptide to the octapeptide that induces the nonexponential fluorescence decay. The 7-azaindole chromophore is furthermore sensitive to structural changes induced by subjecting the octapeptide to reducing or oxidizing conditions: distinct differences are apparent in both the steady-state and time-resolved fluorescence data for the 7-azatryptophan octapeptide (Figures 7.2, 7.6, and 7.7; Tables 7.1, 7.3, and 7.5).

It is important at this point to underline the differences in the behavior of 7-azatryptophan and tryptophan:

1. 7-Azatryptophan is clearly more sensitive than tryptophan to the onset of whatever secondary structure or partial secondary structure the peptide may have assumed.
2. Neither 7-azatryptophan or tryptophan demonstrates itself to be preferable to probing secondary structure *by means of fluorescence quenching studies*.

3. The ability of 7-azatryptophan to probe the secondary structure imposed by the octapeptide must be put into perspective. It is likely that the majority of small peptides capable of assuming some degree of secondary structure will exhibit similar nonexponential fluorescence behavior, presumably from the enhancement of the population of chromophores capable of excited-state tautomerization. Therefore, in situations where it is already known that the peptide in question possesses secondary structure an alternative and possibly more useful optical probe is 1-methyl-7-azaindole [13]: it possesses a high fluorescence quantum yield and a long fluorescence lifetime, 0.55 and 21 ns in water, respectively; and these fluorescence properties are solvent dependent [21]. Also, because its N₁ nitrogen is methylated, it cannot undergo excited-state tautomerization. *7-Azaindole is a chromophore of enormous potential utility because it can be modified to probe different environments and different phenomena.*

A great value of 7-azatryptophan (or 1-methyl-7-azatryptophan) will be to probe the interactions of a smaller peptide or protein containing it with another protein that may contain several tryptophans. These intrinsically tagged molecules can then be studied individually or in complex with their target. This approach will be useful in studying complexes between a small protein or polypeptide containing 7-azatryptophan and a large globular protein that may contain many tryptophans.

Acknowledgment

TCEP•HCl was a gift from A. W. Schwabacher. The 7-azatryptophan peptides were synthesized in the Iowa State University Protein Facility. J.W.P. is an Office of Naval Research Young Investigator. R.L.R. is an Amoco Fellow. D.S.E. is a GAANN Fellow. Additional support was provided by the Iowa State Biotechnology Council, IPRT, University Research Grants, and a Carver Grant.

References and Notes

1. Petrich, J. W.; Chang, M. C.; McDonald, D. B.; Fleming, G. R. *J. Am. Chem. Soc.* **1983**, *105*, 3824; Chang, M. C.; Petrich, J. W.; McDonald, D. B.; Fleming, G. R. *J. Am. Chem. Soc.* **1983**, *105*, 3819.

2. Szabo, A. G. and Rayner, D. M. *J. Am. Chem. Soc.* **1980**, *102*, 554.
3. Szabo, A. G. and Rayner, D. M. *Biochem. Biophys. Res. Commun.* **1980**, *94*, 909.
4. Werner, T. C. and Forster, L. S. *Photochem. Photobiol.* **1979**, *29*, 905.
5. Ross, J. B. A.; Rousslang, K. W.; Brand, L. *Biochemistry* **1981**, *20*, 4361.
6. Chen, L. X.-Q.; Petrich, J. W.; Fleming, G. R.; Perico, A. *Chem. Phys. Lett.* **1987**, *139*, 55.
7. Cockle, S. A. and Szabo, A. G. *Photochem. Photobiol.* **1981**, *34*, 23.
8. Donzel, B.; Gauduchon, P.; Wahl, Ph. *J. Am. Chem. Soc.* **1974**, *96*, 801.
9. Engh, R. A.; Chen, L. X.-Q.; Fleming, G. R. *Chem. Phys. Lett.* **1986**, *126*, 365.
10. Creed, D. *Photochem. Photobiol.* **1984**, *39*, 537.
11. Négrerie, M.; Bellefeuille, S. M.; Whitham, S.; Petrich, J. W.; Thornburg, R. W. *J. Am. Chem. Soc.* **1990**, *112*, 7419.
12. Rich, R. L.; Chen, Y.; Neven, D.; Négrerie, M.; Gai, F; Petrich, J. W. *J. Phys. Chem.* **1993**, *97*, 1781.
13. Chen, Y.; Rich, R. L.; Gai, F; Petrich, J. W. *J. Phys. Chem.* **1993**, *97*, 1770.
14. Rich, R. L.; Négrerie, M.; Li. J.; Elliott, S.; Thornburg, R. W.; Petrich, J. W. *Photochem. Photobiol.* **1993**, *58*, 28.
15. Chen, Y.; Gai, F.; Petrich, J. W. *Chem. Phys. Lett.* **1994**, *222*, 329.
16. Smirnov, A.; Rich, R. L.; Petrich, J. W. *Biochem. Biophys. Res. Commun.* **1994**, *198*, 1007.

17. Rich, R. L.; Gai, F.; Lane, J. W.; Petrich, J. W.; Schwabacher, A. W. *J. Am. Chem. Soc.* **1995**, *117*, 733.
18. Chen, Y.; Gai, F.; Petrich, J. W.; *J. Phys. Chem.* **1994**, *98*, 2203.
19. Seneear, D. F.; Laue, T. M.; Ross, J. B. A.; Waxman, E.; Eaton, S.; Rusinova, E. *Biochemistry* **1993**, *32*, 6179; Ross, J. B. A.; Seneear, D. F.; Waxman, E.; Kombo, B. B.; Rusinova, E.; Huang, Y. T.; Laws, W. R.; Hasselbacher, C. A. *Proc. Natl. Acad. Sci. USA.* **1992**, *89*, 12023; Hogue, C. W. V.; Rasquinha, I.; Szabo, A. G.; MacManus, J. P. *FEBS Lett.* **1992**, *310*, 269; Kishi, T.; Tanaka, M.; Tanaka, J. *Bull. Chem. Soc. Jpn.* **1977**, *50*, 1267.
20. Taylor, C. A.; El-Bayoumi, M. A.; Kasha, M. *Proc. Natl. Acad. Sci. U.S.A.* 1969, **63**, 253.
21. Moog, R. S.; Maroncelli, M. *J. Phys. Chem.* 1991, **95**, 10359.
22. McMorrow, D.; Aartsma, T. J. *Chem. Phys. Lett.* 1986, **125**, 581.
23. Konijnenberg, J.; Huizer, A. H.; Varma, C. A. G. O. *J. Chem. Soc., Faraday Trans. 2* 1988, **84**, 1163.
24. Chou, P.-T.; Martinez, M. L.; Cooper, W. C.; Collins, S. T.; McMorrow, D. P.; Kasha, M. *J. Phys. Chem.* 1992, **96**, 5203.
25. Waluk, J.; Pakula, B.; Komorowski, S. J. *J. Photochem.* **1987**, *39*, 49; Bulska, H.; Grabowska, A.; Pakula, B.; Sepiol, J.; Waluk, J.; Wild, U. P. *J. Lumin.* **1984**, *29*, 65.
26. Lang, K.; Schmid, F. X.; Fischer, G. *Nature* 1987, **17**, 268.
27. *Protein Folding*, ed., Creighton, T. E. W. H. Freeman and Co., New York, 1992.
28. Burns, J. A.; Butler, J. C.; Moran, J.; Whitesides, G. M. *J. Org. Chem.* 1991, **56**, 2648.

29. Cobb, K. A.; Novotny, M. V. *Anal. Chem.* 1992, **64**, 879.
30. Feigl, F. *Spot Tests in Organic Analysis*; Elsevier; Amsterdam, 1960.
31. Schonbaum, G. R.; Zerner, B.; Bender, M. L. *J. Biol. Chem.* **1961**, 236, 2930.
32. Bryant, J.; Green, T. R.; Gurusaddaiah, T.; Ryan, C. A. *Biochemistry* **1976**, *15*, 3418.
33. Some of our earlier reports cite 414 nm as the fluorescence maximum. This is a result of systematic error intrinsic to the fluorimeter used.
34. Tilstra, L.; Sattler, M. C.; Cherry, W. R.; Barkley, M. D. *J. Am. Chem. Soc.* **1990**, *112*, 9176.
35. Arnold, S.; Tang, L.; Sulkes, M. *J. Phys. Chem.* **1994**, *98*, 2325.
36. Chen, Y.; Gai, F.; Petrich, J. W. *J. Am. Chem. Soc.* **1993**, *115*, 10158.
37. Gai, F.; Rich, R. L.; Chen, Y.; Petrich, J. W. *Structure and Reactivity in Aqueous Solution*, ACS Symposium, San Diego, 1994.
38. Foster, R. J.; Niemann, C. *J. Am. Chem. Soc.* **1955**, *77*, 3370.
39. Foster, R. J.; Niemann, C. *J. Am. Chem. Soc.* **1955**, *77*, 3365.
40. Chen, L. X.-Q.; Engh, R. A.; Fleming, G. R. *J. Phys. Chem.* 1988, **92**, 4811.
41. Berger, A.; Schechter, I. *Phil. Trans. R. Soc.* **1970**, *B257*, 249.
42. Hatschek, E. *The Viscosity of Liquids*; G. Bell and Sons, Ltd.: London, 1928, p. 68.
43. Wallace, R. A.; Kurtz, A. N.; Niemann, C. *Biochemistry* **1963**, *2*, 824-836.

44. Stimson, E. R.; Montelione, G. T.; Meinwald, Y. C.; Rudolph, R. K. E.; Scheraga, H. A. *Biochemistry* 1982, **21**, 5252.
45. Rizzo, T. R.; Park, Y. D.; Peteanu, L.; Levy, D. H. *J. Phys. Chem.* **1986**, *84*, 2534; Rizzo, T. R.; Park, Y. D.; Levy, D. H. *J. Chem. Phys.* **1986**, *85*, 6945.
46. Skrabal, P.; Rizzo, V.; Baici, A.; Bangerter,; Luisi, P. L. *Biopolymers* **1979**, *18*, 995; Kobayashi, J.; Higashijima, T.; Sekido, S.; Miyazawa, T. *Int. J. Pept. Protein Res.* **1981**, *17*, 486; Dezube, B.; Dobson, C. M.; Teague, C. E. *J. Chem. Soc. Perkin Trans. 2.* **1981**, 730.
47. Engh, R. A.; Chen, L. X.-Q.; Fleming, G. R. *Chem. Phys. Lett.* **1986**, *126*, 365.

CHAPTER 8. INCORPORATION OF N₁-METHYL-7-AZATRYPTOPHAN INTO PEPTIDE SEQUENCES AND THEIR BINDING INTERACTIONS WITH THE MAJOR HISTOCOMPATIBILITY COMPLEX MOLECULE H-2K^b

A paper in preparation for submittal to the *Journal of the American Chemical Society*

R. L. Rich¹, A. V. Smirnov¹, S. Luo², J. W. Petrich^{1,3}

Introduction

Class I major histocompatibility complex molecules bind antigenic peptides, presenting these sequences to the cytotoxic T-cell receptors (TCR). "When cells are infected by a virus, class I molecules bind processed viral peptides and display them at the cell surface for recognition by cytotoxic T lymphocytes. Thus the binding of foreign peptides to class I molecules is the first step in the subsequent cascade of T-cell activation." [1] We have developed techniques to study these complexes using an intrinsic fluorescent probe and time-resolved spectroscopy.

Currently, we are examining a variety of octapeptide sequences that simulate an octapeptide known to bind tightly to H-2K^b, with N₁-methyl-7-azatryptophan incorporated at different sites in each peptide. The sequence we have chosen to mimic is SIINFEKL (denoted OVA-8 in previous work [1]). We have chosen a variety of site substitutions based on discussion with Luc Teyton at R. W. Johnson Pharmaceutical Research Institute. Residues 1, 4, 6, and 7 of this sequence point toward the TCR and residue 5 is an "anchor" residue positioned in a deep pocket of the MHC molecule binding cleft. The binding studies of these peptides, this class I MHC molecule, and TCR are underway in our laboratory.

¹ Graduate students and Associate Professor, Department of Chemistry, Iowa State University.

² Employed by the Iowa State University Protein Facility.

³ To whom correspondence should be addressed.

Materials and Methods

Determination of Binding Constants

Membrane Preparation. The dialysis membranes used in the EMD101B Equilibrium Microvolume Dialyzer (Hofer Scientific Instruments) require preparation prior to use. Place approximately four membranes in deionized water and let stand for about 30 minutes with occasional gentle agitation. Place the membranes in 500 mL of deionized water containing 2% Na₂CO₃ (2 g/100 mL) and 1 mM EDTA (0.037 g/100 mL) at 60°C. Warm for 30 minutes, stirring briefly and gently periodically. After removing from the wash bath, rinse repeatedly with deionized water. Store membranes in deionized water containing 0.1% NaN₃ at 4°C until use. The company instructions for module preparation and use can be found in my notebook #7.

Sample Preparation. A solution of empty murine class I MHC antigen (approximately 20 mg/mL) was provided by Luc Teyton. Peptides were synthesized and purified by Siquan Luo of the Iowa State University Protein Facility. Dialysis was performed in the buffer system recommended by Fahnestock *et al.* [2]: phosphate-buffered saline containing 0.5% gelatin and 0.02% NaN₃. Concentrations of the MHC and peptide stock solutions was determined using the extinction coefficients: $\epsilon_{280\text{nm}}^{\text{H-2Kb}} = 69,200 \text{ cm}^{-1} \text{ M}^{-1}$ [1] and $\epsilon_{289\text{nm}}^{\text{peptide}} \approx 8300 \text{ cm}^{-1} \text{ M}^{-1}$ [3].

Dialysis Procedure. Side A of each microdialyzer compartment is filled with 90 μL (2 μM) of H2-K^b and side B of each compartment is filled with 90 μL of varying concentrations of peptide (0.25 - 25.0 μM) containing N₁-methyl-7-azatryptophan. The mixtures are allowed to dialyze for 24 hours. After this time, this O.D. of the solutions from both side A and B are measured using 100 μL spectrophotometric cuvettes. The O.D. of blank buffer and H-2K^b dialyzed against buffer alone are measured and subtracted from the other samples. In addition, each cuvette absorbs a slightly different amount of light, so the O.D. of each sample at 400 nm was subtracted from the sample scan. The concentration of bound peptide is therefore: $c(\text{peptide bound}) = c(\text{side A}) - c(\text{side B})$ The data is plotted as (bound)/(free) vs. (bound) and the K_D calculated as $-(1/\text{slope})$.

Preliminary Results

To date, we have performed preliminary binding studies on two peptide sequences: SIIN(1M7AT)EKL and SIINFE(1M7AT)L. Both the D- and L- enantiomers of SIIN(1M7AT) exhibit a $K_D \sim 5 \mu\text{M}$. The D-enantiomer of SIINFE(1M7AT) appears to have a $K_D \sim 0.5 \mu\text{M}$; studies of the L-enantiomer have not yet been performed. Time resolved spectroscopic experiments of these two sequences yield $\tau_f = 16.4 \pm 0.3$, $\tau_r = \pm$, $r(0) =$ for SIIN(1M7AT)EKL and $\tau_f = 16.5 \pm$, $\tau_r = \pm$, $r(0) =$ for SIINFE(1M7AT)L. Studies of these and other peptides in complex with H-2K^b and H-2K^b/TCR are continuing.

References

1. Matsumura, M.; Saito, Y.; Jackson, M. R.; Song, E. S.; Peterson, P. A. *J. Biol. Chem.* **1992**, *267*, 23589. This is the extinction coefficient reported for H-2K^b, $M_r = 43,200$.
2. Fahnestock, M. L.; Johnson, J. L.; Feldman, R. M. R.; Tsomides, T. J.; Mayer, J.; Narhi, L. O.; Bjorkman, P. J. *Biochemistry* **1994**, *33*, 8149.
3. Chen, Y; Rich, R. L.; Gai, F.; Petrich, J. W. *J. Phys. Chem.* **1993**, *97*, 1770. This the extinction coefficient reported for 1-methyl-7-azaindole.

PART III. ANALYSIS OF BIOLOGICAL COFACTORS

**CHAPTER 9. USING 7-AZATRYPTOPHAN TO PROBE SMALL MOLECULE-
PROTEIN INTERACTIONS ON THE PICOSECOND TIME SCALE: THE
COMPLEX OF AVIDIN AND BIOTINYLATED 7-AZATRYPTOPHAN**

A paper published in the *Journal of the American Chemical Society*¹

R. L. Rich², F. Gai², J. W. Lane², J. W. Petrich^{2,3}, and A. W. Schwabacher^{2,3}

Abstract

The utility of 7-azatryptophan as an alternative to tryptophan for optically probing protein structure and dynamics is demonstrated by investigating the complex of egg-white avidin and biotinylated 7-azatryptophan. We report the synthesis of biotinylated 7-azatryptophan and optical measurements of its complex with avidin. Although there are four biotin binding sites, the emission from the 7-azatryptophan tagged to biotin decays by a single exponential, whereas the tryptophyl emission from avidin requires two exponentials in order to be adequately fit. Fluorescence depolarization measurements of the complex probed by emission from 7-azatryptophan reveal both rapid (~ 80 ps) and much longer-lived decay. The former component is attributable to the local motion of the probe with respect to the protein; the latter component represents overall protein tumbling. In addition, energy transfer from tryptophan to 7-azatryptophan and a blue-shift in the spectrum of biotinylated 7-azatryptophan are observed upon formation of the complex. Modified strategies of effecting optical selectivity are also discussed.

¹ Reprinted with permission from *Journal of American Chemical Society* **1995**, *117*, 733.
Copyright © 1995 American Chemical Society.

² Graduate students, Associate Professor, and Assistant Professor; Department of Chemistry; Iowa State University.

³ To whom correspondence should be addressed.

Introduction

We have proposed the nonnatural amino acid, 7-azatryptophan, as an alternative to tryptophan as an optical probe of protein structure and dynamics [1-12]. The merits of 7-azatryptophan lie in its intrinsic single exponential fluorescence decay in water [1,5,10] as compared to the nonexponential decay exhibited by tryptophan [13-19] as well as in its spectroscopic distinguishability with respect to tryptophan in both absorption and emission [3,5,11]. Furthermore, 7-azatryptophan can be incorporated into bacterial protein and is amenable to peptide synthesis [1,3,12]. Important applications of 7-azatryptophan are its incorporation into small peptides, its binding to cofactors, and the subsequent investigation of the dynamics of these smaller, tagged molecules bound to the target protein of interest. In this article, we demonstrate the feasibility of this approach by studying biotinylated 7-azatryptophan (inset of Figure 9.1) bound to avidin.

Avidin is a tetrameric protein found in avian egg white. Each subunit contains 128 residues of which 4 are tryptophan. Avidin is believed to function as an antibacterial agent through its ability to reduce the free concentration of biotin. The dissociation constant of the avidin-biotin complex is about 10^{-15} M [20-27]. The essentially irreversible binding afforded by this complex, the specificity of its formation, and the ready modification of the carboxylate group of biotin have permitted the study of the interactions of several biotin adducts with avidin. Biotin-avidin species have found extensive use as analytical reagents [24,26]. Examples of other uses of biotin-avidin complexes include perturbation of rhodium hydrogenation catalyst activity [27], formation of ordered protein monolayers [22], and hybrid glycoproteins [23]. Recently, X-ray structures of egg-white avidin and its complex with biotin have appeared [25]. Biotin is shown to bind in a β -barrel constructed from eight antiparallel β sheets. The tryptophan residues 70 and 97 of one monomer and tryptophan 110 of an adjacent monomer form part of the avidin binding site and are anchored through hydrogen bonds to other residues, thus stabilizing the binding site. The ureido ring of biotin forms hydrogen bonds with Asn-12, Ser-16, Tyr-33, Thr-35, Asn-118, and possibly Thr-77 [25].

We have prepared a biotin-7-azatryptophan adduct in order to demonstrate further the spectroscopic distinguishability of 7-azatryptophan from tryptophan and to investigate the mobility of the 7-azatryptophan moiety in the complex.

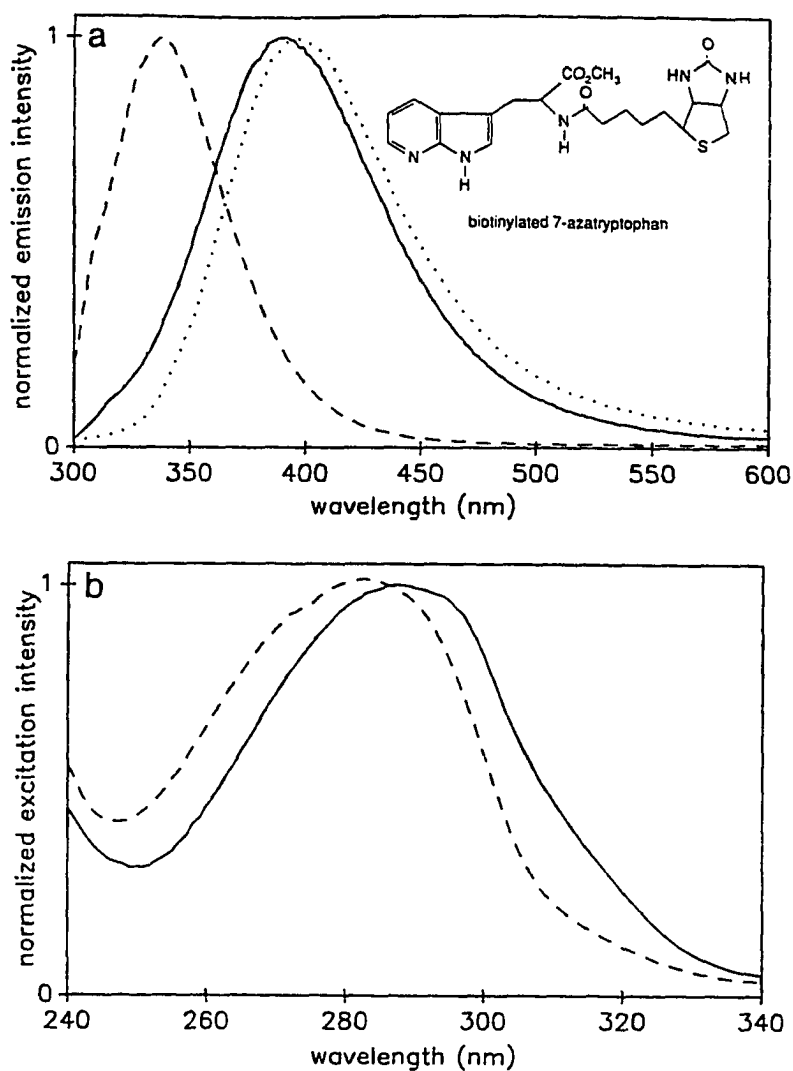


Figure 9.1. (a) Fluorescence spectra of avidin ($\lambda_{em}^{max} = 339$ nm) (- - -); biotinylated-7-azatryptophan ($\lambda_{em}^{max} = 390$ nm) (•••), whose structure is displayed in the inset; and the complex of avidin and the biotinylated 7-azatryptophan (____). $\lambda_{ex} = 310$ nm. The excitation peak has been subtracted out of each spectrum.

(b) Excitation spectra of biotinylated 7-azatryptophan (____) and of biotinylated 7-azatryptophan complexed with avidin (- - -). Samples were dissolved in a 95/5 water/methanol mixture. $\lambda_{em} = 390$ nm.

Experimental

Synthesis of *N*- α -Biotinoyl-D,L-7-Azatryptophan Methyl Ester

Biotin *N*-hydroxysuccinimide ester (100 mg, 0.302 mmol) and D,L-7-azatryptophan methyl ester dihydrochloride (71.2 mg, 0.245 mmol) in 3.0 mL pyridine (distilled from ninhydrin) were stirred under N₂ for 19 hr. The pyridine was removed under vacuum at 40°C and the residue was suspended in approximately 30 mL of ethyl acetate and extracted three times with 50% saturated aqueous NaHCO₃, and once with saturated NaCl. The ethyl acetate layer was then dried over Na₂SO₄, decanted, and the solvent was removed to yield 90 mg (83% yield) of product as a white solid. An analytical sample was obtained by recrystallization from methanol and chloroform (53 mg, 49%, m.p. = 220-222°C). ¹H NMR(300 MHz, CD₃OD): δ 8.07 (d, 4.78 Hz, 1 H); δ 7.92 (d, 7.87 Hz, 1 H); δ 7.81 (s, 1H); δ 7.01 (dd, 4.84 Hz, 7.83 Hz, 1 H); δ 4.66 (m, 1 H); δ 4.39 (m, 1 H); δ 4.12 (m, 1 H); δ 3.59 (s, 3 H); δ 3.09-2.97 (m, 2 H); δ 2.82 (dd, 4.89 Hz, 12.72 Hz, 1 H); δ 2.59 (d, 12.73 Hz, 1 H); δ 2.09 (t, 6.93 Hz, 2 H); δ 1.62-1.39 (m, 6 H). IR (KBr): 1735, 1699, 1536, 1655 cm⁻¹. Anal: calcd for C₂₁H₂₇N₅O₄S(CHCl₃)₁(CH₃OH)₁, C 46.28%, H 5.40%, N 11.73%; found, C 46.54%, H 5.39%, N 11.55%.

Samples used in fluorescence studies were dissolved in a 95/5 water/methanol mixture. The small amount of methanol was necessary to dissolve the biotinylated 7-azatryptophan (7ATB). No degradation of avidin was observed at this concentration of methanol. Affinity-purified, egg-white avidin was obtained from Sigma and used without further purification. Since avidin has four biotin binding sites, the complex was prepared in the ratio of 4 biotinylated 7-azatryptophan molecules to 1 avidin molecule. The concentrations of avidin and biotinylated 7-azatryptophan were determined spectrophotometrically using $\epsilon_{\text{avidin}}(282 \text{ nm}) = 96,000 \text{ cm}^{-1} \text{ M}^{-1}$ [20] and $\epsilon_{\text{biotin-7-azatrp}}(288 \text{ nm}) = 6,200 \text{ cm}^{-1} \text{ M}^{-1}$. Thin-layer chromatography confirms the lack of free biotinylated 7-azatryptophan in solutions of the complex and consequently demonstrates that attachment of 7-azatryptophan to biotin does not affect the ability of the latter to bind to avidin.

Spectroscopic Measurements

Fluorescence lifetimes, $K(t)$, and fluorescence anisotropy decays, $r(t)$, were obtained using the time-correlated, single-photon counting technique [5,6]. Parallel and perpendicular emission intensities for measurements of anisotropy decays were collected alternately with a rotating analyzer polarizer in order to obviate scaling procedures [6]. Unless otherwise

indicated, fluorescence decays were collected to a maximum of 10,000 counts. Fluorescence anisotropy decays were collected so that a maximum of 16,000 counts were obtained in the parallel curve. Data were analyzed as usual [5,6] by an iterative comparison with the convolution of the instrument response function with trial functions for $K(t)$ or for $I_{\parallel}(t)$ and $I_{\perp}(t)$, simultaneously. A nonlinear least-squares fitting procedure was employed, and the quality of fit was determined by the χ^2 criterion. The full-scale time base for all lifetime and anisotropy measurements was 3 ns in order to measure accurately the rapid component of the anisotropy decay. Consequently, long-time depolarizing events (which are not the primary concern of this work) were not fully characterized. All measurements of the 4:1 biotinylated-7-azatryptophan:avidin complex were performed with $\lambda_{\text{ex}} = 310$ nm and $\lambda_{\text{em}} > 400$ nm to minimize the detection of emission from tryptophan residues within the protein. All other measurements were performed with $\lambda_{\text{ex}} = 285$ nm and $\lambda_{\text{em}} > 320$ nm. The values reported for the time-resolved measurements are the average of three to seven measurements.

The dependence of the fluorescence quantum yield on excitation wavelength was determined for indole, 5-methoxyindole, 7-azatryptophan, and the 4:1 complex of biotinylated 7-azatryptophan:avidin. Indole, 5-methoxyindole, and D,L-7-azatryptophan were purchased from Sigma Chemical Co. and used as supplied. Experiments involving biotinylated 7-azatryptophan were performed 95/5 water/methanol solutions; all other samples were dissolved in pure water.

Absorbance measurements were made using a Shimadzu UV-2101PC double-beam spectrometer. Fluorescence measurements were obtained with a Spex Fluoromax fluorimeter whose excitation and emission bandpasses were set to 1 nm. All measurements were conducted at room temperature. Calibration of the absorption spectrometer and of the fluorimeter was performed using indole vapor as a standard. Crystals of indole in a 1-cm cuvette filled with argon were heated to 65°C. Comparison of the absorption and the excitation spectra of the vapor indicated that the position of the sharp 1L_b transition varied by 1 nm. A correction for this discrepancy was applied throughout our calculations. Corrections were also applied for the wavelength-dependent response of the fluorimeter.

The relative excitation-wavelength dependent fluorescence quantum yields were determined by two methods. The first method requires collecting an emission spectrum for each excitation wavelength and employs eq 1:

$$\frac{\phi_F(\lambda_1)}{\phi_F(\lambda_2)} = \frac{1 - 10^{-OD(\lambda_2)} \int_0^{\infty} I_{em}(\lambda_1, \nu) d\nu}{1 - 10^{-OD(\lambda_1)} \int_0^{\infty} I_{em}(\lambda_2, \nu) d\nu} \frac{c(\lambda_2)}{c(\lambda_1)} \quad (1)$$

$OD(\lambda_i)$ is the optical density at the excitation wavelength, λ_i ; $I_{em}(\lambda_i, \nu)$ is the emission intensity at the excitation wavelength λ_i ; and $c(\lambda_i)$ is a correction factor taking into account fluctuations of the intensity of the xenon lamp of the fluorimeter as well as other factors discussed above. (Alternatively, the peak height may be used instead of the integrated spectrum since in the systems studied here the emission profile does not change shape or position over the range of excitation wavelengths investigated.)

The second method is based upon a comparison of the fluorescence excitation spectrum and the optical density as a function of the excitation wavelength, eq 2:

$$\frac{\phi_F(\lambda_1)}{\phi_F(\lambda_2)} = \frac{1 - 10^{-OD(\lambda_2)} I_{ex}(\lambda_1)}{1 - 10^{-OD(\lambda_1)} I_{ex}(\lambda_2)} \quad (2)$$

$I_{ex}(\lambda_i)$ is the intensity of the excitation spectrum (monitored, in our case, at the emission maximum) at the excitation wavelength, λ_i .

As a check of our procedures, we determined the excitation-wavelength dependence of the fluorescence quantum yield for rhodamine B and pyrene. The fluorescence quantum yield across the range of excitation wavelengths scanned remained constant within an experimental error of $\pm 15\%$ for all the systems studied here except for that of the complex of biotinylated 7-azatryptophan and avidin. The excitation-wavelength dependence of the fluorescence quantum yield reported elsewhere is in error [36].

Results

Figure 9.1 displays the fluorescence emission and excitation spectra of avidin, the biotin-7-azatryptophan adduct, and the complex of the biotin-7-azatryptophan adduct with

avidin. Figure 9.2 demonstrates that with an excitation wavelength of 310 nm, 7-azatryptophan is detected predominantly in the complex.

Figure 9.3 presents the fluorescence anisotropy decay of the biotinylated 7-azatryptophan; Figure 9.4, of avidin alone. Figure 9.5 presents the fluorescence anisotropy decay of the complex of biotinylated 7-azatryptophan with avidin. Even in the presence of 16 tryptophan residues, the 7-azatryptophan (1 per subunit) is detected unambiguously. The fluorescence anisotropy decay of the avidin-biotin complex that is detected by means of the 7-azatryptophan chromophore is clearly different from that observed from avidin itself (detected by means of the tryptophyl residues). Fluorescence lifetime and anisotropy decay data are summarized in Table 9.1.

The fluorescence lifetime of biotinylated 7-azatryptophan is dominated by emission from 7-azatryptophan and is well described by the function: $K(t) = 0.98 \pm 0.02 \exp(-t/646 \pm 9 \text{ ps}) + 0.02 \pm 0.02 \exp(-t/2690 \pm 970 \text{ ps})$. The residual 2% of this fluorescence decay is attributed to biotin itself, which is characterized by a fluorescence lifetime with a long component of about 3 ns.

The complex of avidin and biotinylated 7-azatryptophan is fit well to a double-exponential fluorescence decay. The dominant component is again attributed to 7-azatryptophan and has an apparent time constant of 420 ps. *Because we have chosen a 3-ns full-scale time base to investigate the rapid dynamics, we consequently have not made a very precise determination of either the magnitude or the duration of the longer-lived component, which arises mostly from tryptophan itself but contains a small contribution from biotin.* Fitting the data collected on a full scale of 3 ns indicates that about 50% of the emission collected arises from 7-azatryptophan.

It is important to note that detection of such a relatively small contribution of 7-azatryptophan emission in the complex is unexpected given the respective optical properties of 7-azatryptophan and tryptophan. The contribution of fluorescence detected from a particular chromophore as a function of time, $C(t)$, depends on several factors: the optical density at the excitation wavelength, the radiative rate, the fraction of the emission spectrum over which the fluorescence lifetime is measured, and the fluorescence lifetime of the chromophore itself. The expression used for determining the contribution of fluorescence observed from 7-azatryptophan in the presence of four tryptophyl residues (a model system for avidin) when the excitation wavelength is 310 nm and when fluorescence is collected at wavelengths longer than 400 nm is:

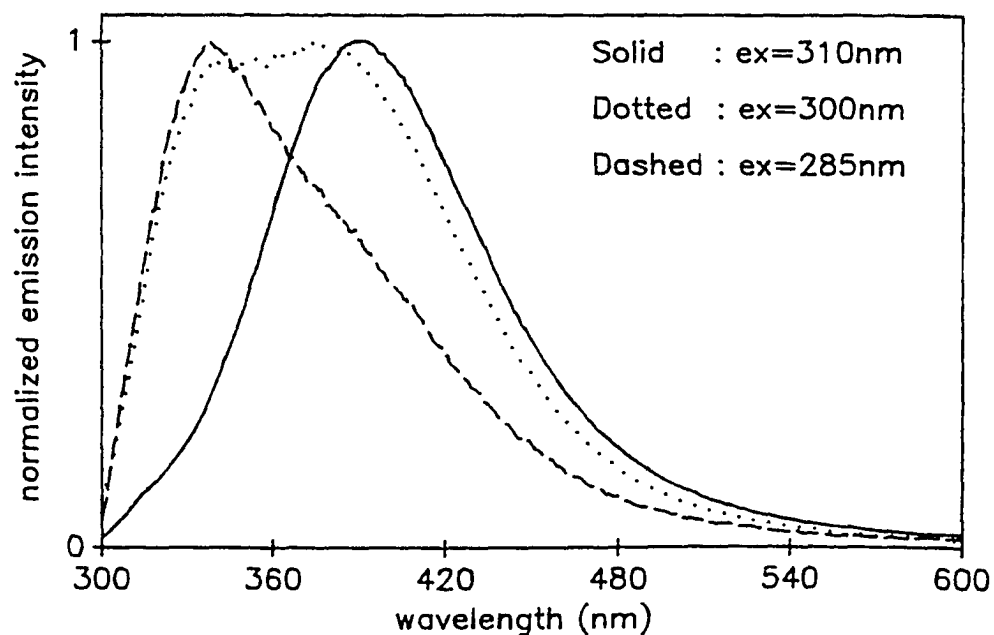


Figure 9.2. Fluorescence spectra of the complex of avidin and biotinylated 7-azatryptophan (1 per binding site) as a function of excitation wavelength. Note that at $\lambda_{ex} = 310\text{ nm}$ essentially only emission from 7-azatryptophan is observed whereas at bluer excitation wavelengths the contribution from tryptophan in avidin is more pronounced. For $\lambda_{ex} = 310\text{ nm}$, the excitation peak has been subtracted out of the spectrum.

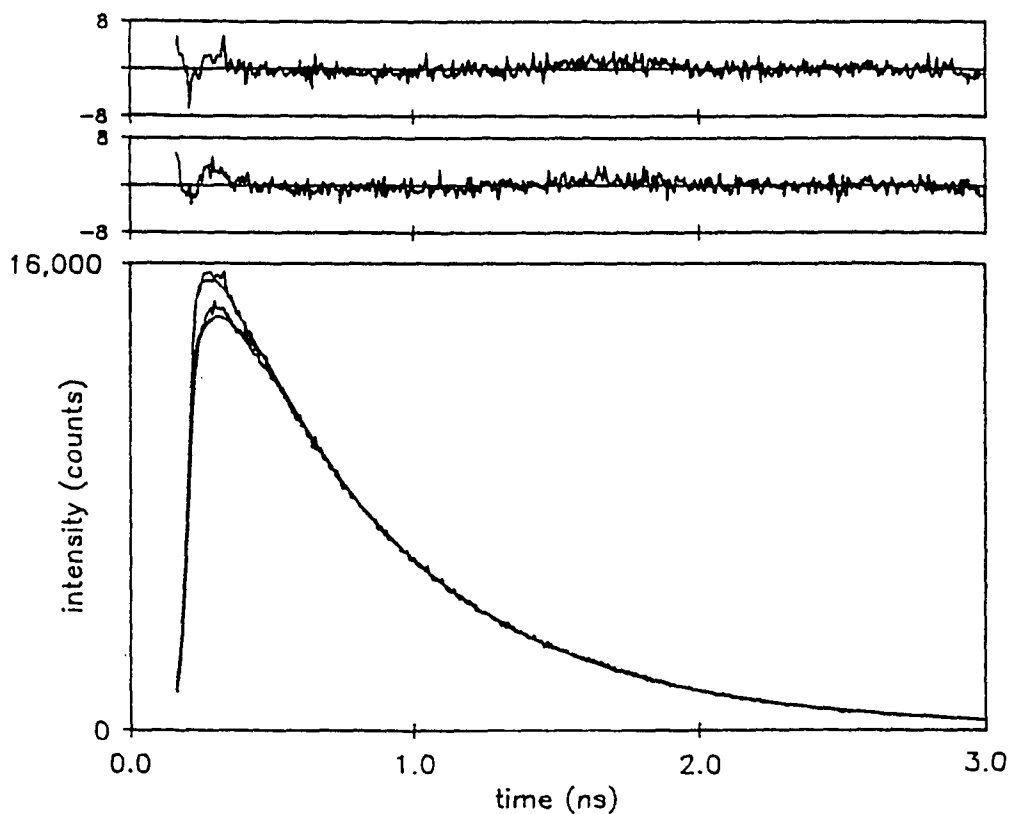


Figure 9.3. Parallel and perpendicular fluorescence intensity profiles from which the anisotropy decay is calculated [6] for biotinylated 7-azatryptophan: $\lambda_{\text{ex}} = 285 \text{ nm}$, $\lambda_{\text{em}} > 335 \text{ nm}$, 20°C . The fluorescence anisotropy decay was fit to a single exponential: $r(t) = 0.06 \exp(-t/110 \text{ ps})$, $\chi^2 = 1.62$. Displayed above the polarized fluorescence profiles are the residuals for the parallel and the perpendicular emission, respectively. The fluorescence lifetime of this compound was fit to the function: $K(t) = 0.98 \exp(-t/642 \text{ ps}) + 0.02 \exp(-t/2484 \text{ ps})$, $\chi^2 = 1.50$. The residual contribution of long-lived component is due to biotin itself, which is weakly fluorescent. Biotin has an average fluorescence lifetime of 1.5 ns (and a long-lived component of about 3 ns) in a 95/5 water/methanol mixture. The values of the limiting anisotropies, $r(0)$, reported here and in Figures 4 and 5 are consistent with steady-state measurements obtained in glasses [6,34,35].

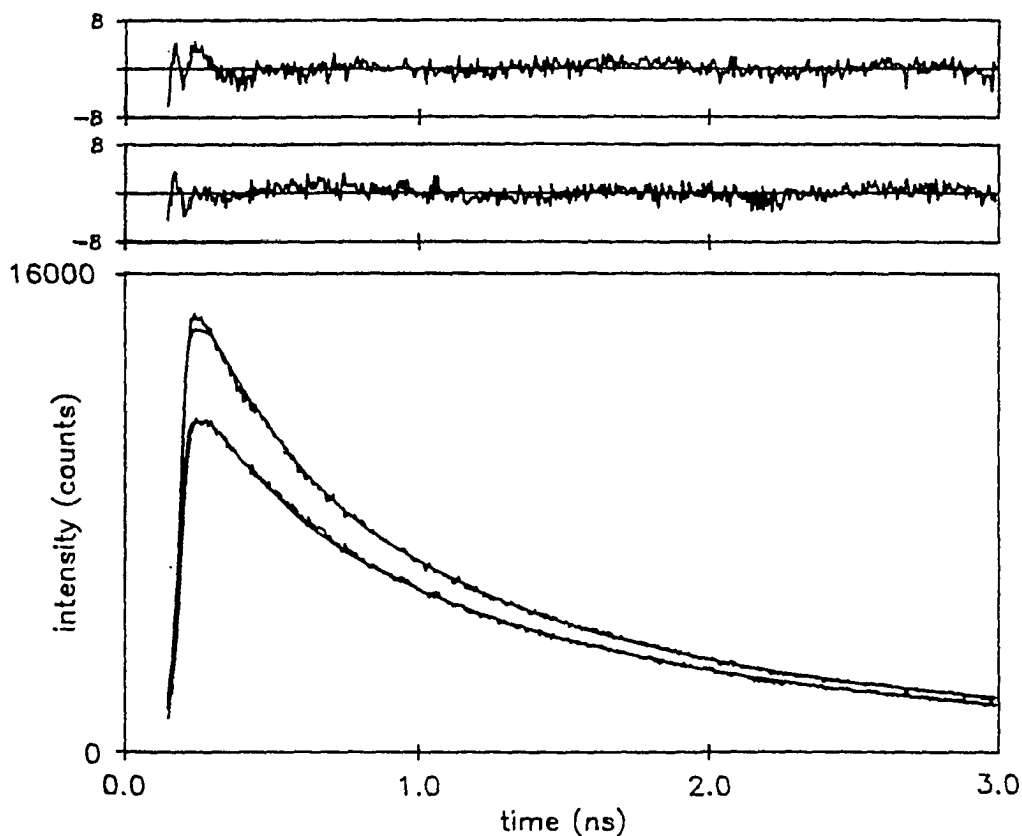


Figure 9.4 Parallel and perpendicular fluorescence intensity profiles from which the anisotropy decay is calculated for avidin: $\lambda_{\text{ex}} = 285 \text{ nm}$, $\lambda_{\text{em}} > 335 \text{ nm}$, 20°C . The fluorescence anisotropy decay was fit to a single exponential: $r(t) = 0.08 \exp(-t/1586 \text{ ps})$, $\chi^2 = 1.56$. The fluorescence lifetime of avidin was fit to the function: $K(t) = 0.41 \exp(-t/272 \text{ ps}) + 0.59 \exp(-t/1757 \text{ ps})$, $\chi^2 = 1.36$. The upper set of residuals corresponds to emission polarized parallel to the excitation source; the lower, perpendicular to the excitation source.

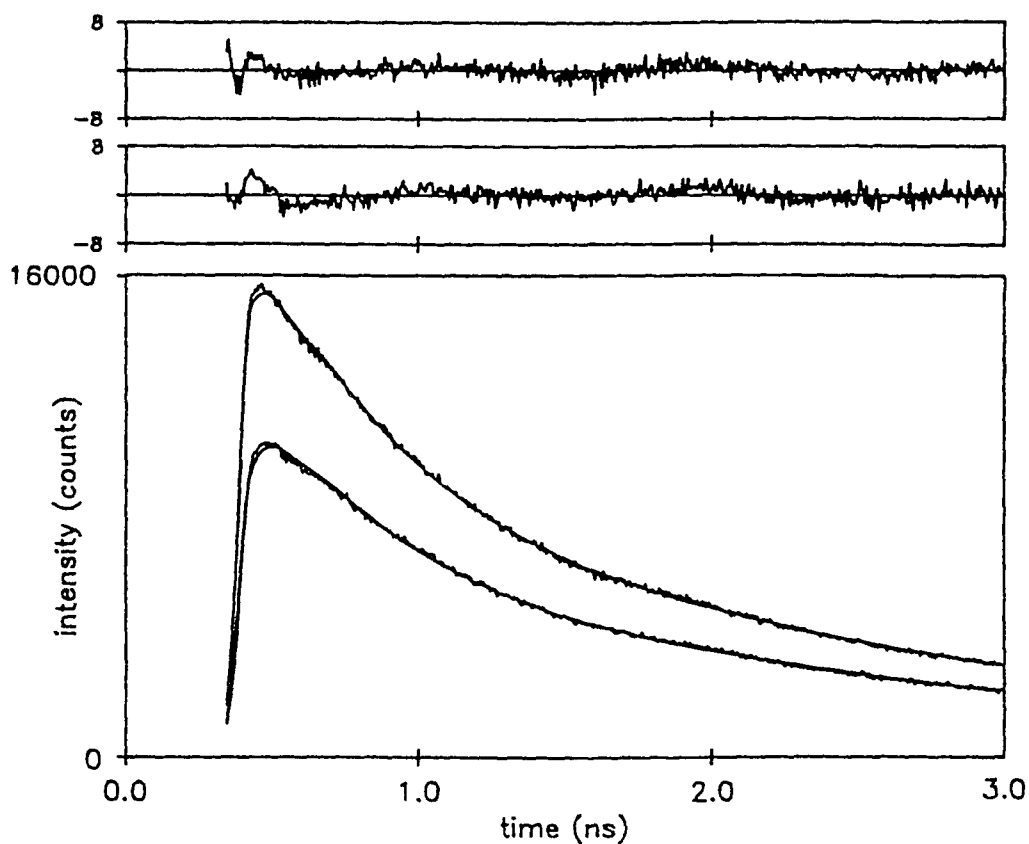


Figure 9.5. Parallel and perpendicular fluorescence intensity profiles from which the anisotropy decay is calculated for the complex of avidin and biotinylated 7-azatryptophan (1 per binding site), $\lambda_{\text{ex}} = 310 \text{ nm}$, $\lambda_{\text{em}} > 400 \text{ nm}$. As indicated in the Results section, about 50% of the emission comprising the anisotropy decay is due to the 7-azatryptophan chromophore. The anisotropy decay is well described by two components: $r(t) = 0.06 \exp(-t/64 \text{ ps}) + 0.13$; $\chi^2 = 1.51$. The second component of the anisotropy decay reflects the overall tumbling of the protein itself and is too long-lived to be accurately determined on a 3-ns time scale, on which it appears to be infinite. The fluorescence lifetime of the biotinylated 7-azatryptophan in the complex was fit the function: $K(t) = 0.48 \exp(-t/423 \text{ ps}) + 0.52 \exp(-t/2265 \text{ ps})$, $\chi^2 = 1.17$. The upper set of residuals corresponds to emission polarized parallel to the excitation source; the lower, perpendicular to the excitation source.

Table 9.1
Fluorescence Lifetime and Anisotropy Decay Parameters^a

species	τ_{F1} (ps)	τ_{F2} (ps)	A_1	τ_{r1} (ps)	τ_{r2} (ps)	$r_1(0)$	$r_2(0)$
7ATB	646 ± 9	2690 ± 970	0.98 ± 0.02	108 ± 2	---	0.08 ± 0.01	---
avidin	268 ± 9	1730 ± 70	0.42 ± 0.03	1300 ± 260	---	0.09 ± 0.01	---
complex ^b	417 ± 14^c	2300 ± 40	0.48 ± 0.01	80 ± 18	∞	0.06 ± 0.02	0.14 ± 0.01

^a Fluorescence decays are fit to the function $K(t) = A_1 \exp(-t/\tau_{F1}) + A_2 \exp(-t/\tau_{F2})$. Anisotropy decays are fit to the function $r(t) = r_1(0) \exp(-t/\tau_{r1}) + r_2(0) \exp(-t/\tau_{r2})$. All measurements were performed at 20°C and with $\lambda_{ex} = 285$ nm and $\lambda_{em} \geq 335$ nm, unless otherwise specified.

^b $\lambda_{ex} = 310$ nm, $\lambda_{em} \geq 400$ nm.

^c The apparent shortening of the lifetime of 7-azatryptophan in the complex may be attributed in part to a weighted average of emission from itself and tryptophan.

$$C^{7AT}(t) = \frac{e_{310}^{7AT} k_R^{7AT} F_{em}^{7AT} \exp(-t/780ps)}{e_{310}^{7AT} k_R^{7AT} F_{em}^{7AT}} \exp(-t/780ps) + 4 e_{310}^{Trp} k_R^{Trp} F_{em}^{Trp} [0.22 \exp(-t/620ps) + 0.78 \exp(-t/3210ps)] \quad (3)$$

$$\text{where } F_{em} = \frac{\int_0^{\infty} I_{em}(\nu) d\nu}{\int_0^{\infty} I_{em}(\nu) d\nu}$$

$\epsilon_{Trp}(310 \text{ nm}) = 100 \text{ cm}^{-1} \text{ M}^{-1}$ and $\epsilon_{7AT}(310 \text{ nm}) = 1100 \text{ cm}^{-1} \text{ M}^{-1}$ [3]. The radiative rates used for 7-azatryptophan and for tryptophan are $3.8 \times 10^7 \text{ s}^{-1}$ and $5.0 \times 10^7 \text{ s}^{-1}$, respectively. The quantity, $C(t)$, is plotted for 7-azatryptophan in the presence of 4 tryptophan residues and for 1-methyl-7-azaindole in the presence of 4 tryptophan residues for different excitation wavelengths and on different time scales to demonstrate the selectivity of the 7-azatryptophan chromophore as an optical probe (Figure 9.6). 1-Methyl-7-azaindole is presented to illustrate the enormous optical selectivity that persists at longer times as a result of blocking the nonradiative processes afforded by the interactions of the N_1 proton with the solvent [5,12] (see Conclusions).

Detection of emission wavelengths longer than 400 nm was chosen to accelerate the data collection time and to ensure discrimination against emission from tryptophan itself. In principle, the "homogeneity" of the signal can be improved by selecting a combination of a lower energy emission wavelength cutoff and a lower energy excitation wavelength, as is demonstrated elsewhere and in Figure 9.6.

Our data reveal an interesting complication in the photophysics of the complex of avidin and biotinylated 7-azatryptophan. Namely, despite the high 7-azatryptophan to tryptophan ratio in the complex, the contribution of 7-azatryptophan emission detected is essentially constant (50-60%) regardless of whether the excitation wavelength is 285, 290, or 310 nm. The explanation of this phenomenon is revealed by Figure 9.1b, which compares the fluorescence excitation spectra of biotinylated 7-azatryptophan free and complexed with avidin. Complexation induces a blue-shift and a slight change in shape of the absorption spectrum that renders preferential optical excitation of 7-azatryptophan less efficient.

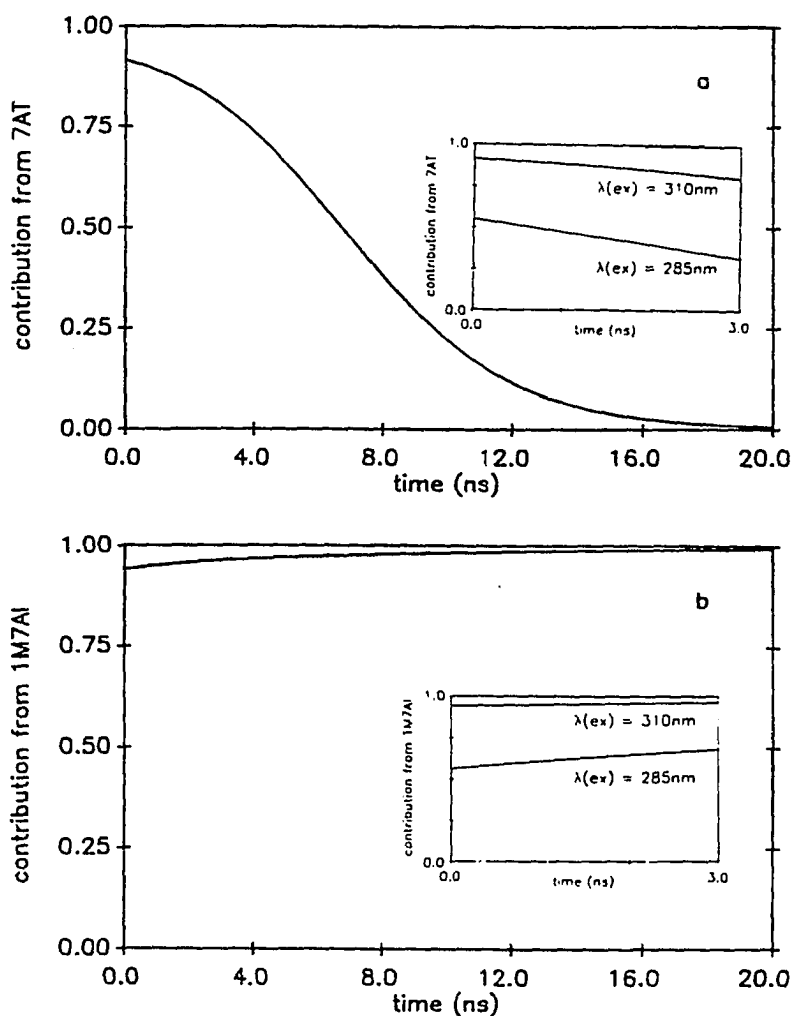


Figure 9.6. Percentage of emission observed from 7-azatryptophan and related compounds as a function of time for various experimental conditions as determined from eq 3.

(a) 7-azatryptophan/4 tryptophans, $\lambda_{\text{ex}} = 310 \text{ nm}$, $\lambda_{\text{em}} \geq 400$, 20-ns full scale. The inset depicts the difference in emission (on a 3-ns scale) observed from 7-azatryptophan when the excitation wavelength is changed from 310 nm to 285 nm.

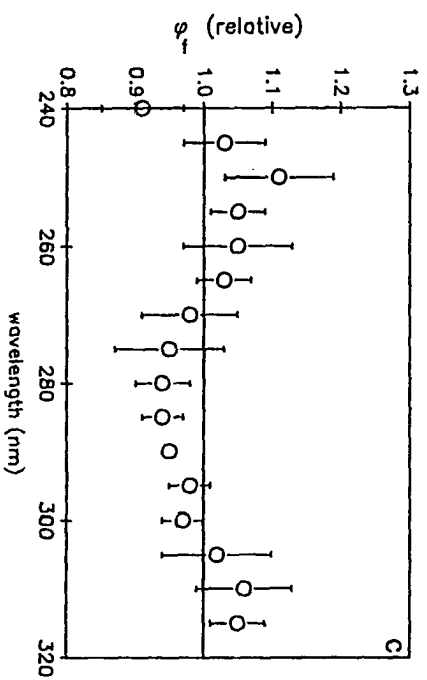
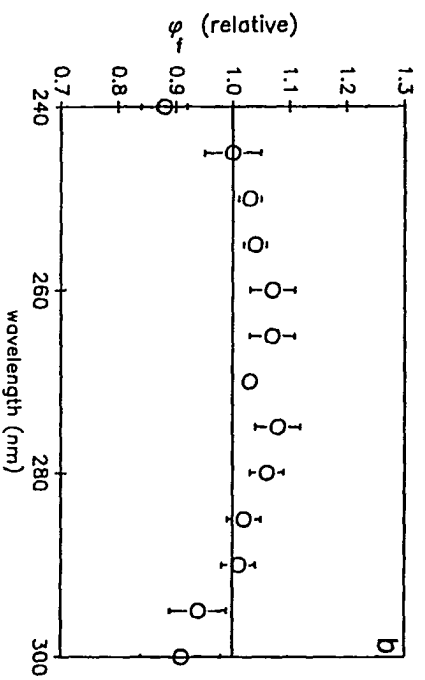
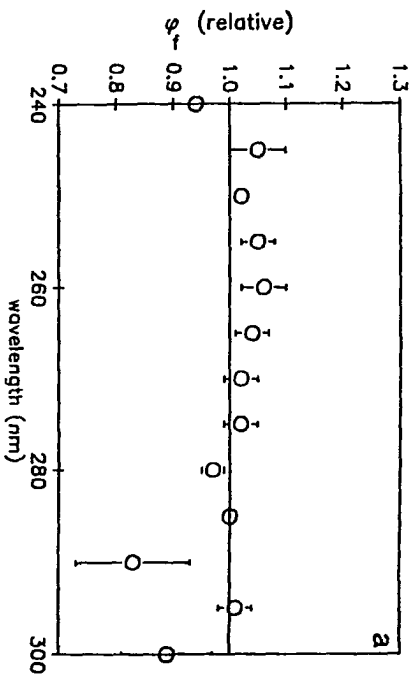
(b) 1-Methyl-7-azaindole/4 tryptophans, $\lambda_{\text{ex}} = 310 \text{ nm}$, $\lambda_{\text{em}} \geq 400$, 20-ns full scale. The inset depicts the difference in emission observed from 7-azaindole when the excitation wavelength is changed from 310 nm to 285 nm. The rise in percentage emission is a result of the 21-ns fluorescence lifetime of 1-methyl-7-azaindole as compared to the ~ 2.6 -ns average fluorescence lifetime of tryptophan (eq 3).

Despite the shift of the absorption spectrum induced upon complexation, there is significant spectral overlap between the absorption spectrum of biotinylated 7-azatryptophan and the emission spectrum of tryptophan. The possibility of thus exploiting tryptophan to 7-azatryptophan energy transfer as an additional tool is confirmed by Figures 9.7 and 9.8. Figure 9.7e demonstrates that the *fluorescence quantum yield of 7-azatryptophan increases when the excitation wavelength is scanned through the region corresponding to tryptophyl absorption*. Figures 9.7a-d indicate no such variation of fluorescence quantum yield and are presented as control experiments. Figure 9.8 presents time-resolved data that verify the presence of energy transfer: at 330 nm where the emission of tryptophan is predominant, the average lifetime is significantly shorter than that of uncomplexed avidin; at emission wavelengths greater than 505 nm where the emission of 7-azatryptophan is predominant, a rise time in the emission is evident and is fit to a time constant of ~ 800 ps. Determination of the energy transfer time employed the spectral overlap integral determined from the absorption spectrum of biotinylated 7-azatryptophan bound to avidin (Figure 9.1b) and the emission spectrum of avidin: 2.84×10^{-15} cm⁶/mol. This corresponds to a critical distance, R_0 , of 12.3 Å. Distances between the tryptophan donor and the 7-azatryptophan acceptor were estimated as the distance from the midpoint between the 8 and 9 carbons of the indole ring of tryptophan and the carbonyl carbon of the biotin alkyl chain [25]. Three potential donors were investigated: tryptophans 70 and 97 of one monomer and tryptophan 110 of the other monomer. These tryptophans yielded the following donor-acceptor distances and energy transfer times, respectively: 4.9 Å, 6.7 ps; 11.2 Å, 960 ps; 29.1 Å, 290 ns. (An orientation factor of 2/3 was employed.) Our measured energy transfer time is in excellent agreement with Trp-97 being the donor.

Discussion

The steady-state absorption and fluorescence properties of 7-azatryptophan are sufficiently different from those of tryptophan that selective excitation and detection may be effected. The absorption maximum of 7-azatryptophan is red shifted by 10 nm with respect to that of tryptophan. There is also a significant red shift of about 50 nm of the maximum of the fluorescence spectrum of 7-azatryptophan with respect to that of tryptophan. We have measured the fluorescence decays of mixtures of tryptophan and 7-azatryptophan. Only when the ratio of tryptophan to 7-azatryptophan is as great as 10:1 does the tryptophyl emission

Figure 9.7. Relative fluorescence quantum yields, ϕ_F , as a function of excitation wavelength at neutral pH (unless otherwise indicated) for (a) indole, (b) 5-methoxyindole, (c) 7-azatryptophan, (d) rhodamine B in ethylene glycol, (e) complex of biotinylated 7-azatryptophan and avidin. The quantum yields presented here are relative to those obtained at the absorption maximum.



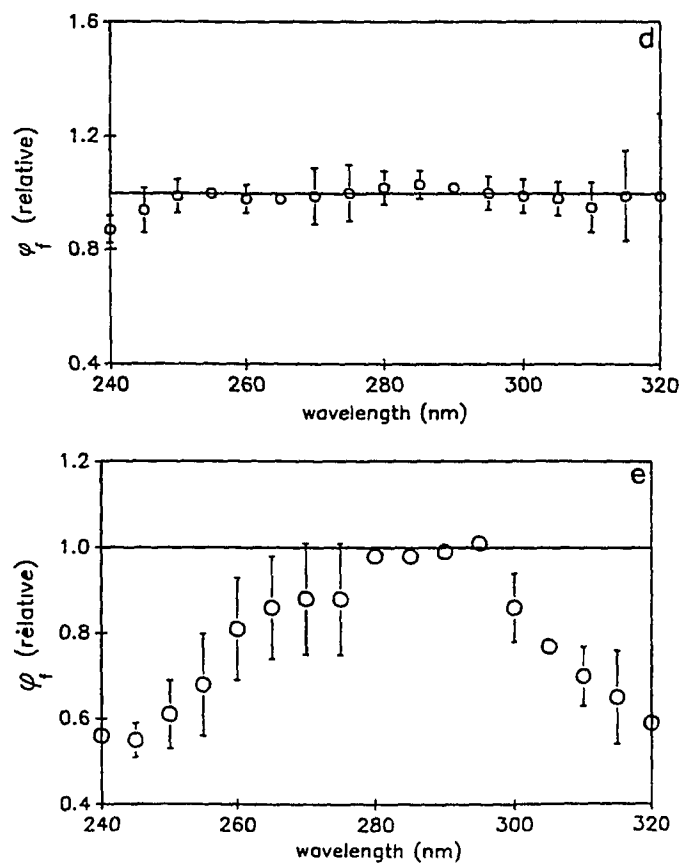


Figure 9.7 (continued)

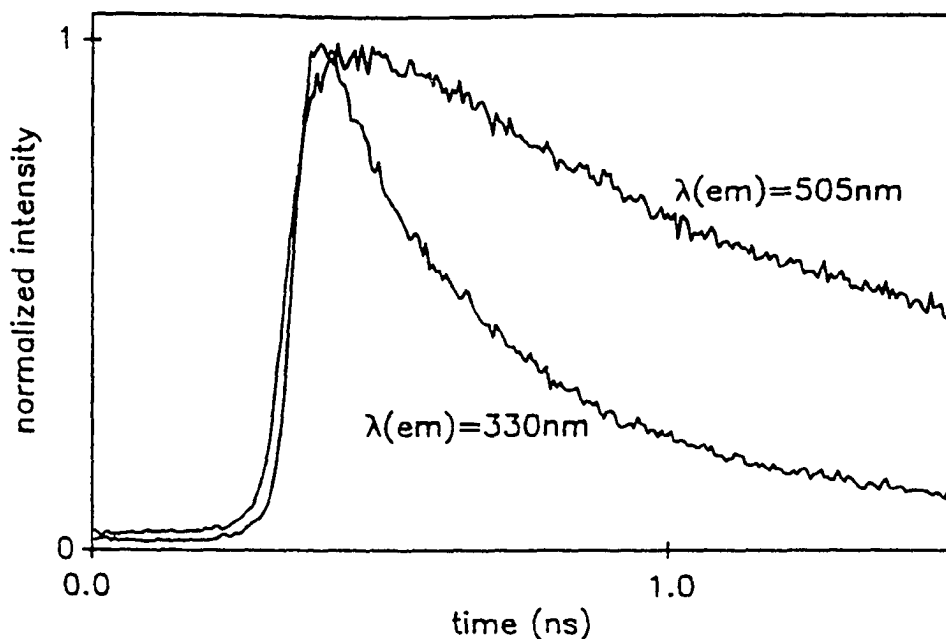


Figure 9.8. Fluorescence decay of biotinylated 7-azatryptophan bound to avidin at emission wavelengths of 330 ± 8 nm and ≥ 505 nm at 20°C . $\lambda_{\text{ex}} = 290$ nm.

(a) $\lambda_{\text{em}} = 330 \pm 8$ nm, $K(t) = 0.60 \exp(-t/78 \text{ ps}) + 0.34 \exp(-t/420 \text{ ps}) + 0.06 \exp(-t/1830 \text{ ps})$, $\chi^2 = 1.65$.

(b) $\lambda_{\text{em}} \geq 505$ nm, $K(t) = -0.26 \exp(-t/828 \text{ ps}) + 1.03 \exp(-t/822 \text{ ps}) + 0.23 \exp(-t/6580 \text{ ps})$, $\chi^2 = 1.40$.

In both measurements, data were collected only to a maximum of 3800 counts given the low fluorescence intensity in the emission wavelength range of interest.

become detectable. Furthermore, as opposed to aqueous tryptophan at pH 7, the fluorescence decay of 7-azatryptophan is single exponential. This result holds across the emission band and over the pH range we have studied, from 4 to 13. The monoexponential fluorescence decay in itself indicates the enormous preference for using 7-azatryptophan instead of tryptophan as a fluorescent probe.

Recently, there have been reports suggesting that 5-hydroxytryptophan is a useful biological probe as well [28]. While in some cases 5-hydroxytryptophan may prove useful (if relatively long excitation wavelengths, ~ 320 nm, are employed), we have demonstrated [10] that because its fluorescence spectrum and lifetime are similar to those of tryptophyl chromophores, it can be more difficult to distinguish from tryptophan than is 7-azatryptophan. *This is due in large part to the 3.8-ns lifetime of 5-hydroxytryptophan, which is similar to that of the long component of tryptophan.* In mixtures of 5-hydroxytryptophan and the tryptophyl chromophore, NATA (N-acetyl tryptophanamide), in a ratio as high as 1/10, the presence of 5-hydroxytryptophan cannot be discriminated from the mixture ($\lambda_{\text{ex}} = 305$ nm; $\lambda_{\text{em}} > 335$ nm). On the other hand, when the ratio of 7-azatryptophan to NATA is as low as 1/40, the 7-azatryptophan is easily detected [10].

The spectroscopic distinguishability of 7-azatryptophan in the presence of avidin is demonstrated clearly in the Figures. As is noted above and in the caption to Figure 9.5, about 50% of the emission of the complex of biotinylated 7-azatryptophan with avidin is attributable to 7-azatryptophan. *More importantly, the emission attributable to 7-azatryptophan decays according to a single exponential even though there are four biotin binding sites in avidin.* As indicated in the caption to Figure 9.4, however, the fluorescence decay of avidin itself requires two exponentials in order to be adequately fit. This is not surprising considering that there are 16 tryptophans present and that the fluorescence decay of tryptophan is intrinsically nonexponential.

The fluorescence anisotropy decay of biotinylated 7-azatryptophan in complex with avidin is fit well to two exponentially decaying components, the second of which is very long lived: $r(t) = r_1(0)\exp(-t/\tau_1) + r_2(0)\exp(-t/\tau_2) = 0.06 \pm 0.02 \exp(-t/80 \pm 8 \text{ ps}) + 0.14 \pm 0.01$ (Figure 5). That the fluorescence anisotropy is fit to two exponentials indicates that we are probing the rapid librational motion of the 7-azatryptophan probe with respect to avidin as well as the overall tumbling motion of the avidin itself. For probes attached to globular proteins, the order parameter, S^2 , is a model independent measure of the extent to which restricted motion can occur [29]. $S^2 = [r(t)/r(0)] \exp(t/\tau_r) = r(0^+)/r_{\text{eff}}(0)$. τ_r and $r(0^+)$ are determined by the fit of the long-time behavior of the anisotropy decay (the overall protein

reorientation or tumbling) to a single exponential and are equivalent to τ_2 and $r_2(0)$, respectively. $r_{\text{eff}}(0)$ is the initial value of the anisotropy less those nonmotional factors contributing to the anisotropy decay [30]. In the treatment of the data, $r_{\text{eff}}(0) = r_1(0) + r_2(0)$. S^2 gives an indication of the magnitude of the depolarizing motions that are present in addition to the overall protein reorientation. Thus a value of $S^2 < 1$ implies local motion of the chromophore with respect to the body of the protein, and $S^2 = 1$ implies a rigid chromophore that undergoes depolarization only by means of overall protein motion. The order parameter can be related to a *hypothetical* cone semiangle, θ_0 , within which the transition dipole moment can diffuse [29,31]: $S = 1/2 \cos\theta_0 (1 + \cos\theta_0)$. In this example, $\theta_0 = 29 \pm 5^\circ$. The relatively large value for the cone semiangle indicates that while the biotin itself is firmly attached to the avidin, the 7-azatryptophan tag lies either in a mobile part of the protein or is partially exposed at the exterior of the protein. The latter of these possibilities is more likely given the large contribution of the rapid component of the anisotropy decay and the similarity of the fluorescence spectrum of 7-azatryptophan in the complex (Figures 9.1 and 9.2) to 7-azatryptophan in water [5,10]. If 7-azatryptophan were buried in the protein interior, not only would the rapid component be much less pronounced (or absent) but its fluorescence spectrum would be expected to resemble more closely what is observed in pure alcohols. In alcohols, a second maximum is observed at lower energies. This second band arises from excited-state tautomerization [2,5,8,9,32], which does not occur to any significant extent either in pure water [5,8,9,33] or in the complex studied here. The conclusion concerning the degree of freedom afforded to the 7-azatryptophan moiety is also confirmed by the X-ray structure of the avidin-biotin complex [25], which indicates that carboxylate groups of the valeryl side chain of biotin (used to form the linkage with 7-azatryptophan), lie at the surface of the protein.

Conclusions

1. Fluorescence anisotropy measurements of the complex of biotinylated 7-azatryptophan with avidin suggests the utility of 7-azatryptophan as probe of small molecule-protein interactions owing to its spectroscopic distinguishability with respect to tryptophan and to its intrinsic single-exponential fluorescence decay.
2. The spectroscopic distinguishability of 7-azatryptophan in the complex of biotinylated 7-azatryptophan and avidin is less than that expected from a comparison of the

the individual optical properties of 7-azatryptophan and tryptophan (50-60% as opposed to 85% at time zero, Figure 9.6). This result provides an example of the sensitivity of the 7-azaindole chromophore to its environment and indicates that not all such interactions may be favorable to its role as a probe molecule. As we have discussed elsewhere, much of the sensitivity of the fluorescence of 7-azaindole to its environment is a consequence of the proton bound to the 1-nitrogen, which can interact with the solvent and promote either internal conversion to the ground state or states of solvation that favor excited-state tautomerization [4,5,8,9,12]. In certain circumstances, it may be more convenient to use a chromophore where this interaction with the solvent is prohibited [12]. An excellent candidate is afforded by 1-methyl-7-azaindole, which has a fluorescence lifetime and quantum yield in water of 21 ns and 0.55, respectively [5,32]. The long fluorescence lifetime of 1-methyl-7-azaindole provides the additional advantage of permitting the measurement of rotational diffusion times on a time scale of tens of nanoseconds. The spectroscopic distinguishability of this chromophore is clearly demonstrated in Figure 9.6.

3. The occurrence of energy transfer from tryptophan to 7-azatryptophan is demonstrated and suggests another role for 7-azatryptophan as a probe of structure and environment.

4. Biotinylated 7-azatryptophan binds tightly to avidin (as demonstrated by chromatography). The 7-azatryptophan moiety can be modelled as diffusing in a cone with a half angle of $29 \pm 5^\circ$.

5. The four avidin binding sites provide equivalent environments as indicated by the fluorescence lifetime and anisotropy decay of the bound biotinylated 7-azatryptophan.

Acknowledgment

R. L. R. is the recipient of a fellowship from Amoco. J. W. P is an Office of Naval Research Young Investigator. We thank Professor P. Callis for his very helpful comments.

References

1. Négrerie, M.; Bellefeuille, S. M.; Whitham, S.; Petrich, J. W.; Thornburg, R. W. *J. Am. Chem. Soc.* 1990, **112**, 7419.
2. Négrerie, M.; Gai, F.; Bellefeuille, S. M.; Petrich, J. W. *J. Phys. Chem.* 1991, **95**, 8663.
3. Rich, R. L.; Négrerie, M.; Li, J.; Elliott, S.; Thornburg, R. W.; Petrich, J. W. *Photochem. Photobiol.* 1993, **58**, 28.
4. Gai, F.; Chen, Y.; Petrich, J. W. *J. Am. Chem. Soc.* 1992, **114**, 8343.
5. Chen, Y.; Rich, R. L.; Gai, F.; Petrich, J. W. *J. Phys. Chem.* 1993, **97**, 1770.
6. Rich, R. L.; Chen, Y.; Neven, D.; Négrerie, M.; Gai, F.; Petrich, J. W. *J. Phys. Chem.* 1993, **97**, 1781.
7. Négrerie, M.; Gai, F.; Lambry, J.-C.; Martin, J.-L.; Petrich, J. W. *J. Phys. Chem.* 1993, **97**, 5046.
8. Chen, Y.; Gai, F.; Petrich, J. W. *J. Am. Chem. Soc.* 1993, **115**, 10158.
9. Chen, Y.; Gai, F.; Petrich, J. W. *Chem. Phys. Lett.* 1994, **222**, 329.
10. Chen, Y.; Gai, F.; Petrich, J. W. *J. Phys. Chem.* 1994, **98**, 2203.
11. Smirnov, A. V.; Rich, R. L.; Petrich, J. W. *Biochem. Biophys. Res. Comm.* 1994, **198**, 1007.
12. Rich, R. L.; English, D. S.; Thornburg, R. W.; Petrich, J. W. In preparation.
13. Beechem, J. M.; Brand, L. *Ann. Rev. Biochem.* 1985, **54**, 43.

14. Creed, D. *Photochem. Photobiol.* **1984**, *39*, 537.
15. Szabo, A. G.; Rayner, D. M. *J. Am. Chem. Soc.* **1980**, *102*, 554.
16. Petrich, J. W.; Chang, M. C.; McDonald, D. B.; Fleming, G. R. *J. Am. Chem. Soc.* **1983**, *105*, 3824.
17. Donzel, B.; Gauduchon, P.; Wahl, Ph. *J. Am. Chem. Soc.* **1974**, *96*, 801.
18. Gudgin, E.; Lopez-Delgado, R.; Ware, W. R. *J. Phys. Chem.* **1983**, *87*, 1559.
19. Tilstra, L.; Sattler, M. C.; Cherry, W. R.; Barkely, M. D. *J. Am. Chem. Soc.* **1990**, *112*, 9176.
20. Green, N. M. *Adv. Protein Chem.* **1975**, *29*, 85.
21. Kurzban, G. P.; Gitlin, G.; Bayer, E. A.; Wilchek, M.; Horowitz, P. M. *Biochemistry* **1989**, *28*, 8537.
22. Blankenburg, R.; Meller, P.; Ringsdorf, H.; Salesse, C. *Biochemistry* **1989**, *28*, 8214.
23. Chen, V. J.; Wold, F. *Biochemistry* **1986**, *25*, 939.
24. *Meth. Enzymology*; Wilchek, M.; Bayer, E., Eds.; Academic Press: San Diego, **1990**, 184.
25. Livnah, O.; Bayer, E. A.; Wilchek, M.; Sussman, J. L. *Proc. Natl. Acad. Sci. USA* **1993**, *90*, 5076.
26. Lane, J. W.; Hong, X.; Schwabacher, A. W. *J. Am. Chem. Soc.* **1993**, *115*, 2078.
27. Wilson, M. E.; Whitesides, G. M. *J. Am. Chem. Soc.* **1978**, *100*, 306.

28. Hogue, C. W. V.; Rasquinha, I.; Szabo, A. G.; MacManus, J. P. *FEBS Lett.* **1992**, *310*, 269. Senear, D. F.; Laue, T. M.; Ross, J. B. A.; Waxman, E.; Eaton, S.; Rusinova, E. *Biochemistry.* **1993**, *32*, 6179. Ross, J. B. A.; Senear, D. F.; Waxman, E.; Kombo, B. B.; Rusinova, E.; Huang, Y. T.; Laws, W. R.; Hasselbacher, C. A. *Proc. Natl. Acad. Sci. USA.* **1992**, *89*, 12023. Kishi, T.; Tanaka, M.; Tanaka, J. *Bull. Chem. Soc. Jpn.* **1977**, *50*, 1267.
29. Lipari, G.; Szabo, A. *J. Am. Chem. Soc.* **1982**, *104*, 4559.
30. Cross, A. J.; Waldeck, D. H.; Fleming, G. R. *J. Chem. Phys.* **1983**, *78*, 6455. Ruggiero, A. J.; Todd, D. C.; Fleming, G. R. *J. Am. Chem. Soc.* **1990**, *112*, 1003.
31. Petrich, J. W.; Longworth, J. W.; Fleming, G. R. *Biochemistry* **1987**, *26*, 2711.
32. Moog, R. S.; Maroncelli, M. *J. Phys. Chem.* **1991**, *95*, 10359.
33. This conclusion [5,8,9] is in general agreement with that presented by Chou *et al.* (*J. Phys. Chem.* **1992**, *96*, 5203). We note, however, that Chapman and Maroncelli (*J. Phys. Chem.* **1992**, *96*, 8430) have presented an alternative explanation in which *all* of the 7-azaindole population tautomerizes in water.
34. Valeur, B.; Weber, G. *Photochem. Photobiol.* **1977**, *25*, 441.
35. Eftink, M. R.; Selvidge, L. A.; Callis, P. R.; Rehms, A. A. *J. Phys. Chem.* **1990**, *94*, 3469.
36. Gai, F.; Rich, R. L.; Petrich, J. W. *J. Am. Chem. Soc.* **1994**, *116*, 735.

CHAPTER 10. SYNTHESIS AND SPECTRAL CHARACTERIZATION OF 5'-PHOSPHOPYRIDOXAL-D,L-7-AZATRYPTOPHAN, A PHOTOPHYSICAL PROBE OF PROTEIN STRUCTURE AND DYNAMICS

A paper published in *Biochemical and Biophysical Research Communications*¹

A. V. Smirnov², R. L. Rich^{3,4}, J. W. Petrich^{3,5}

Abstract

We report the first isolation of an unique adduct of pyridoxal 5'-phosphate, 5'-phosphopyridoxyl-D,L-7-azatryptophan, and suggest a new and easier route for synthesis and purification of 5'-phosphopyridoxyl-L-(or -D-)tryptophan. The absorbance and emission spectra of the 7-azatryptophan adduct are distinctly different than those of pyridoxal 5'-phosphate or the tryptophan adduct. We propose that 5'-phosphopyridoxyl-D,L-7-azatryptophan has great potential as an intrinsic probe in optical studies of protein dynamics.

Introduction

We have previously proposed 7-azatryptophan (Figure 10.1) as an alternative to tryptophan as an optical probe of protein structure and dynamics. The absorption and emission spectra of 7-azatryptophan are sufficiently different from those of tryptophan that it

¹ Reprinted with permission from *Biochemical and Biophysical Research Communications* **1994**, 198, 1007. Copyright © 1994 Academic Press.

² Undergraduate summer student from the Higher Chemical College of the Russian Academy of Sciences who worked under the direction of J. W. Petrich. Currently a graduate student in J. W. Petrich's group, Department of Chemistry, Iowa State University.

³ Graduate student and Associate Professor, respectively, Department of Chemistry, Iowa State University.

⁴ The major portion of the work published in this publication was performed by A. V. Smirnov. This paper is included in this dissertation for completeness in describing the cofactor projects currently underway in our laboratory.

⁵ To whom correspondence should be addressed.

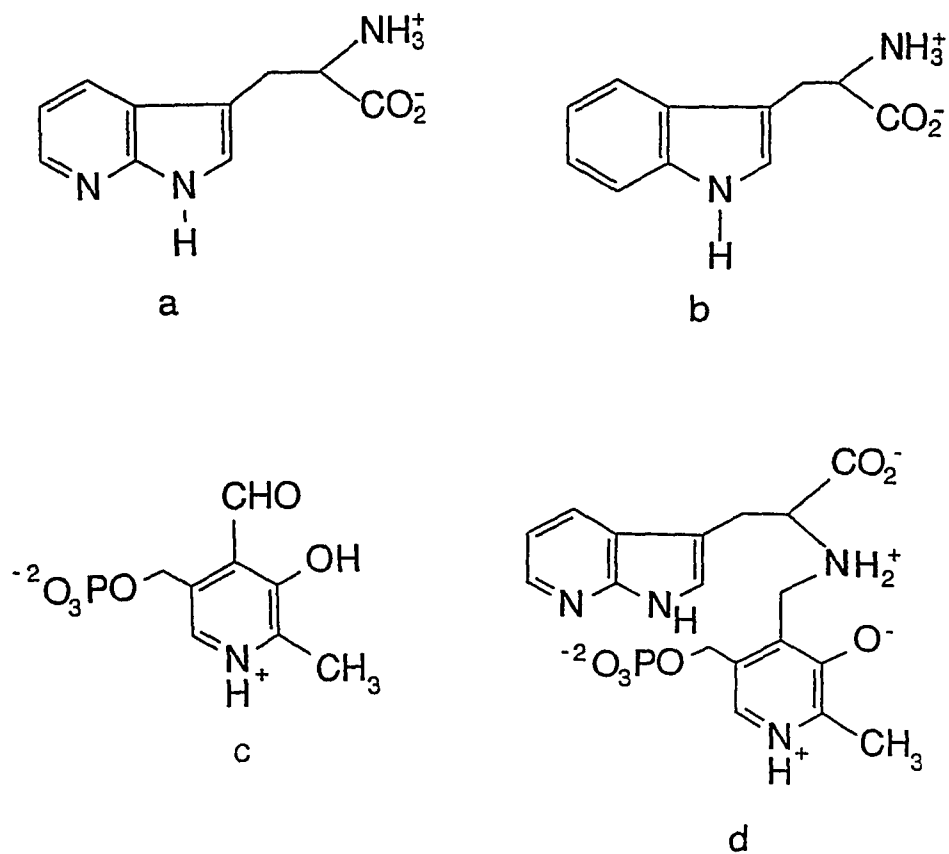


Figure 10.1. Structures of: (a) 7-azatryptophan; (b) tryptophan; (c) pyridoxal 5'-phosphate; and (d) 5'-phosphopyridoxyl-D,L-7-azatryptophan.

is possible to observe selectively and uniquely emission from 7-azatryptophan in the presence of at least ten tryptophans [1-5]. Furthermore, whereas the intrinsic fluorescence decay of aqueous tryptophan is nonexponential, that of 7-azatryptophan is single exponential [1-5]. In addition, we have successfully replaced tryptophan with 7-azatryptophan in bacterial enzymes [1,6], incorporated 7-azatryptophan into synthetic peptides, and have shown that the binding characteristics of a 7-azatryptophan-containing peptide resemble those of the native tryptophan-containing sequence [3]. Tethering 7-azatryptophan to a coenzyme that binds in the enzymatic active site would ensure that examination of the protein dynamics indeed would be of the active site. We chose to synthesize 5'-phosphopyridoxyl-D,L-7-azatryptophan, an adduct of pyridoxal 5'-phosphate, a vitamin B₆ derivative that is a required cofactor for a number of enzymes. Such a modified coenzyme would permit one to observe fluorescence emission preferentially from the adduct, up to a limit of ten tryptophans within the enzyme per coenzyme adduct molecule [3].

Experimental

Materials and Methods

Pyridoxal 5'-phosphate, D- and L-tryptophan, and D,L-7-azatryptophan were purchased from Sigma Chemical Co. Acetic acid, potassium hydroxide, hydrochloric acid, and sodium borohydride were reagent-grade chemicals from Fisher Chemical Co. Dowex-1 and Amberlite IRA-743 resins were products of Dow Co. and Rohm & Haas Co., respectively. All reagents and resins were used as purchased.

UV-visible spectra were obtained at room temperature using a Hewlett-Packard HP 8452A diode-array spectrophotometer. ¹H NMR spectra were recorded on a Nicolet NT300 spectrometer. Column preparation/regeneration of the Dowex-1 resin required flushing thoroughly with 4 M CH₃COOH (approximately 50 mL), then washing the column with water until the effluent was at neutral pH. The preparation/regeneration of the Amberlite IRA-743 column required flushing with 50 mL of 2 M H₂SO₄, followed by washing with water until the effluent was at neutral pH, and then flushing with 30 mL of 2 M NH₄OH [10].

Preparation of 5'-Phosphopyridoxyl-D,L-7-Azatryptophan

The synthetic methods described in this paper are based on a combination of techniques published previously [7-9]. All operations were performed at room temperature and under yellow light to prevent photolysis. The solutions were stirred throughout the synthetic procedure.

0.5 mmol each of pyridoxal 5'-phosphate and D,L-7-azatryptophan were dissolved in five mL water, forming a light yellow solution. After 30 minutes, the pH was adjusted slowly to 8 using 5 M KOH and the solution gradually became clear and light brown. At this time 1.5 mmol NaBH₄ was added slowly while pH 8 was maintained by occasional addition of dilute HCl and the solution became light yellow. The pH was lowered to 2 using 6 N HCl and the reaction mixture became colorless.

In order to remove boric acid produced in the synthesis, the solution was layered on a column of Amberlite IRA-743 (1 x 15 cm) and eluted with 30 mL 0.1 M HCl, followed by 30 ml of 0.5 M HCl. Collected fractions showing an absorption maximum at 328-330 nm were combined, evaporated *in vacuo* to approximately one mL, and neutralized. A viscous yellow liquid was obtained. The compound was further purified by layering on a column of Dowex-1 (1 x 40 cm) previously equilibrated with water. A linear gradient of 0 to 0.7 M CH₃COOH was then applied to the column. A total of 400 mL of eluent was used. The residual pyridoxal 5'-phosphate and 7-azatryptophan eluted at the beginning of the gradient, while the product eluted at 0.5 M CH₃COOH. Once again, fractions showing an absorption maximum of 328-330 nm were combined, evaporated *in vacuo* to approximately one mL, neutralized, and evaporated until dry. Light yellow crystals were obtained. These were dried overnight in a drying box with NaOH to remove all traces of CH₃COOH.

UV-vis (rel. int.): 260 (0.64), 292 (1.00), 330 nm (0.75). ¹H NMR (D₂O/NaOD): δ 2.42 (s, ArCH₃), 3.28 (m, -CH_AH_B-CH_X-), 3.71 (t, -CH_AH_B-CH_X-), 3.89 (d, -CH_AH_BAr), 4.06 (d, -CH_AH_BAr), 4.97 (m, ArCH_AH_B-NH-), 7.36 (m, ArH), 7.58 (s, ArH), 7.69 (s, ArH), 8.21 (m, ArH), 8.45 (m, ArH).

Preparation of 5'-Phosphopyridoxyl-L-Tryptophan and 5'-Phosphopyridoxyl-D-Tryptophan

Since tryptophan is not stable under extreme acidic conditions and the 5'-phosphopyridoxyl-tryptophan compounds are not as soluble in water as 5'-phosphopyridoxyl-D,L-7-azatryptophan, a slightly different route was employed for these syntheses. A total of 0.5 mmol each of pyridoxal 5'-phosphate and L-tryptophan were dissolved in 5 ml of water,

forming a deep orange solution. The pH was adjusted to 8 with 3-4 drops of 50% KOH and the reaction mixture became light green-yellow. After 15 min, 2 mmol of NaBH₄ were added slowly while pH 8 was maintained by occasional addition of dilute HCl. After another 5 minutes, the pH was slowly lowered to 3-4 with 6 N HCl and the reaction mixture was allowed to sit for about 2 hours while light yellow needle-like crystals formed. The product was filtered and washed with a small amount of water followed by MeOH and dried in a drying box with CaSO₄ overnight. The product was purified by dissolving it in water with a minimum of KOH and then adding HCl solution dropwise until the pH was 3-4.

Synthesis of the D-tryptophan adduct followed the same procedure as that of the L-tryptophan adduct described above. The absorption and emission spectra of the two enantiomeric compounds show the same maxima.

UV-vis (rel. int.): 260 (1.00), 280 (0.82), 288 (0.76), 332 nm (0.93). ¹H NMR (D₂O/NaOD): δ 2.42 (s, ArCH₃), 3.23 (m, -CH_AH_B-CH_X-), 3.69 (t, -CH_AH_B-CH_X-), 3.81 (d, -CH_AH_BAr), 3.99 (d, -CH_AH_BAr), 4.94 (m, ArCH_AH_B-NH-), 7.31 (m, ArH), 7.39 (s, ArH), 7.43 (m, ArH), 7.69 (d, ArH), 7.72 (s, ArH), 8.21 (d, ArH).

Results and Discussion

Most of the reported derivatives of pyridoxyl 5'-phosphate with natural amino acids were obtained in 1966 by Ikawa [7]. Further work [8-10] revealed improved methods for the synthesis of the L-tryptophan derivative. None of these methods, however, offers a convenient synthesis and purification technique. Ikawa [7] uses platinum oxide in the initial synthetic steps and other methods [8,9] involve maintaining the reaction product at low pH values known to be destructive for the tryptophan moiety [11]. In addition, when chromatography on a column of DEAE-Sephadex A-25 [9] was tried for product purification, the effluent was too dilute to be unambiguously analyzed by thin-layer chromatography with a fluorescent indicator. After concentrating the column effluent, both methods [8,9] produce a brownish yellow substance, in contrast to the one described by Ikawa [7] and here (see Materials and Methods).

In order to examine the possible effects of the D- and L-enantiomers, both of the tryptophan derivatives were obtained. Any differences in protein-adduct behavior between these two species may then be directly attributed to the α-carbon. In the event that no differences are observed between the D- and L- species, it is not necessary to isolate the

individual enantiomers. The synthesis presented here for the 7-azatryptophan adduct produces a racemic mixture. Should evidence of enantiomeric factors be observed, separation of the D- and L- species would be required.

There are no reports of 5'-phosphopyridoxyl-7-azatryptophan synthesis. The synthetic procedure to obtain the 7-azatryptophan adduct is less straightforward than that of the tryptophan analog. Most importantly, the reaction mixture should be maintained at a lower pH and for longer period of time to achieve equilibrium. Also, the relatively high solubility of 5'-phosphopyridoxyl-D,L-7-azatryptophan in water does not permit the use of recrystallization as a convenient purification procedure. Fortunately, the greater stability of 7-azatryptophan than tryptophan in acidic solution allows for purification via column chromatography.

Figures 10.2-10.4 illustrate the significant differences in the absorption and emission spectra of the two adducts and pyridoxal 5'-phosphate. The contributions from tryptophan and 7-azatryptophan are easily observed in the absorption spectra, producing maxima (280 and 292 nm, respectively) not present in the pyridoxal 5'-phosphate spectrum. The emission spectra yield maxima in the expected ranges for derivatives of these amino acids. Clearly, preferential excitation and emission collection of 5'-phosphopyridoxyl-D,L-7-azatryptophan may be performed in the holoenzyme complex.

Conclusions

5'-Phosphopyridoxyl-D,L-7-azatryptophan offers a unique opportunity to study protein dynamics without significantly altering the enzyme structure while employing an intrinsic probe. Previous work has shown the 5'-phosphopyridoxyl-L-tryptophan adduct to bind successfully to tryptophanase [8] and tryptophan synthase [9]. The 7-azatryptophan adduct is expected to bind similarly based on earlier comparisons of tryptophan and 7-azatryptophan binding in an enzymatic active site [3]. This probe presents a novel approach to study steady-state and time-resolved spectroscopy of enzymatic systems requiring pyridoxal 5'-phosphate as a cofactor.

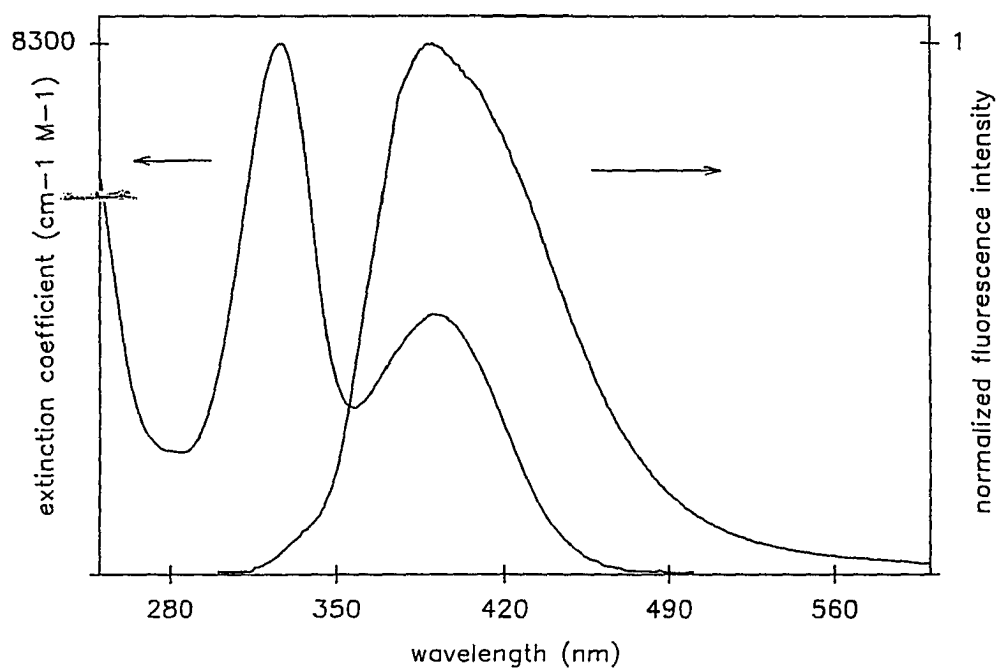


Figure 10.2. Absorption and emission spectra ($\lambda_{\text{ex}} = 320 \text{ nm}$) of pyridoxal 5'-phosphate.

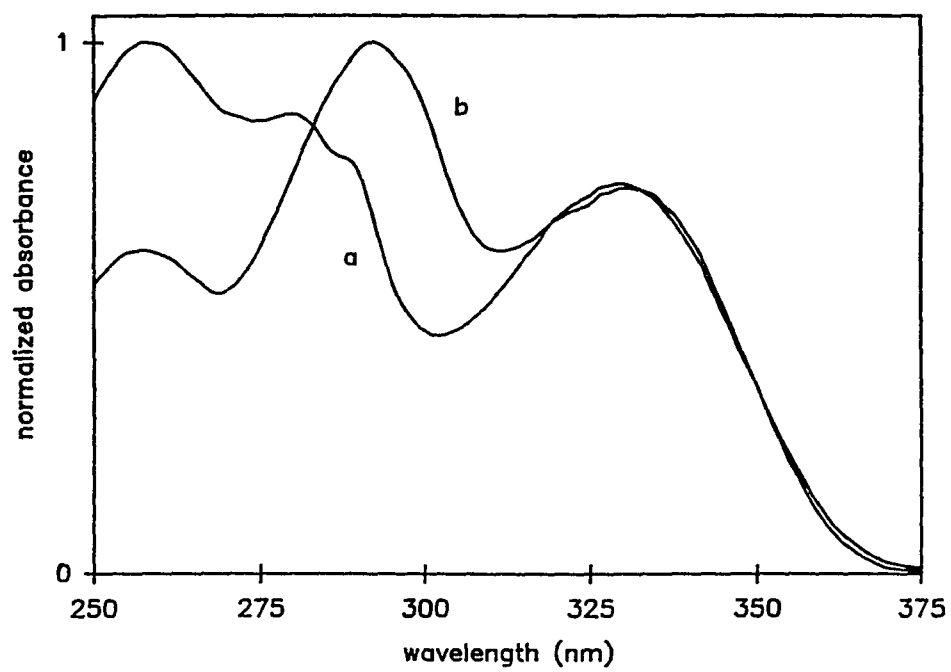


Figure 10.3. Absorption spectra of: (a) 5'-phosphopyridoxyl-L-tryptophan and (b) 5'-phosphopyridoxyl-D,L-7-azatryptophan.

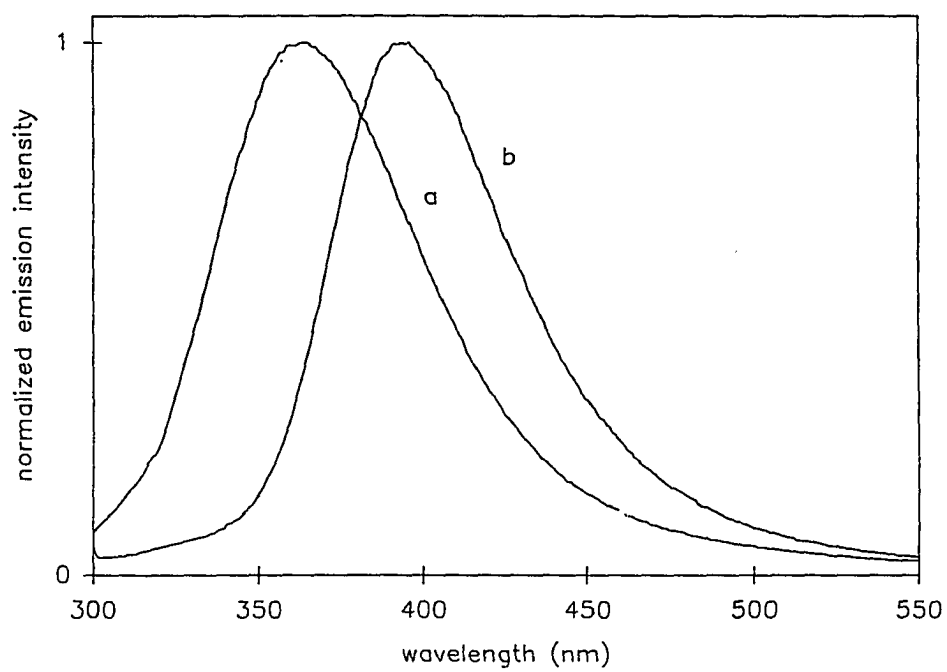


Figure 10.4. Emission spectra of: (a) 5'-phosphopyridoxyl-L-tryptophan ($\lambda_{em}^{max} = 364$ nm; $\lambda_{ex} = 281$ nm) and (b) 5'-phosphopyridoxyl-D,L-7-azatryptophan ($\lambda_{em}^{max} = 394$ nm; $\lambda_{ex} = 292$ nm).

Acknowledgments

A.V.S. was a summer student from the Higher Chemical College of the Russian Academy of Sciences. R.L.R. is the recipient of an Amoco fellowship. J.W.P. is an Office of Naval Research Young Investigator.

References

1. Négrerie, M., Bellefeuille, S.M., Whitham, S., Petrich, J.W., Thornburg, R.W. *J. Am. Chem. Soc.* **1990**, *112*, 7419.
2. Négrerie, M., Gai, F., Bellefeuille, S.M., Petrich, J.W. *J. Phys. Chem.* **1991**, *95*, 8663.
3. Rich, R.L., Négrerie, M., Li, J., Elliott, S., Thornburg, R.W., Petrich, J.W. *Photochem. Photobiol.* **1993**, *58*, 28.
4. Chen, Y., Rich, R.L., Gai, F., Petrich, J.W. *J. Phys. Chem.* **1993**, *97*, 1770.
5. Rich, R.L., Chen, Y., Neven, D., Négrerie, M., Gai, F., Petrich, J.W. *J. Phys. Chem.* **1993**, *97*, 1781.
6. Rich, R.L., Thornburg, R.W., Petrich, J.W. unpublished results.
7. Ikawa, M. *Arch. Biochem. Biophys.* **1967**, *118*, 497.
8. Raibaud, O. and Goldberg, M. E. *J. Biol. Chem.* **1976**, *251*, 2814.
9. Tschopp, J. and Kirschner, K. *Biochem.* **1980**, *19*, 4514.

10. Mair, J. W. and Day, H. G. *Anal. Chem.* **1972**, *44*, 2015.
11. Holt, L.A., Milligan, B., Rivett, D.E. *Biochem.* **1971**, *10*, 3559.

PART IV. ANALYSIS OF PROTEINS

CHAPTER 11. PROPOSED INCORPORATION OF 7-AZATRYPTOPHAN INTO BACTERIAL PROTEINS

Introduction

Incorporation of intrinsic probes into proteins is the ultimate goal of this research project. A nonnatural amino acid such as 7-azatryptophan or one of its analogs as a replacement for a particular residue in the protein's peptide sequence allows for highly selective yet relatively non-disruptive study of the protein alone or in complex with cofactors, peptides, another protein, or other biological entities. This replacement approach has numerous advantages, particularly when employing 7-azatryptophan and its analogs. As discussed in previous chapters, 7-azatryptophan is spectroscopically distinct from tryptophan and can be detected in an environment containing multiple tryptophans. The following is a description of the 7-azatryptophan incorporation into proteins project underway in our [1] laboratory; included are a list of clone donations provided to our laboratory for this project and the procedures and techniques required.

Materials and Methods

Donations

Below are listed the clones donated to our laboratory and a short description of each. Actual correspondence from the donors can be found in my notebooks.

1. pUCW248F tryptophanase containing one tryptophan (JM109) from Yasushi Kawata, Department of Biotechnology, Tottori University, Japan, 1/26/1993. We have been given a W248F mutant cell of tryptophanase (JM109/pUCWF) that overproduces the enzyme under IPTG inducing conditions. This mutant contains only one tryptophan, W330. The optimal conditions for cell growth known by Dr. Wen-Chy, a postdoctoral fellow in Dr. Metzler's lab, Department of Biochemistry and Biophysics, Iowa State University. Previous work with this enzyme includes incorporating 5-fluorotryptophan at positions 330 or 248 and /330. SVS370 tryptophanase (wild-type that contains two tryptophans) was also provided by Dr. Wen-Chy.

2. Y147W LDH (42 kDa) from J. J. Holbrook, Department of Biochemistry, University of Bristol, U.K.. The actual correspondence was from D. J. Halsall, a postdoctoral fellow in Dr. Holbrook's lab, 3/2/1993: "The crystal structure of the Y147W mutant has been solved and is essentially identical to that of the wild type [2] The plasmid is pkk derived and transformed into *E. coli* TG2 cells and transformants are selected for by growth on ampicillin. The LDH expresses routinely at at least 20% of the total cell protein. Purification is relatively simple: the group used a heat step (70°C for 20 minutes, a blue sepharose or oxamate affinity step, then ion-exchange on Q-sepharose)."

3. pTZW31-3 DHFR (18.5 kDa) from Benkovic, pUCW289F, pJGR luciferase (62 kDa): I have no information about these donations.

Production and Isolation of Tryptophanase

The procedures for growth of competent cells and transformation of plasmids described below are general techniques; the procedure for isolation of tryptophanase from the cell milieu and determination of enzymatic activity is that of Behbahani-Nejad *et al.* [3] and Metzler *et al.* [4], with slight modifications noted.

We have obtained a mutant cell (JM109/pUCWF) that has only one tryptophan (at residue 330) from Y. Kawata and overproduces tryptophanase upon induction with IPTG. I transformed the DNA from this mutant into a tryptophan auxotroph *E. coli* K-12 strain, ATCC 23802. I call this 2W1.

Single colonies of 2W1 cells are grown on 2yT agar plates having an ampicillin pressure of 50 µg/mL, then harvested into 1 L of culture media. If incorporation of 7-azatryptophan was intended, the media used was M56' media (M56' is M56 [5], but using glycerol as the carbon source); if not, cultures were grown in 2yT media. Cultures were grown for approximately 40 hours at 37°C with gentle agitation. The broth was then centrifuged and the supernatant discarded. The pellet was resuspended in M56' media in which the tryptophan had been replaced with D,L-7-azatryptophan. IPTG was added 45 minutes later to initiate tryptophanase production and this culture was gently agitated at 37°C for approximately 15 hours longer. At this time, the broth was centrifuged and the pellet was frozen at -20°C overnight.

Growth of Competent E. coli Cells. Grow one mL 2yT culture overnight, then inoculate 200 µL this broth into 50 mL 2yT media. Grow this culture until it reaches the mid-log phase. Put the culture on ice for 30 minutes, then centrifuge for 30 minutes. Centrifuge for 10 minutes at 4°C and resuspend in the cells in 20 mL cold trisCa (10 mM tris

HCl pH 8.0, 50 mM CaCl_2). Keep the cells on ice for 30 minutes, then centrifuge the suspension for 10 minutes. Resuspend the cells in 2 mL of cold tris Ca.

Transformation of Plasmids. Add five μL DNA to 200 μL of cells and put on ice for 30 minutes. Heat shock at 42°C for two minutes, then add one mL 2yT culture broth. Incubate at 37°C with gentle agitation for one hour and then plate out 50 μL , 100 μL , and 200 μL culture on (2yT + amp) plates. Collect cells containing plasmid by: selecting a single colony from culture grown on (2yT + amp) plate, inoculating one mL (2yT + amp) media, and allowing this to grow overnight at 37°C with gentle agitation, and harvest when at mid-log phase. Centrifuge and discard the supernatant (use approximately 1.5 mL culture). Resuspend the pellet in 150 μL solution I (50 mM glucose, 10 mM EDTA, 25 mM trisCl pH 8.0). Add 350 μL soln II (10% SDS, 0.4 M NaOH). Mix gently and put on ice for 15 minutes. After a precipitate forms add 250 μL solution III. Put on ice for 15 minutes, then centrifuge at 4°C for five minutes. Transfer 700 μL supernatant to a new vial without transferring the scum from the top. Add 700 μL isopropanol, centrifuge five minutes, and decant the supernatant. Wash the pellet with one mL 70% ethanol and remove all the ethanol before drying. Dry in a Speedvac for 15 minutes and resuspend in 50 μL TE80. Store at -20°C until use.

Purification of Enzyme. A number of different buffer systems are used throughout the isolation of tryptophanase. A recipe for each is given below, followed by step-by-step instructions for the enzyme purification.

buffer 1: 17.42 g K_2HPO_4 in 1 L water (0.1 M), pH 7.0 adjusted with dilute H_3PO_4 , 0.05 g PLP (0.1 mM), 0.585 g EDTA (2 mM), 0.391 g β -mercaptoethanol (5 mM).

buffer 2: 17.42 g K_2HPO_4 in 1 L water (0.1 M), pH 7.8 with dilute H_3PO_4 , 0.05 g PLP (0.2 mM), 0.585 g EDTA (2 mM), 0.391 g β -mercaptoethanol (5 mM), 110 g $(\text{NH}_4)_2\text{SO}_4$ (11 g/100 mL).

buffer 3: 17.42 g K_2HPO_4 in 1 L water (0.1 M), pH 7.8 with dilute H_3PO_4 , 0.025 g PLP (0.1 mM), 0.585 g EDTA (2 mM), 0.391 g β -mercaptoethanol (5 mM).

buffer 4: 17.42 g K_2HPO_4 in 1 L water (0.1M), pH 7.8 with dilute H_3PO_4 , 0.005 g PLP (0.02 mM).

buffer 5: 4.35 g K_2HPO_4 in 900 mL water (0.025 M), pH 7.0 with dilute H_3PO_4 , 100 mL glycerol (10%), 0.025 g PLP (0.1 mM), 0.585 g EDTA (2 mM), 0.391 g β -mercaptoethanol (5 mM).

buffer 6: 34.84 g K_2HPO_4 in 900 mL water (0.2 M), pH 7.8 with dilute H_3PO_4 , 0.2 M NH_4Cl (2.14 g), 0.585 g EDTA (2 mM), 1.56 g β -mercaptoethanol, (20mM), 100 mL glycerol (10%).

12.7 g cells are suspended in 50 mL 50 mM tris-HCl pH 7.5, 5 mM EDTA buffer. 0.15 g lysozyme is added and the solution is put on ice for two hours. 3.5 mL 5 M NH_4Cl is added and the solution mixed by inversion. 3.76 mL 10% Nonidet P-40 is added and the solution is again mixed. The solution is sonicated at 80% full power until most viscosity is lost (solution can drip from a pipette) and then diluted to 165 mL with buffer solution to make a final concentration of 0.1 M K_2HPO_4 , 0.1 M pyridoxal 5'-phosphate (PLP), 2mM EDTA, 5 mM β -mercaptoethanol, adjusted to pH 7.0 with dilute H_3PO_4 (buffer 1). The burst cells are centrifuged at 3800 rpm for 25 minutes. The supernatant is collected and adjusted to pH 6.0 with 10% CH_3COOH . 30 mL of 2% protamine sulfate solution is added dropwise with stirring over 20 minutes and the mixture is centrifuged for 30 minutes. The pH of the supernatant is then adjusted to 7.0 with 10% NH_4OH . 44.6 g $(NH_4)_2SO_4$ is added over 30 minutes while stirring the solution at 4°C and maintaining pH 7.0 by periodically adding 10% NH_4OH . The solution is then centrifuged for 30 minutes and the precipitate is discarded. 28.1 g $(NH_4)_2SO_4$ is added over 30 minutes while stirring at 4°C and maintaining pH 7.0. The precipitate was dissolved in 17.5 mL buffer 2. The solution is heated to 65°C and this temperature is maintained for 5 minutes. The solution is centrifuged for 30 minutes and the supernatant is dialyzed against 3 x 2 L buffer 3. The solution is concentrated to 10 mL by ultrafiltration, loaded onto a Sephacryl HR-200 column, and eluted with buffer 4. Fractions showing tryptophanase activity are pooled and dialyzed against 3 x 2 L buffer 5. After concentration by ultrafiltration, the sample is loaded onto a DEAE cellulose column, washed with 2 x bed volume of buffer 5, and eluted with 0.025 M K_2HPO_4 and a gradient of 0.5 NH_4Cl . Fractions showing tryptophanase activity are pooled and dialyzed against buffer 6. The sample is stored at 4°C in the dark. SDS-PAGE gel analysis shows one band at 52 kDa. Enzyme activity is determined at each step as described by Behbahani-Nejad [3] using *S*-*o*-nitrophenyl-L-cysteine (SOPC) provided by Professor Metzler, Department of Biochemistry and Biophysics, Iowa State University. The two solutions required for the activity measurements are: (1) SOPC solution, 0.05 M K_2HPO_4 pH 8.0, 0.05 M KCl, 0.6 mM SOPC (m.w. 242 g/mol) and (2) tryptophanase activation buffer, 25 mM EPPS pH 8.0, 1mM EDTA, 0.2 M KCl, 0.2 PLP, 50 mM β -mercaptoethanol. The K_m and k_{cat} values I obtain for

the isolated tryptophanase agree with published results [3,4,6] and the optical spectra duplicate those of Metzler *et al.* [4] and Kawata *et al.* [7].

References

1. References to "our" laboratory throughout this chapter explicitly refer to the laboratories of J. W. Petrich and R. W. Thornburg. Most of the work described herein was directly supervised by R. W. T. and the clones and other materials for this project are to be found in his laboratory.
2. Roper et al *Protein Engineering* **1992**, 5, 611.
3. Behbahani-Nejad, I. Dye, J. L., Suelter, C. H. *Methods Enzymol.* **1987**, 142, , 414.
4. Metzler, C. A.; Viswanath, R.; Metzler, D. E. *J. Biol. Chem.* **1991**, 266, 9374.
5. Monod et al. *Biochem. Biophys. Acta* **1951**, 7, 585.
6. Phillips, R. S.; Gollnick, P. *FEBS Lett.* **1990**, 268, 213.
7. Kawata, Y.; Tsujimoto, N.; Tani, S.; Mizobata, T.; Tokushige *Biochem. Biophys. Res. Comm.* **1990**, 173, 756.

GENERAL SUMMARY AND CONCLUSIONS

This work has demonstrated the viability of 7-azatryptophan and its derivatives as optical probes of biological systems. The red-shifted optical spectra and monoexponential fluorescence lifetimes (in water at pH 7) of these compounds provide us with a unique opportunity to study protein structure and dynamics of proteins, even those that contain multiple tryptophans.

Detailed analysis of the chromophore, 7-azaindole, and its methylated derivatives has supplied a solid basis for interpreting spectroscopic data for the amino acid, 7-azatryptophan, in a variety of biological environments due to this probe's sensitivity since the appearance of nonexponentiality and changes in lifetime are due to the local environment. Development of a new nonnatural amino acid, N₁-methyl-7-azatryptophan, shows great promise. Its high fluorescence quantum yield and long fluorescence lifetime indicate that this molecule may be an even better intrinsic probe than 7-azatryptophan. The other 7-azatryptophan derivatives we are preparing may have similar advantages and prove useful as optical probes.

We have demonstrated that incorporation of these amino acids into peptides, biological cofactors, and proteins is possible and these systems remain viable. Our work on the peptide/proteinase and peptide/MHC systems has proved that 7-azatryptophan and N₁-methyl-7-azatryptophan are suitable as intrinsic probes in these complexes. These tryptophan derivatives have demonstrated particular sensitivity to their surrounding environment; thereby yielding valuable information about their specific location and the overall complex. Studies of the "optically tagged" biological cofactors, (biotinylated-7-azatryptophan and -N₁-methyl-7-azatryptophan, and 5'-phosphopyridoxal-D,L,-7-azatryptophan) are still underway; our data collected thusfar illustrate the usefulness of using such modified cofactors: the native complex is disturbed minimally, if at all, and the probe is placed directly into a well-characterized binding site. We continue to improve our techniques of direct incorporation of 7-azatryptophan into proteins.

Throughout the work described in this dissertation, we have shown the great advantages of 7-azatryptophan and its analogs over tryptophan, (and other chromophores currently in use), as tools in the photophysical analyses of proteins and other systems of biological interest.

ACKNOWLEDGMENTS

Many people have contributed supplies, insight, and encouragement to me throughout my graduate studies. Sincere appreciation is due to my advisor, mentor, and friend, J. Petrich, for his continual guidance and support. Other faculty and committee members have given me valuable advice and assistance; in particular, I thank R. Thornburg for teaching me techniques in biochemistry and sharing his laboratory equipment, supplies, and space, and A. Schwabacher for helping me with my synthetic work.

No project in our research group has been performed in isolation, but rather, has required input from each of us. I thankfully acknowledge the efforts contributed by the other members of my research group. I am grateful to F. Gai for teaching me about our laser systems in particular and science in general, and commend M. Fehr for his *joie de vivre*.

Friends and family have proved invaluable. L. Berreau is a dear friend and a fine example of dedication and perseverance. My family, immediate and extended, each deserve a heartfelt thank-you for their constant encouragement. My parents taught me to work hard and believe in myself — any credit for my completion of this work is ultimately theirs.

APPENDIX A: FUTURE PROJECTS

The following are a number of projects related to our 7-azatryptophan and N₁-methyl-7-azatryptophan work that we have either considered, but not begun, or started, but not fully developed.

Rigid Octameric Peptide Studies

We would like to determine the local environment effects upon the binding and photophysics of octapeptides containing 7-azatryptophan. Effects due to peptide secondary structure may be examined by using two octapeptides we have had synthesized by the ISU Protein Facility: KACPLNCD and KACP(7AT)NCD. Incorporation of "spacers" into the disulfide bond of these octameric peptide and subsequent determination of the inhibition ability of the modified octameric peptide would demonstrate the optimum configuration of the peptide for enzymatic binding.

The selection of appropriate spacer length could be performed as follows. Add a mixture of alkylating agents (e.g., ICH₂C(=O)NH(CH₂)_nNHC(=O)CH₂I) to a solution of the peptide bound to enzyme, such as α-chymotrypsin. If the solution is sufficiently dilute and the binding of the alkylating agent is reversible, the alkyl chain of optimal length should bind to the peptide. Analysis of the alkylated peptide (after removal of the enzyme by denaturation and dialysis) by mass spectrometry should reveal the preferred chain length for alkylation. After this initial screen, synthesis using the chosen alkylating agent may be performed on a larger scale and under conditions not requiring an enzyme. At this stage, inhibition studies and photophysical analyses could be performed using this rigid peptide alone and bound to an appropriate enzyme. Notebook reference: ntbk 5, p. 194-195.

Verification of Peptide Cleavage Site

It is generally assumed that proteinases cleave peptides on the carboxylic acid side of amino acids containing large aromatic side chains. The following is a test to verify this assumption for the peptide sequences and proteinases that we use. The buffer system to use is 0.1 M tris buffer solution (2.422 g tris, 0.588 g CaCl₂ · 2H₂O), 1 drop Triton X-100 in 200 mL water and adjusted to pH 8.3 using 1 M HCl. As an example, the procedure for the tripeptide, NAc-pro-trp-asn-NH₂, is described. Mix the peptide and proteinase in equimolar

ratio (an overwhelming excess of proteinase should guarantee significant peptide cleavage).

On a silica gel TLC plate, make lanes for:

1. proteinase
2. peptide
3. peptide/proteinase (1:1) at pH of complex under normal condition
4. peptide/proteinase (1:1) at pH that causes hydrolysis to occur
5. NAc-pro-trp
6. asn-NH₂
7. buffer alone.

The TLC solvent system is *n*-BuOH, acetic acid, water (4:1:1) and its identification is suggested to be by Ninhydrin (0.1% Ninhydrin, 5% HAc, 10 pyridine in acetone, made immediately prior to use), an alternative staining agent, and/or *uv* light. The lane of buffer alone is necessary since this buffer will produce a spot on the TLC plate (tris is C(MeOH)₃NH₂). A conjugated system is necessary for *uv* detection and a NH₃⁺ group is necessary for Ninhydrin analysis. Note, however, that by these methods no spot should be apparent if NAc-pro exists in a lane on the TLC plate. By comparison of the lanes after elution, the cleavage site of the peptide should be readily apparent.

5'-Phosphopyridoxal-D,L-7-Azatriptophan Studies

Pyridoxal 5'-phosphate (PLP), a derivative of vitamin B₆, is a cofactor in a wide variety of enzymatic reactions: transaminations, elimination and replacement reactions, decarboxylations, deaminations, racemizations, and aldol cleavages [1]. The synthesis of an optically-tagged cofactor, 5'-phosphopyridoxal-D,L-7-azatriptophan (7AT-PLP), is discussed in Chapter 10. We have performed some preliminary photophysical analyses of this compound and the others reported in Chapter 10. The data for these compounds at $\lambda_{ex}=285\text{nm}$, 20°C in water are shown below:

compound	λ_{em} (nm)	A ₁	A ₂	τ_1 (ps)	τ_2 (ps)	τ_3 (ps)
PLP	345	0.90	0.10	68	521	
7AT-PLP	435	0.54	0.46	157	637	
trp-PLP	434.5	0.51	0.41	51	266	1574

It should be noted that these data should be remeasured to verify that the short lifetime components are valid and not due to instrument instability.

We propose that the binding of these tagged cofactors with PLP-requiring enzymes, e.g. tryptophanase, tryptophan synthase and aspartate aminotransferase, should yield information about the role of this cofactor in particular and active site dynamics in general. Tschopp and Kirschner [2] have previously reported the synthesis of PLP tagged with tryptophan (N-phosphopyridoxal-L-tryptophan) and presented ligand binding parameters for their derivative bound to tryptophan synthase: For PLP, $K_D = 0.12$ mM; for trp-PLP $K_D = 1.10$ mM. These results imply that tagged cofactors are viable, yet show a ten-fold decrease in binding ability. We assume the substitution of a nitrogen at the 7-position should make a small, if non-negligible, change in the binding of the tagged PLP from that of trp-PLP.

1. Biochemistry, Stryer, L. 2nd ed. 1975, W. H. Freeman and Company, New York
2. Tschopp, J.; Kirschner, K. *Biochem.* **1980**, *19*, 4514.

1M7AT bound to avidin

Current studies of the biotinylated 1M7AT are underway in our laboratory. This cofactor was synthesized by J. Lane at using similar techniques and procedures as described for the synthesis of biotinylated 7-azatryptophan. With this tagged biotin, we hope to verify the assumptions we proposed in the preceding paper; that is, that such a probe as a 7-azatryptophan derivative methylated at the aromatic N_1 position is indeed a most viable tool in the study of protein structure and dynamics.

APPENDIX B: NOTES ON INSTRUMENTATION

The following is a collection of notes concerning two instruments in our laboratory: the Spex Fluoromax and the Perkin-Elmer Lambda 18 UV/vis spectrometer. These notes include techniques required for daily use and procedures that I have performed in unusual circumstances. Manuals for these instruments may be found in the bench drawers beneath each instrument.

Spex Fluoromax

Start Up

The start-up sequence for the Fluoromax is important. Turn the lamp power on and wait for the red light next to the Lamp On toggle switch to remain lit. Turn on the computer and monitor. Wait for the computer to boot up and select the option "Fluoromax". When the company logo appears on the screen and a message appears at the bottom prompting you to turn on the Fluoromax power, do so. This message will flash periodically until the the Power On toggle switch is tripped. If you turn the power on at the correct time, the message will change to "downloading" and the system will initialize. If the prompt message continues to appear after you have tripped the Power On toggle switch, you must reboot the computer and begin again. The system requires a few minutes to initialize and is finished when graph axes appear on the screen. The system is now ready for calibration.

Daily Calibration

The excitation and emission calibrations that are required upon initializing the instrument are fully described in the manual. When calibrating the excitation spectrum, the maximum should be 467.125 nm. If it is not, repeat this calibration until the maximum is correct. When calibrating the emission spectrum, the maximum should be 397 nm, with an intensity of $1-2 \times 10^5$ cps. If the maximum is off by less than 10 nm, repeat this calibration until it is correct. This is the calibration that is more often performed incorrectly. If you should have problems, verify that the excitation is set at 350 nm and run an emission scan from 300 to 500 nm to observe the excitation and Raman peaks. The excitation peak should appear centered at 350 nm ($> 1 \times 10^6$ cps) and the maximum of the Raman peak should be at

397 nm ($1-2 \times 10^5$ cps). If the fluorimeter needs to be drastically recalibrated (the Raman peak is $> \pm 10$ nm from 397 nm), the calibration must be performed in increments of 10 nm. Move the Raman peak 10 nm in the direction desired, run the calibration, and observe the peak shift 10 nm. Repeat this step until the calibration is correct.

Generation of XC.SPT and MC.SPT files

The generation of excitation (xc.spt) and emission (mc.spt) files is described in the manual. These should be performed regularly, particularly when careful examinations of intensities at various wavelengths are required.

Comparative Calibration of UV/vis Spectrophotometer and Fluorimeter

The comparative calibration of a UV/vis spectrophotometer and the fluorimeter has been described previously in this work, but is included here for reference. Such a comparison is necessary when evaluating any differences between the absorption and excitation spectra obtained for a sample. Calibration of the absorption spectrometer and of the fluorimeter is performed using indole vapor as a standard. Crystals of indole in a 1-cm cuvette filled with argon are heated to 65°C. Absorption and excitation spectra are obtained and overlaid. In our experiments, comparison of the absorption and the excitation spectra of the vapor indicated that the position of the sharp 1L_b transition varied by 1 nm and were accounted for in our calculations.

Lamp Replacement

The lamp should be replaced when the spectra begin to appear "shaky" (the excitation spectra are particularly sensitive to lamp degradation). For example, the excitation calibration scan will show unusual oscillations when the lamp needs to be replaced. A 150 W Xenon lamp is required and we have purchased such lamps (#XBO-150W/CROFR (69237)) from Adventure Lighting, 750 E. Elm St., Des Moines, IA 50309 for \$350.00

Contact People at Spex

I have worked with a number of representatives from Spex when I required advice or parts. These contacts include: Pete Kepper (at Chicago) at 708-620-4520, FAX 708-620-4551; Doug Keenan and Scott McDowell (in N. J.) at 908-549-7144 ext. 104 and Rich

Ruzzi (in N. J.) at ext. 228; Karen Rubalowski, Jim Matthias, and Dot Mitch (in N. J.) at 908-549-2571.

UV/vis Lambda 18 Spectrophotometer

General information

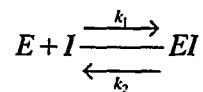
To date, we have performed typical wavelength scans that are simply described in the manual. Our sales representative, Chris Getz, may be contacted at 1-800-762-4000 and technical service representatives may be contacted at 1-800-762-8288. The serial number must be provided when one asks for assistance; our serial number is 75033.

Lamp Replacement

On the lamp housing is a gauge that measures total lamp hours. when a new lamp is required, it may be purchased from Perkin-Elmer. It is easily replaced since the lamp (already fixed in its housing) slides, then snaps, into place.

APPENDIX C. CALCULATIONS TO DETERMINE 90% INHIBITOR BOUND TO ENZYME.

The original reference for this calculation may be found in my notebook 4, p. 91. For an enzyme/inhibitor complex, we can assume the following:



$$K_I = k_2/k_1$$

$$[I] = [I_0] - [EI]$$

$$[E] = [E_0] - [EI]$$

where E is the free enzyme, I is the free inhibitor, EI is the enzyme/inhibitor complex, E_0 is the total enzyme, I_0 is the total inhibitor, and K_I is the inhibition constant. Under steady-state conditions,

$$d[EI]/dt = 0 = k_1[E][I] - k_2[EI] = [E][I] - K_I[EI]$$

which can also be written as

$$[EI]^2 - [EI]([E_0] + [I_0] + K_I) + [E][I] = 0$$

Solving for the roots of this quadratic equation using

$$\frac{-b \pm \sqrt{b^2 - 4ac}}{2a}$$

where $a=1$, $b = [E_0] + [I_0] + K_I$, and $c = [E_0][I_0]$, one can calculate the concentration of E_0 and I_0 required for 90% of the inhibitor to be bound; i.e., the concentrations of E_0 and I_0 required so that $I/I_0 < 0.10$.